

**Structural and functional analysis of yeast proteins involved
in ER-to-Golgi transport:
Sec24p family proteins and the GTPase activating protein Gyp5p**

Dissertation
zur Erlangung des Doktorgrades
der Mathematisch-Naturwissenschaftlichen Fakultäten
der Georg-August-Universität zu Göttingen

vorgelegt von
Anna De Antoni
aus Vicenza, Italien

Göttingen 2001

D7

Referent: Prof. Dr. Gerhard Braus

Korreferent: Prof. Dr. Dieter Gallwitz

Tag der mündlichen Prüfung: 30 April 2001

a mio padre
to my father

Acknowledgements

I thank Prof. Dr. Dieter Gallwitz for giving me the opportunity to work in his Department, for proposing this project, for his interest, support and invaluable criticisms. I am also grateful for his critical reading and discussion of this manuscript.

To Prof. Dr. Gerhard Braus, of the Dept. of Molecular Microbiology, my thanks for agreeing to be the referee for the faculty of Biology of the University of Göttingen.

A special thank to Dr. Thomas Lazar, for invaluable help (this thesis would not exist without him) for his advice and encouragement, and above all for being a very good friend.

I thank my lab-mates, Christian Votsmeier and Dr. Xiaoping Yang, for critical discussion, cooperation, for the supportive and lively atmosphere created in laboratory 211.

I am grateful to Dr. Stefan Albert and Dr. Renwang Peng for their cooperation in the projects I reported on this thesis, and for their critical discussion. I also thank Renwang for the support he gave to me during the first period I was in Germany.

I thank Dr. Jana Schmitzová for useful discussion on my thesis and on Gyp5p.

I thank Ursula Welscher-Altschäfel, Peter Mienkus, Rita Schmitz-Salve, Heike Behr, for useful and skilful technical assistance; Hans-Peter Geithe for DNA sequencing; Dr. Hans-Heinrich Trepte for the excellent electron microscopy pictures.

I thank Dr. Hans Dieter Schmitt and Dr. Stephan Schröder for critical discussion and useful advice.

I thank Ingrid Balshüsemann for helping me to overcome german bureaucracy.

I am also grateful to all the other members and to former colleagues of the Dept. of Molecular Genetics, Max Planck institute for Biophysical Chemistry, for creating a nice and stimulating working environment and comfortable atmosphere at the department.

I am indebted to Prof. Mary Osborn and colleagues of the Dept. of Biochemistry and Cell Biology, Max Planck institute for Biophysical Chemistry, for introducing me to culture and immunofluorescence of mammalian cells, and for allowing me to use their equipment. A special thank to Heinz-Jürgen Dehne for all the help he gave to me, for his kindness and his friendship.

I thank Dr. Stefan W. Hell, Alexander Egner and Andreas Schönle of the High Resolution Optical Microscopy Group, Max Planck institute for Biophysical Chemistry, for allowing me to use their confocal microscope and for teaching me how to use it.

I am grateful to Dr. David Ferrari and Dr. Phil Palma for critical reading of this manuscript.

I am deeply grateful to Fabiana Ganz, Phil Palma, Joanna Zergioti, David and Jane Britt, Francesco and Antonella Cecconi for their friendship, and the nice time we had together.

I thank fam. Meiwes for the lovely atmosphere I could breath in their house.

Extra special thanks to my family, my mother, my father (he is still alive in my heart), my sister and my fiancé Renato for their support and love.

Finally I want to thank all my friends from different parts of the world I did not mention before.

CONTENTS

1 INTRODUCTION	1
1.1 Intracellular protein transport in eukaryotic cells	1
1.2 ER-Golgi transport	3
1.3 Budding	5
1.3.1 COPII-coated vesicles (Table 1.1)	5
1.3.2 The Sec24p family (Table 1.2)	9
1.4 Tethering, docking and fusion	11
1.4.1 SNAREs	12
1.4.2 The Ypt/Rab family of small GTPases	14
1.4.3 Ypt1p	18
1.4.4 The Gyp protein family (Table 1.3)	20
2 MATERIALS	23
2.1 Growth media	23
2.1.1 Media components	23
2.1.2 Bacterial media	23
2.1.3 Yeast media	24
2.1.4 Mammalian cell media	25
2.2 Frequently used buffers and solutions	25
2.3 Chemicals	26
2.4 Enzymes	27
2.5 Reaction systems, Kits	27
2.6 Disposable supplies	28
2.7 Laboratory gadgets	28
3 METHODS	29
3.1 Bacteria and yeast culture techniques	29
3.2 DNA preparation, manipulation, amplification and analysis	29
3.2.1 Bacterial plasmid DNA preparation	29
3.2.2 Yeast genomic and plasmid DNA preparation	30
3.2.3 Spectrophotometric estimation of DNA purity and quantitation	30
3.2.4 Enzymatic treatment of DNA	30
3.2.5 <i>E. coli</i> transformation	31
a) Preparation of competent cells and transformation by heat shock	31
b) Preparation of competent cells and transformation by electroporation	32
3.2.6 PCR amplification of DNA	32
3.2.7 <i>In vitro</i> mutagenesis	33
3.2.8 DNA-Sequencing	34
3.2.9 DNA-DNA hybridization (Southern blotting)	34
3.3 Yeast genetics and yeast cell biology methods	34
3.3.1 <i>S. cerevisiae</i> transformation	34
3.3.2 Yeast gene knock-out	35
3.3.3 Yeast PCR mediated epitope tagging	36
3.3.4 Growth analysis	39
3.3.5 Invertase assay	39
3.3.6 Pulse-chase	40

3.4 Biochemical methods	42
3.4.1 Polyacrylamide gel electrophoresis (PAGE)	42
a) Denaturing polyacrylamide gel electrophoresis (SDS-PAGE)	42
b) Non-denaturing PAGE	43
3.4.2 Preparative gel electrophoresis and electro-elution	43
3.4.3 Staining of proteins in polyacrylamide gels	44
a) Coomassie brilliant blue staining	44
b) Silver staining	44
3.4.4 Western blotting and immunological detection of proteins on nitrocellulose filters	44
3.4.5 Protein quantitation	45
3.4.6 Concentrating proteins	45
3.4.7 Protein extraction	46
a) Protein extraction from bacteria	46
b) Protein extraction from yeast	46
c) Protein extraction from mammalian cells	48
3.4.8 Expression of proteins and recombinant proteins	48
a) Fusion tags	48
b) Expression of proteins in bacteria	49
c) Expression of proteins in yeast	50
3.4.9 Protein purification	50
a) 6xHis-fusion protein purification	50
b) GST-fusion protein purification	51
c) MBP-fusion protein purification	52
d) Anion exchange chromatography	52
e) Superdex 200 HR and Sephacryl S-200 HR size exclusion gel filtration chromatography	52
f) Ypt1p purification	53
g) Gyp5 ₍₄₀₀₋₈₉₂₎ -6His protein purification	53
3.4.10 Subcellular fractionation	53
a) Subcellular fractionation by differential centrifugation	53
b) Subcellular fractionation by velocity sedimentation on sucrose gradient	54
3.4.11 Analytical separation of protein complexes by gel filtration	55
3.4.12 Affinity binding assay with GST-fusion proteins	55
3.4.13 Immunoprecipitation	56
3.4.14 GAP assay	57
a) Quantitative HPLC-based GAP assay	57
b) Kinetic analysis of GTPase-GAP interaction	59
c) Filter GAP assay	60
3.5 Antibody production	60
3.6 Microscopic analysis	61
3.6.1 Indirect immunofluorescence of yeast cells	61
3.6.2 Vacuole detection by FM 4-64 staining	62
3.6.3 Indirect immunofluorescence of mammalian cells	62
3.7 Electron microscopic analysis	63
3.8 DNA and protein sequence computer analysis	64
4 RESULTS	65
4.1 SECTION I (Gyp5p)	65
4.1.1 Cloning and expression of different fragments of <i>GYP5</i>	65

4.1.2 Ypt1p is the preferred substrate for Gyp5p (Table 4.1)	69
4.1.3 Kinetic investigation of the Gyp5p/Ypt1p interaction	71
4.1.4 Arginine 496 is important for the catalytic activity of Gyp5p	73
4.1.5 Gyp5p can accelerate the GTPase activity of the Ypt1p ^{Q67L} mutant	74
4.1.6 Mutant strains with different <i>GYP</i> genes deleted in combination with <i>ypt1</i> ^{Q67L}	75
4.1.7 Growth analysis of different strains carrying <i>ypt1</i> ^{Q67L}	78
4.1.8 Partial rescue of the growth defect of the <i>ypt1</i> ^{Q67L} mutant by high expression of Gyp5p	81
4.1.9 Analysis of possible transport defects in the different mutants	81
4.1.10 Gyp5p is primarily a cytosolic protein	84
4.1.11 Electron microscopic inspection of $\Delta gyp5/ypt1$ ^{Q67L} mutant cells	85
4.1.12 Visualization of vacuolar membranes in living cells by FM 4-64 vital staining	85
4.2 SECTION II (Sec24p family)	89
4.2.1 Sec24 family proteins are differently expressed in the cell	89
4.2.2 Sec24p, Sfb2p and Sfb3p form complexes with Sec23p	92
4.2.3 Sfb2p behaves differently from Sec24p and Sfb3p on gel filtration chromatography	93
4.2.4 Intracellular distribution of Sec24p and its orthologues	93
4.2.5 Sfb2p, like Sec24p, binds Sed5p	96
4.2.6 Sfb2p can rescue the growth defect of <i>sec24-11</i>	97
4.2.7 Effects on protein transport of $\Delta sfb2$ in combination with the <i>sec24-11</i> allele	97
4.2.8 Electron microscopic inspection of the $\Delta sfb2/sec24-11$ mutant	99
4.2.9 Immunofluorescence detection of one member of the mammalian Sec24p family in monkey CV1 cells	99
4.3 SECTION III (Epitope tagging vectors)	104
5 DISCUSSION	106
5.1 Sec24p family	107
5.1.1 Sfb2p	107
5.1.2 Sfb3p	109
5.1.3 Why are there three Sec24 related proteins?	110
5.2 Ypt/Rab proteins as regulators of p protein transport	111
5.3 Gyp proteins and the "GYP domain"	111
5.4 Gyp5p	113
5.4.1 Ypt1p is the preferred substrate of Gyp5p (Table 5.1)	113
5.4.2 Gyp5, like other Gyp proteins, contains a putative catalytic arginine finger	114
5.4.3 Gyp5p can accelerate the GTPase activity of the Ypt1p ^{Q67L} mutant	115
5.4.4 Is GTP hydrolysis important <i>in vivo</i> ?	115
6 SUMMARY	119
7 APPENDIX	121
7.1 Bacterial and yeast strains and mammalian cell lines	121
7.1.1 Bacterial <i>E. coli</i> strains (Table 7.1)	121
7.1.2 Yeast strains (Table 7.2)	121
7.1.3 Mammalian tissue culture cell lines (Table 7.3)	124
7.2 Plasmids	124

7.2.1 <i>E. coli</i> cloning and expression vectors (Table 7.4).....	124
7.2.2 Yeast vectors (Table 7.5).....	125
7.2.3 Recombinant plasmids created in this work (Table 7.6).....	126
7.3 Oligonucleotides (Table 7.7).....	130
7.4 Antibodies	135
7.4.1 Primary antibodies (Table 7.8).....	136
7.4.2 Secondary antibodies (Table 7.9).....	136
8 ABBREVIATIONS	137
9 REFERENCES	140

1 INTRODUCTION

During my Ph.D. work I studied some of the mechanisms that regulate the complex machinery of vesicular transport from the endoplasmic reticulum to the Golgi apparatus in the single-celled eukaryote *Saccharomyces cerevisiae*. I focused my attention on certain proteins involved in vesicular budding, particularly on Sec24p family members. In addition I studied proteins involved in tethering/docking processes, in particular a new member of the Gyp family of GTPase activating proteins (GAP), Gyp5p, the preferred substrate of which is the small Ras-like Ypt1 protein.

1.1 Intracellular protein transport in eukaryotic cells

Eukaryotic cells are subdivided into membrane-enclosed compartments called organelles. Each organelle is endowed with a specific subset of lipids and cellular proteins according to its physiological specialization. This has been known since the introduction of electron microscopic analyses combined with cell fractionation studies (de Duve, 1975; Palade, 1975). Cellular life and differentiation depend on keeping the integrity of the complex network of membranous compartments, however, macromolecules also have to be transported from one compartment to another and into and out of the cell. In order to achieve this without compromising membrane integrity, an efficient and elaborate transport machinery that ensures temporal and spatial specificity has been developed (Fig. 1.1). Secretory proteins are synthesized and assembled in the endoplasmic reticulum (ER). Then they pass through the Golgi apparatus where they undergo a variety of carbohydrate and other modifications before being delivered to their final destinations, such as the plasma membrane, endosomes or the lysosome (vacuole). A related pathway exists for the uptake of proteins and extracellular fluids from the cell surface via endosomes to lysosomes and traffic can occur in both directions along the two pathways (Fig. 1.1). Retrograde transport between endocytic and exocytic compartments ensures that the quantitative and qualitative balance in the protein and lipid contents of the cell's organelles is maintained.

Since the pioneering work of George Palade (Palade, 1975) it has been known that proteins get to their final destination in membrane-derived transport vesicles (for reviews see Mellman and Warren, 2000; Rothman, 1994). The vesicular protein transport through the secretory and endocytic pathways is directional and tightly controlled through the action of a variety of evolutionary conserved proteins (Bennett and Scheller, 1993; Ferro-Novick and Jahn, 1994; Kaiser and Schekman, 1990; Novick and Zerial, 1997). In principle, the transport process "simply" requires the selective packaging of cargo into a vesicle carrier and the transport, docking and fusion of the vesicle intermediate with the appropriate target membrane. This set of biochemical reactions depends on a considerable array of proteins, lipids and enzyme complexes (coats, SNAREs, GTPases, ATPases, kinases, phosphoinositides, etc.), some of which function as structural components while others catalyze the assembly/disassembly of reaction intermediates or regulate spatial and temporal aspects of the process. The vesicular transport can be separated into three steps: budding (see Section 1.3), tethering/docking, and fusion of vesicles with the target membrane (see Section 1.4).

The three main classes of vesicles, classified on the basis of their protein coats, are: COPII vesicles, which mediate ER to Golgi traffic (see 1.3.1); COPI vesicles, which are responsible for retrograde traffic from the Golgi to the ER and for traffic between the cisternae of the Golgi; and the clathrin-coated vesicles, which mediate various endocytic and post-Golgi vesicular trafficking steps (for reviews see Kirchhausen, 2001; Scales *et al.*, 2000b). The assembly of a protein coat provides not only the driving energy to deform the vesicle membrane into a spherical shell but also an affinity matrix for the selective partitioning of cargo molecules into the vesicle. In addition to the coat proteins, the budding process also involves monomeric GTPases of the dynamin and ARF family, as well as adaptor proteins (for reviews see Aridor and Balch, 1996; Cosson and Letourneur, 1997; Kirchhausen, 1999; Springer *et al.*, 1999). Once the cargo-containing vesicles have pinched off from the donor organelle membrane, they must be targeted to and fuse with the correct target membrane. It is thought that vesicles travel to their target membrane along cytoskeletal structures (Kamal and Goldstein, 2000). Members of the SNARE, Ypt/Rab and Sec1 families of proteins appear to direct and regulate these vesicle docking and fusion reactions (see Section 1.4). In addition, a regulatory function in vesicular trafficking has also been demonstrated for phosphatidylinositol and its phosphorylated derivatives (for reviews see De Camilli *et al.*, 1996; Odorizzi *et al.*, 2000).

Protein transport to peroxisomes, mitochondria and chloroplasts differs mechanistically from the vesicular transport discussed here (for reviews see Haucke and Gottfried, 1997; Hettema *et al.*, 1999; Schatz, 1996; Schleiff and Soll, 2000).

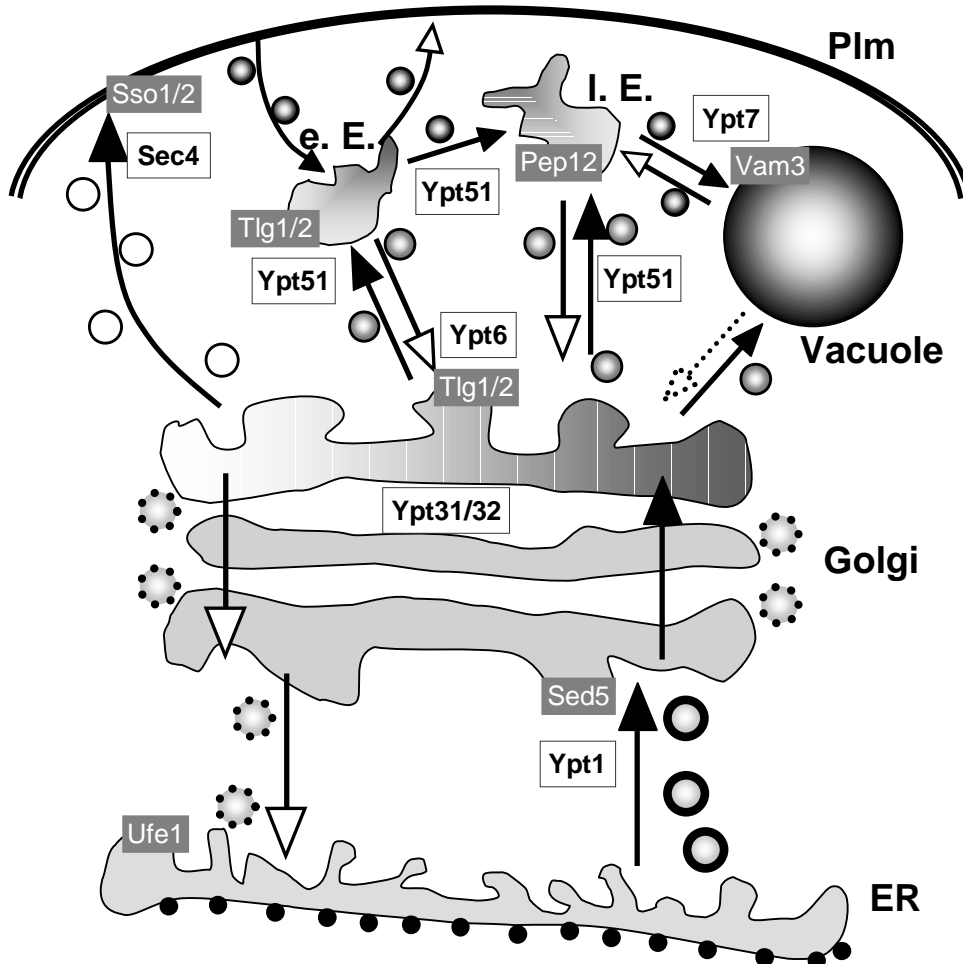


Fig 1.1 Vesicular protein transport pathways in a *S. cerevisiae* cell. Filled arrows indicate forward traffic, while open arrows indicate retrograde trafficking, dotted arrows indicate hypothetical routes. The known sites of action of Ypt GTPases are in white boxes and those of syntaxins in gray boxes. e.E.= early endosome, I.E.= late endosome, Plm= plasma membrane. Figure modified from (Götte *et al.*, 2000).

1.2 ER-Golgi transport

Transport of proteins between the endoplasmic reticulum and the Golgi apparatus is mediated by COPII and COPI coated vesicles (Bannykh *et al.*, 1996; Bednarek *et al.*, 1996). In addition, there are many accessory proteins that facilitate

the forward movement of proteins from the ER and their uptake into transport vesicles (for review see Herrmann *et al.*, 1999).

The endoplasmic reticulum consists of an elaborate and dynamic tubular and cisternal network that is continuous with the outer nuclear membrane. It is divided in smooth and rough ER. The rough ER is the place where proteins are assembled and it can be considered the first station in the secretory pathway. The Golgi apparatus is typically represented as a series of stable compartments, *cis*-, *medial*-, *trans*-Golgi and *trans*-Golgi-network (TGN), with transport vesicles serving as carriers of the secretory cargo from one compartment to the next (in *S. cerevisiae*, the Golgi apparatus does not form stacks of organelles but consists of individual cisternae interspersed throughout the cytoplasm). An alternative model considers the Golgi compartments as transitory structures continuously undergoing renewal, and the Golgi apparatus is viewed as a dynamic outgrowth of the ER (Fig. 1.2). According to this "cisternal maturation" hypothesis, COPII vesicles fuse to form the ERGIC (ER-Golgi intermediate compartment) clusters, which coalesce to form a new *cis*-cisterna that progresses through the stack, until it ultimately disintegrates into various types of transport carriers.

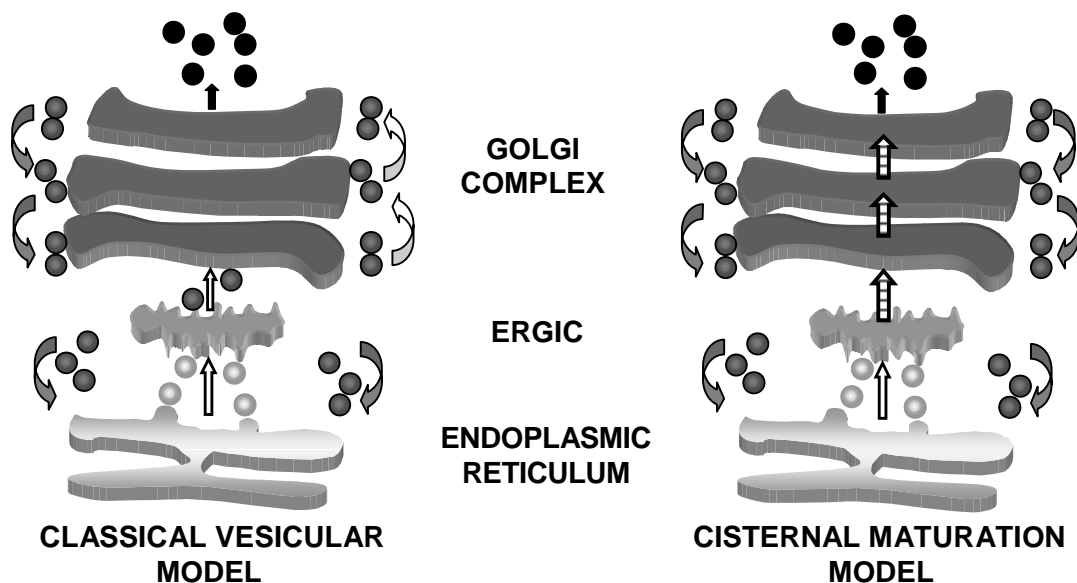


Fig. 1.2 Schematic representation of the two proposed mechanisms for transport of secretory cargo to and through the Golgi apparatus. In the first model, the Golgi consist of stable compartments, membrane-bounded carriers transport cargo molecules from ER to *cis*-Golgi and between the different Golgi compartments. In the second model, ER-derived membranes coalesce to form a new *cis*-cisterna which then progresses through the stack, carrying the secretory cargo forward, while retrograde COPI vesicles recycle resident Golgi proteins to younger cisternae. ERGIC= ER-Golgi intermediate compartment

● = COPII ● = COPI ● = Clathrin

While cisternae progress, carrying the secretory cargo forward, retrograde COPI vesicles recycle resident Golgi proteins to younger cisternae. In both models the intermediate compartment (ERGIC) residing between the ER and the Golgi is considered to be a dynamic structure that captures cargo released from the ER in COPII vesicular carriers and promotes recycling by COPI vesicular carriers (Bannykh and Balch, 1997). In yeast, there is no clear evidence for the existence of an intermediate compartment and *cis*-Golgi is regarded as the first compartment after the ER.

Up to now, the dilemma of whether transport through the Golgi complex occurs via vesicular transport or by cisternal maturation remains unsolved. Nevertheless, in both models COPII vesicles mediate the first transport step in the secretory pathway. It is in fact generally accepted that most, if not all, of the forward vesicular traffic from the ER to the Golgi involves COPII vesicles (Mellman and Warren, 2000; Pelham and Rothman, 2000)

1.3 Budding

Once a protein is properly core-glycosylated, folded and assembled in the ER it may be incorporated into COPII vesicles. COPII-coated vesicles, as mentioned before, represent the major, and perhaps the sole, vehicle for anterograde protein traffic from the ER, and COPII components are involved in cargo selection and export from the ER.

1.3.1 COPII-coated vesicles

COPII coat is composed of five cytosolic components: Sar1p, a small GTP-binding protein (Barlowe *et al.*, 1993; Nakano and Muramatsu, 1989), and the two heterodimeric protein complexes Sec23p/Sec24p (Hicke *et al.*, 1992; Yeung *et al.*, 1995a) and Sec13p/Sec31p (Salama *et al.*, 1997; Salama *et al.*, 1993). By morphological studies on yeast *sec* mutants and by cell-free assays (Baker *et al.*, 1988; Barlowe *et al.*, 1994; Rexach and Schekman, 1991) it was demonstrated that these five cytosolic proteins represent the minimal requirements for vesicular budding.

Several homologs of COPII components exist in yeast, in mammals (Table 1.1) and in other organisms.

Table 1.1 COPII components in yeast and mammals

Protein	Main characteristics	Yeast	Mammals
Sar1p ~ 21 kDa	- GTPase.	Sar1p (<i>YPL218W</i>) (190 aa) (Nakano and Muramatsu, 1989; Oka <i>et al.</i> , 1991)	mSar1Ap (198 aa) mSar1Bp (Kuge <i>et al.</i> , 1994; Shen <i>et al.</i> , 1993)
Sec23p ~ 85 kDa	- GAP for Sar1p. - Always in complex with Sec24p. - Sequence similarity with Sec24p.	Sec23p (<i>YPR181C</i>) (768 aa) (Hicke and Schekman, 1989; Yoshihisa <i>et al.</i> , 1993)	hSec23Ap (765 aa) hSec23Bp (767 aa) (Orci <i>et al.</i> , 1991; Paccaud <i>et al.</i> , 1996)
Sec24p ~ 105 kDa	- Always in complex with Sec23p. - Putative Zinc binding motif. - Sequence similarity with Sec23p.	Sec24 (<i>YIL109C</i>) (926 aa) Sfb2p (<i>YNL049C</i>) (876 aa) Sfb3p (<i>YHR098C</i>) (929 aa) (Hicke <i>et al.</i> , 1992; Kurihara <i>et al.</i> , 2000; Peng <i>et al.</i> , 2000; Roberg <i>et al.</i> , 1999)	hSec24Ap (1078 aa) hSec24Bp (1268 aa) hSec24Cp (1094 aa) hSec24Dp (1032 aa) (Pagano <i>et al.</i> , 1999; Tang <i>et al.</i> , 1999; Tani <i>et al.</i> , 1999)
Sec13p ~ 34 kDa	- Always in complex with Sec31p. - six WD-40 repeat motifs.	Sec13p (<i>YLR208W</i>) (297 aa) Seh1p (<i>YGL100W</i>) (349 aa) (Pryer <i>et al.</i> , 1993; Saxena <i>et al.</i> , 1996; Siniosoglou <i>et al.</i> , 1996)	Sec13Rp (322 aa) (Swaroop <i>et al.</i> , 1994; Tang <i>et al.</i> , 1997)
Sec31p ~ 150 kDa	-phosphoprotein. -Always in complex with Sec13p. -seven WD-40 repeats near the N terminus.	Sec31p (<i>YDL195W</i>) (1273 aa) (Salama <i>et al.</i> , 1997)	Sec31Ap (1220 aa) Sec31Bp (1179 aa) (Tang <i>et al.</i> , 2000).

The vesicle budding process starts (see Fig. 1.3) with the recruitment of Sar1p to the ER (Yoshihisa *et al.*, 1993). Sar1p recruitment to membranes requires ATP. This could allow the export machinery to respond to extracellular signaling pathways, thus integrating the secretory pathway with the cellular physiology (Aridor and Balch, 2000). At the ER membrane, Sar1p exchanges GDP for GTP under the influence of a specific guanine nucleotide exchange factor, Sec12p, an integral membrane glycoprotein (Barlowe and Schekman, 1993). This activation step leads to the recruitment of Sec23p/Sec24p from the cytosol to the membrane to form a ternary complex that interacts with cargo and cargo receptors (Aridor *et al.*, 1998; Kuehn *et*

al., 1998; Springer and Schekman, 1998; Springer *et al.*, 1999). Finally the Sec13p/Sec31p complex binds to initiate the formation of the budding vesicle. Sec23p is a GTPase activating protein for Sar1p (Yoshihisa *et al.*, 1993). GTP hydrolysis (step preceding fusion) allows Sar1p to dissociate from the membrane, this would render COPII components easily displaceable from the completed vesicle. In fact, it is thought that the vesicular coat has to be removed to allow fusion to take place.

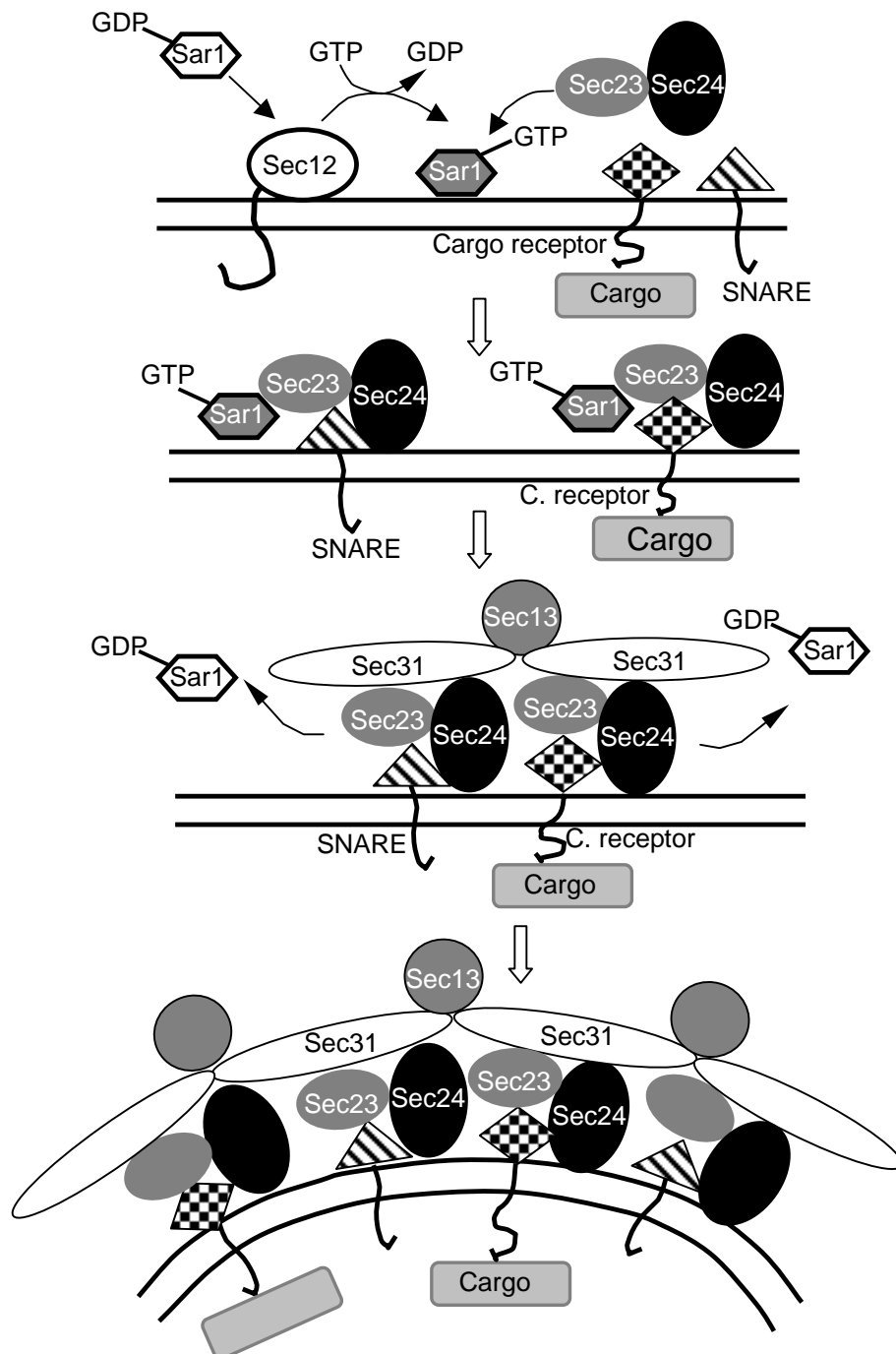


Fig. 1.3 Scheme of COPII vesicle formation (modified from Schekman and Orci, 1996).

Direct interactions among COPII components have been shown by two-hybrid analysis and *in vitro* binding assays. The N-terminus of Sec24p binds to Sec23p (Gimeno *et al.*, 1996; Peng *et al.*, 1999); Sec13p and the N-terminal region of Sec31p interact with each other, while Sec23p and Sec24p interact with a central region of Sec31p (Shaywitz *et al.*, 1997), see Fig. 1.4.

In vivo, an additional gene, *SEC16*, is important for budding and probably also for cargo sorting, but it may not contribute directly to vesicle morphogenesis. Sec16p is a large (240 kDa) peripheral membrane protein that is tightly associated with the cytosolic face of the ER. It was shown to interact genetically with all five COPII proteins and to bind, through independent domains, Sec23p, Sec24p and Sec31p. Sec16p was proposed to organize and to stabilize COPII coat assemblage (Espenshade *et al.*, 1995; Shaywitz *et al.*, 1997).

In vitro experiments using reconstituted COPII-coated vesicles from chemically defined liposomes showed that the "binding sites" for coat proteins could be lipids rather than membrane proteins, in particular the acidic phospholipids phosphatidylinositol-4-phosphate (PIP) and phosphatidylinositol-4-5-bisphosphate (PIP₂) (Matsuoka *et al.*, 1998b). Acidic phospholipids present in a membrane in high amounts favor the binding of coat proteins and the formation of buds and vesicles, nevertheless it is not clear whether they represent the essential minimal components of a biological process (Nickel *et al.*, 1998).

Several experiments suggest that cargo is selected and actively concentrated into COPII vesicles (Aridor *et al.*, 1998; Balch *et al.*, 1994; Bannykh *et al.*, 1996; Campbell and Schekman, 1997; Matsuoka *et al.*, 1998a; Springer *et al.*, 1999). In particular, it was demonstrated that Sar1p-GTP and Sec23p/Sec24p form a specific "prebudding" complex with integral membrane proteins such as the SNAREs Bet1p and Bos1p and with membrane proteins of the p24 family (such as Emp24p) in yeast (Kuehn *et al.*, 1998; Springer and Schekman, 1998) and with vesicular stomatitis virus glycoprotein (VSV-G) in mammalian systems (Aridor *et al.*, 1998). Sec23p/Sec24p in the presence of Sar1-GTP can also interact with cytosolic cargo such as the glycosylated pro-alpha

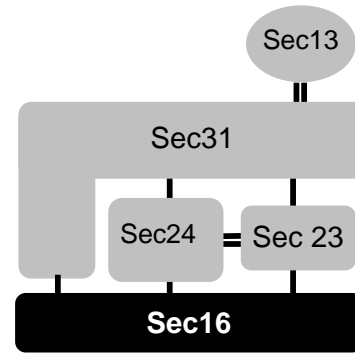


Fig. 1.4 Sec16p interactions with COPII components as described in (Shaywitz *et al.*, 1997).

factor (gp α F), probably with the help of membrane spanning receptors/adaptors (Kuehn *et al.*, 1998). Furthermore, it was demonstrated that resident ER proteins (such as Sec61p and Kar2p) are excluded from the prebudding complex (Kuehn *et al.*, 1998; Matsuoka *et al.*, 1998b). A direct interaction of Sec24p and the Golgi syntaxin Sed5p suggests that it is mainly this COPII component that binds membrane cargo molecules (Peng *et al.*, 1999). Proteins of the p24 family (type I transmembrane proteins) were thought to be cargo receptor/adaptors that could serve as a link between luminal cargo molecules and coat proteins (Fiedler *et al.*, 1996; Muniz *et al.*, 2000; Schimmoller *et al.*, 1995; Stamnes *et al.*, 1995). It was recently demonstrated, however (with a strain lacking all eight members of the p24 gene family) (Springer *et al.*, 2000), that in *S. cerevisiae* p24 proteins are not essential for vesicular transport. Therefore, a possible role as quality control factors, which restrict the entry of proteins into COPII vesicles, was postulated for p24 proteins. Recently, data have been published supporting the role of the mannose specific lectin-like ERGIC-53 (a non-glycosylated type I membrane protein) as a receptor facilitating the ER-to-ERGIC (ER-Golgi intermediate compartment) transport of soluble glycoprotein cargo in mammalian cells (Appenzeller *et al.*, 1999; Hauri *et al.*, 2000). In addition, studies on mammalian cells have identified two sorting motifs within the cytoplasmic domains of transmembrane cargo molecules which are important for their efficient exit out of the ER: a di-acidic motif (Asp-X-Glu, where X represents any amino acid) on the cytoplasmic tail of vesicular stomatitis virus glycoprotein (Nishimura and Balch, 1997; Nishimura *et al.*, 1999), and a double phenylalanine motif (Phe-Phe) on the cytoplasmic tail of p24 proteins (Dominguez *et al.*, 1998) and ERGIC-53 (Hauri *et al.*, 2000; Kappeler *et al.*, 1997). It was also demonstrated that peptides containing the double phenylalanine motif were able to bind to several proteins, among them the mammalian Sec23p/Sec24p complex (Dominguez *et al.*, 1998; Kappeler *et al.*, 1997). Furthermore, novel data from mammalian cells, suggest a more active role of Sar1p in cargo sorting. According to these researchers cargo capture would happen in two integrated stages, the first of which would be supported by Sar1p before the recruitment and the assembly of the coat complexes (Aridor *et al.*, 2001).

1.3.2 The Sec24p family

In yeast, there are two close orthologues of Sec24p (Sfb2p and Sfb3p) that were characterized during this work (Kurihara *et al.*, 2000; Peng *et al.*, 2000; Roberg *et al.*, 1999). Whereas Sec24p is an essential protein, Sfb2p and Sfb3p are dispensable for

cell viability. As Sec24p, both Sfb2p and Sfb3p form stable complexes with Sec23p. Interestingly, all three proteins harbor within the N-terminal region a domain with a GATA-type zinc finger-like motif (CysX₂CysX₁₈CysX₂Cys) (Mackay and Crossley, 1998; Trainor *et al.*, 1990). In Table 1.2, the main characteristics of these proteins are listed.

Table 1.2 Main characteristics of *S. cerevisiae* Sec24 family proteins.

	Sec24p (ORF: <i>YIL109C</i>)	Sfb2p (Iss1p) (ORF: <i>YNL049C</i>)	Sfb3p (Lst1p) (ORF: <i>YHR098C</i>)
Length	926 aa	876 aa	929 aa
MW	103.6 kDa	98.9 kDa	103.9 kDa
Chromosome	IX	XIV	VIII
pI	5.83	5.16	5.87
% identity with Sec24p	100%	56%	23.5%
% similarity with Sec24p	100%	71%	42%
Gene deletion phenotype	Lethal	no significant effect	no significant effect
Protein interactions (physical)	Sec23p, Sec31p, Sec16p, Bet1p, Bos1p, Sed5p, Pma1p (Gimeno <i>et al.</i> , 1996; Peng <i>et al.</i> , 1999; Shaywitz <i>et al.</i> , 1997; Shimoni <i>et al.</i> , 2000; Springer and Schekman, 1998; Yeung <i>et al.</i> , 1995b).	Sec23p, Sed5p, Sec16p (Higashio <i>et al.</i> , 2000; Kurihara <i>et al.</i> , 2000; Peng <i>et al.</i> , 2000)	Sec23p, Pma1p (Peng <i>et al.</i> , 2000; Shimoni <i>et al.</i> , 2000)
Synthetic lethal interactions	<i>BET1</i> , <i>SEC12</i> , <i>SEC13</i> , <i>SEC16</i> , <i>SEC17</i> , <i>SEC18</i> , <i>SEC22</i> , <i>SEC23</i> , <i>SFB3</i> , <i>BET1</i> (Kurihara <i>et al.</i> , 2000; Peng <i>et al.</i> , 2000)	<i>BET1</i> , <i>SEC22</i> (Kurihara <i>et al.</i> , 2000)	<i>SEC12</i> , <i>SEC13</i> , <i>SEC16</i> , <i>SEC23</i> , <i>SEC24</i> , <i>SEC31</i> . (Peng <i>et al.</i> , 2000; Roberg <i>et al.</i> , 1999; Shimoni <i>et al.</i> , 2000)

Database searches revealed a whole family of Sec24-related proteins from many other organisms (three isoforms in *S. pombe*, two isoforms in *C. elegans*, three isoforms in *D. melanogaster*, four isoforms in *H. sapiens*).

1.4 Tethering, docking and fusion

The fusion of a transport vesicle with its target membrane involves two types of events: first the transport vesicle must specifically recognize the correct target membrane, then it has to fuse with that membrane. Interaction of two membranes can be considered a multi-stage process in which different protein complexes are involved. The first stage, during which the two membranes come close to each other, has been termed "tethering". Then follows the interaction of SNAREs (SNAP receptors) on opposing membranes (see Section 1.4.1), and this strong interaction (called "docking") ultimately leads to membrane fusion. The docking/fusion process is probably initiated by the binding of two soluble proteins, NSF (Sec18p in yeast) and SNAP (Sec17p in yeast), that open the cis-SNARE complexes (Ungermann *et al.*, 1998). NSF (N-ethyl-maleimide sensitive factor) is a soluble ATPase (Beckers *et al.*, 1989; Block *et al.*, 1988; Malhotra *et al.*, 1988), SNAPs (no relation with SNAP-25) are soluble NSF attachment proteins (Clary *et al.*, 1990).

Many different "tethering components" involved at different transport steps have recently been identified in yeast and mammalian cells (for review see Guo *et al.*, 2000; Waters and Pfeffer, 1999). The use of multiple tethering factors is likely to ensure the high selectivity and spatial and temporal regulation of membrane targeting. Tethering complexes and proteins implicated in ER-Golgi transport in yeast are: TRAPP (transport protein particle, a ten subunits complex) (Barrowman *et al.*, 2000; Sacher *et al.*, 2000; Sacher *et al.*, 1998; Wang *et al.*, 2000b), p115/Uso1p (Allan *et al.*, 2000; Cao *et al.*, 1998; Sapperstein *et al.*, 1996; Sapperstein *et al.*, 1995), and Sec34p-Sec35p (VanRheenen *et al.*, 1998; VanRheenen *et al.*, 1999). In mammalian cells, the protein p115 probably also acts at other transport steps (Nelson *et al.*, 1998; Waters *et al.*, 1992).

The intricate tethering/docking process is regulated by small Ras-like GTPases termed Ypt in yeast or Rab in mammals (for reviews see Götte *et al.*, 2000; Lazar *et al.*, 1997; Zerial and McBride, 2001) (see Section 1.4.2). Ypt/Rab proteins might be involved in recruiting tethering and docking factors (Allan *et al.*, 2000; Cao *et al.*, 1998; Guo *et al.*, 2000; Seals *et al.*, 2000; Wickner and Haas, 2000) and/or in the removal of inhibitors of SNARE complex assembly such as could be the proteins of the Sec1 family (Lian *et al.*, 1994; Lupashin and Waters, 1997; Sogaard *et al.*, 1994).

The Sec1 family is another group of proteins important in fusion. In yeast, there are four proteins belonging to this family: Sec1p, Sly1p, Vps33p and Vps45p. Sec1p

acts exclusively at the plasma membrane. It was demonstrated to bind to assembled exocytic SNARE complexes in yeast (Carr *et al.*, 1999). In mammals, n-Sec1p binds to the closed conformation of Syntaxin1A inhibiting it from interacting with other SNAREs (Yang *et al.*, 2000). Sly1p participates in docking events of ER-derived vesicles to the Golgi compartment; it binds to the Golgi syntaxin Sed5p (Grabowski and Gallwitz, 1997). The *SLY1-20* mutant is a dominant allele that can suppress the functional loss of *YPT1* (Dascher *et al.*, 1991; Ossig *et al.*, 1991). Vps45p is involved in endosomal trafficking, and it was shown to bind to the syntaxin Tlg2p (Nichols *et al.*, 1998). Vps33p is part of a large protein complex (C-VPS complex / HOPS) involved in Golgi-to-vacuole protein transport and in homotypic vacuole fusion (Sato *et al.*, 2000; Seals *et al.*, 2000). The function of Sec1 proteins is not well understood yet, they have been described both as activators and inhibitors of SNARE complex assembly and membrane fusion (for review see Halachmi and Lev, 1996).

1.4.1 SNAREs

SNAREs (SNAP receptors) comprise distinct families of conserved transmembrane or membrane-associated proteins that were independently discovered in yeast, mammalian cells and neurons (for review see Bennett and Scheller, 1993; Ferro-Novick and Jahn, 1994) and which are considered the core machinery for membrane fusion (Weber *et al.*, 1998). They are grouped into three large families (the names derive from the synaptic proteins first recognized to be SNAREs): the syntaxin (Bennett *et al.*, 1992), the SNAP-25 (synaptosomal-associated protein of 25 kDa) (McMahon and Sudhof, 1995) and the VAMP/synaptobrevin family (VAMP= vesicle-associated membrane protein) (Baumert *et al.*, 1989; Trimble *et al.*, 1988). The term SNARE was coined by J. Rothman and colleagues (Söllner *et al.*, 1993b) to describe entities which could bind soluble factors that had previously been described to be important components of the intracellular membrane fusion apparatus, namely NSF (N-ethylmaleimide-sensitive fusion protein) and SNAP (soluble NSF attachment protein; no relation to SNAP-25). Based on their localization and overall structure, SNAREs were initially classified into t-SNAREs (SNAREs localized to target membrane) and v-SNAREs (SNAREs localized to the membrane of a trafficking vesicle) (Söllner *et al.*, 1993a). The Syntaxin and SNAP-25 families were originally classified as t-SNAREs and the VAMP/synaptobrevin family as v-SNAREs. Since proteins related to SNAREs were also found in non-neuronal cells and were localized

to specific subcellular compartments, Rothman and colleagues in 1993 formulated the "SNARE hypothesis" (Rothman, 1994; Rothman and Warren, 1994; Söllner *et al.*, 1993b) on the basis of which SNAREs would provide a general mechanism for the specific docking and fusion of transport vesicles (containing v-SNAREs) with their target membranes (containing the cognate t-SNAREs).

Every cell expresses a large number of SNARE proteins that exhibit characteristic subcellular distributions (see Fig. 1.1), suggesting that the fidelity of vesicle trafficking might in part be determined by specific SNARE pairings. However, the promiscuity of SNARE pairing observed *in vitro* (Fasshauer *et al.*, 1999; Grote and Novick, 1999) and the fact that they shuttle between trafficking compartments associated with transport vesicles (Wooding and Pelham, 1998) suggest that the information for membrane compartment organization is not in the inherent ability of SNAREs to form complexes. This point remains quite controversial since several researchers still support the idea of specificity by SNARE pairing. These investigators observed that whereas SNAREs pair almost randomly in solution they are not at all promiscuous in the presence of lipid bilayers (McNew *et al.*, 2000; Parlati *et al.*, 2000; Scales *et al.*, 2000a). SNAREs involved in ER-to-Golgi transport in yeast are Bos1p, Bet1p, Sec22p and Sed5p (Cao and Barlowe, 2000; Parlati *et al.*, 2000).

Structural and biochemical data highlighted the mechanism by which trans-SNARE complexes catalyze the merging of lipid bilayers during intracellular membrane fusion. SNAREs are coiled-coil proteins and during membrane fusion, four α -helices from proteins on the vesicle and target membrane come together to form a stable, four-helix bundle (see Fig. 1.5). The trans-SNARE complex consists of syntaxin and SNAP25 family members on the target membrane and a VAMP/synaptobrevin family member on the vesicle.

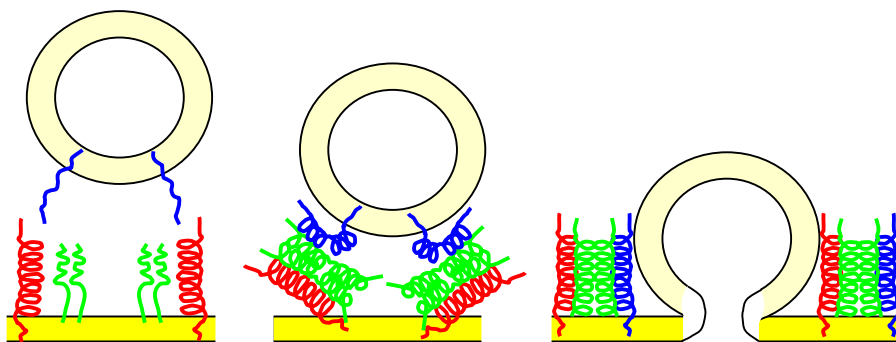


Fig. 1.5 Trans-SNARE complex formation and membrane fusion. For vesicle fusion, three SNAREs of the syntaxin (red) and the SNAP25 family (green) are required on the target membrane and a VAMP family member (blue) on the vesicle (modified from Scales *et al.*, 2000a).

The formation of the four-helix bundle may bring interacting membranes in close enough opposition to facilitate, if not complete, bilayer fusion (Lin and Scheller, 1997; Otto *et al.*, 1997; Poirier *et al.*, 1998; Sutton *et al.*, 1998; Weber *et al.*, 1998).

There is evidence that, at least in the case of vacuole-to-vacuole fusion, for the terminal step of the fusion event to take place, a calcium signal that is sensed by calmodulin is necessary (Peters and Mayer, 1998). The action of protein phosphatase-1 has been found to be essential for fusion, too (Peters *et al.*, 1999).

The association of the four α -helices in the synaptic fusion complex structure produces highly conserved layers of interacting amino acid side chains in the center of the four-helix bundle, and on the basis of these features SNAREs were reclassified into Q-SNAREs and R-SNAREs (Q= glutamine, R= arginine). Fusion-competent SNARE complexes generally consist of four-helix bundles composed of three Q-SNAREs and one R-SNARE (Fasshauer *et al.*, 1998; Ossig *et al.*, 2000), however exceptions to this rule have been described (Katz and Brennwald, 2000).

Because the core complex is extremely stable, cells have evolved a specialized chaperone whose function is to dissociate the SNARE complex under the hydrolysis of ATP. This chaperone is the previously mentioned NSF (Sec18p in yeast) which acts in conjunction with SNAP (Sec17p in yeast). Both NSF and SNAP are structurally and functionally conserved in evolution. They are known to function at virtually all intracellular transport steps (Rothman, 1994). SNAP/Sec17p needs to bind to the SNARE complex before NSF/Sec18p can bind. Sec18p action also depends on the heterodimeric protein complex LMA1 (a heterodimer composed of thioredoxin and the proteinase inhibitor IB2) that is thought to stabilize SNARE proteins after their separation (Barlowe, 1997; Xu *et al.*, 1997; Xu *et al.*, 1998). Recent data suggest that only cis-SNARE complexes (formed when SNAREs combine on the same membrane) are disrupted by the action of the ATPase NSF, and that this would be necessary to maintain a supply in cells of uncombined SNAREs for fusion (Wang *et al.*, 2000a; Weber *et al.*, 2000). For further reviews on SNARE proteins see (Chen and Scheller, 2001; Gerst, 1999; Jahn and Südhof, 1999; Pelham, 1999).

1.4.2 The Ypt/Rab family of small GTPases

Ypt/Rab proteins form the largest subfamily of the Ras superfamily of GTPases (Götte *et al.*, 2000; Novick and Zerial, 1997; Zerial and McBride, 2001). The Ras-superfamily includes more than 700 members in species from yeast to man and it can

be divided into at least five subfamilies: the Ras, the Rho/Rac/Cdc42, the Ypt/Rab, the Sar1/Arf, and the Ran families (Garcia-Ranea and Valencia, 1998; Kahn *et al.*, 1992; Matozaki *et al.*, 2000). Different members of these families play key roles in a variety of cellular processes including signal transduction, cytoskeletal organization and protein transport (Garcia-Ranea and Valencia, 1998; Zerial and Huber, 1995). Like heterotrimeric G proteins they act as molecular switches, where the "switching" process relies on GTP hydrolysis (for review see Bourne *et al.*, 1990; Kjeldgaard *et al.*, 1996; Sprang, 1997).

Ras and Ras-like proteins are related in size (approximately 200-230 amino acids), secondary and tertiary structure (six-stranded β -sheet surrounded by α -helices) and they share significant sequence identity and similar biochemical properties (Bourne *et al.*, 1990; Gamblin and Smerdon, 1998; Wittinghofer and Pai, 1991). They bind guanine nucleotides with high affinity and are endowed with a very slow intrinsic GTPase activity. The superfamily is characterized by a C-terminal cysteine motif subject to post-translational modifications and by the presence of a set of highly conserved regions, G1-G5 (loops between the secondary structure elements), that are critical for GDP/GTP exchange, for GTP-induced conformational change and for GTP hydrolysis (Bourne *et al.*, 1991; Valencia *et al.*, 1991) (see Fig. 1.6). The G1-region or "P-loop" (residues 10-17 in p21^{ras}, 15-22 in Ypt1p) is responsible for the binding of the alpha- and beta- phosphate groups of GTP/GDP. The G2-region or "effector region" (residues 32-40 in p21^{ras}, 37-45 in Ypt1p) is the part of the molecule which undergoes the most extensive changes upon GTP hydrolysis (Schlichting *et al.*, 1990) and is thought to bind effector proteins (Becker *et al.*, 1991; Sigal *et al.*, 1986). The conserved threonine residue in this region binds a Mg²⁺ ion, essential for GTP hydrolysis, that is coordinated to the oxygens of the β - and γ - phosphates of GTP.

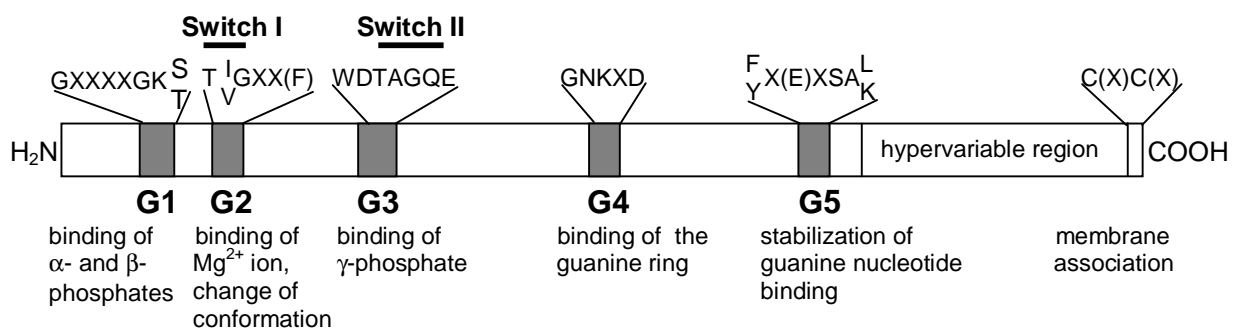


Fig. 1.6 Schematic representation of the conserved G1-G5 (gray boxes) regions in members of the Ras-superfamily and their involvement in the binding of guanine nucleotides. Conserved sequence motifs for Ypt/Rab GTPases are shown at the top.

The G3-region (residues 53-62 in p21^{ras}, 59-68 in Ypt1p) binds the gamma-phosphate of GTP, the glutamine in this region (Q61 in p21^{ras} and Q67 in Ypt1p) is critical for GTP hydrolysis. The G4-region (residues 112-119 in p21^{ras}, 117-124 in Ypt1p) binds the guanine ring of GTP/GDP whereas the G5-region (residues 140-146 in p21^{ras}, 147-153 in Ypt1p) is required for stabilization of the G4-interactions. The C-terminal cysteine-containing motif in Ypt/Rab proteins (Fig. 1.6) is post-translationally modified with a lipid moiety (geranylgeranyl), which is necessary for insertion into the membrane (Cox and Der, 1992; Peter *et al.*, 1992).

Depending on the nucleotide being bound (GDP or GTP), Ras and Ras-like GTPases adopt different conformations that allow them to interact with different effector proteins. The conformational changes, upon GTP hydrolysis, are mainly localized in two distinct regions of the molecule, named "switch I" and "switch II". Switch I (residues 30-38 in p21^{ras}) overlaps with the effector region G2 while switch II (residues 60-76 in p21^{ras}) encompasses the G3-region (Milburn *et al.*, 1990; Wittinghofer and Pai, 1991).

Ypt/Rab proteins are regulators of vesicular protein transport in both the biosynthetic/secretory and endocytic pathways. They are located on distinct cellular compartments, and participate in molecular events that underlie the targeting and/or docking/fusion of transport vesicles with their acceptor membrane (Schimmoller *et al.*, 1998; Zerial and McBride, 2001). Ypt/Rab GTPases are thought to act prior to SNAREs in vesicle docking. There are many hints indicating that they act directly or indirectly to promote SNARE-complex formation (Sogaard *et al.*, 1994; VanRheenen *et al.*, 1999). They might be involved in recruiting tethering and docking factors and/or in the removal of inhibitors of SNARE complex assembly (Allan *et al.*, 2000; Cao *et al.*, 1998; Lupashin and Waters, 1997; Pfeffer, 1999; Seals *et al.*, 2000). There are also studies that support an additional role of some Rab proteins in regulating the movement of vesicles and organelles along the cytoskeleton (Echard *et al.*, 1998; Nielsen *et al.*, 1999; Peranen *et al.*, 1996; Pruyne *et al.*, 1998; Schott *et al.*, 1999).

Rab protein activity seems to be modulated by different effectors. Several proteins were actually identified as Rab effectors and the list is rapidly growing, among them are: rabphilin3A, rabin3 and Rim for Rab3 (Brondyk *et al.*, 1995; Shirataki *et al.*, 1993; Wang *et al.*, 1997); rabaptin-5, rabaptin-5 β and EEA1 for Rab5 (Gournier *et al.*, 1998; Simonsen *et al.*, 1998; Stenmark *et al.*, 1995); Rab8ip for Rab8 (Ren *et al.*, 1996); p40 for Rab9 (Diaz *et al.*, 1997); Rab11BP for Rab11 (Zeng *et al.*, 1999).

Ypt/Rab GTPases and their involvement in membrane trafficking were first discovered in yeast (Gallwitz *et al.*, 1983; Salminen and Novick, 1987; Schmitt *et al.*, 1988; Segev *et al.*, 1988). In *S. cerevisiae*, there are 11 Ypt GTPases: Ypt1p, Ypt31p, Ypt32p, Sec4p, Ypt51p, Ypt52p, Ypt53p, Ypt6p, Ypt7p, Ypt10p and Ypt11p (Fig. 1.1 shows the localization and sites of action of Ypt proteins in the yeast cell; for review see Götte *et al.*, 2000; Lazar *et al.*, 1997). Only the functional loss of those involved in the biosynthetic pathways results in lethality, these proteins are: Ypt1p (Schmitt *et al.*, 1986), Ypt31p/Ypt32p (Benli *et al.*, 1996), and Sec4p (Salminen and Novick, 1987). In mammalian cells, over 30 Rab proteins are known (for review see Martinez and Goud, 1998; Novick and Zerial, 1997; Zerial and McBride, 2001).

Ypt/Rab proteins cycle between a GTP-bound (active) and GDP-bound (inactive) form, and between a membrane-attached and a soluble form (see Fig. 1.7). The soluble fraction of the proteins is complexed with a cytosolic protein, the GDP dissociation inhibitor GDI (Gdi1p/Sec19p in yeast; mammalian cells express several GDI isoforms) (Garrett *et al.*, 1994). GDI indiscriminately interacts with all types of Ypt/Rab proteins (Ullrich *et al.*, 1993). It is able to solubilize the inactive, GDP-bound Ypt protein from target membranes and thought to guide it to the correct donor membrane (Garrett *et al.*, 1994; Pfeffer *et al.*, 1995).

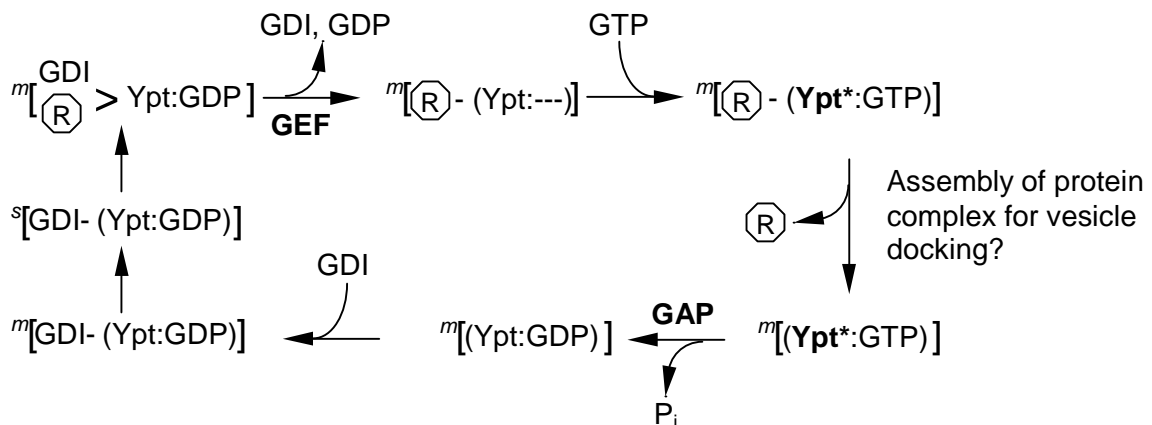


Fig. 1.7 Model of the Ypt GTPase cycle as described in [Götte, 2000 #38] (to be followed clockwise from middle left). The inactive GDP-bound form of the Ypt protein is kept in a soluble state by the GDP-dissociation inhibitor (GDI). After docking to a putative membrane receptor (R), GDI dissociates from transport GTPases. Upon membrane binding, a guanine nucleotide exchange factor (GEF) catalyzes GDP/GTP exchange. The activated Ypt GTPase (Ypt*) most likely acts in the assembly of a protein complex which facilitates membrane docking. A GTPase activating protein (GAP) accelerates the GTP hydrolysis and the GDP-bound form of the Ypt can be solubilized by GDI and used in a new cycle. *s* = soluble, *m* = membrane-bound.

The mechanism by which the interaction with the correct membrane is achieved is poorly understood, but it appears that the hypervariable C-terminus is involved in specific membrane interaction (Brennwald and Novick, 1993; Chavrier *et al.*, 1991). In addition hypothetical receptors could be important to mediate a correct membrane interaction (Dirac-Svejstrup *et al.*, 1997; Soldati *et al.*, 1995; Ullrich *et al.*, 1994). The recently described complex of Yip1p and Yif1p is a candidate membrane receptor for Ypt1 and Ypt31/Ypt32 GTPases on Golgi compartments (Matern *et al.*, 2000; Yang *et al.*, 1998).

After membrane association, GDI dissociates from transport GTPases. A GDI displacement factor (GDF), with specific action on endosomal Rab proteins, was isolated in mammalian cells (Dirac-Svejstrup *et al.*, 1997). Such a factor has not been identified in yeast yet. Once a GDP-bound GTPase associates with the membrane, GDP has to be exchanged for GTP, in order to activate the protein (Soldati *et al.*, 1994; Ullrich *et al.*, 1994). The exchange reaction is catalyzed by a guanine nucleotide exchange factor (GEF) (Cherfils and Chardin, 1999; Day *et al.*, 1998; Sprang and Coleman, 1998). Known Ypt/Rab specific GEFs are Rabex-5 for Rab5 (Horiuchi *et al.*, 1997), Vps9p for Ypt51p (Hama *et al.*, 1999) and Sec2p for Sec4p (Walch-Solimena *et al.*, 1997). GEF activity for Ypt1p and Ypt31/32 appears to reside in the 10-component TRAP complex (Jones *et al.*, 2000; Wang *et al.*, 2000b) Ypt6p-GEF activity in the heterodimeric Ric1/Rgp1 complex (Siniosoglou *et al.*, 2000) and Vps39p, a component of the multi-protein complex C-VPS/HOPS, stimulates the nucleotide exchange on Ypt7p (Wurmser *et al.*, 2000). Finally, when a GTPase has fulfilled its function, GTP is hydrolyzed. The Ypt's weak intrinsic GTPase activity ($<0.01 \text{ min}^{-1}$ at 30 °C; see Table 4.1) is accelerated many orders of magnitude by GTPase activating proteins (GAPs). In yeast, eight GAPs for Ypt/Rab proteins have been identified (see Section 1.4.4). In mammals, only two Rab-GAPs are currently known: GAPCenA that prefers Rab6 as substrate (Cuif *et al.*, 1999) and Rab3-GAP that is specific for Rab3 subfamily members (Burstein and Macara, 1992; Clabecq *et al.*, 2000; Fukui *et al.*, 1997). GAPCenA shares sequence similarity with yeast Ypt/Rab-GAPs, but the sequence of Rab3-GAP seems to be totally different.

1.4.3 Ypt1p

Ypt1p is a 23 kDa GTP-binding protein (Gallwitz *et al.*, 1983), and together with Sec4p (Salminen and Novick, 1987) is the founding member of the Ypt/Rab family of small GTPases. After its discovery in yeast, Ypt1p homologues were found in mouse

(Haubruck *et al.*, 1987) and rat (Rab1p, the acronym Rab stays for rat brain) (Touchot *et al.*, 1987) and subsequently in many others species. Ypt1p is predominantly localized to Golgi membranes (Segev *et al.*, 1988), the mammalian homolog Rab1p is found on ER membranes, pre-Golgi intermediates, and early compartments of the Golgi complex (Saraste *et al.*, 1995). Ypt1p acts in ER-to-Golgi transport and intra-Golgi transport (Jedd *et al.*, 1995). As shown by the use of mutants (Becker *et al.*, 1991; Schmitt *et al.*, 1988; Segev *et al.*, 1988) and of cell-free transport systems (Rexach and Schekman, 1991; Segev, 1991), the GTPase is required for docking of ER-derived vesicles to Golgi membranes. There are data indicating a role of Ypt1p in recruiting the docking factor Uso1p (Cao *et al.*, 1998; Sapperstein *et al.*, 1996). This was also observed in mammalian cells, where it has been demonstrated that Rab1p recruits p115 (the mammalian homolog of Uso1p) onto COPII vesicles where it interacts with a select set of SNARE proteins (Allan *et al.*, 2000). Other *in vitro* transport studies indicated that Ypt1p is functionally required on the Golgi acceptor membrane (Cao and Barlowe, 2000). Genetic interactions between *YPT1* and both *SEC34* and *SEC35* genes (encoding for the proteins of the tethering Sec34p/Sec35p complex) have been also documented (VanRheenen *et al.*, 1998; VanRheenen *et al.*, 1999).

Loss of Ypt1p function results in the accumulation of vesicles and ER membranes and finally in cell death. This phenotype can be suppressed by high expression of the SNAREs Sec22p and Bet1p (Dascher *et al.*, 1991). The suppressive effect is even stronger when there is co-overexpression of Bos1p with either Sec22p (Lian *et al.*, 1994) or Bet1p (Stone *et al.*, 1997), all SNAREs involved in ER-Golgi transport. Furthermore, the loss of Ypt1p can be efficiently suppressed by a dominant mutant allele of *SLY1* (*SLY1-20*) (Dascher *et al.*, 1991; Ossig *et al.*, 1991) that encodes a member of the Sec1p protein family (see Section 1.4). These and other experiments (Lupashin and Waters, 1997; Sogaard *et al.*, 1994) showed that Ypt1p is required to facilitate SNAREs complex formation.

To study the function of Ypt1p, several mutants created by site-directed mutagenesis have been used; of special interest are single amino acid substitutions within the conserved domains G4 (N121I) and G3 (Q67L). The N121I substitution turned out to be a dominant negative inhibitor of transport (Schmitt *et al.*, 1988; Schmitt *et al.*, 1986) most likely because of its tight interaction with a still unknown effector. The Q67L mutation, in analogy to the equivalent substitution in Ras, believed to lock Ypt1p in the active GTP-bound form, apparently does not induce any

easily observable phenotype (Richardson *et al.*, 1998). From this, it was concluded that GTP hydrolysis is not important for the GTPases function in transport, but this view will be challenged by the data presented in this Ph.D. thesis.

1.4.4 The Gyp protein family

The slow intrinsic GTPase activity of Ypt/Rab GTPases ($<0.01 \text{ min}^{-1}$) has to be accelerated by GAPs in order to allow the termination of the GTPases function and the recycling of the regulators. Ypt/Rab-GAP proteins were first identified in yeast by high expression cloning and named Gyp (**G**AP for **Y**pt) (Strom *et al.*, 1993; Vollmer and Gallwitz, 1995). Gyp proteins form a family with several structurally related members. This was predicted by a sophisticated computer search (Neuwald, 1997; Neuwald *et al.*, 1997), and subsequently proven by biochemical analysis (Albert and Gallwitz, 1999; Albert and Gallwitz, 2000; Albert *et al.*, 1999; Cuif *et al.*, 1999). To date, there are eight yeast proteins proven to be Ypt/Rab-GAPs (Gyp1p-Gyp8p) (see Table 1.3). In addition, there are other yeast proteins (the products of *YMRO55c/BUB2*, *YMR192w* and *YGL036w* reading frames) that share sequence similarity with Gyp family members.

Table 1.3 Yeast Ypt/Rab-GAPs.

GAP	ORF	Length	MW (kDa)	pI	Substrate (main substrates are underlined)	References
Gyp1p	<i>YOR070c</i>	637	73.3	6.71	<u>Sec4p</u> , <u>Ypt51p</u> , Ypt1p, Ypt7p.	(Albert <i>et al.</i> , 1999; Du <i>et al.</i> , 1998; Rak <i>et al.</i> , 2000).
Gyp2p (Mic1/Mdr1)	<i>YGR100w</i>	950	109.23	5.25	<u>Ypt6p</u> , <u>Sec4p</u> .	(Albert and Gallwitz, 1999).
Gyp3p (Msb3)	<i>YNL293w</i>	633	73	7.3	<u>Sec4p</u> , <u>Ypt6p</u> , <u>Ypt51p</u> , Ypt31p	(Albert and Gallwitz, 1999).
Gyp4p (Msb4)	<i>YOL112w</i>	492	57.1	5.39	<u>Ypt6p</u> , <u>Ypt7p</u> , Sec4p.	(Albert and Gallwitz, 2000).
Gyp5p	<i>YPL249c</i>	894	101.8	4.73	<u>Ypt1p</u> , Sec4p.	This work.
Gyp6p	<i>YJL044c</i>	458	53.8	5.84	<u>Ypt6p</u> , Ypt7p.	(Strom <i>et al.</i> , 1993; Will and Gallwitz, 2001)
Gyp7p	<i>YDL234c</i>	746	87.3	5.02	<u>Ypt7p</u> , Ypt6p, Ypt31p, Ypt32p.	(Albert <i>et al.</i> , 1999; Vollmer <i>et al.</i> , 1999).
Gyp8p	<i>YFL027c</i>	497	57.7	8.81	<u>Ypt6p</u> , <u>Ypt1p</u> , Sec4p.	S. Albert unpublished data.

Gyp proteins share six conserved sequence motifs (A, B, C, D, E, F) (Neuwald, 1997) (Fig. 4.2). These sequence motifs (present also in several proteins in different eukaryotic organisms) are localized within the catalytic domain of Gyp proteins and will be referred to as the "GYP domain". However, the GYP domain does not represent the complete catalytic domain, additional sequences downstream of the conserved motifs are required for GAP activity. A detailed mutational analysis of the catalytically active regions in Gyp1p and Gyp7p has revealed a conserved arginine residue in motif B which is critical for the catalytic activity (Albert *et al.*, 1999). It was therefore postulated that Ypt/Rab-GAPs exhibit an "arginine finger" mechanism of GTPase accelerating activity similar to that previously described for Ras- and Rho-GAPs (Ahmadian *et al.*, 1997; Rittinger *et al.*, 1997a; Rittinger *et al.*, 1997b; Scheffzek *et al.*, 1997; Scheffzek *et al.*, 1998). According to the "arginine finger hypothesis" GAP supplies an arginine residue into the active site of the GTPase to favor GTP hydrolysis and thereby to stabilize the transition state of the reaction (see Fig. 1.8).

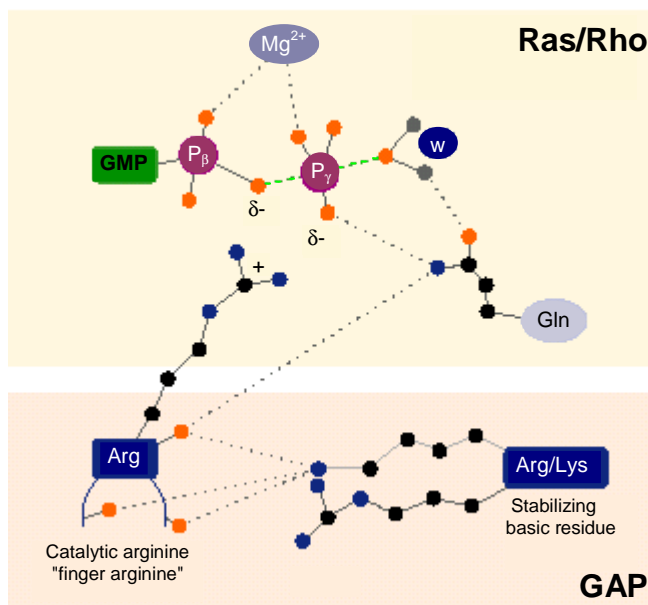


Fig. 1.8 Scheme of the Ras/Rho GAP complex from (Scheffzek *et al.*, 1998). The transition state is shown as having a pentacoordinate γ -phosphate group due to nucleophilic attack of a water molecule (w). The catalytic arginine residue of GAP "arginine finger", together with a "finger loop", crosses the "gap" between the proteins in order to neutralize developing charges during the transition state of the reaction and stabilize the critical catalytic glutamine residue in Ras/Rho proteins (Q61 in Ras and Q63 in Rho). A

"secondary", positively charged residue, (Arg in Ras-GAP and Lys in Rho-GAP), stabilizes the "finger loop". GMP = guanosine monophosphate.

The crystal structure of the Gyp1p GAP-domain, recently solved (Fig. 1.9) (Rak *et al.*, 2000), revealed that the protein is purely α -helical (16 α -helices) and V-shaped. In accordance with the biochemical data, the critical arginine (R343) is positioned in the presumed GTPase-binding cleft where it could come into close contact with the bound GTP. It is interesting to note that while Ras- Rho- and

Ypt/Rab-GTPases are significantly related in primary and tertiary structure, the corresponding GTPase-activating proteins are not at all related in primary structure and display distinct folds, however, their overall structures are nearly exclusively α -helical and their catalytic activities are based on same mechanistic principle (Barrett *et al.*, 1997; Rak *et al.*, 2000; Scheffzek *et al.*, 1996).

None of the eight yeast Ypt/Rab-GAPs studied so far is essential for cell viability or, after gene deletion, results in a observable phenotype. This might be due to overlapping substrate specificity as all Gyp proteins accept more than one GTPase as substrate (Table 1.3).

One of the aims of this work was the detailed characterization of a member of the family of Ypt/Rab-GAPs, Gyp5p, the preferred substrate of which turned out to be Ypt1p. In addition, an attempt was made to explain the biological relevance of its GAP activity within the living cell.

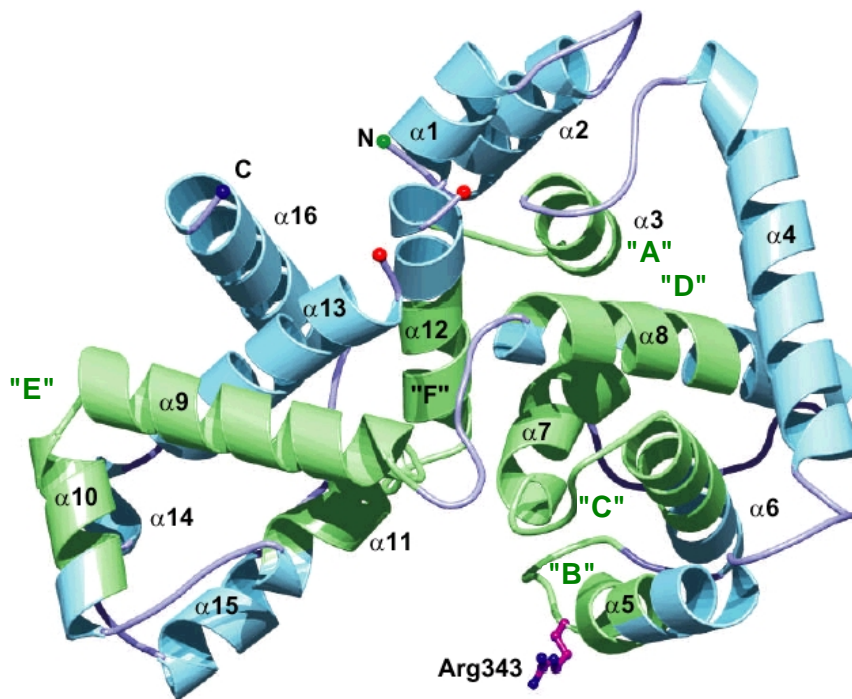


Fig. 1.9 The three-dimensional structure of Ypt-GAP of Gyp1p (from A. Rak *et al.*, 2000). The ribbon diagram displays the secondary structure elements and the catalytic active arginine (Arg 343) in a ball-and-stick representation. Regions of the conserved motifs A-F are highlighted in green.

2 MATERIALS

Bacterial and yeast strains, mammalian cell lines, plasmids, oligonucleotides and antibodies are listed and described in Appendix (Chapter 7).

2.1 Growth media

2.1.1 Media components

Bacto-agar, bacto-peptone 140, bacto-yeast-extract, and bacto-yeast nitrogen base w/o amino acids from Difco (Detroit, USA). D-glucose, D-raffinose, D-galactose, D-fructose, ammonium sulfate, potassium acetate and amino acids from SERVA (Heidelberg, Germany). Geneticin G418 Sulfate from Calbiochem (La Jolla, CA, USA), Ampicillin Na-salt, kanamycin sulfate, chloramphenicol and tetracycline from SERVA, Penicillin-Streptomycin from Gibco BRL. (Karlsruhe, Germany). 3-Amino-1,2,4-Triazole (3-AT) and 5-Fluoroorotic acid (5-FOA) from Sigma-Aldrich (Deisenhofen, Germany). Dulbecco's Mod. Eagle Medium and Sodium Bicarbonate from Gibco BRL. (Karlsruhe, Germany). Fetal Bovine Serum F-7524 from Sigma (Deisenhofen, Germany)

2.1.2 Bacterial media

All media were autoclaved for 20 min at 120°C and stored at 4°C. Solid media were obtained adding bacto-agar at the final concentration of 1.5 % (w/v).

<u>LB (Luria Bertani)</u>	5 g/l	Yeast extract	
	10 g/l	Bacto-peptone	
	5 g/l	NaCl	
	5 ml/l	NaOH 1N	
<u>SOC</u>	20 g/l	Bacto-peptone	
	5 g/l	Yeast extract	
	0.5 g/l	NaCl	
	prior to use add:	10 ml/l	1M MgCl ₂ (filter sterilized)
		10 ml/l	1M MgSO ₄ (filter sterilized)
		1 ml/l	2M Glucose (filter sterilized)

Additives

0.1-1 mM IPTG

Antibiotics:	100 µg/ml Ampicillin
	50 µg/ml Kanamycin
	30 µg/ml Chloramphenicol
	15 µg/ml Tetracycline

2.1.3 Yeast media

All media were autoclaved for 20 min at 120°C and stored at 4°C. Solid media were obtained adding bacto-agar at the final concentration of 2 % (w/v).

<u>YEPG (YEPGal)</u>	10 g/l	Yeast extract
	20 g/l	Peptone 140
	20 g/l	D-glucose (D-galactose)
	20 mg/l	Uracil
	20 mg/l	Adenine sulphate
<u>YEPG 0.1%</u>	10 g/l	Yeast extract
	20 g/l	Peptone 140
	1 g/l	D-glucose
	20 mg/l	Uracil
	20 mg/l	Adenine sulphate
<u>PM-glucose</u>	1.7 g/l	Yeast nitrogen base w/o amino acids
<u>(PM-galactose)</u>	5 g/l	Peptone 140
<u>(PM-raffinose)</u>	5 g/l	Ammonium sulfate
	20 g/l	D-glucose (D-galactose) (D-raffinose)
<u>SD</u>	1.7 g/l	Yeast nitrogen base w/o amino acids
	5 g/l	Ammonium sulfate
	20 g/l	D-glucose
<u>SMM</u>	1 g/l	KH ₂ PO ₄
	1 g/l	NH ₄ Cl
	0.2 g/l	CaCl ₂
	0.6 g/l	MgCl ₂
	0.5 g/l	NaCl
	3 g/l	Yeast extract
	20 g/l	Glucose
<u>Additives</u>		
Amino acids:	20 mg/l	Uracil
	20 mg/l	Adenine sulphate
	20 mg/l	L-tryptophan
	20 mg/l	L-histidine
	30 mg/l	L-leucine
	30 mg/l	L-Lysine/HCl
Antibiotics:	200 mg/l	geneticin G418

2.1.4 Mammalian cell media

<u>DME 10% FCS (10 l)</u>	1 Package 37 g 200 ml 1 l	Dulbecco's Mod. Eagle Medium Sodium Bicarbonate Penicillin-Streptomycin (10000 IU/ml) Foetal Bovine Serum
---------------------------	------------------------------------	--

2.2 Frequently used buffers and solutions

<u>TAE 50X</u>	242 g/l 57.1 ml/l 18.612 g/l	Tris-base Glacial acetic acid EDTA
<u>DNA loading buffer 10X</u>	30% (w/v) 0.25% (w/v) 0.25% (w/v) 0.5 M	Ficoll Xylene Cyanol FF Bromophenol Blue EDTA, pH 8.0
<u>30% Acrylamide-stock sol.</u>	29.2%(w/v) 0.8% (w/v)	Acrylamide Bisacrylamide
<u>APS</u>	10% (w/v)	
<u>Laemmli loading buf. 2X</u>	0.1M 2% (w/v) 2% (v/v) 20% (v/v) 0.002%(w/v)	Tris-HCl, pH 6.8 SDS β-Mercaptoethanol Glycerol Bromophenol Blue
<u>SDS electrophoresis buf.</u>	0.19 M 25 mM 0.1% (w/v)	Glycine Tris-base SDS
<u>Coomassie fixing sol.</u>	25% (v/v) 10% (v/v)	Isopropanol Glacial acetic acid
<u>Coomassie staining sol.</u>	10% (v/v) 60 mg/l	Glacial acetic acid Coomassie brilliant blue R250
<u>Western blot transfer buffer</u>	20 mM 150 mM 20% (v/v)	Tris-base Glycine Methanol
<u>Ponceau S solution</u>	2.5 g/l 15% (v/v) 40% (v/v)	Ponceau S Glacial acetic acid Methanol

<u>Western blot washing buffer A</u>	10 mM 0.9% (w/v) 0.05% (v/v)	Tris-HCl, pH 7.4 NaCl Tween 20
<u>Western blot washing buffer B</u>	0.2% (w/v) 0.9% (w/v) 0.5% (v/v) 0.5% (w/v)	SDS NaCl Triton X-100 BSA
<u>HPLC buffer</u>	10 mM 100 mM 0.2 mM 2-4% (v/v)	Tetrabutylammonium bromide K ₂ HPO ₄ /KH ₂ PO ₄ , pH 6.5 NaN ₃ Acetonitrile
<u>GAP reaction buffer</u>	50 mM 5 mM 1 mM	Tris-HCl, pH 8.0 MgCl ₂ DTT
<u>PBS</u>	137 mM 2.7 mM 4.3 mM 1.4 mM pH 7.3	NaCl KCl Na ₂ HPO ₄ 7H ₂ O KH ₂ PO ₄
<u>Phenol</u>	Phenol saturated with TE 0.1% (w/v)	Hydroxyquinoline
<u>SSC 20X</u>	3 M 0.3 M	NaCl Na-citrate
<u>TE</u>	10 mM 1 mM	Tris-HCl, pH 7.4-8.0 EDTA, pH 8.0
<u>TBS</u>	100 mM 0.9%	Tris-HCl, pH 7.5 NaCl
<u>Buffer 88</u>	20 mM 0.25 M 0.15 M 5 mM	HEPES pH 7.0 Sorbitol KOAc MgOAc

2.3 Chemicals

All chemicals used were of analytical grade and were purchased from Boehringer (Mannheim, Germany), Merck (Darmstadt, Germany), Sigma Deisenhofen, Germany) or Serva (Heidelberg, Germany) unless otherwise stated. Tran³⁵S-label from ICN (Meckenheim, Germany) and Amplify fluorographic reagent from Amersham (Braunschweig, Germany). Glutathione sepharose 4B, protein A sepharose fast flow

and protein G sepharose fast flow were from Pharmacia (Freiburg, Germany). Ni-NTA agarose from QIAGEN (Hilden, Germany). Bradford protein assay reagent and Chelex 100 resin from Bio-Rad (Munich, Germany). Protease inhibitors cocktail tablets and PefablocSC (4-2-Aminoethyl-benzenesulfonyl fluoride) from Roche (Mannheim, Germany). Prestained protein ladder BenchMark from Gibco Brl (Karlsruhe, Germany), Rainbow protein marker from Amersham (Braunschweig, Germany).

2.4 Enzymes

Restriction endonucleases were from Boehringer (Mannheim, Germany), New England Biolabs (Frankfurt, Germany), and Promega (Mannheim, Germany). T4-polymerase, T4-DNA ligase and RNase were from Boehringer (Mannheim, Germany). Taq DNA polymerase was from Perkin Elmer (New Jersey, USA), Deep Vent DNA polymerase from *Thermococcus litoralis* was from New England Biolabs (Frankfurt, Germany), Pfu DNA polymerase from Stratagene (Heidelberg, Germany). Zymolyase 100T from *Arthrobacter luteus* was from Seikagaku Corp. (Tokyo, Japan), Lyticase partially purified from *Arthrobacter luteus* was from Sigma (Deisenhofen, Germany), β -glucuronidase/arylsulfatase from *Helix pomatia* was from Boehringer (Mannheim, Germany). Thrombin was from Sigma (Deisenhofen, Germany).

2.5 Reaction systems, Kits

Plasmid DNA extraction from *E. coli*, DNA extraction from agarose gels and purification of PCR products were performed with a QIAGEN Spin Miniprep or Midiprep kit, a QIAquick Gel Extraction kit, a QIAquick PCR purification kit respectively, from QIAGEN (Hilden, Germany).

ECL western blotting detection reagents, ECL direct nucleic acid labeling, 3'-oligo-labeling and detection system, and Lumi-LightPLUS western blotting substrate from Amersham-Buchler (Braunschweig, Germany).

QIAexpressionist (His-tag) from QIAGEN, GST-fusion system from Pharmacia (Freiburg, Germany) and MBP-fusion system from New England Biolabs (Frankfurt, Germany).

For Sequencing the Thermo Sequenase dye terminator cycle sequencing kit from Amersham was used.

2.6 Disposable supplies

Autoradiography films X-Omat from Kodak-Eastman (Rochester, New York, USA). Nitrocellulose membrane filters BA 85 and Nylon membrane filters Nytran-N from Schleicher and Schuell (Dassel, Germany). Whatman 541 Filter and Whatman 3MM paper from Whatman (Maidstone, UK). Filtropur BT50 0.2 μ m 500ml from Sarstedt (Nümbrecht, Germany), non pyrogenetic 0.22 μ m filter Millex-GS from Millipore (Molsheim, France). Centricon concentrators from Amicon (Beverly, USA), and membra-spin PES columns (membraPure, Bodenheim, Germany). Reaction vials 0.5 ml, 1.5 ml and 2 ml from Eppendorf (Hamburg, Germany). Polypropylene Falcon vials 15 ml and 50 ml from Becton –Dickinson (Heidelberg, Germany). Petri dishes from Nunc (Wiesbaden, Germany). Electroporation cuvettes from Invitrogen (Leek, The Netherlands). All other materials including glassware were purchased from Schütt (Göttingen, Germany).

2.7 Laboratory gadgets

Centrifuges: Eppendorf bench centrifuge 5415 (Eppendorf, Hamburg, Germany), Hereaus Laborfuge GL, Sorvall RC-5B with rotors HS-4, HB-4, GSA, SS-34 and SA600 (DuPont Instruments, Bad Homburg, Germany), Ultracentrifuges TL-100, L7, L8-M with rotors TLA100.3 45Ti 70Ti SW40Ti and SW60 Ti (Beckman, Munich, Germany). Electroporation chamber BioRad Gene-Pulser with pulse-controller from BioRad Laboratories (Munich, Germany). Gel dryer BioRad Slab Dryer 443 and 448 from BioRad Laboratories (Munich, Germany). Homogenizer Gaulin Micron Lab 40 “French Press” from APV Gaulin (Lübeck, Germany). HPLC (High performance liquid chromatography) “System GOLD” from Beckman (Munich, Germany). Incubators: Gyrotory Shaker and controlled environment incubators from New Brunswick (Edison, NJ, USA). Lumi-imager from Boehringer (Mannheim, Germany). Micromanipulator from Singer Instruments (Watchet, GB). Spectrophotometer Uvikon 860 from Kontron instruments (Eching, Germany). Microscopes: Zeiss Photomicroscope Axiophot (Zeiss, Oberkochen, Germany), Leitz Laborlux (Leitz, Bad Bensheim, Germany), Confocal Leica TCS NT laser scanning microscope. PCR thermocycler devices PTC-100 from MJ Research Inc. (MA, USA), and RoboCycler gradient 40 from Stratagene (Heidelberg, Germany). Radiography developing machine Gevamatik 60 from AGFA Gevaert (Hannover, Germany). DNA Sequencer 373A from Applied Biosystems (Weiterstadt, Germany). Transilluminators 302 and 366nm from Bachofer (Reutlingen, Germany). Sonicator: sonifier-B15 and 250 from Branson ultrasonics (Schwäbisch Gmünd, Germany)

3 METHODS

Molecular biological and biochemical methods used in this work are in more detail described in standard manuals like: “Molecular Cloning” (Sambrook *et al.*, 1989), “Current Protocols in Molecular Biology” (Ausubel *et al.*, 1997), “Current Protocols in Protein Science (Coligan *et al.*, 1997), Current protocols in cell biology (Bonifacino *et al.*, 1999).

3.1 Bacteria and yeast culture techniques

Bacterial strains were grown in the described media (see 2.1.2) at 37°C or at lower temperatures. For short-time storage, bacteria plates were sealed with Parafilm and stored at 4°C. For long time storage, 0.9 ml of overnight cultures were mixed with an equal volume of 50% sterile glycerol (50% glycerol / 50% LB medium), rapidly frozen in liquid nitrogen and then kept at –80°C.

Yeast strains were grown in the described media (see 2.1.3), usually at 30°C, or, when required, at different temperatures ranging from 15°C to 37°C. For short time storage, streaked yeast plates were sealed with Parafilm and stored at 4°C. For long time storage, 0.9 ml of overnight cultures were mixed with equal volume of 60% sterile glycerol (60% glycerol 50% SD medium), rapidly frozen in liquid nitrogen and then stored at –80 °C.

3.2 DNA preparation, manipulation, amplification and analysis

3.2.1 Bacterial plasmid DNA preparation

Small-, medium- and large-scale plasmid extractions were performed using Plasmid mini-, midi- and maxi-prep from QIAGEN according to the manufacturer's recommendations.

3.2.2 Yeast genomic and plasmid DNA preparation

10 ml of overnight cultures were centrifuged to collect the cells. The cell pellets were washed with distilled water and resuspended in 200 μ l of “braking buffer”. To this mixture 200 μ l of phenol/chloroform/isoamyl alcohol (25:24:1) and 0.3 g of acid-washed glass beads were added. Cells were broken by vortexing for 5 min. After vortexing, 200 μ l of TE buffer were added to each tube and subsequently the tubes were centrifuged for 10 min at 14.000 rpm. The aqueous phase was collected in new test tubes and 2-5 μ l used directly for transformation of *E. coli* when plasmid DNA was isolated. In the case of genomic DNA isolation, the DNA and the RNA present in the aqueous phase was precipitated with 1 ml 96% ethanol. The DNA/RNA pellet, obtained after 5 min centrifugation at 14.000 rpm, was dissolved in 400 μ l of TE buffer containing 0.1 mg/ml RNase A and incubated for 5 min at 37 °C. Finally, the genomic DNA was precipitated adding 10 μ l of 4 M Ammonium acetate and 1 ml of 96% Ethanol. The DNA pellet was dissolved in 50-70 μ l 10 mM Tris-HCl pH 8.0.

<u>Breaking buffer</u>	2%	Triton X-100
	1%	SDS
	100 mM	NaCl
	10 mM	Tris-HCl pH 8.0
	1 mM	EDTA pH 8.0

3.2.3 Spectrophotometric estimation of DNA purity and quantitation

As described in “Molecular Cloning” (Sambrook *et al.*, 1989), it is possible to quantify nucleic acids and to evaluate their purity by spectrophotometric analysis. DNA and RNA absorb light of 260 nm wavelength, proteins (aromatic amino acids) absorb light of 260 nm wavelength too, but absorption is much stronger at 280 nm.

The ratio A_{260}/A_{280} gives an estimation of DNA purity. For pure DNA, A_{260}/A_{280} ratio is about 1.8.

Spectrophotometric conversion: $1A_{260}$ of double-stranded DNA = 50 μ g/ml

$1A_{260}$ of single-stranded DNA = 33 μ g/ml

$1A_{260}$ of single-stranded RNA = 40 μ g/ml

3.2.4 Enzymatic treatment of DNA

Restriction enzyme digestion was carried out according to standard procedures (Sambrook *et al.*, 1989). Depending on the enzymes used and their cutting sites,

sticky-ended (5'- or 3'-protruding single strand DNA) or blunt-ended DNA fragments can be generated. Restricted DNA fragments were purified either by gel electrophoresis and extraction using a QIAGEN gel extraction kit, or by using a QIAGEN PCR and nucleotides purification kit.

DNA fragments with compatible cohesive ends can be ligated using T4 DNA ligase which catalyses the ATP-dependent ligation of blunt or complementary sticky ends of DNA. Sticky-end ligations were carried out at room temperature for 2-4 h using a 1:1 - 1:5 vector:insert molar ratio. Blunt-ended ligations were carried out at 14°C overnight, with a 1:5 molar ratio of vector:insert. A typical 20 µl reaction mixture contain: 50-100 ng insert DNA, 10-50 ng vector DNA, 1x ligase buffer, 0.5-1 mM ATP, 1U T4 DNA ligase, water.

3.2.5 *E. coli* transformation

E. coli cells were transformed either by heat shock or by electroporation. The two methods differ in the efficiency, in the first the efficiency can be 10^6 - 10^8 transformants per µg of DNA, in the second 10^7 - 10^9 transformants per µg of DNA.

a) Preparation of competent cells and transformation by heat shock

To render the cells competent, the method of Hanahan (Hanahan *et al.*, 1991) was employed. Upon reaching an OD₆₀₀ of 0.5-0.9, a 50 ml culture was harvested by centrifugation (10 min at 4.000g, 4°C) . Cells were resuspended in 20 ml of cold RF1 buffer and left on ice for 15 min, then the cells were centrifuged again and resuspended in 4 ml RF2 buffer. 70 µl aliquots were taken, rapidly frozen in liquid nitrogen and stored at -80°C.

<u>RF1</u>	100 mM	RbCl
	50 mM	MnCl ₂
	30 mM	KOAc
	10 mM	CaCl ₂
	15% (v/v)	Glycerol

(pH adjusted to 5.8 with 0.2 M acetic acid; sterilized by filtration through 0.2µm filters)

<u>RF2</u>	10 mM	MOPS
	10 mM	RbCl
	75 mM	CaCl ₂
	15% (v/v)	Glycerol

(pH adjusted to 6.8 with NaOH; sterilized by filtration through 0.2µm filters)

Transformation: 1-10 ng of plasmid DNA or 10 μ l ligation mixture were added to 70 μ l competent cells (thawed on ice). Cells were incubated for 40 min on ice, then heat-shocked for 90 sec at 42°C. Thereafter, 1 ml SOC medium was added and the samples were incubated with agitation at 37°C for 45 min. Finally, cells were plated onto LB-agar plates containing the appropriate antibiotic and incubated overnight at 37°C.

b) Preparation of competent cells and transformation by electroporation

10 ml of overnight culture of *E. coli* were used to inoculate 1l of fresh LB medium. The culture was grown at 37 with agitation until an OD₆₀₀ of 0.5-0.9 was achieved. Cells were harvested by centrifugation (10 min at 4.000g, 4°C). The cell pellet was washed 2 times with 1 volume sterile cold water and 1 time with 20 ml sterile cold 10% glycerol. Finally, cells were resuspended in 2 ml sterile cold 10% glycerol, dispensed in 40 μ l aliquots and frozen in liquid nitrogen. The frozen cells were stored at -80°C.

Transformation: 40 μ l electro-competent cells were thawed on ice and transferred to a chilled 0.2 cm electroporation cuvette. 1-2 μ l of ligation mixture was added and the sample was kept on ice for 1 min. Thereafter, the cuvette was transferred to a Gene Pulser electroporation chamber and pulsed once with 25 μ F, 2500 V, 200 Ohms. 1 ml SOC medium was added immediately after the pulse and the sample transferred to a 2 ml Eppendorf tube and incubated with agitation at 37°C for 45 min. Cells were then plated onto LB-agar plates containing the appropriate antibiotic and incubated overnight at 37°C.

3.2.6 PCR amplification of DNA

The polymerase chain reaction (PCR) is a very useful technique that allows to produce high yields of specific DNA target sequences (Saiki *et al.*, 1988). PCR was used in this work:

- to isolate specific genes from yeast genomic DNA.
- to create appropriate restriction sites at the termini of DNA fragments to be cloned into different vectors.
- to check whether a specific DNA fragment was correctly cloned into a vector or correctly inserted into the genome.
- to check whether a gene was correctly deleted.
- to amplify specific “cassettes” for gene disruption or gene tagging (see 3.3.2 and 3.3.3).
- for *in vitro* mutagenesis (see 3.2.7)

Most PCR protocols are performed at the 25 μ l -100 μ l scale, larger volumes are not recommended.

A typical 50 μ l reaction mixture consist of:

- 1-10 ng plasmid DNA or 50-100 ng genomic DNA
- 20 pmol forward primer
- 20 pmol reverse primer
- 1x nucleotide mix (200 μ M of each dNTP)
- 1x PCR buffer with MgCl₂ (10 mM Tris-HCl pH8.3, 50 mM KCl, 1.5 mM MgCl₂)
- 1 U DNA polymerase (Taq or a mixture Taq/Deep-Vent 5/1)
- dH₂O

The reaction is incubated in a thermocycler device where the temperature can be changed rapidly. Usually there is a preheating step of 3 min at 93°C during which the template DNA is denatured. This is followed by 30-32 cycles of:

- denaturing 30-60 sec at 92°C
- annealing 30-60 sec at 45-60°C
- elongation 30-120 sec at 72°C

the last cycle is followed by an extra elongation step of 5-10 min at 72°C.

The annealing temperature is dependent on the primers composition, on their T_m (melting temperature) and on their homology with the template. The primers may have modifications such as extensions at their 5' ends or point mutations.

PCR can be done directly from bacteria colonies. Bacteria were taken with a toothpick from agar plates, dissolved in 60 μ l PCR buffer 1x and boiled at 95°C for 5 min, after that 5 μ l of the mixture were used as template for the PCR reaction.

PCR products were purified by using a QIAGEN PCR purification kit according to the manufacturer's instructions.

3.2.7 *In vitro* mutagenesis

The Quick Change site-directed mutagenesis kit from STRATAGENE was used to create point mutations in plasmid DNA containing cloned genes. The basic procedure starts with a supercoiled, dsDNA vector, with an insert of interest and two long oligonucleotide primers (30-45 bases) containing the desired mutation. The oligonucleotide primers, each complementary to opposite strands of the vector, are extended during temperature cycling by Pfu-Turbo DNA polymerase. Incorporation of the oligonucleotide primers generates a mutated plasmid. After temperature cycling, the product is treated with DpnI. The DpnI is used to digest the methylated non mutated

parental DNA template since DpnI is specific for methylated and hemimethylated DNA. The nicked vector DNA incorporating the desired mutations is then transformed into *E. coli*.

3.2.8 DNA-Sequencing

DNA fragments were sequenced using the thermo Sequenase dye terminator cycle sequencing kit from Amersham on an ABI373A sequencing device according to the manufacturer's instructions. Automated sequencing was performed by H. P. Geithe in this department.

3.2.9 DNA-DNA hybridization (Southern blotting)

2-4 μg of genomic DNA (see 3.2.2) were digested overnight with the appropriate restriction enzyme, run on an agarose gel, and then transferred to a nitrocellulose membrane as described in (Sambrook *et al.*, 1989, Southern, 1992 #26; Southern, 1975). Specific DNA fragments obtained by PCR or by plasmid digestion or synthetic oligonucleotides, were used as probe. The probes were labeled with horseradish peroxidase (HRP) using the ECL direct nucleic acid labeling system or the 3'-oligo-labeling and detection system (Amersham) according to the manufacturer's instructions.

3.3 Yeast genetics and yeast cell biology methods

3.3.1 *S. cerevisiae* transformation

Transformation of yeast was carried out using a modified lithium acetate method (Schiestl and Gietz, 1989). A 50 ml yeast culture was harvested by centrifugation (4 min at 500g, RT) upon reaching an OD_{600} of 0.8-1.0. The cells were washed once with 20 ml sterile distilled water and once with 2 ml filter-sterilized LiOAc/TE/Sorbitol (100 mM LiOAc, 10 mM Tris-HCl pH 7.5, 1 mM EDTA pH 7.5, 1M Sorbitol), transferred to 2 ml tubes, harvested by centrifugation, resuspended in 0.5 ml LiOAc/TE/Sorbitol, and incubated at 30°C for 10 min. 50 μl cells mixture were transferred to a new tube and to them were added: 300 μl of filter-sterilized 40% PEG-3350 (40% w/v PEG-3350, 100 mM LiOAc, 10 mM Tris-HCl, 1 mM EDTA), 25 μl 2 mg/ml denatured salmon sperm DNA (this can be omitted, but the efficiency of transformation will be lower) and 1-5 μg PCR product or 0.1-1 μg plasmid DNA. The samples were mixed by vortexing and incubated at 30°C for 30 min, then heat-

shocked at 42°C for 20 min. Finally, cells were collected by centrifugation, washed with 1 ml YEPG medium, resuspended in 2-3 ml YEPG medium (no vortexing) and incubated for 2-3 h at 30°C (this incubation time can be avoided when cells are not selected on geneticin). After that cells were plated onto YEPG plates or SD plates containing the appropriate selecting additives and incubated at 30 °C (or at the required temperature) until colonies appeared.

3.3.2 Yeast PCR-mediated gene knock-out

A PCR-based gene deletion method as described in (Güldener *et al.*, 1996) was used. The method relies on the amplification by PCR (see also 3.3.3) of the selectable module *loxP-kanMX-loxP* from the pUG6 vector, using two primers with tail sequences homologous to the yeast genomic sequences flanking the ORF to be deleted (the PCR product is ~1600 bp long), followed by transformation and homologous recombination into the yeast genome (see Fig. 3.1). The minimum amount of homology sequence required for homologous integration in *S. cerevisiae*'s genome is 30 bp on each side of a genomic locus (Manivasakam *et al.*, 1995). Transformants were selected on YEPG plates containing 200 µg/ml G418). The *loxP* sites flanking *kanMX* allow the excision of the cassette (1507 bp) upon the expression of the Cre-recombinase (Güldener *et al.*, 1996; Sauer, 1987) (see Fig. 3.1.B). In this way it is possible to delete different genes using the same system repeatedly. For Cre-mediated marker rescue the cells were transformed with the pSH47 plasmid containing the *cre* gene under the control of the yeast *GAL1* promoter. Expression of the Cre-recombinase was induced by incubating the transformants for 2-4 hours at 30°C in YEPGal medium (1 colony in 2 ml medium). The loss of the *kan^r* marker was verified by replica plating onto YEPG/G418 selective medium. pSH47 plasmid can be removed by streaking the cells on plates containing 5-fluoroorotic acid.

With this method the strains ADY20-ADY28 and ADY40-ADY48 were created, in which the genes *GYP1*, *GYP5*, *GYP7* and *GYP8* were deleted either alone or in combinations (see Appendix, Table 7.2). The primers used are listed in Table 7.7. The correct deletion of these genes was verified by PCR (using primers that anneal with sequences outside the deleted genes in combination with primers that anneal with sequences inside the *kanMX* cassette) and by Southern blotting.

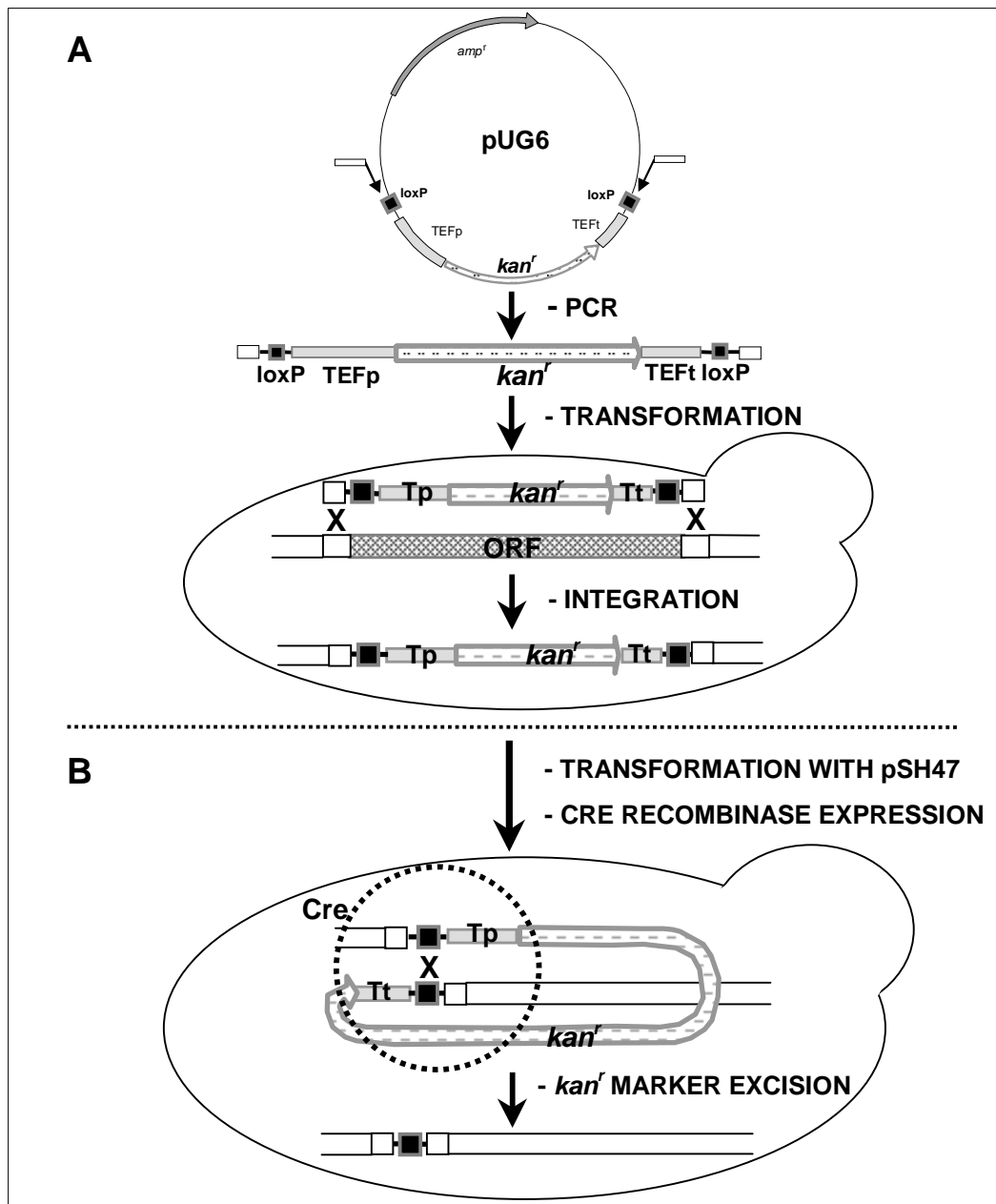


Fig. 3.1 Scheme of PCR-based gene deletion. **(A)** PCR amplification of the *loxP-kanMX-loxP* cassette from pUG6 using primers with tail sequences homologous to yeast genomic sequences flanking the ORF to be deleted, and successive integration into that locus. **(B)** Excision of the *kan^r* selection marker (1507bp DNA fragment) induced by the Cre recombinase; one *loxP* sequence remains in the genome.

3.3.3 Yeast PCR mediated epitope tagging

An epitope (also called antigenic determinant) is any structure or sequence that is recognized by an antibody. Epitope tagging is the addition of a short peptide to a

target protein. This technique has provided the means for the characterization and purification of proteins without the need of specific antibodies.

A new method for PCR-mediated C-terminal epitope tagging, that allows the tagging of chromosomal genes with sequences expressing the MYC, HA or VSV epitopes, was created during this work (De Antoni and Gallwitz, 2000). Three new plasmids named pU6H2MYC, pU6H3HA and pU6H3VSV (pU-tag vectors) were created (see Results, Section 4.3). These plasmids contain the new modules 6His-2MYC-loxP-*kanMX*-loxP, 6His-3HA-loxP-*kanMX*-loxP or 6His-3VSV-loxP-*kanMX*-loxP that allow tagging of different genes by using the *kan^r* marker repeatedly (see Fig. 3.2). The method relies on the amplification by PCR of the *tag-loxP-kanMX-loxP* cassettes using the tag-forward and tag-reverse primers. tag-forward = 5'-... .. TCC CAC CAC CAT CAT CAT CAC-3', is a chimeric primer composed of 42-45 nucleotides derived from the 3'-end of the gene of interest (excluding the stop codon, and in frame with the epitope-encoding sequence), plus the 21 nucleotides shown, annealing to the 5'-end of the cassette; tag-reverse = 5'-... .. ACT ATA GGG AGA CCG GCA GAT C-3', is composed of 42-45 nucleotides derived from the sequence downstream of the gene of interest (starting at either the stop codon or 50-100 nucleotides after the stop codon) plus the 22 nucleotides shown, annealing to a sequence downstream of the cassette (see Fig. 3.2). The length of the amplified cassettes is 1711 bp from pU6H2MYC, 1735 bp from pU6H3HA, and 1753 bp from pU6H3VSV. The primers used in this study are listed in Table 7.7. A 100 μ l preparative PCR contains: 5-10 ng template (pU6H2MYC, pU6H3HA or pU6H3VSV), 30 pmol of each primer (tag-forward and tag-reverse), 200 μ M of each dNTP, 1.5 U AmpliTaq (Perkin Elmer), 0.4U Deep Vent DNA polymerase (NEB) and 10 μ l 10X PCR buffer (Perkin Elmer, containing 15 mM MgCl₂). PCR conditions were: denaturation at 93°C for 3 min, followed by 32 cycles (93°C for 1 min, 55°C for 1 min, 72 °C for 1.5 min) and a final elongation step at 72 °C for 10 min. The PCR products were purified with QIAquick PCR columns and 1-5 μ g used to transform yeast cells. Transformants were plated onto YEPG plates containing 200 μ g/ml G418. Plates were incubated at 30°C until colonies appeared. Well grown colonies were re-streaked onto YEPG/G418 plates.

It is possible to excise the *Kan^r* marker, by inducing the Cre-recombinase (see 3.3.2) and subsequently to tag other genes.

With this method the strains ADY1-ADY16 were created, that express different tagged proteins such as Sec24p-MYC, Sec24p-HA, Sec24p-VSV, Sec23p-MYC,

Sfb2p-MYC, Sfb2p-HA, Sfb2p-VSV, Sfb3p-MYC, Sfb3p-HA, Sfb3p-VSV, Gyp5p-MYC, Gyp5p-HA and Gyp5p-VSV.

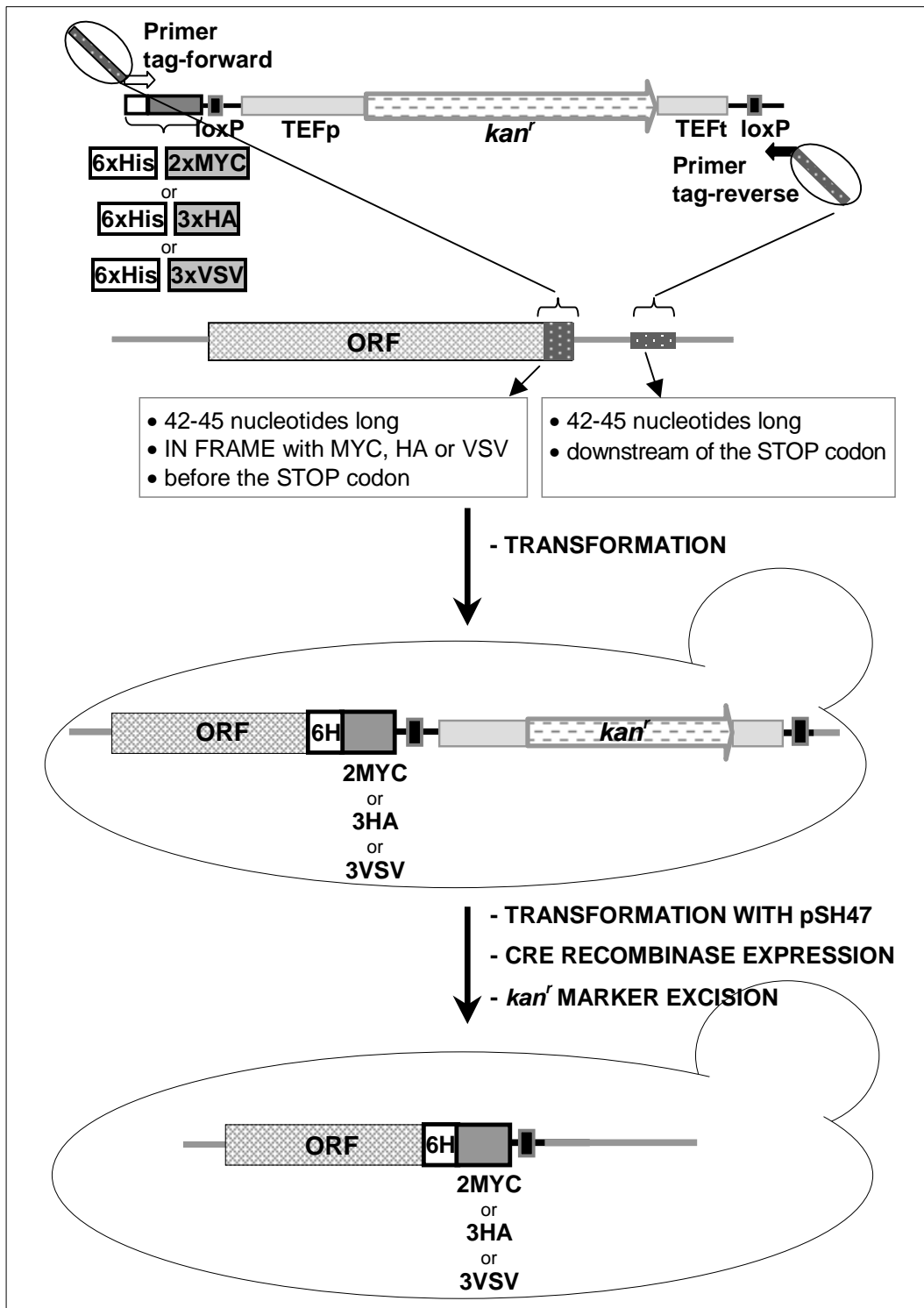


Fig. 3.2 Schematic representation of PCR-mediated epitope tagging. The tag-loxP-*kanMX*-loxP cassettes are amplified by PCR using pU6H2MYC, pU6H3HA and pU6H3VSV as templates and chimeric primers (for more details see in the text). The PCR products are then used to transform yeast cells and the tag-cassette will be integrated in frame with the desired ORF. Finally, the *kan^r* selection marker (1507 bp DNA fragment) is excised from the genome by action of the Cre-recombinase so that another protein can be tagged.

3.3.4 Growth analysis

To analyze growth defects of different mutant strains at different temperatures, overnight cultures were diluted in fresh medium to reach an optical density $OD_{600} \sim 0.01$, subsequently serial 10-fold dilutions were done. 5 μ l cells from each dilution were spotted onto a plate and put to grow at the appropriate temperature.

3.3.5 Invertase assay

Invertase catalyze the hydrolysis of sucrose in glucose and fructose. Invertase secretion is induced by low glucose concentration in the medium. Secreted invertase migrates in non-denaturing polyacrylamide gels as heterogeneous species with an apparent molecular mass of 100-140 kDa. The glycosylated ER-form has an apparent molecular mass of 80-86 kDa.

Cells of different strains were grown in YEPG medium at 30°C to mid-log phase and 10 OD units of cells were collected by centrifugation at 4.000g for 5 min at room temperature. Cells were washed with YEPG 0.1% (YEPG medium containing 0.1% glucose) resuspended in 10 ml of YEPG 0.1% and incubated at the desired temperature for 1-6 hours (1h at 37°C or 30°C, 2h at 25 °C, 4h at 20 °C, 6h at 15 °C) (Esmon *et al.*, 1981). After induction, cells were collected, washed in 10 mM NaN_3 and resuspended in 100 μ l lyticase buffer. Spheroplasts were formed by incubating the cells at 30 °C for 1 hour with 200 units Lyticase (Sigma). Subsequently, to isolate periplasmic and intracellular invertase, the spheroplasts were fractionated as described by (Schauer *et al.*, 1985). Spheroplasts were gently centrifuged at 1.000g for 5 min at RT and the supernatant containing the periplasmic invertase was transferred to a new tube. The pellet, containing the intracellular invertase, was gently washed with 1M sorbitol, resuspended in 100 μ l lysis buffer and vortexed for 5 min at 4°C, finally the samples were centrifuged to eliminate cell debris, and the supernatant (containing the intracellular invertase) was transferred to a new tube. 20 μ l of each sample were loaded onto a non denaturing 7% polyacrylamide gel. Staining of active invertase was performed as described by (Grossmann and Zimmermann, 1979). The gel was soaked in 200 ml sucrose buffer for one hour at 37°C, washed with water and soaked in 150 ml staining buffer over a boiling bath till a red staining appeared. The reaction was blocked washing the gel with cold water and 10% acetic acid.

<u>Lyticase buffer</u>	1.4 M 50 mM 10 mM 80 mM	Sorbitol K ₂ HPO ₄ /KH ₂ PO ₄ , pH 7.5 NaN ₃ β-mercaptoethanol
<u>Lysis buffer</u>	50 mM 10 mM 0.1%	K ₂ HPO ₄ /KH ₂ PO ₄ , pH 7.5 NaN ₃ Triton X-100
<u>Sucrose buffer</u>	0.1 M 0.1 M (pH 4.5-5.0)	Sucrose NaOAc
<u>Staining buffer (150 ml)</u>	300 mg 4 g (dissolve separately then mix)	Triphenyltetrazoliumchloride NaOH
<u>7% Polyacrylamide gel</u> (non denaturing)	5 ml 8.7 ml 26 ml 0.3 ml 17 μl	0.6M Tris-HCl pH 8.4 30% Acrylamide stock solution H ₂ O 10% APS TEMED
<u>Running buffer (1l)</u>	5.19 g 2.5 g (pH 9.5)	Tris-HCl Glycine

3.3.6 Pulse-chase

Overnight cultures of the appropriate strains were used to inoculate fresh SMM medium and grown at the required temperature to reach an OD₆₀₀ of 0.6-1.2. Six OD units of cells were harvested, resuspended in 500 μl SMM medium containing 1 mg/ml ovalbumin and incubated at the appropriate temperature for 30-60 min. After that cells were pulsed for 10 min with 250 μCi Trans^[35S]-label mix (a mix of ^[35S]-cysteine and ^[35S]-methionine) followed by a chase of 30 minutes with methionine and cysteine (1.5 mg/ml each). The incubation time for both pulse and chase was longer if the temperature was lower than 30 °C. To stop the reaction the samples were placed on ice and NaN₃, PMSF and Pefablock were added (final concentration was: 10 mM NaN₃, 1 mM PMSF, 2 mM Pefablock). The labeled samples were fractionated into intracellular and extracellular fractions by centrifugation (1.000g for 5 min). 250 μl medium (the extracellular fraction) was collected in new tubes and 10 μl 10% SDS were added, the pellet (intracellular fraction) was washed once with PBS containing 10 mM NaN₃ and resuspended in 100 μl 1% SDS, both fractions were frozen in liquid nitrogen (they can

be stored several days at -80°C). The pellet samples were subsequently lysed by vortexing for 5 min in the presence of 0.1 g glass beads, boiled for 5 min and centrifuged at 14.000 rpm for 5 min. The supernatant ($\sim 100\ \mu\text{l}$) containing the intracellular fraction was transferred to new tubes and 500 μl 2x IP buffer plus 400 μl water were added. The 250 μl extracellular fractions were treated in a similar way. They were boiled for 5 min, centrifuged at maximum speed for 5 min and the supernatants transferred to new tubes containing 500 μl 2x IP buffer plus 250 μl water. The samples so treated were ready for the immunoprecipitation with anti-carboxypeptidase Y (CPY), anti-Gas1p, or anti alkaline phosphatase (ALP). 5-10 μl antiserum and 5 mg protein-A sepharose CL-4B were added to each sample. The samples were incubated overnight at 4°C (end-over-end rotation). After that the sepharose "beads" were sequentially washed with 1 ml ice-cold washing buffer-1, washing buffer-2, and washing buffer-3. The "beads" were resuspended in 50 μl Laemmli buffer and boiled for 5 min at 95°C . The immunoprecipitated proteins were separated by SDS-PAGE on 10% Acrylamide gels (see 3.4.1.a). After electrophoresis the gels were fixated for 20 min in a [10% acetic acid / 25% methanol] solution, treated with Amplify (Amersham) according to the manufacturer's instruction, dried and exposed to Kodak X-Omat AR films at -80°C for 2-10 days.

CPY is a soluble vacuolar hydrolase. It leaves the ER as a core-glycosylated precursor protein of 67 kDa, is further glycosylated in the Golgi apparatus (69 kDa), and finally reaches the vacuole, where after a short proteolytic truncation, it becomes active. This mature form has a molecular mass of 61 kDa. Gas1p is a 125 kDa glycolipid-anchored plasma membrane protein. The ER glycosylphosphatidylinositol-containing precursor has a molecular mass of 105 kDa and, upon arrival in the Golgi, is further glycosylated, reaching a molecular mass of 125 kDa. ALP is a vacuolar type II transmembrane enzyme. The ER/Golgi glycosylated 76 kDa precursor protein become active by proteolytic truncation after arrival to the vacuole. The mature form of ALP has a molecular mass of 72 kDa.

<u>SMM</u>	0.1%	KH_2PO_4
	0.1%	NH_4Cl
	0.02%	CaCl_2
	0.06%	MgCl_2
	0.05%	NaCl
	0.3%	Yeast extract
	2%	Glucose
		Amino acids (according to the auxotrophy requirement)

<u>2x IP buffer</u>	100 mM	Tris-HCl, pH 7.5
	2%	Triton X-100
	0.2%	SDS
	300 mM	NaCl
	2 mg/ml	Ovalbumin
	10 mM	EDTA
	4 mM	Pefabloc
	1 tablet/5ml protease inhibitors	
<u>Washing buff.-1</u>	1x	IP buffer
	2M	Urea
<u>Washing buff.-2:</u>	1x	IP buffer
	500 mM	NaCl
<u>Washing buff.-3</u>	150 mM	NaCl
	5 mM	EDTA
	50 mM	Tris -HCl, pH 7.5

3.4 Biochemical methods

3.4.1 Polyacrylamide gel electrophoresis (PAGE)

The principle of polyacrylamide gel electrophoresis is the separation of a large range of proteins of varying molecular masses under the influence of an electrical field by means of a continuous, cross-linked polymer matrix. Here, the polymer is polyacrylamide and the cross-linking agent bis-acrylamide. Cross-linking is effected through a radical-induced pathway by the addition of APS and TEMED (Ogden and Adams, 1987). In polyacrylamide gel electrophoresis, proteins migrate in response to an electric field through pores in the gel matrix. The pore size decreases with higher acrylamide concentration. The combination of gel pore size and protein charge, size and shape determines the migration rate of the proteins (Coligan *et al.*, 1997; Sambrook *et al.*, 1989).

a) Denaturing polyacrylamide gel electrophoresis (SDS-PAGE)

One dimensional gel electrophoresis under denaturing conditions (in presence of 0.1% SDS) separates proteins on the base of their molecular size. The mobility of the proteins is inversely proportional to the logarithm of their molecular mass. SDS is employed to effect denaturation of the proteins, to dissociate protein complexes and to impart upon the polypeptide chains net negative charge densities proportional to

the length of the molecule. A reducing agent such as DTT or 2-ME is used to reduce any existing disulphide bond. The method used is that described by Laemmli (Laemmli, 1970). Two gels are employed: a "stacking gel" with a low level of cross-linkage and low pH, allowing proteins to enter the gel and collect without smearing, and a "resolving gel" with a higher pH, in which the proteins are separated. For an 8x10x0.1 cm gel the following volumes were used:

5% Stacking gel (5 ml)	3.4 ml	H ₂ O		
	0.83 ml	30% Acrylamide stock solution (see 2.2)		
	0.63 ml	1M Tris-HCl, pH 6.8		
	50 µl	10% SDS		
	50 µl	10% APS		
	5 µl	TEMED		
<u>Resolving gel (10 ml)</u>	<u>10%</u>	<u>12%</u>	<u>15%</u>	
	4 ml	3.3 ml	2.3 ml	H ₂ O
	3.3 ml	4 ml	5 ml	30% Acrylamide stock sol
	2.5 ml	2.5 ml	2.5 ml	1.5 M Tris-HCl, pH 8.8
	100 µl	100 µl	100 µl	10% SDS
	100 µl	100 µl	100 µl	10% APS
	4 µl	4 µl	4 µl	TEMED

For Laemmli loading buffer and electrophoresis buffer, see Materials 2.2.

b) Non-denaturing PAGE

The basis of separation in this case is as described above, with the exception that proteins now separate with an apparent molecular mass based on the overall size and shape of the molecule. SDS is not added to such gels. Electrophoresis is performed at lower voltages and temperatures to reduce the risk of heat-denaturation of the proteins. In this study non-denaturing gel PAGE was used for analyzing samples after invertase assay (see 3.3.5).

3.4.2 Preparative gel electrophoresis and electro-elution

To obtain up to milligrams amounts of proteins from an impure mixture, preparative gel electrophoresis was employed. The principle is the same as above (3.4.1), here however, a gel of larger dimensions is poured, and a comb with a single slot is used that allows the application of larger amounts of sample. The band of interest is excised from the gel after standard Coomassie staining (3.4.3.a) and eluted using an electro-elution chamber.

3.4.3 Staining of proteins in polyacrylamide gels

a) Coomassie brilliant blue staining

Gels were soaked in fixating solution with gentle shaking for 10 min, stained in staining solution for 1 hour or for longer time at room temperature. The background was subsequently reduced by soaking the gel in 10% acetic acid solution in which the gels can be kept for several days. After that gels can be dried.

<u>Fixating solution</u>	25% (v/v) 10% (v/v)	Isopropanol Glacial acetic acid
<u>Staining solution</u>	10% (v/v) 60 mg/l	Glacial acetic acid Coomassie brilliant blue R250

b) Silver staining

Gels were first fixated in fixating solution for 1 hour at room temperature, then soaked for 30 min in incubation solution and washed 3x10 min in distilled water. After that the gels were placed in binding solution for 20 min. Finally the gels were washed with water and put into developing solution till brown band appeared. The staining reaction was stopped by washing with 50 mM EDTA and subsequently the gels were soaked in 10% acetic acid. All the solutions should be freshly prepared.

<u>Fixating solution</u>	50% 10%	Ethanol Acetic acid
<u>Incubation solution</u>	30% 0.83 M 13 mM 0.25%	Ethanol NaOAc Na ₂ S ₂ O ₃ (sodium thiosulfate) Glutaraldehyde (to be added just before use)
<u>Binding solution</u>	6 mM 0.02%	AgNO ₃ (silver nitrate) Formaldehyde
<u>Developing solution</u>	0.25 M 0.01%	Na ₂ CO ₃ Formaldehyde

3.4.4 Western blotting and immunological detection of proteins on nitrocellulose filters

Proteins were separated by SDS-PAGE and electrophoretically transferred from the polyacrylamide gels to nitrocellulose membranes as described by (Burnette, 1981). The transfer was carried out at 100 mA constant current for 1 hour or at 30 mA overnight.

<u>Transfer buffer</u>	20 mM	Tris-base
	150 mM	Glycine
	20% (v/v)	Methanol

After the transfer onto nitrocellulose the proteins were stained with Ponceau S solution. Then the membranes were washed briefly with washing buffer-A, treated with blocking solution for 1 h at RT and incubated with the primary antibody in blocking solution for 1 h at RT. After 2x 5 min washes in buffer-A, 2x 5 min in buffer-B and once again for 5 min in buffer-A, the membrane was incubated for 1 h at RT with the horseradish peroxidase-coupled secondary antibody (1:10.000 dilution). Finally, the membranes were washed as described above. Detection by chemiluminescence was performed using the ECL detection system as recommended by the manufacturer.

<u>Ponceau S solution</u>	2.5 g/l	Ponceau S
	15% (v/v)	Glacial acetic acid
	40% (v/v)	Methanol
<u>Blocking solution</u>	5% (w/v)	low fat milk powder in washing buffer A
<u>Washing buffer-A</u>	10 mM	Tris-HCl, pH 7.4
	0.9% (w/v)	NaCl
	0.05% (v/v)	Tween 20
<u>Washing buffer-B</u>	0.2% (w/v)	SDS
	0.9% (w/v)	NaCl
	0.5% (v/v)	Triton X-100
	0.5% (w/v)	BSA

3.4.5 Protein quantitation

Protein concentrations were estimated according to the method of Bradford (Bradford, 1976). The method is based on the observation that the absorbance for the protein-specific dye, Coomassie brilliant blue G-250 shift from 465 nm to 595 when binding to protein occurs. Therefore, the A_{595} yields a good linear concentration dependence for most soluble proteins. 800 μ l of a proteins solution of unknown concentration was mixed with 200 μ l of the dye solution (BioRad) and the measured A_{595} was plotted against a reference curve obtained with known concentrations of BSA.

3.4.6 Concentrating proteins

Protein solutions were concentrated using Centricon spin columns (Amicon), or membra-spin PES columns (membraPure) as recommended by the manufacturer.

3.4.7 Protein extraction

For a more detailed description about extraction conditions, see (Janson and Ryden, 1989).

a) Proteins extraction from bacteria

Bacteria were harvested by centrifugation, suspended in cold lysis buffer (2-5 volumes per gram of wet weight) and sonicated 3 times on ice (1 min bursts/1 min cooling/200-300 Watt). The lysis buffer composition depended on the subsequent use of the protein extracts (see 3.4.9). After sonication the cell debris was separated from the solubilized proteins by centrifugation (2x10 min at 5.000g).

Alternatively, total protein extracts for SDS-PAGE and western blotting were obtained easily by resuspending the pellet from 1 OD₆₀₀ cells with 100 µl Mg²⁺/SDS buffer (Tris-HCl, pH 6.8 / 0.1 M MgCl₂ / 4% SDS / 10% glycerol/ 5% 2-ME / 0.01% bromophenol blue) and subsequently centrifuging for 2 min at 14000 rpm to remove the precipitate (Chen and Christen, 1997).

b) Protein extraction from yeast

Total protein extracts from yeast can be obtained using several methods that differ mainly in the way the cells are broken. Those used during this work are described below.

- Cell disruption by alkaline lysis

It is a fast method suitable to obtain denatured proteins for SDS-PAGE and western-blotting analysis.

One OD₆₀₀ unit of cells (~10⁷ cells) was centrifuged (2 min at 10.000 rpm), and the cell pellet washed with cold water, resuspended in 180 µl lysis buffer (2 M NaOH / 0.5% β-mercaptoethanol) and incubated on ice for 5 min. Proteins were precipitated adding 20 µl 100% TCA. After incubation on ice for 5 min, proteins were pelleted by centrifugation (10 min at 14.000 rpm). The pellet was then washed with acetone, left to air dry thoroughly and resuspended in 100 µl Laemmli loading buffer. After being boiled for 5 min proteins were separated by SDS-PAGE.

- Cell disruption by sonication

It is another fast method to obtain protein extracts for western blot analysis. Five OD₆₀₀ units of cells were centrifuged, washed with cold water, resuspended in 100 µl of lysis buffer (20 mM HEPES-KOH, pH 7.2 / 150 mM KOAc / 1 mM MgOAc / 0.9% CHAPS / 2 mM

Pefabloc) and sonicated for 5 sec. To each sample were added 100 μ l of 2X Laemmli loading buffer. After being boiled for 5 min proteins were separated by SDS/PAGE.

- Cell disruption by glass beads

This procedure is suitable for small-scale protein preparation. It is very flexible because it can be carried out easily on multiple small cell cultures, but the proteins can be subjected to proteolysis due to the harsh treatment and heat developed during the mechanical breakage. These protein extracts are suitable for different applications such as cell fractionation (see 3.4.10), immunoprecipitation (see 3.4.13) and gel filtration (see 3.4.11).

Five ml of a mid-log phase culture was centrifuged, the cell pellet washed with cold water was and resuspended with 200 μ l cold lysis buffer. The lysis buffer composition was different depending on the subsequent use of the protein extract. A typical glass beads lysis buffer is composed of: 10 mM Tris-HCl, pH 8 / 2 mM MgCl₂ / 1 mM DTT / 1 mM EGTA / 2 mM Pefabloc / protease inhibitors. To each sample was added the same volume of chilled acid-washed glass beads (0.45-0.55 mm) and the tubes were vortexed 3 times for 30-60 sec (maximum speed, at 4°C), with a pause on ice of 2 min each time. Finally the tubes were centrifuged for 10 min at 500g. The supernatant containing the total protein extract was ready to be further processed.

- Cell disruption by liquid nitrogen

This method is designed for the processing of 50-500 ml of liquid culture. The proteins obtained in this way are suitable for many applications. This method was mainly used in this work for cell fractionation (3.4.10).

The pellet from a 50-500 ml-culture was transferred to a mortar containing liquid nitrogen and smashed until a fine powder was obtained. The powder was dissolved in the desired buffer and centrifuged 2 times at 500g for 5 min. The supernatant containing the total protein extract was ready to be further processed.

- Cell disruption by high-pressure homogenization (by french-press)

This is a method designed for processing big amounts of cells (> 1l liquid culture). It was mainly used in this work to get big amounts of proteins to be purified by affinity chromatography (3.4.9).

A 5 ml cell pellet was dissolved in 40 ml ice cold lysis buffer and the cell solution was subjected for 3 times (with a pause on ice of 5 min each time) to 1380 bars pressure produced by the "French press". After centrifuging twice at 500g for 5 min, the total protein extract was ready to be further processed.

- Cell disruption by spheroplast formation and lysis

This is the most gentle way to break yeast cells, but also the most time consuming. Cells are converted to spheroplasts by zymolyase treatment, and then lysed by osmotic shock. This method was used in this work to obtain cell extracts suitable for sucrose gradients (see 3.4.10.b).

c) Protein extraction from mammalian cells

During this work protein extracts from CV1 and Hela cells were used for western-blotting analysis. Cells were first washed twice with cold PBS, scraped off the Petri dishes in PBS buffer with the aid of a rubber "policeman", then briefly sonicated on ice and resuspended in Laemmli loading buffer.

3.4.8 Expression of proteins and recombinant proteins

Genes can be cloned into expression vectors, and expressed in the appropriate cell systems. An expression vector is a vector that contains the necessary regulatory sequences for gene expression. Both prokaryotic and eukaryotic expression vectors exist, many of them are shuttle vectors (cloning vectors that can replicate in two or more dissimilar hosts). Many factors (number of copies of the gene per cell, promoter strength and regulation, translation initiation, codon usage and protein stability) can influence the level of expression of a gene. In addition a suitable host must be used in which the expression vector is most effective. Often it is advantageous to express proteins as a fusion product with a protein or an epitope. Some of the sequence "tags" can facilitate detection and purification of the target proteins, other increase the probability of biological activity by affecting the solubility in the cytoplasm or the export into the periplasm.

a) Fusion tags

Here is a list of the fusion sequence tags (proteins or epitopes) used during this work.

c-myc (MYC) is a 10 aa peptide from the human c-myc protein (sequence: EQKLISEEDL, aa 410-419). It is recognized by the rabbit polyclonal or by the mouse monoclonal anti-c-myc antibody (clone 9E10 (Evan *et al.*, 1985). PCR-mediated epitope tagging (see 3.3.3) is one of the methods used for tagging yeast proteins with this epitope.

HA is a 9 aa peptide from the human influenza virus hemagglutinin protein (sequence: YPYDVPDYA, aa 98-106). It is recognized by the mouse monoclonal

anti-HA antibody (clone 12CA5 (Wilson *et al.*, 1984). PCR-mediated epitope tagging (3.3.3) is one of the methods used for tagging yeast proteins with this epitope.

VSV-G (VSV) is a 11 aa peptide from the vesicular stomatitis virus glycoprotein (sequence: YTDIEMNRLGK, aa 501-511). It is recognized by the mouse monoclonal anti-VSV-G antibody (clone P5D4 (Kreis, 1986). PCR-mediated epitope tagging (3.3.3) is one of the methods used for tagging yeast proteins with this epitope.

6xHis and polyhistidine tags bind metal ligands. Proteins containing this tag can be purified by affinity chromatography on Ni-NTA matrices (see 3.4.9.a). This tag is present in the expression vectors pQE30, pQE50, pET30 and pET32. It can be also produced by PCR using primers containing the 6xhistidine coding sequence, or by PCR-mediated epitope tagging (3.3.3).

S-tag is a 15 aa peptide that binds with high affinity to the 104 aa S-protein (derived from pancreatic ribonuclease A). It is recommended for detection, quantitation and purification of target proteins. S-tag is present in the expression vectors pET30 and pET32.

Trx: thioredoxin (109 aa). It increases protein solubility. This tag is present in the expression vector pET32.

GST: glutathione S-transferase (220 aa). It is useful to purify proteins by affinity chromatography on glutathione sepharose matrix (see 3.4.9.b). This tag is present in the expression vectors pGEX-TT (for expression in bacteria) and pEG(KT) (for expression in yeast).

MBP: maltose binding protein (483 aa). It is useful to purify protein by affinity chromatography on amylose resin (see 3.4.9.c). This tag is present in the expression vectors pMAL-c2 and pMAL-p2.

b) Expression of proteins in bacteria

To be expressed in bacteria, genes were cloned into expression vector containing inducible promoters: pQE50, pQE30, pET12c, pET30a, pET32a, pGEX-TT, and pMAL-c2 (see Appendix Tables 7.4 and 7.6). After being established in a non-expression host, the plasmids were transferred into hosts more suitable for protein expression such as M15(pREP), B121, B121(DE3) or origami(DE3) (see Appendix Table. 7.1). The last two strains contain the T7 RNA polymerase gene (λ DE3 lysogens) and have to be used when the target genes are under T7 promoter control since it is not recognized by *E. coli*

RNA polymerase. Protein expression was induced with 1 mM IPTG (IPTG was added when an OD₆₀₀ of 0.5-0.8 was reached) at 25-30°C for 4-6 hours.

c) Expression of proteins in Yeast

Yeast expression vectors used in this work are pEG(KT), pYX112, pYX143, pYX212, pYX243 (see Appendix Tables 7.5 and 7.6). They are shuttle vectors containing either the 2 μ or *CEN/ARS* sequences and the strong *TPI* promoter or the inducible *GAL1* promoter. Moreover, proteins can be expressed by genes carrying their natural yeast promoter cloned into multi-copy vectors such as pRS315, pRS316, pRS325, pRS326. To induce protein expression of genes under *GAL* promoter, yeast strains were first grown overnight in raffinose selection medium and then transferred to fresh pre-warmed YEPGal medium and induced for at least 8 hours.

3.4.9 Protein purification

Different chromatography techniques were used to purify the target proteins from total bacterial or yeast protein extracts (for more details see Janson and Ryden, 1989).

a) 6xHis-fusion protein purification

6xHis-fusion proteins can be purified on Ni-NTA metal affinity chromatography matrices (Janknecht *et al.*, 1991). Purification can be performed under native or denaturing conditions.

Purification under native conditions: A 5 ml cell pellet from 1 l IPTG-induced bacteria were dissolved in 20 ml lysis buffer and sonicated 3x1 min. Cell debris was eliminated by centrifugation for 10 min at 2.000g (4°C), then the supernatant was further centrifuged at 10.000g for 30 min (4°C). The 10.000g supernatant was transferred to a new tube containing 0.5-1 ml of a 50% slurry of Ni-NTA resin (pre-washed with lysis buffer), and incubated at 4°C for 1-2 h with end-over-end rotation. After that the resin was loaded onto a column and washed with 200 ml buffer-1, 200 ml buffer-2, and 200 ml buffer-3. Finally, the protein was eluted with elution buffer.

When the 6xHis-fusion proteins were produced in yeast, the same procedure was used with the only difference that cells were lysed by French press (see 3.4.7.b).

<u>Lysis buffer</u>	20 mM	Tris-HCl pH 7.5-8.00
	500 mM	NaCl
	10 mM	CHAPS
	Proteinase inhibitors EDTA free (cocktail tablets, Roche)	

<u>Buffer-1</u>	20 mM 500 mM 20 mM (pH 7.5)	Tris-HCl NaCl Imidazole
<u>Buffer-2</u>	20 mM 300 mM 20 mM (pH 7.5)	Tris-HCl pH 7.5 NaCl Imidazole
<u>Buffer-3</u>	50 mM 300 mM 10 mM (pH 7.5)	NaH ₂ PO ₄ NaCl Imidazole
<u>Elution buffer</u>	50 mM 300 mM 250 mM (pH 7.5)	NaH ₂ PO ₄ NaCl Imidazole

Purification under denaturing conditions: The cell pellet from 100 ml culture was dissolved in 10 ml buffer-B and sonicated. The lysate was centrifuged for 30 min at 10.000g. The supernatant was transferred to a new tube containing 250-500 µl of a 50% slurry of Ni-NTA resin and incubated at 4°C for 1-2 h with end-over-end rotation. After that the resin was loaded onto a column and washed twice with 10 ml buffer-C. Finally the protein was eluted with Laemmli buffer and analyzed by SDS-PAGE.

<u>Buffer-B</u>	100 mM 10 mM 8M (pH 8.0)	NaH ₂ PO ₄ Tris-HCl urea
<u>Buffer-C</u>	100 mM 10 mM 8M (pH 6.3)	NaH ₂ PO ₄ Tris-HCl urea

b) GST-fusion protein purification

GST-fusion proteins bind to a glutathione sepharose matrix with high affinity in almost any biological buffer. The solubility of fusion proteins is increased by the presence of detergents (1% Triton X100 or 0.5% CHAPS). GST-fusion proteins were purified according to standard protocols as described by (Smith and Johnson, 1988) (see also 3.4.12).

c) MBP-fusion protein purification

The vectors containing the maltose binding proteins were developed by the New England Biolabs company, the MBP-fusion proteins were purified as described in the manufacturer's protocols manual. A complete description can be downloaded from http://www.neb.com/neb/tech/tech_resource/fusion/fusion_frame.html.

d) Anion exchange chromatography

By anion exchange chromatography biomolecules are separated on the basis of differences in charge characteristics. MonoQ (Pharmacia) is a strong anion exchanger with trimethyl-aminomethyl ($-\text{CH}_2\text{N}^+(\text{CH}_3)_3$) moieties as functional groups. Proteins were diluted with 3 volumes MonoQ buffer and loaded onto FPLC monoQ HR (high resolution) 10/10 columns or onto HiLoad 16/10 Q sepharose HP (high performance), at a flow rate of 1 ml/min. The columns were washed extensively with monoQ buffer until the baseline was reached. Proteins bound to the column were eluted with a linear gradient of 0-0.4 or 0-0.6 M NaCl solution in MonoQ buffer and 1 ml fractions were collected.

MonoQ buffer 20 mM Tris-HCl, pH 8.0
2 mM MgCl_2
1 mM EGTA
1 mM DTT
10 % glycerol

e) Superdex 200 HR and Sephacryl S-200 HR size exclusion gel filtration chromatography

In Superdex 200 (Pharmacia) the gel material is composed of covalently bound dextran to highly cross-linked porous agarose beads. Sephacryl S-200 (Pharmacia) is composed of allyl dextran and N,N'-methylenebisacrylamide. Large proteins are excluded from the porous cavity within the gel material and flow around the beads. Therefore, having a shorter distance to travel, they migrate faster through the column and elute before smaller proteins.

Protein samples were loaded onto Superdex 200 HR 16/60 or onto Sephacryl S-200 HR 16/60 columns, equilibrated with the desired buffer, at a flow rate of 0.5 ml/min. 2 ml fractions were collected. This was the last purification step to obtain pure Gyp5p constructs and Ypt1p. As determined by SDS-PAGE the purity, typically achieved at this stage, was above 95%.

f) Ypt1p purification

The Ypt1p purification protocol is based on the method described in (Wagner *et al.*, 1992). Two liters of liquid culture of BI21(DE3) containing pET12c-*YPT1* were induced by 1 mM IPTG at 30 °C for 6 hours. After induction the cells were harvested by centrifugation, suspended in 40 ml (20 mM Tris-HCl, pH 8.0, 10 mM MgCl₂ 1 mM DTT, 1% Triton X100, 1 mM Pefabloc) and sonicated twice for 2 min on ice. The cell lysate was centrifuged for 10 min at 10.000g, and the supernatant was loaded onto a HiLoad 16/10 Q Sepharose HP column and subjected to anion exchange chromatography as described before with a 0-0.4 M NaCl linear gradient. Ypt1p eluted with 0.19 M NaCl and the purity was higher than 75%. The fractions containing Ypt1p were further purified by Superdex 200 HR gel filtration chromatography in the reaction buffer (200 mM Tris-HCl, pH 8.0 / 10 mM MgCl₂ / 1 mM DTT / 0.2 mM GDP). Fractions containing Ypt1p were identified by spectrophotometric analysis at 280 nm and by SDS-PAGE and collected. These fractions were pooled, quantified by Bio-Rad protein assay (3.4.5), frozen in liquid nitrogen and stored at -80 °C. About 8 mg of protein with >95% purity could be obtained.

g) Gyp5₍₄₀₀₋₈₉₂₎-6His protein purification

One liter liquid culture of BI21(DE3) containing pET30-*GYP5*₍₄₀₀₋₈₉₂₎A was induced with 1 mM IPTG at 25 °C for 5 hours. The 6xHis fusion protein was first purified as described in 3.4.9.a (yielding ~6 mg protein with a purity of 75-80%), then subjected to anion exchange chromatography (MonoQ HR 10/10 column, 1ml/min flow rate, 0-0.6 M NaCl linear gradient; see 3.4.9.d) and finally to gel filtration chromatography (see 3.4.9.e) using a Sephacryl S-200 HR 16/60 column equilibrated with reaction buffer (0.1 M NaCl, 50 mM Tris-HCl, pH 8.0, 5 mM MgCl₂ 1 mM DTT). The fractions containing the purified proteins were pooled, quantified by Bio-Rad protein assay (3.4.5), frozen in liquid nitrogen and stored at -80 °C. From a monoQ column ~3 mg of Gyp5₍₄₀₀₋₈₉₂₎-6His protein eluted with 0.45 M NaCl with a purity higher than 85%; after gel filtration, ~2 mg of protein with >95% purity could be obtained.

3.4.10 Subcellular fractionation

a) Subcellular fractionation by differential centrifugation

The pellet from 250 ml culture was transferred to a mortar containing liquid nitrogen and smashed until a fine powder was obtained. The powder was dissolved in 5 ml of buffer-A and centrifuged for 15 min at 500g. The supernatant was divided into 4 tubes

(500 μ l each), and to each tube were added 500 μ l of buffers A, B, C, D, respectively. After incubation on ice for 15 min, the samples were centrifuged at 4°C for 15 min at 10.000g, the pellet (p10) was resuspended in 2 ml 1xLaemmli buffer. 950 μ l of the supernatant were transferred to new tubes and subjected to further centrifugation for 1 h at 100.000g at 4°C, the pellet (p100) was resuspended in 1.9 ml of 1xLaemmli buffer and to 900 μ l of the supernatant (S100) were added 900 μ l 2xLaemmli buffer. All samples were subjected to SDS-PAGE, followed by immunoblotting.

Buffer-A 20 mM HEPES-KOH pH 7.2
100 mM KCl
4 mM MgCl₂
2 mM Pefabloc
protease inhibitors EDTA free (cocktail tablets, Roche)

Buffer-B Buffer A containing 2% Triton X-100

Buffer-C Buffer A containing 3M KCl

Buffer-D Buffer A containing 8 M urea

b) Subcellular fractionation by velocity sedimentation on sucrose gradient

200 ml cells grown to mid-log phase were harvested and resuspended in 5 ml buffer-1 and incubated for 10 min at RT. Cells were collected by centrifugation (5 min at 2.000g), washed once with 10 ml buffer-2 (same composition as buffer-1 without 2-ME) and resuspended in 2 ml buffer-2. 2.000 units of lyticase (Sigma) were added and the mixture was incubated for 30min-1h at 30°C (spheroplast formation was checked under the microscope). When spheroplasting was completed, cells were centrifuged for 5 min at 2.500 rpm (Eppendorf bench centrifuge) and the cell pellet was resuspended in 2 ml water containing protease inhibitors EDTA free (1 tablet in 6 ml). At this step spheroplasts are osmotically lysed. Unbroken cells were removed by centrifuging at 3.500 rpm for 2 min, the centrifugation should be repeated as many times as necessary to remove all unbroken cells (this was checked under the microscope). 1.5 ml cleared lysate was loaded carefully onto sucrose-gradient tubes (thawed at 4°C). The samples were centrifuged for 2.5 hours at 37.000 rpm at 4 °C in an ultracentrifuge using a SW40 rotor. 12 fractions of 1 ml each, plus a fraction of 500 μ l containing the pellet, were carefully collected. To each fraction was added an equal volume of 2x Laemmli buffer containing 8M urea, the fractions were then analyzed by SDS-PAGE and by immunoblotting. The chemiluminescence signals were quantified with a Lumi-Imager.

Fractions 1 and 2 contain the cytosolic and vacuolar proteins, Golgi proteins are in fractions 4-9 and ER proteins are in the last four fractions of the gradient.

<u>Buffer-1</u>	10 mM	HEPES, pH 7
	1 mM	MgCl ₂
	1.2 M	Sorbitol
	100 mM	β-mercaptoethanol
	10 mM	NaN ₃

Preparation of frozen step-gradient tubes: eleven sucrose solutions were prepared containing respectively, 18%, 22%, 26%, 30%, 34%, 38%, 42%, 46%, 50%, 54% and 60% (w/v) sucrose / 10 mM HEPES, pH 7.5 / 1 mM MgCl₂. Starting with the 60% sucrose solution, 1 ml aliquot was loaded onto the bottom of a 13 ml centrifuge tube, the tube was put into liquid nitrogen until the solution was frozen, then 1 ml of the next solution was added. The freezing procedure was repeated for all the solutions. The gradients were stored at -80 °C. 4-5 hours prior to use, the gradients were put at 4°C for slow thawing.

3.4.11 Analytical separation of protein complexes by gel filtration

The pellet from a 500 ml culture grown to mid-log phase was suspended in 6 ml of lysis buffer. Cells were lysed by vortexing with glass beads at 4°C. The supernatant was centrifuged for 1 h at 100.000g. 5 ml of the supernatant were loaded onto a Sephacryl S-400 or a Sephacryl S-300 column (Pharmacia). The column was eluted at 0.5 ml/min and 2 ml fractions were collected. Proteins from each fraction were separated by SDS-PAGE, transferred to nitrocellulose filters and probed with different antibodies. The chemiluminescence signals were quantified with a Lumi-Imager.

<u>lysis buffer</u>	20 mM	HEPES, pH 7.0
	150 mM	KOAc
	5 mM	MgOAc
	250 mM	Sorbitol
	0.5%	CHAPS
	2 mM	Pefabloc
		protease inhibitors EDTA free (cocktail tablets, Roche)

3.4.12 Affinity binding assay with GST-fusion proteins

E. coli or *S. cerevisiae* strains expressing the desired GST-fusion protein were lysed as described before (3.4.7). The proteins were solubilized in lysis buffer and

immobilized on glutathione sepharose 4B beads. 200 μ l yeast protein extracts (500-1000 μ g) were added to 1-2 μ g recombinant protein bound to 30 μ l glutathione sepharose beads, and incubated at 4 °C for 1-2 h with end-over-end rotation. The beads were washed 4 times with 1 ml lysis buffer and subsequently resuspended in Laemmli buffer, boiled and analyzed by SDS-PAGE and immunoblotting.

<u>Lysis buffer</u>	25 mM	HEPES, pH 7.0
	150 mM	KOAc
	5 mM	MgCl ₂
	1 mM	DTT
	1 mM	EDTA
	1%	Triton X-100
		protease inhibitors (cocktail tablets, Roche)

3.4.13 Immunoprecipitation

The cell pellets from 50 ml cultures grown to mid-log phase were resuspended in 1.5 ml of lysis buffer. The cells were lysed by vortexing with glass beads at 4°C (3.4.7.b). The lysates were centrifuged for 30 min at 16.000g at 4°C. The supernatants were incubated for 30 min at 4°C with 100 μ l of Protein A/G Sepharose-4B fast flow (Pharmacia) with end-over-end rotation. After centrifugation (in a table centrifuge for 1 min at top speed) 600 μ l of the supernatant were transferred to a new tube, and 100 μ l of Protein A/G Sepharose-4B, previously coupled with anti-MYC, or anti-HA antibodies, and 10 μ l of 10% BSA were added. The samples were then incubated for 1.5 h at 4°C with end-over-end rotation. After centrifugation at 5.000g for 1 min, the supernatant (S) was transferred to a new tube and an equal volume of 2x Laemmli sample buffer was added. The beads with the immunoprecipitated bound proteins (IP) were washed three times (for 5 min each) with 1 ml lysis buffer and twice with PBS, resuspended in 60 μ l 1x Laemmli buffer and boiled for 3 min. 20 μ l from the IP sample (corresponding to 1/3 of the total IP) and 20 μ l from the supernatant sample (S) (corresponding to 1/70 of the total supernatant) were separated by SDS/PAGE, followed by immunoblotting with the desired antibodies. For more details see also (Harlow and Lane, 1999).

<u>lysis buffer</u>	20 mM	HEPES, pH 7.5
	150 mM	KOAc
	5 mM	MgOAc
	1%	Triton X-100
	2 mM	Pefabloc
		protease inhibitors (cocktail tablets, Roche)

Antibody coupling: 200 μg of antibody were added to 200 μl protein A/G sepharose and incubated at RT for 1 h with gentle rocking (protein A is recommended for rabbit polyclonal antibodies and for mouse monoclonal antibodies from IgG_{2a}, IgG_{2b}, IgG₃; protein G is recommended for mouse IgG₁ and rat monoclonal antibodies). The beads were washed twice with 2 ml of 0.2 M Sodium borate (pH 9.0) and resuspended in 2 ml of 0.2 M Sodium borate (pH 9.0). Dimethylpimelimidate (solid) was added to reach a final concentration of 20 mM (5.2 mg/ml) and the samples were incubated for 30 min at RT with gentle rocking. The reaction was stopped by washing the beads once with 0.2 M ethanolamine (pH 8.0) and incubating for 2 h at RT in 0.2 M ethanolamine (pH 8.0) with gentle mixing. Finally the beads were washed with PBS and resuspended in 1 ml PBS with 0.01% merthiolate. For more details see also (Harlow and Lane, 1999).

3.4.14 GAP assay

The small GTPases of the Ypt/Rab family have a low intrinsic GTPase activity which can be significantly accelerated by GTPase-activating proteins (GAPs). The GTP-bound form of the GTPase is the substrate for the GAP, the GDP-bound form of the GTPase is the product of the GAP-mediated hydrolysis reaction. The activity of a GTPase activating protein can be detected *in vitro* by one of the methods described in the sections below.

a) Quantitative HPLC-based GAP assay

The protocol is based on the method described by (Will *et al.*, 2001). The starting material for the assay are GTPases loaded with GTP and purified Gyp proteins.

GTP loading: After purification, the GTPases are bound to GDP, a condition which is stabilized by Mg^{2+} ions present in the buffer. The underlying principle of the method, which is being applied here, relies on the fact that the exchange activity of the substrate can be raised temporarily by a decrease in the concentration of free Mg^{2+} ions (for example by complexing them with EDTA). During this time, GTP offered in excess, will be exchanged for the (lost) GDP at the protein's binding site.

To 200 μl of purified Ypt/Rab protein solution (at least 80 μM) in GAP reaction buffer, a 50-fold molar excess of GTP (4 mM final concentration) and 4 μl of 0.5 M EDTA (10 mM final concentration) were added. The mixture was incubated at RT for 20 min and in the meantime two NAP5 columns (Pharmacia) were equilibrated with

ice-cold GAP reaction buffer (the next steps must be done in the cold room as fast as possible, because Ypt/Rab proteins intrinsically hydrolyze bound GTP). The mixture was passed over one of the columns at 4°C to separate the protein and free nucleotides. Drop-fractions were collected and protein-containing fractions (identified by Bio-Rad protein assay) were pooled and passed over the second column. The protein-bound GTP was assessed by HPLC analysis on a calibrated reversed phase 5 µm ODS Hypersil column (250x4.6 mm, Bischoff, Germany) run under isocratic conditions (Tucker *et al.*, 1986). Calibration of the column was done with GDP solutions (more stable than GTP) of known concentration. Guanine nucleotides were detected by their absorbance at 254 nm (see Fig. 4.5). Aliquots of the GTP-loaded GTPase were shock-frozen in liquid nitrogen and stored at -80°C.

GAP reaction and HPLC analysis: 2 nmols of GTP-loaded protein were incubated at 30°C together with 1-50 pmols (depending on their specific activity) of purified GAPs in 200 µl GAP reaction buffer (pre-warmed). To measure the intrinsic activity, the same reaction is done without GAP. Aliquots of 12 µl are taken at different intervals, pipetted into cooled tubes that are immediately transferred to liquid nitrogen. To determine the GTP/GDP ratio, the frozen aliquots are thawed in a boiling water bath for 30 seconds and immediately subjected to HPLC (see above). HPLC was performed at 1.5 ml/min with HPLC buffer on the HPLC system Gold (Beckman) with the pump module 126 and the detector module 166. From the GTP and GDP peak areas at each time point (see Fig. 4.5), the relative amount of GTP is calculated according to:

$$\frac{GTP}{GDP + GTP}$$

and plotted as a function of time that can be fitted with the simple exponential decay function:

$$y = Y_0 + e^{-kt}$$

where Y_0 is the GTP/(GTP+GDP) ratio at the start of the reaction and t is the interval time.

<u>GAP reaction buffer</u>	50 mM	Tris-HCl, pH 8.0
	5 mM	MgCl ₂
	1 mM	DTT
<u>HPLC buffer</u>	10 mM	Tetrabutylammonium bromide
	100 mM	K ₂ HPO ₄ /KH ₂ PO ₄ , pH 6.5
	0.2 mM	NaN ₃
	2-4%(v/v)	Acetonitrile

b) Kinetic analysis of GTPase-GAP interaction

As described in the Results Section 4.1.2, Gyp5p is a GAP for Ypt1p. Under single turnover conditions Ypt1p-GTP can be considered the substrate and Ypt1p-GDP the product of the reaction. As the intrinsic rate of GTP hydrolysis is negligible compared to the GAP-activated rate, Gyp5p is regarded as an enzyme despite the fact that the catalytic center of the reaction is present on Ypt1p. To calculate K_m and k_{cat} of the reaction an alternative method to that described by the classical Michaelis-Menten equation was used. With this method, as has been described for the interaction of Ras and Ras-Gap (Schweins *et al.*, 1996), K_m and k_{cat} can be calculated from a single reaction. The single reaction was started at a high substrate concentration (100 μ M Ypt-GTP or more). The concentration of Ypt-GTP after GAP addition, was determined by HPLC at different time points (at least 15). The fitting procedure involves numerical integration and simulation, and leads to a representation of the concentration of Ypt-GTP as a function of time (see Fig. 4.7). For this procedure the reasonable assumption was done that the reaction product (Ypt-GDP) does not interact with GAP. Data fitting was performed using a model file (kindly provided by Prof. R. Goody, MPI for Molecular Physiology, Dortmund, Germany) and the software "SCIENTIST" (Micromath, Salt Lake City, Utah, USA). The model file, below shown, defines the concentration of the GAP-Ypt-GTP complex (EC1) at a given time as a function of the K_m , of the concentration of GAP (E1) and of the concentration of Ypt-GTP (C1) at that time, and the rate (C1') at a given time as the product of the k_{cat} for the concentration of the ternary complex (EC1). The rate is entered as a differential equation into the model file. T= time, E1₀= starting concentration of the enzyme (GAP), C₀= starting concentration of the substrate (Ypt-GTP).

```
//MM model file according to R. Goody
IndVars: T
DepVars:C1, E1, EC1
Params:kcat, KM, E1o, C1o
EC1=E1*C1/KM
C1'=-kcat*EC1
E1o=E1+EC1
C1o=C1+EC1
0<E1<E1o
//Parameter values
kcat= 100
KM=100
E1o=0.01
C1o=200
//initial conditions
T=0
C1=C1o-(E1o/(1+KM/C1o))
```

c) Filter GAP assay

The assay is performed with a [γ^{32}]GTP loaded GTPase (Ypt1p in this work). 100 pmols of Ypt1p (pre-run over a NAP5 column to eliminate GDP present in the buffer) were incubated for 10 min with 200 μ l of exchange buffer (put on ice thereafter). To the mixture, $MgCl_2$ to a final concentration of 5 mM (so that the protein-GTP complex was stabilized) and GTP to a final concentration of 0.1 mM, were added.

<u>exchange buffer</u>	50 mM	Tris-HCl, pH 8.0
	2 mM	EDTA
	0.5 mg/ml	BSA
	1 mM	DTT
	0.5 μ M	GTP
	0.025 μ M	[γ^{32}]GTP (6000 Ci/mmol, NEN, DuPont)

Two OD₆₀₀ units of bacteria strains expressing different fragments of Gyp5p were sonicated in 100 μ l GAP reaction buffer (see 3.4.14.a). 10 μ l of the bacterial lysate were added to 10 μ l of the exchange mixture (described above) to which were added further 30 μ l of GAP reaction buffer. The reaction was allowed to proceed at 30°C for 30 min. 10 μ l (taken at time points 0 and 30 min) were vacuum-filtered through nitrocellulose filters (45 μ m BA-Filter, Schleicher and Schüll) with the help of a vacuum pump (Schleicher and Schüll). Free nucleotides and γ -phosphate pass through the filter while proteins together with the bound-nucleotides stay on the filters. The filters were washed 3 times with 3 ml washing buffer. Dried filters were overlaid with scintillation liquid (Quicksafe A, Zinsser, Germany) and subjected to scintillation counting. The hydrolysis of GTP was measured as decrease of the radioactivity trapped on the filters (due to the release of γ -phosphate).

<u>Washing buffer</u>	20 mM	Tris-HCl, pH 8.0
	5 mM	$MgCl_2$
	10 mM	NH_4Cl
	1 mM	2-ME

3.5 Antibody production

Antibodies against two fragments of human Sec24C protein were produced in rabbit according to standard procedures. Human 6His-Sec24C₍₃₆₃₋₅₂₂₎, Sec24C₍₃₆₃₋₅₂₂₎-6His and 6His-Sec24C₍₇₄₇₋₉₉₂₎ peptides were expressed in *E. coli* by using the plasmids

pQE30-KIAA0079₍₃₆₃₋₅₂₂₎, pQE50-KIAA0079₍₃₆₃₋₅₂₂₎, pQE30-KIAA0079₍₇₄₇₋₉₉₂₎ (see Table 7.6). The 6xHis-fusion protein fragments were purified under denaturing conditions as described before (3.4.9a), electroeluted from a gel (3.4.2) and used to immunize four rabbits. Two rabbits, n° 166 and n° 167, were immunized with a mix of 6His-hSec24C₍₃₆₃₋₅₂₂₎ and hSec24C₍₃₆₃₋₅₂₂₎-6His proteins; two rabbits, n° 168 and n° 169, were immunized with 6His-hSec24C₍₆₃₅₋₈₂₇₎ protein. Antibodies were first purified from serum over a protein-A sepharose column, then over Amino-Links plus coupling gel columns (PIERCE) coupled with purified MBP-hSec24C₍₃₆₃₋₅₂₂₎ or MBP-hSec24C₍₇₄₇₋₉₉₂₎ proteins (produced in bacteria using the plasmids pMAL-KIAA0079₍₃₆₃₋₅₂₂₎ and pMAL-KIAA0079₍₆₃₅₋₈₂₇₎) according to the manufacturer's recommendations. For more details about antibody production and purification see (Harlow and Lane, 1999).

3.6 Microscopic analysis

3.6.1 Indirect immunofluorescence of yeast cells

Indirect immunofluorescence of yeast cells was performed with a modified method after (Pringle *et al.*, 1991). Yeast cultures were grown to an OD₆₀₀ of 0.7-1.2. 10 ml cells were harvested by centrifugation for 3 minutes at 1.000g, resuspended in 1 ml fixative buffer and left at RT for 1-2 hours. Cells were then centrifuged for 1 min at 5.000 rpm (Eppendorf centrifuge), washed once with PBS/10%sorbitol, resuspended in 1 ml PBS/10%sorbitol to which were added 5 µl 2-ME and 20 µl 10 mg/ml zymolyase T-100. The cell mixture was incubated at 30°C for an appropriate period of time (~1h). After spheroplasting cells were collected by centrifugation at 2.000 rpm for 1 min, washed once with 1 ml of PBS/10%sorbitol and resuspended in 0.5-1 ml PBS/10%sorbitol. 15-20 µl of the cell suspension were put on a polylysine-coated multi-well slide and allowed to attach for 10-15 minutes. The supernatant was removed by suction and blocking solution added to block unspecific binding sites. After 15-20 minutes the liquid was removed again and 15 µl of the first antibody (adequately diluted in blocking solution) were added. Incubation was allowed to proceed at room temperature in a moist chamber for an appropriate period of time. Hereafter the supernatants were removed and the slides washed 10 times with PBS/10%sorbitol. 20 µl of the fluorochrome-conjugated secondary antibody (Cy3-conjugated) were added (1:400 dilution). After incubation in a dark moist chamber for 2-3 hours at RT, the supernatant was removed and the slides washed 10 times with

PBS/10% sorbitol. 20 μ l of DAPI solution were added (1:1000 dilution in PBS/10% sorbitol, from a 1mg/ml stock solution) and incubated in the dark for 5 minutes. After washing twice again with PBS, a sufficient amount of mounting medium was pipetted onto the slides (along the middle ridge) and a 60 mm cover slip carefully put on top. After removing (squeezing out) excess of mounting medium, the edges were sealed with nail-polish. Finally, the sealed slides were rinsed with tap water before microscopic inspection.

<u>fixative buffer</u>	3.5% (v/v) Paraformaldehyde 10% (w/v) Sorbitol 1x PBS
<u>blocking solution</u>	1% (w/v) BSA 1% (w/v) Triton X-100 10% (w/v) Sorbitol 1x PBS
<u>mounting medium</u>	1mg/ml p-Phenylenediamine 90% Glycerol 1X PBS (pH 8.5-9.0 adjusted with 0.5M Na ₂ CO ₃)

3.6.2 Vacuole detection by FM 4-64 staining

The lipophilic styryl dye N-(3-triethylammoniumpropyl)-4-(p-diethylaminophenyl)-hexatrienyl pyridinium dibromide (FM 4-64) is a vital stain that can be used to follow membrane internalization and transport to the vacuole in yeast. The method used is basically that described in (Vida and Emr, 1995). 10 OD₆₀₀ cells from a logarithmic growing culture were harvested and resuspended in 250 μ l YEPG medium. 0.5 μ l of 16 mM FM 4-64 (stock solution of 16 mM FM 4-64 in DMSO) were added. Cells were then incubated at 30°C for 15 min with shaking. Subsequently cells were harvested, washed one time with YEPG, resuspended in 1 ml YEPG medium and incubated at 30°C for 1 h. After this chase period, cells were harvested at 700g for 3 min, resuspended in 250 μ l water placed on standard slides and viewed. To immobilize the cells, the coverslips were treated with 1 mg/ml solution of concavalin A and air dried before use. A 564 nm filter was used to detect FM 4-64 fluorescence under a fluorescence microscope.

3.6.3 Indirect immunofluorescence of mammalian cells

CV1 and Hela cells were grown on round (1 cm \varnothing) sterilized coverslips to about 15% confluence. The coverslips were transferred to a ceramics mini racket (Coors,

USA), washed 3 times with cold PBS then fixated putting the racket for 4 min in cold methanol followed by 4 min in cold acetone. Subsequently they were washed once with PBS and put for 5 min in 0.1% saponin solution that permeabilize cell membranes. Coverslips were transferred to a moist chamber (put on wet filter paper with the side containing the cells up) and 20 μ l of the first antibody (adequately diluted in TBS containing 0.5 mg/ml BSA) were added. Incubation was allowed to proceed at 37°C for 1h. After washing the coverslips 3 times with PBS, 20 μ l of the fluorochrome-conjugated second antibody, adequately diluted in TBS/0.05% BSA, were added (Oregon Green 488 conjugated antibody, 1:500 dilution, or Rhodamine Red-X conjugated antibody, 1:100 dilution). Incubation was allowed to proceed at 37°C for 1 h. After that the coverslips were washed 3 times with PBS. One drop of embedding medium was added to each of them and subsequently they were mounted on a microscope slide and sealed with nail-polish.

Embedding medium preparation:

6g	Glycerol
+ 2,4 g	MOWIOL, stirr 1 h at RT
+ 6 ml	sterile distilled water, stirr 2 h at RT
+ 12 ml	0.2 M Tris-HCl, pH 8.5

-Heat up to 50°C for 10-15 min stirring.
-Centrifuge at 5.000g for 15 min.
-Store at -20°C.

3.7 Electron microscopic analysis of yeast cells

Electron microscopy analysis has be done by Dr. H. H. Trepte (this department). Cells were fixated either with potassium permanganate and processed as described previously (Benli *et al.*, 1996) or by freeze-fixation/freeze-substitution as follows. Yeast cultures were grown to an OD₆₀₀ of 0.7-1.2. 5 μ l of cell pellet were freeze fixated on a copper mirror chilled to -190°C in liquid nitrogen. For freeze-substitution, the samples were soaked in 0.2% uranyl-acetate/acetone solution and maintained at -85°C for three days. The samples were then allowed to warm slowly (in 10 hours) to -35°C. After that the substitution medium was replaced with cold acetone. During the next two days the samples were infiltrated with increasing concentration of HM20 resin. The resin was polymerized for two days at -35°C and for one day at +15°C.

3.8 DNA and protein sequence computer analysis

Here are listed some of the programs used. DNA sequences analysis and alignment in contigs were done with "SEQUENCHER" (Gene Code, Michigan, USA). Primer analysis with "OLIGO" (Med Probe, Sweden). For molecular and atomic visualization WebLab Viewer was used.

For multiple sequence alignments "clustal-w" was used (available at <http://www2.ebi.ac.uk/clustalw/help.html> or at <http://dot.imgen.bcm.tmc.edu:9331/multi-align/multi-align.html>). Other sequence analysis tools are available at the ExPASy site: <http://www.expasy.ch/>; or at the NPSA (network protein sequence analysis) site: <http://pbil.ibcp.fr/>. It is possible to retrieve sequences from different databases (such as GENE BANK, EMBL, TREMBL, SWISSPROT etc.) at the SRS (Sequence Retrieval System) site: <http://www.embl-heidelberg.de/srs5/>. For sequences database search, "WU-Blast2" or "Fasta3" were used, both available at the EBI (European Bioinformatics Institute) site: <http://www2.ebi.ac.uk/>. Other important database sites are: MIPS (Munich Information Centre for Protein Sequences) <http://www.mips.biochem.mpg.de/>; SGD (*Saccharomyces* Genome Database) <http://genome-www.stanford.edu/Saccharomyces/>; and the proteome database <http://www.proteome.com/databases/index.html>.

4 RESULTS

In this work, two different topics on ER-to-Golgi transport were treated, one regarding the characterization of the Ypt1p-GAP Gyp5p, the second one regarding the characterization of Sec24p family proteins. Therefore, the results will be divided into two sections in which the two topics will be considered separately. In addition, there will be a short third section regarding a new tagging technique that has been invented during my work.

4.1 SECTION I (Gyp5p)

4.1.1 Cloning and expression of different fragments of *GYP5*

By a sophisticated computer search (Neuwald, 1997), many proteins sharing a common domain with Ypt/Rab-specific GTPase-activators, were found. We named this domain the "GYP domain". The protein product of the ORF *YPL249c* was in this group, and we called it Gyp5p since other Ypt-GAP proteins had already been characterized and named "Gyp" (the acronym "Gyp" stands for "GAP for Ypt"); see Introduction 1.4.4. The eight Gyp proteins characterized to date are quite different in size and amino acid composition (see Table 1.3, and Fig. 4.1).

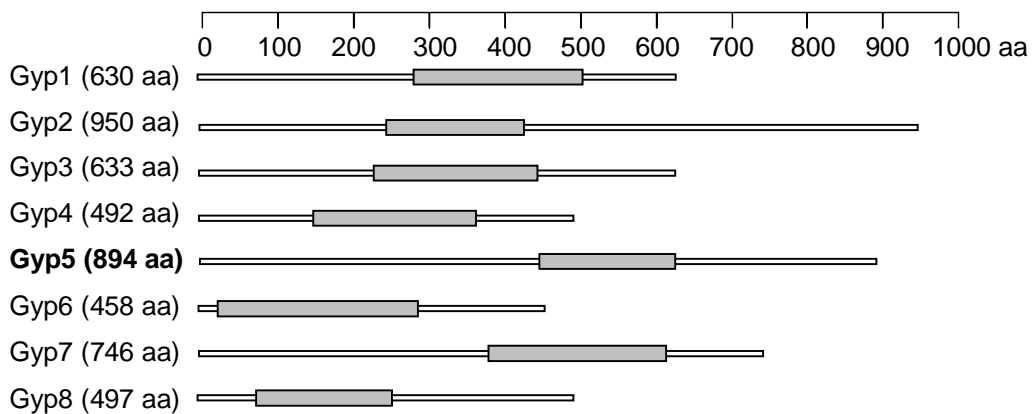


Fig. 4.1 Schematic representation of the eight Ypt/Rab-GAP proteins showing the "GYP domain" as gray rectangles.

They share sequence homologies only in the "GYP domain" in which it is possible to distinguish six conserved motifs (A-F) harboring the highly conserved "fingerprint sequences" (RxxW, IxxDxxR, YxQ) (see Figs. 4.2 and 5.2).

In Fig. 4.2, the alignment of Gyp5p and Gyp1p sequences is shown. The crystal structure of the Gyp1 catalytic domain (Fig. 1.9) (Rak *et al.*, 2000) confirmed that the conserved amino acids are located in critical positions for either the active site or for the conservation of the structure of the protein (see Fig. 5.2).

Different fragments of the Gyp5 protein were expressed as 6xHis fusion proteins. The different peptides obtained are shown in Fig. 4.3. The different DNA fragments were obtained by PCR amplification using the primers schematically shown by arrows in Figs. 4.2 and 4.3 (for the primer sequences, see Appendix Table 7.7). The PCR fragments were cloned into pET30 or pET32 vectors (see Table 7.6). For simplicity, I called the different fragments pep0-pep14. Except for Gyp5₍₈₋₄₄₈₎ (pep0_B) and Gyp5₍₈₋₈₉₂₎ (pep1_B) which were cloned as NcoI-NotI restriction fragments into pET32, and which were expressed in bacteria as fusion proteins with N-terminal Trx-6xHis-S-tags (see 3.4.8.a), all others were cloned into pET30 as NdeI-SalI restricted fragments, and were expressed in bacteria as fusion proteins with C-terminal 6xHis-tags. The "GYP domain" of Gyp5p is contained between amino acids 451-624 (highlighted in Fig. 4.3, by a red frame).

The GAP activity on Ypt1p was assayed for all the different constructs by the filter assay (see Methods 3.4.14.c), pep2 and pep5 were also tested by the HPLC-GAP-assay (3.4.14.a). The fragments, which have retained or which have lost the GAP activity for Ypt1p, are indicated in Fig 4.3 by "+" or "-". The data clearly show that there is a region downstream of the "GYP domain" (up to the amino acid 759) that is required for the catalytic activity. Instead, the N-terminal part (up to amino acid 429, and probably up to amino acid 451) is not important for its catalytic activity. Computer analysis with the program COILS (Lupas *et al.*, 1991) revealed also a potential coiled-coil region at C-terminus of Gyp5p (between amino acids 730-870).

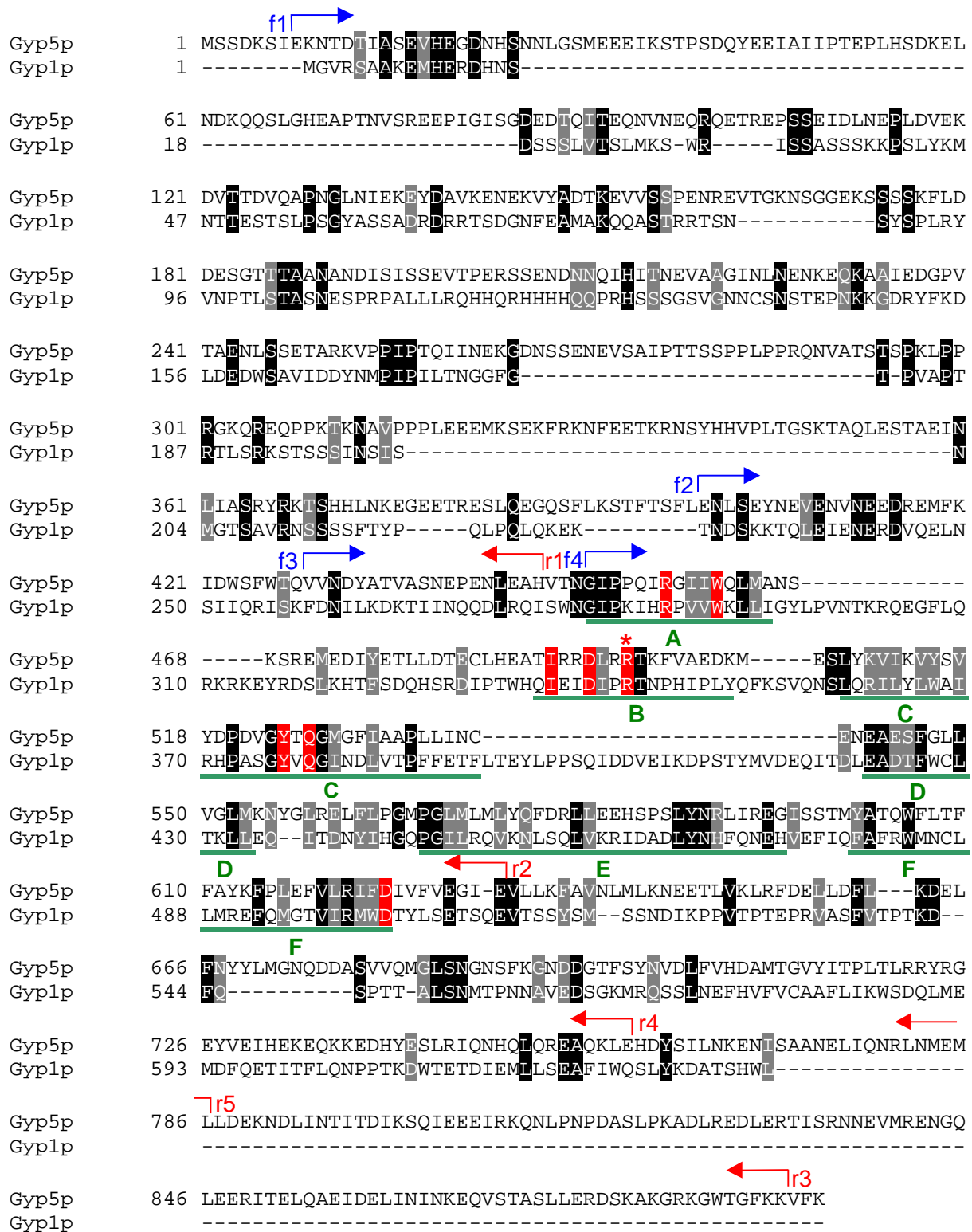


Fig. 4.2 Alignment of Gyp5p and Gyp1p sequences. Identical or similar amino acids are shown on black or shaded background, respectively. The six conserved motifs (A, B, C, D, E, F) are indicated by green bars [Neuwald A. F., 1997 ; Raket *et al.*, 2000]. The conserved amino acids of the "fingerprint sequences" RxxxW, IxxDxxR and YxQ and the conserved aspartic acid (D502 in Gyp1p and D624 in Gyp5p) are highlighted in red. The critical catalytic arginine (R343 in Gyp1p and R496 in Gyp5p) is indicated by an asterisk. Blue and red arrows represent the forward (f) and the reverse (r) primers used to amplify different fragments of *GYP5*.

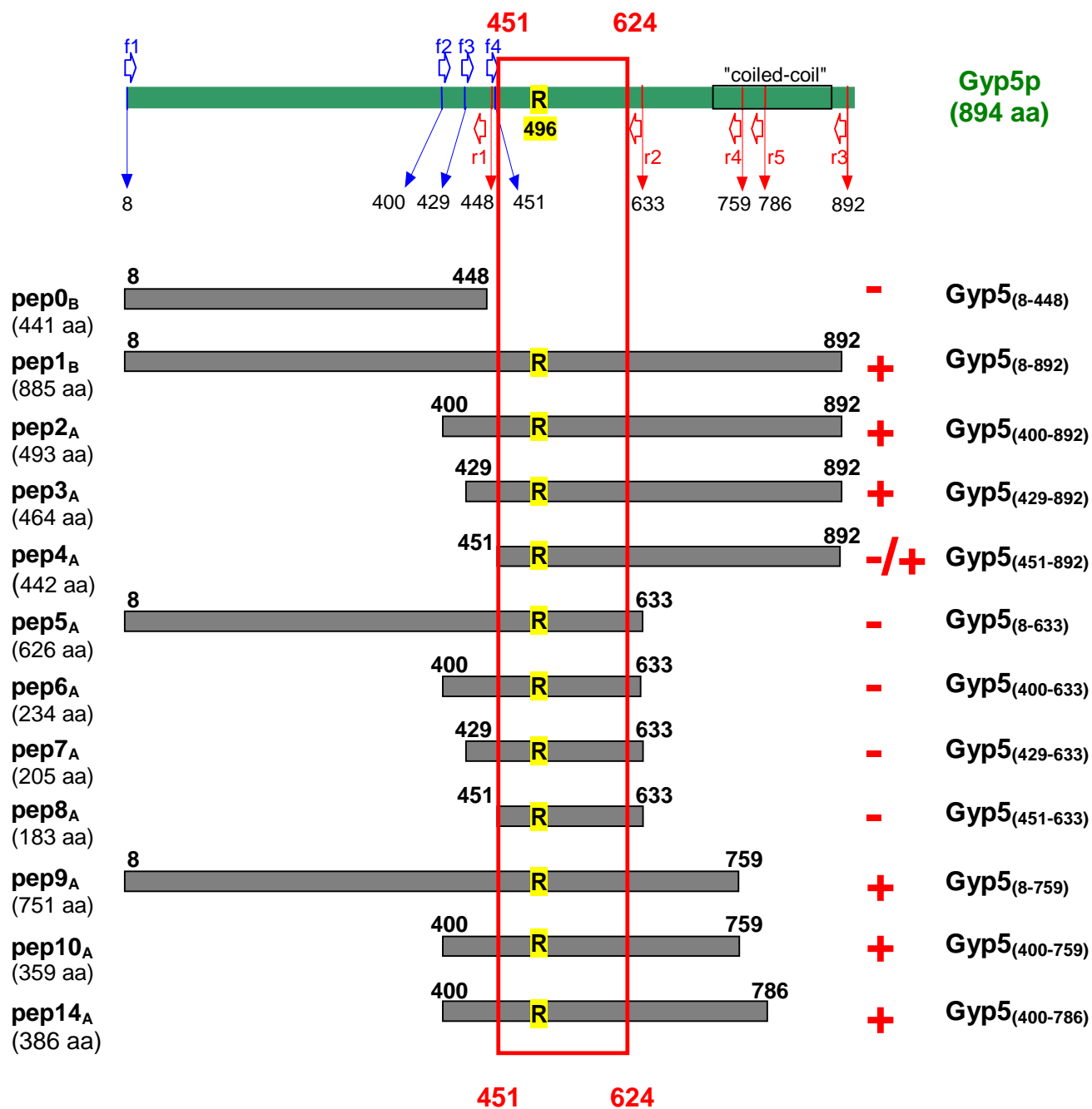


Fig. 4.3 Schematic representation of Gyp5p and its different fragments expressed as 6xHis fusion proteins in bacteria (see Table 7.6). Arrows represent the forward (f) and reverse (r) primers used to amplify the fragments from genomic DNA for subsequently cloning into pET30 or pET32 vectors (see also Fig. 4.2). Fragments showing GAP activity on Ypt1p (determined by a filter test) are indicated by "+"; when the catalytic activity is lost, they are indicated by "-". The critical catalytic arginine-496 is highlighted in yellow. The "GYP" domain" is contained inside the red frame (between amino acids 451-624). A putative coiled-coil region is contained between amino acids 730-870.

4.1.2 Ypt1p is the preferred substrate for Gyp5p

Gyp5p₍₄₀₀₋₈₉₂₎-6His (pep2_A) was expressed in *E. coli*, purified as described in Methods 3.4.9.g on Ni-NTA resin, and subsequently by anion exchange and gel filtration chromatography, see Fig. 4.4. The purified protein was stored frozen or used in GAP assays.

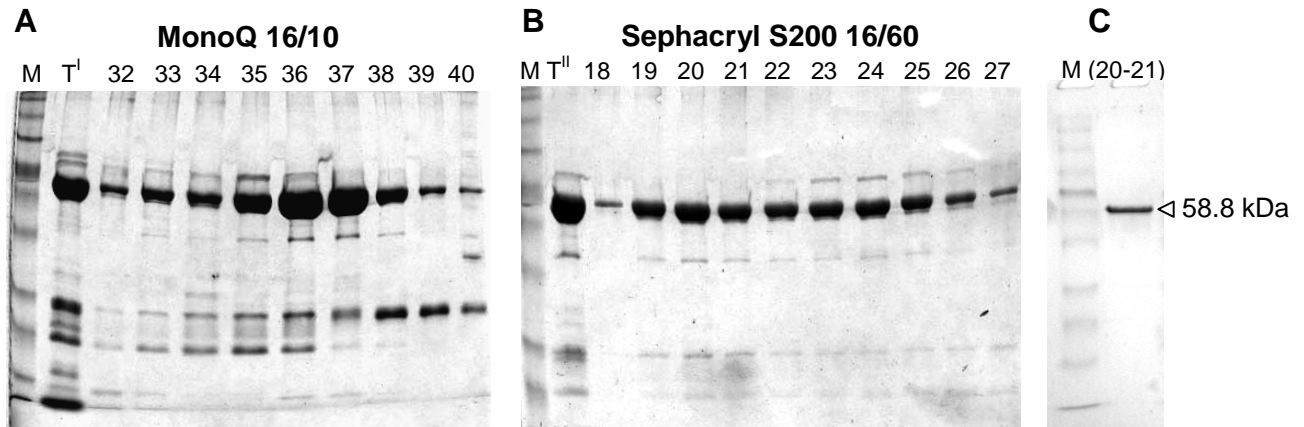


Fig. 4.4 Gyp5p₍₄₀₀₋₈₉₂₎-6His was produced in *E. coli* and purified on Ni-NTA resin. (A) The eluted protein (T^I is the protein sample after Ni-NTA purification) was further purified by anion exchange chromatography and subsequently (B) by gel filtration chromatography. Fractions 35-37 (T^{II}) from MonoQ columns were loaded on Sephacryl-200 column. Fractions 19-21 and 22-25 were pooled separately. (C) 5 μ l of the pooled fractions 19-21. The purity achieved at this stage was greater than 95%. M= Molecular mass marker.

The GAP activity of Gyp5p₍₄₀₀₋₈₉₂₎-6His (for simplicity, named Gyp5p₍₄₀₀₋₈₉₂₎ in the following sections) was tested with different GTPases in a standard HPLC-based GAP assay (3.4.14.a). 20 μ M GTP-loaded GTPases were incubated with 0.1 μ M Gyp5p₍₄₀₀₋₈₉₂₎ at 30°C, and aliquots were taken at different time points. Each sample was subjected to HPLC that allows to separate GDP from GTP (see Fig. 4.5). With the help of the "Gold-System-software", the peak areas were evaluated and the relative GTP amount $GTP/(GDP+GTP)$, at each time point, was calculated. These values were plotted as a function of time that can be fitted with the simple exponential decay function: $y = Y_0 + e^{-kt}$. Y_0 is the $GTP/(GTP+GDP)$ ratio at the start of the reaction, t is the incubation time and k represents the rate constant of the reaction. The different GTPases have different intrinsic GTP hydrolysis rates (see Table 4.1) that can be accelerated several-fold by GAP proteins. The acceleration

rate of the reaction in the presence of its GAP is given by the ratio between the GAP-catalyzed GTP hydrolysis rate and the intrinsic hydrolysis rate.

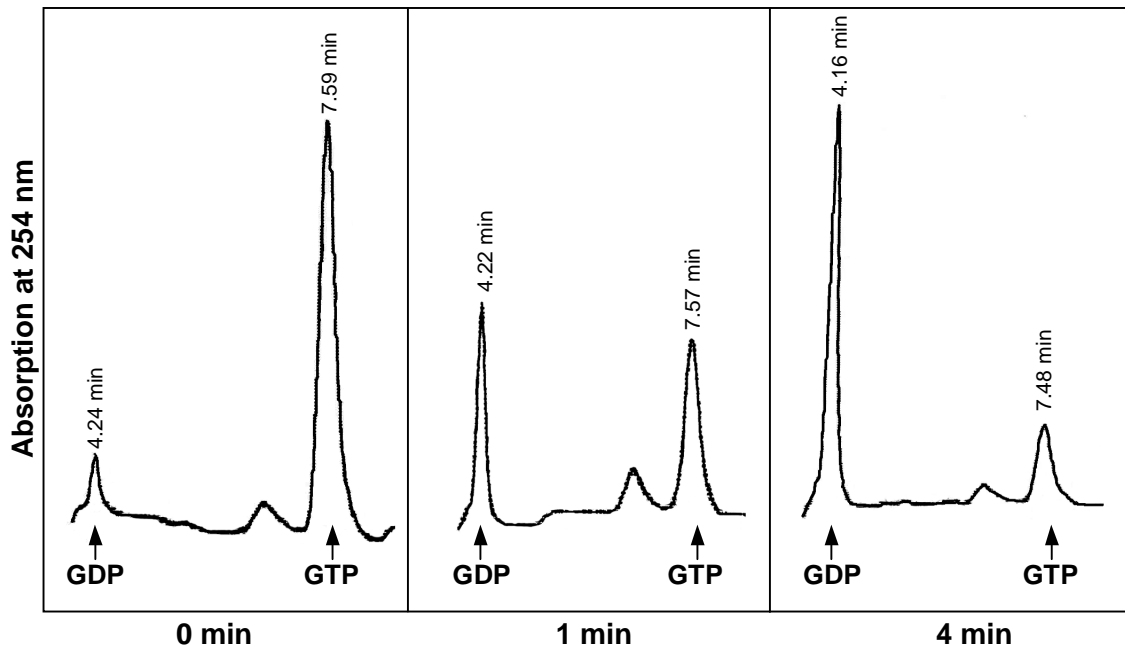


Fig. 4.5 Analysis of GTP hydrolysis through separation of the guanosine nucleotides by HPLC. GDP is detected after ~ 4.2 min, GTP after ~ 7.5 min. 20 μ M Ypt1p-GTP was incubated with 0.1 μ M Gyp5p₍₄₀₀₋₈₉₂₎ at 30°C for 0 min, 1 min and 4 min (standard HPLC-based GAP assay). Samples were shock-frozen in liquid nitrogen and boiled for 30 sec before being injected into the HPLC apparatus (see Methods 3.4.14.a-b). With the "Gold-System-Software", the peak areas are calculated and the ratio GTP/(GDP+GTP) can be calculated.

Table 4.1 Intrinsic GTP hydrolysis rates of Ypt GTPases measured at 30°C

GTPase	GTP hydrolysis rate (min ⁻¹)
Ypt1p	0.0035
Sec4p	0.0013
Ypt31p	0.0072
Ypt32p	0.0062
Ypt6p	0.0004
Ypt7p	0.0027
Ypt51p	0.0059
Ypt52p	0.0989
Ypt53p	0.0065

The acceleration of intrinsic GTPase activity of different Ypt-GTPases induced by Gyp5p₍₄₀₀₋₈₉₂₎ is documented in Fig. 4.6. Ypt1p is by far the best substrate for Gyp5p. Also the Sec4p GTPase activity is accelerated but, in comparison with Ypt1p, much less efficiently .

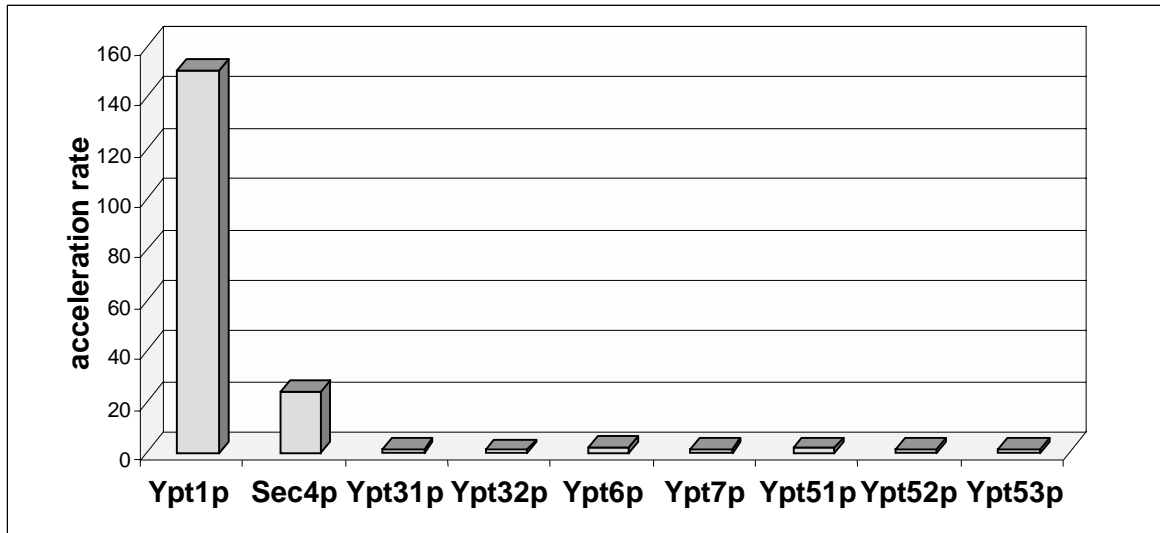


Fig. 4.6 Specificity of the Gyp5₍₄₀₀₋₈₉₂₎ protein for different GTPases, as determined by standard HPLC-based GAP assay. 20 μ M GTP-loaded GTPases were incubated at 30°C with or without 0.1 μ M Gyp5p₍₄₀₀₋₈₉₂₎. The ratio of the GTP hydrolysis velocity with and without GAP (intrinsic GTPase activity), gives the acceleration rate. The best, if not the only, substrate for Gyp5p is Ypt1p. The data are the average of two independent experiments.

4.1.3 Kinetic investigation of the Gyp5p/Ypt1p interaction

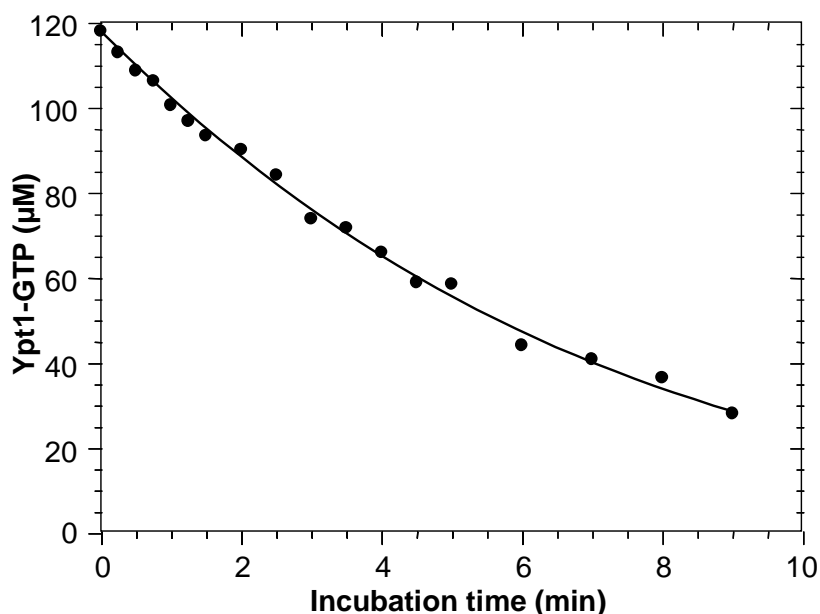
To characterize the efficiency of the catalysis, the kinetic constants of the Gyp5p/Ypt1p interaction were determined. Ypt1p-GTP can be considered the substrate, Ypt1p-GDP the product of the reaction, and Gyp5p is regarded as the enzyme. The Michaelis-Menten model says that the velocity of the reaction will increase with increasing substrate concentrations and asymptotically reach a saturation value (V_{max}). By dividing V_{max} by the enzyme concentration, one gets the maximal number of substrate molecules which an enzyme molecule can chemically transform within a given period of time (k_{cat}). The substrate concentration at the half-maximal reaction velocity (K_m) can be regarded as a measure for the affinity of an enzyme for its corresponding substrate. K_m is the Michaelis constant.

To calculate K_m and k_{cat} of the Gyp5p/Ypt1p reaction, an alternative method to the classical Michaelis-Menten equation was used. An integrated Michaelis-Menten

equation (Duggleby and Clarke, 1991) was used, that allows to calculate k_{cat} and K_m from a single time curve. The time curve is derived from a reaction with highly concentrated substrate. The absolute substrate concentration will decrease while the reaction proceeds (see Fig. 4.7). This method is generally applicable for stable enzymes which catalyze irreversible reactions with none of the reaction products having inhibitory effects.

The fitting procedure involves numerical integration and simulation, and leads to a representation of the concentration of Ypt-GTP as a function of time. This was performed using a model file (kindly provided by Prof. R. Goody, MPI for Molecular Physiology, Dortmund, Germany) and the software "SCIENTIST" (Micromath, Salt Lake City, Utah, USA) (see Methods, 3.4.14.b).

In Fig. 4.7, a time curve obtained from a reaction with 118 μM Ypt1p-GTP and 0.134 μM Gyp5p₍₄₀₀₋₈₉₂₎ is shown. The reaction was carried out at 30°C.



K_m (μM)	k_{cat} (s^{-1})	Activation (-fold)
400	9	1.6×10^5

Fig. 4.7 Kinetic analysis of Ypt1p-bound GTP hydrolysis accelerated by Gyp5p₍₄₀₀₋₈₉₂₎. 118 μM Ypt1p-GTP was incubated with 0.134 μM Gyp5p₍₄₀₀₋₈₉₂₎ at 30°C. K_m and k_{cat} values were calculated according to the integrated Michaelis-Menten equation using the program Scientist (as described in Methods 3.4.14.b).

From the integration of this curve and from two other curves, a K_m of 400 (μM) and a k_{cat} of 9 (s^{-1}) were calculated. This means that Gyp5p does not have a high affinity for its substrate GTPase, but the turnover rate is quite high. With an intrinsic GTP hydrolysis rate of 0.0035 per minute, the GTPase activity is maximally accelerated 1.6×10^5 -fold by the action of Gyp5p₍₄₀₀₋₈₉₂₎. These values are comparable with values obtained for other GAPs (See Discussion, Table 5.1)

4.1.4 Arginine 496 is important for the catalytic activity of Gyp5p

It was shown previously, that Gyp1p and Gyp7p have a conserved arginine residue (in motif B) which is critical for the catalytic activity (Albert *et al.*, 1999). The "arginine finger" mechanism of the GTPase accelerating activity has been described for other GAP proteins, Ras-GAP and Cdc42p-GAP (Scheffzek *et al.*, 1998), (see Fig. 1.8). To verify whether this is also true for Gyp5p, the arginine-496 coding triplet was mutated to one for either alanine or lysine. The mutations were introduced into pET30-GYP5₍₄₀₀₋₈₉₂₎A by PCR (using the primers GYP5-R/A_f, GYP5-R/A_r, GYP5-R/K_f and GYP5-R/K_r; see Methods, 3.2.7 and Tables 7.6 and 7.7). The proteins Gyp5^{R496A}₍₄₀₀₋₈₉₂₎ and Gyp5^{R496K}₍₄₀₀₋₈₉₂₎ were produced and purified as described above (see 3.4.9.g and 4.1.2) and their GAP activity for Ypt1p was tested (for simplicity, I will call them Gyp5p^{R496A}, or Gyp5p^{R496K}). 20 μM GTP-loaded Ypt1p was incubated at 30°C with 0.2 μM Gyp5p^{R496A} or with 0.2 μM Gyp5p^{R496K} and the GTP hydrolysis was evaluated by HPLC. As shown in Fig. 4.8.A, both mutations have a dramatic effect on the catalytic activity. Both mutant proteins are unable (at the concentration used) to stimulate the GTPase activity while the wild type protein (0.1 μM Gyp5p₍₄₀₀₋₈₉₂₎) can accelerate the same reaction 200 fold. By strongly increasing the concentration of Gyp5p^{R496K} it is possible to see a weak enzymatic activity (see Fig. 4.8.B). 55 μM GTP-loaded Ypt1p was incubated at 30°C with 11 μM Gyp5p^{R496K} or with 0.13 μM Gyp5p₍₄₀₀₋₈₉₂₎. While the wild type protein can accelerate the GTPase activity 61-fold, the mutant protein can accelerate it only 4-fold.

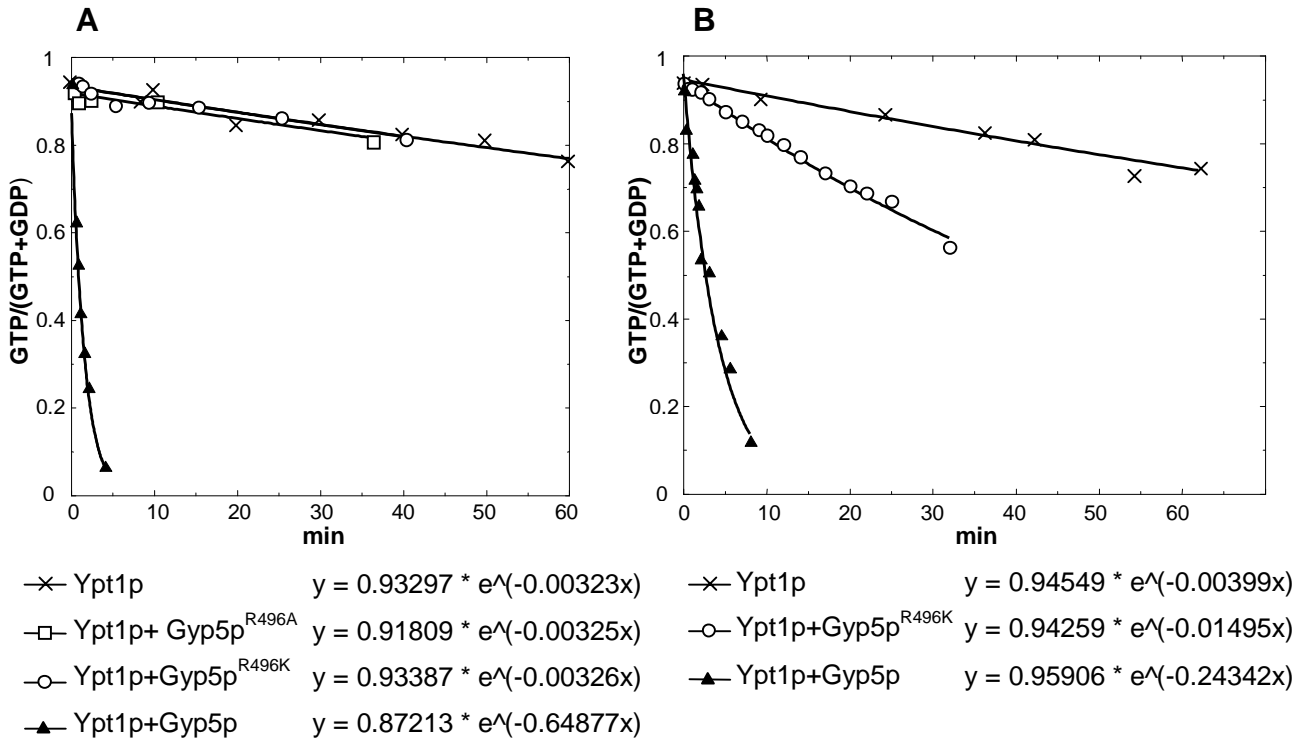
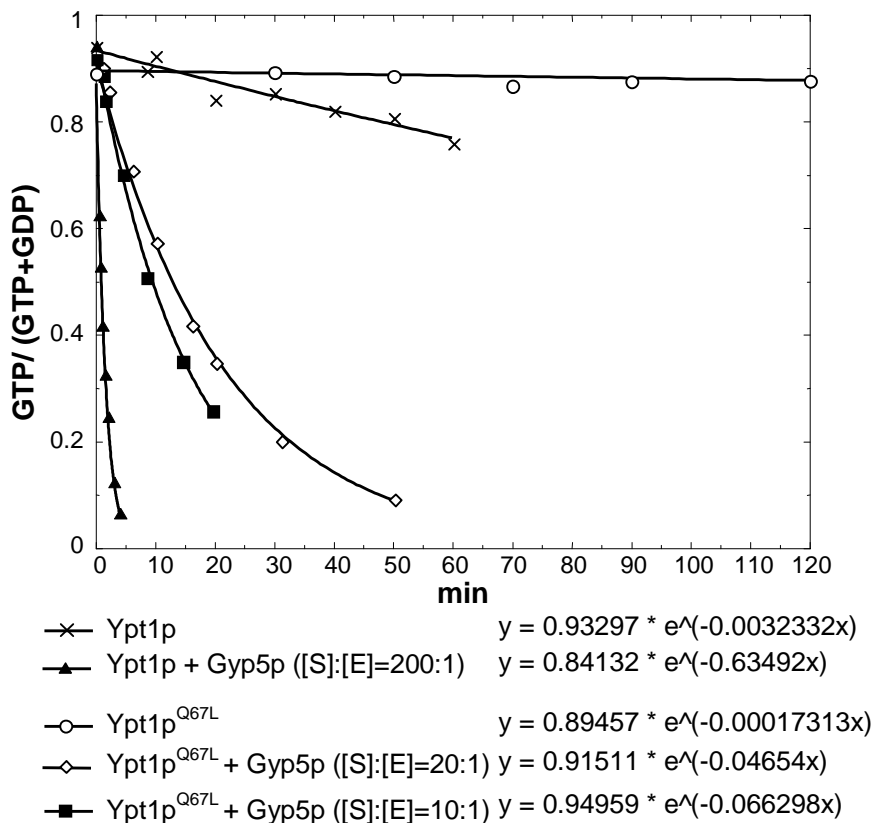


Fig. 4.8 Kinetic analysis of the Ypt1p-bound GTP hydrolysis acceleration induced by Gyp5₍₄₀₀₋₈₉₂₎ mutant proteins (Gyp5p^{R496A} and Gyp5p^{R496K}). **(A)** 20 μ M Ypt1p was incubated at 30°C together with 0.2 μ M Gyp5p^{R496A} or with 0.2 μ M Gyp5p^{R496K} or with 0.1 μ M Gyp5p₍₄₀₀₋₈₉₂₎. The mutant proteins are not able to accelerate the GTP hydrolysis at this concentration while the wild type can accelerate it 200-fold. **(B)** 55 μ M Ypt1p-GTP was incubated at 30°C together with 11 μ M Gyp5p^{R496K}, or with 0.13 μ M Gyp5p; GTPase hydrolysis is accelerated 61-fold by the wild type and 4-fold by the mutant protein.

4.1.5 Gyp5p can accelerate the GTPase activity of the Ypt1p^{Q67L} mutant

The Q67L mutation in Ypt1p is homologous to the well known oncogenic Q61L mutation of Ras that impairs its GTPase activity (Der *et al.*, 1986; Frech *et al.*, 1994). This glutamine residue in Ras is thought to form a hydrogen bond with an H₂O molecule which is positioned to attack the phosphoryl bond of GTP (Krengel *et al.*, 1990); see also Fig. 1.8. Importantly, Ras-GAP cannot accelerate the intrinsic GTPase activity of this mutant (Bollag and McCormick, 1991; Scheffzek *et al.*, 1997; Vogel *et al.*, 1988). The homologous mutation in many members of the Ras superfamily was shown to impair their GTPase activity, among them also a number of Ypt/Rab proteins: Rab2p^{Q65L} (Tisdale, 1999), Rab3Ap^{Q81L} (Brondyk *et al.*, 1993), Rab5p^{Q79L} (Stenmark *et al.*, 1994), Rab6p^{Q72L} (Martinez *et al.*, 1997), Sec4p^{Q79L} (Walworth *et al.*, 1992) and Ypt51p^{Q66L} (Singer-Kruger *et al.*, 1995).

To test whether Gyp5p could stimulate the GTPase activity of Ypt1p^{Q67L}, I introduced by PCR (using the primers *YPT1-Q/L_f* and *YPT1-Q/L_r*; see Methods, 3.2.7) this mutation in pET12c-*YPT1*. The protein was produced in *E. coli* and purified as described in 3.4.9.f (for GTP loading, see 3.4.14.a). 20 μ M GTP-loaded Ypt1p^{Q67L} was incubated at 30°C with 1 μ M and 2 μ M Gyp5p₍₄₀₀₋₈₉₂₎ and a kinetic analysis was done (Fig. 4.9). The intrinsic GTPase activity of Ypt1p^{Q67L} (0.00017 min⁻¹) is reduced ~20-fold in comparison to that of the wild type protein (0.003 min⁻¹). Nevertheless, Gyp5p is able to accelerate it several-fold: 269-fold when [Ypt1p^{Q67L}]:[Gyp5p] is 20:1, 382-fold when the ratio is 10:1.



GTPase	Gyp5p ₍₄₀₀₋₈₉₂₎	Acceleration GTPase activity (-fold)
Ypt1p (20 μ M)	0.1 μ M	196
Ypt1p ^{Q67L} (20 μ M)	1 μ M	269
Ypt1p ^{Q67L} (20 μ M)	2 μ M	382

Fig. 4.9 Gyp5p₍₄₀₀₋₈₉₂₎ can accelerate the intrinsic GTP hydrolysis of the GTPase-activity-deficient Ypt1p^{Q67L}. The reaction was done at 30 °C. "[S]:[E]" is [Substrate]:[Enzyme].

4.1.6 Mutant strains with different *GYP* genes deleted in combination with *ypt1*^{Q67L}

In order to understand the biological meaning of the GTPase-accelerating activity observed *in vitro*, the genes *GYP5*, *GYP1* and *GYP8* (Gyp1p and Gyp8p are

also GAPs for Ypt1p, see Table 1.3) were deleted in two different haploid yeast strains (MSUC-3D and the protease-deficient strain cl3-ABYS-86). The genes were deleted using *loxP-kanMX-loxP* cassettes and the PCR-based method described in the Section 3.3.2. The correct gene deletion was checked by both PCR and Southern blotting. Strains with one, two or the three *GYP* genes deleted didn't have any particular phenotype. Only a weak growth retardation at 15°C was observed in cl3-ABYS-86 $\Delta gyp5/\Delta gyp1/\Delta gyp8$ strains (ADY27 and ADY28) (data not shown). Since there was no evident mutant phenotype, it was decided to combine the deletions with *ypt1*^{Q67L}. To introduce the Q67L mutation into the yeast *YPT1* locus, the plasmid pRE-*YPT1*^{Q67L} was used (from U. Vespermann, this department); pRE-*YPT1* is described by (Schmitt *et al.*, 1988). This plasmid contains *ypt1*^{Q67L} in addition to the genomic flanking regions (where there are *TUB2* and *ACT1*; see Fig 4.10).

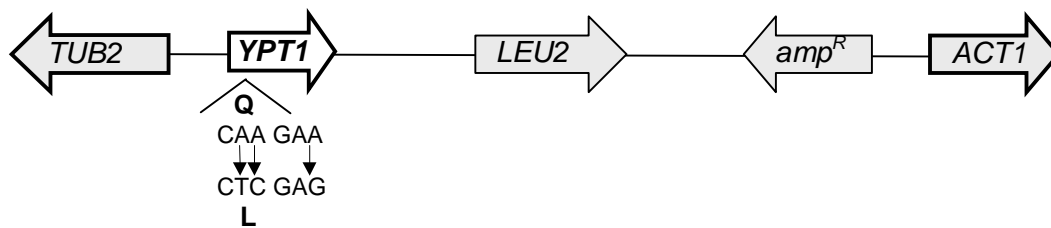


Fig. 4.10 Schematic representation of pRE-*YPT1*^{Q67L} linearized by HindIII digestion. An XhoI site is present in *ypt1*^{Q67L}. This "cassette" is used to transform yeast cells and in order to replace the wild type *YPT1* gene with the *ypt1*^{Q67L} allele.

Haploid strains with the different *GYP* genes deleted were transformed with linearized pRE-*YPT1*^{Q67L} and selected on LEU⁻ media. To check for the presence of the Q67L mutation, the *YPT1* gene was amplified by PCR (using the primers YPT1_f0 and YPT1_r0_b) and subsequently digested with XhoI (see Fig. 4.11). As shown in Fig. 4.11, when more than one *GYP* gene was deleted the probability of getting *ypt1*^{Q67L} was lower. This could be an indication of functional interplay of *YPT1*, *GYP5*, *GYP1* and *GYP8*.

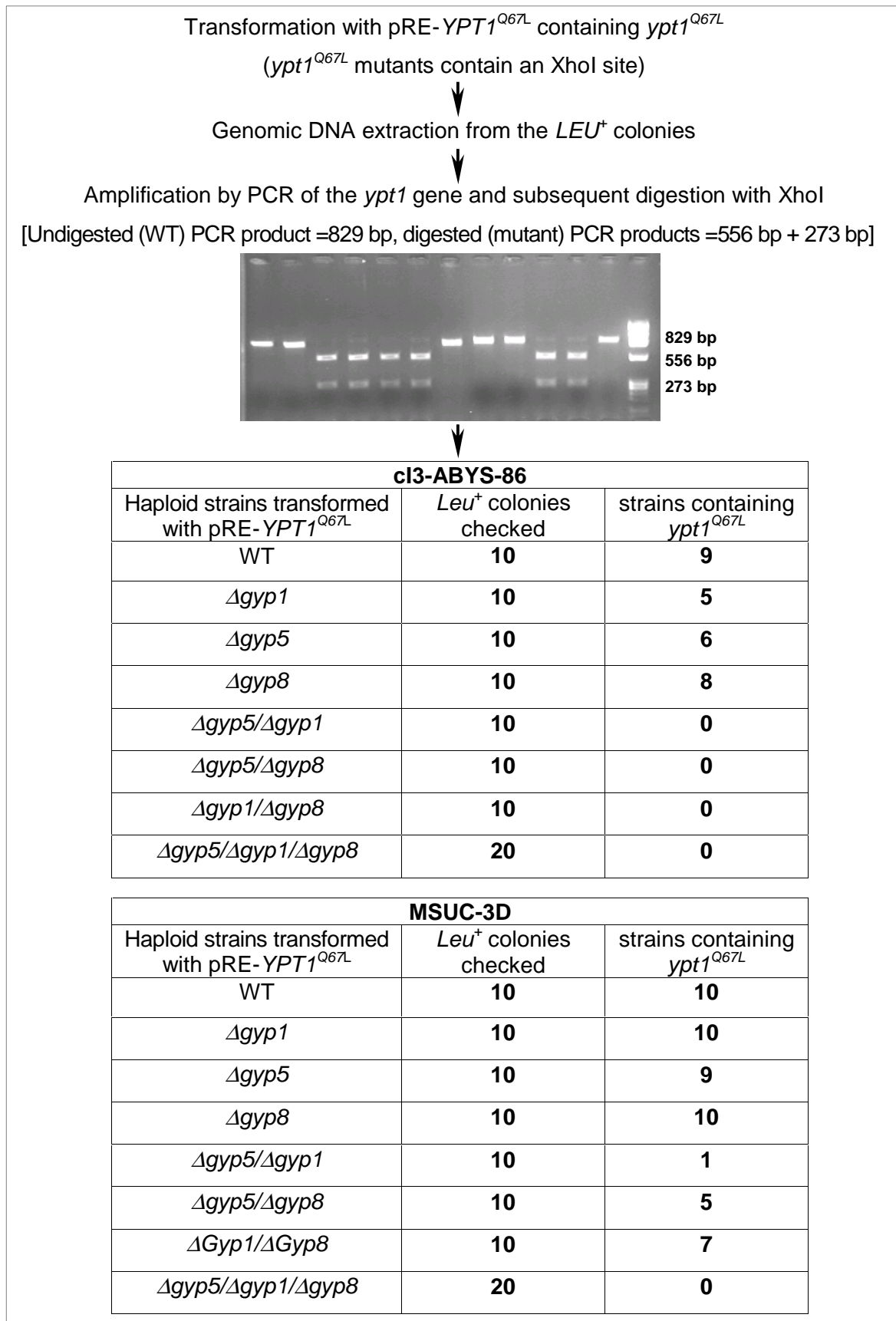


Fig. 4.11 Schematic view of the method to obtain *ypt1*^{Q67L} mutants, and their verification. It is evident that it is more difficult to obtain *ypt1*^{Q67L} mutants when more than one *GYP* gene is deleted.

4.1.7 Growth analysis of different strains carrying *ypt1*^{Q67L}

To assess the effect on cell growth of *ypt1*^{Q67L} alone or in combination with *GYP5*, *GYP1* or *GYP8* deletions, serial 10-fold dilutions of cells (see Methods 3.3.4) were spotted onto YEPG plates and grown at temperatures ranging from 15°C to 37°C (see Fig. 4.12 and Fig. 4.13). In the protease deficient strain cl3-ABYS-86, it was not possible to introduce the *ypt1*^{Q67L} mutation when more than one *GYP* gene was deleted, while in MSUC-3D *ypt1*^{Q67L} was obtained also in strains where two *GYP* genes were disrupted (see Fig. 4.11). *ypt1*^{Q67L}/ Δ *gyp7* (ADY32 and ADY52) strains were used as negative controls since Ypt1p is not a substrate for Gyp7p. A first observation was that mutants based on cl3-ABYS-86 strain background showed stronger growth defects than mutants based on MSUC-3D. The *ypt1*^{Q67L} mutant in the cl3-ABYS-86 genetic background (ADY29) was not able to grow at 15°C (see Fig. 4.12, lane 2, last panel) while *ypt1*^{Q67L} mutants in a MSUC-3D genetic background (ADY49) could grow at 15°C (see Fig. 4.13 lane 2, last panel). Interestingly, cell growth of MSUC-3D based mutants at 15°C was dramatically slowed down when, in combination with *ypt1*^{Q67L}, *GYP5* was deleted (see Fig. 4.13, last panel, lane 5, 7 and 8). The cl3-ABYS-86 *ypt1*^{Q67L}/ Δ *gyp5* strain (ADY31) showed a defect in growth already at 20°C (see Fig. 4.12, lane 4, fourth panel). The strains *ypt1*^{Q67L}/ Δ *gyp1* or *ypt1*^{Q67L}/ Δ *gyp8* (in both cl3-ABYS-86 and MSUC-3D genetic background) did not show a growth defect at low temperatures. The cl3-ABYS-86 based *ypt1*^{Q67L}/ Δ *gyp8* (ADY33) showed a growth retardation at 37°C. The MSUC-3D based strains with *ypt1*^{Q67L} combined with double *GYP* deletions (*ypt1*^{Q67L}/ Δ *gyp5*/ Δ *gyp1*, ADY54; *ypt1*^{Q67L}/ Δ *gyp5*/ Δ *gyp8*, ADY55; *ypt1*^{Q67L}/ Δ *gyp1*/ Δ *gyp8*, ADY56) showed slower growth at all temperatures, but the strongest effect was in the strains lacking *GYP5*. The growth of these strains at 15°C was almost completely blocked (see Fig. 4.12, last panel).

From these data it became evident that *ypt1*^{Q67L} mutants show a stronger growth defect at low temperature when *GYP5* is missing. This was the first indication supporting the importance of GTP hydrolysis for the function of Ypt1p, and for a role *in vivo* of Gyp5p as Ypt1p-GAP.

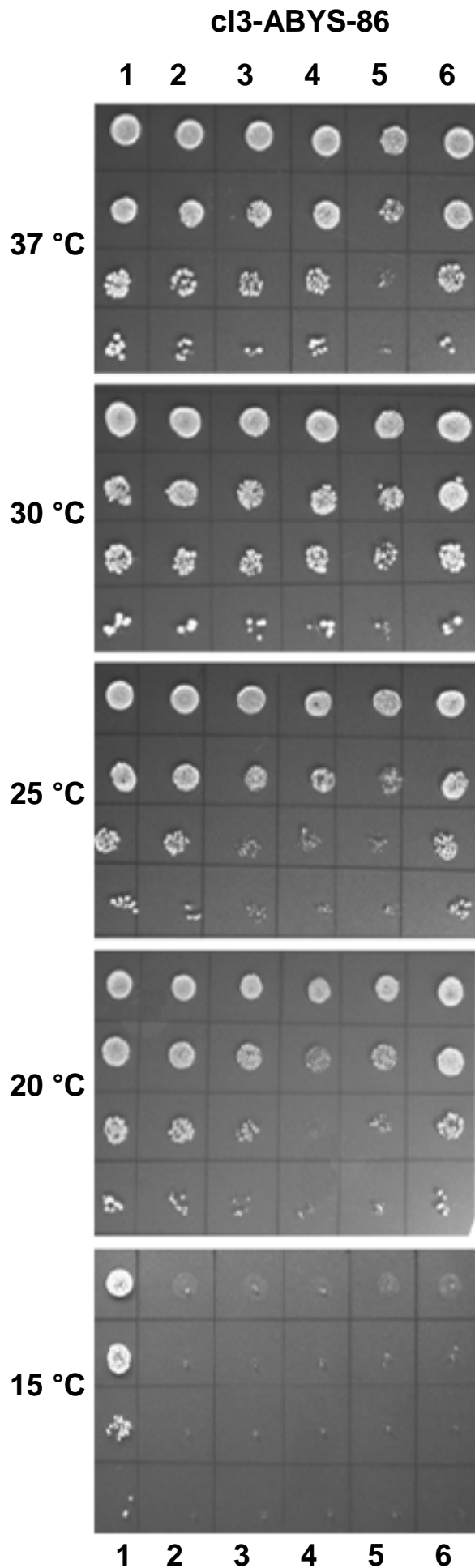


Fig. 4.12 Synthetic growth defect analysis of the strains

1) **wt** (cl3-ABYS-86)

2) ***ypt1^{Q67L}*** (ADY29)

3) ***ypt1^{Q67L}/Δgyp1*** (ADY30)

4) ***ypt1^{Q67L}/Δgyp5*** (ADY31)

5) ***ypt1^{Q67L}/Δgyp8*** (ADY33)

6) ***ypt1^{Q67L}/Δgyp7*** (ADY32)

(for genotype description, see Appendix Table 7.2).

10-fold serial dilutions of cells (starting at 0.01 OD) were spotted on YEPG plates and grown at different temperatures for 3 days, (7 days at 15° C).

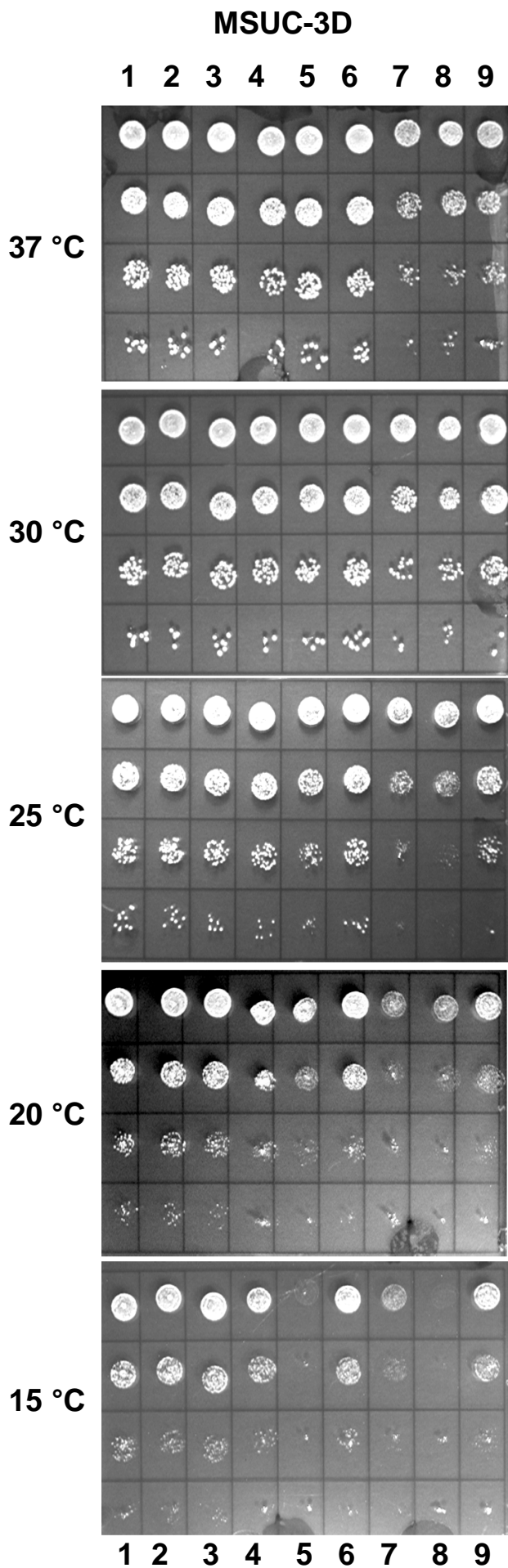


Fig. 4.13 Synthetic growth defect analysis of the strains

1) wt (MSUC-3D)

2) *ypt1*^{Q67L} (ADY49)

3) *ypt1*^{Q67L}/Δ*gyp7* (ADY52)

4) *ypt1*^{Q67L}/Δ*gyp1* (ADY50)

5) *ypt1*^{Q67L}/Δ*gyp5* (ADY51/K)

6) *ypt1*^{Q67L}/Δ*gyp8* (ADY53)

7) *ypt1*^{Q67L}/Δ*gyp5*/Δ*gyp1* (ADY54)

8) *ypt1*^{Q67L}/Δ*gyp5*/Δ*gyp8* (ADY55)

9) *ypt1*^{Q67L}/Δ*gyp1*/Δ*gyp8* (ADY56)

(for genotype description, see Appendix Table 7.2).

10-fold serial dilutions of cells (starting at 0.01 OD) were spotted on YEPG plates and grown at different temperatures for 3 days, (7 days at 15° C).

4.1.8 Partial rescue of the growth defect of the *ypt1*^{Q67L} mutant by high expression of Gyp5p

As shown in Fig. 4.14.A, the cold sensitivity of cl3-ABYS-86 *ypt1*^{Q67L} (ADY29) could be partially rescued by overexpression of Gyp5p₍₈₋₈₉₂₎ but not by the catalytically active fragment Gyp5p₍₄₀₀₋₈₉₂₎ lacking the N-terminus. The two gene fragments were cloned into the pYX212 shuttle vector (see Appendix, Table 7.6), a 2 μ vector containing the strong constitutive *TPI*-promoter. The two proteins with a 6xHis-tag at their C-terminus could be detected by immunoblot analysis using anti-6xHis antibody (Fig. 4.14.B). The near full-length Gyp5p was prone to degradation even in the protease -deficient strain.

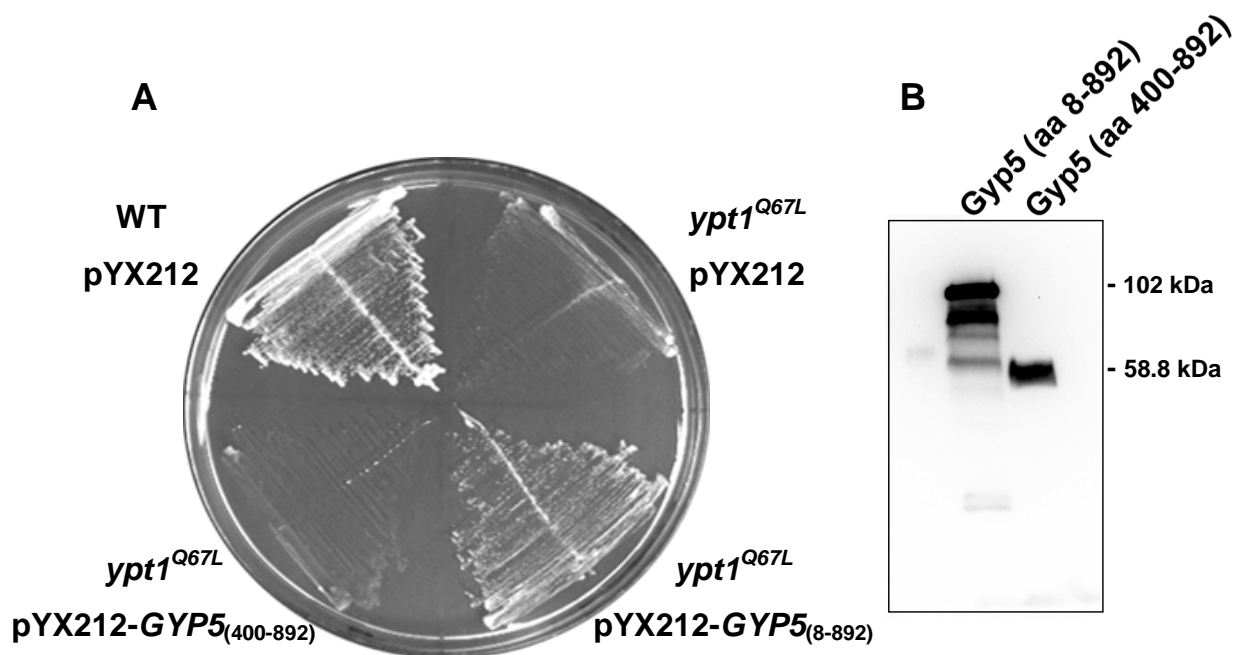


Fig. 4.14 (A) Partial rescue of the growth defect at 15°C of cl3-ABYS-86 *ypt1*^{Q67L} (ADY29) by high expression of Gyp5p (aa 8-892). The catalytically active fragment Gyp5p₍₄₀₀₋₈₉₂₎ cannot rescue the same mutant. The strains were grown on uracil-free plates, at 15 °C for 2 weeks. **(B)** Western blot showing Gyp5p expression in the strains containing pY212-GYP5-6H₍₈₋₈₉₂₎ and pY212-GYP5-6H₍₄₀₀₋₈₉₂₎. For the immunoblot, anti-6xHis antibody was used.

4.1.9 Analysis of possible transport defects in the different mutants

To verify whether the reduction of Ypt1p GTPase activity could affect vesicular ER-to-Golgi transport, the transport of different proteins (secreted invertase, vacuolar carboxypeptidase Y and plasma membrane-localized Gas1p), that pass through the ER and the Golgi compartments on the way to their final destinations, was tested in different mutants. Carboxypeptidase Y (CPY) is a soluble vacuolar hydrolase. It

leaves the ER as a core-glycosylated precursor protein of 67 kDa (p1), it is further glycosylated in the Golgi apparatus (p2, 69 kDa), and finally reaches the vacuole, where after a short proteolytic truncation, it becomes active. This mature form (m) has a molecular mass of 61 kDa. Gas1p is a 125 kDa glycolipid-anchored plasma membrane protein. The ER glycosylphosphatidylinositol-containing precursor has a molecular mass of 105 kDa and, upon arrival in the Golgi, is further glycosylated, reaching a molecular mass of 125 kDa. Invertase is a secreted protein (induced by low glucose concentration in the medium) that is modified by 14 core oligosaccharides in the ER, and by outer chain glycosylation in the Golgi apparatus. Secreted invertase migrates on non-denaturing polyacrylamide gels as heterogeneous species with an apparent molecular mass of 100-140 kDa, the glycosylated ER-form has an apparent molecular mass of 80-86 kDa.

MSUC-3D based strains ($\Delta gyp5$, $ypt1^{Q67L}$, and $ypt1^{Q67L}/\Delta gyp5$) were tested for invertase secretion at 30°C and 15°C (see Methods 3.3.5). As can be seen in Fig. 4.15, no significant differences were found between the mutant and the wild type strains. Similar results were also observed with cl3-ABYS-86 based strains. In the $ypt1^{Q67L}$ containing mutants the secreted invertase seems to be under-glycosylated to some extent, and there is probably a slight accumulation of the ER core-glycosylated invertase form; this is more visible in cells induced at 15°C. *sec18-1*, a mutant with a block at multiple steps in the secretory and endocytic pathways at non permissive temperature of 37°C, was used here as positive control.

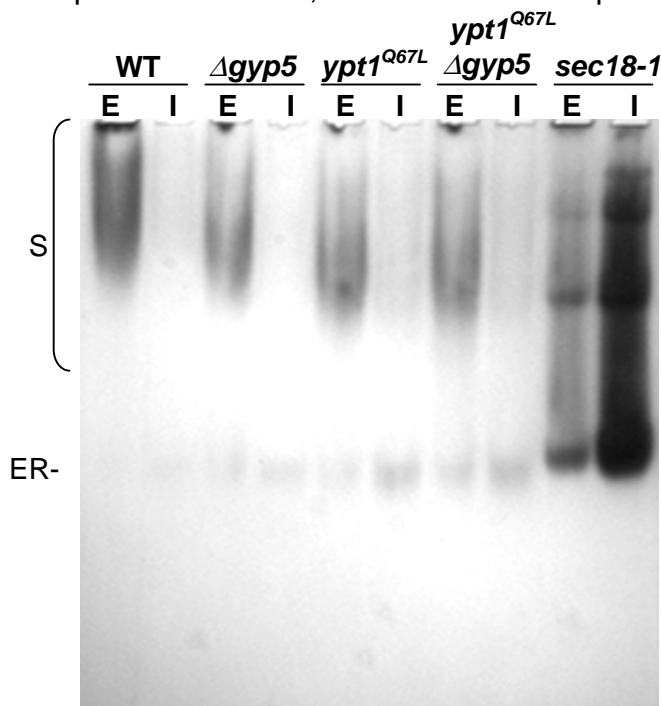


Fig. 4.15 Staining of active invertase in non-denaturing gels. MSUC-3D based strains $\Delta gyp5$ (ADY41/K), $ypt1^{Q67L}$ (ADY49), $ypt1^{Q67L}/\Delta gyp5$ (ADY51/K), induced for invertase synthesis at 15°C for 2 h; *sec18-1* induced at 37°C for 1h. For genotype description, see Appendix Table 7.2. "I"= intracellular fraction, "E"= periplasmic fraction, "S"= secreted form, "ER" = ER form.

Transport of CPY and Gas1p was tested in MSUC-3D based strains (for genotype description, see Appendix, Table 7.2). Cells were grown at 30°C until reaching an optical density of 0.5. The cells were then incubated for 1 h at 20°C, pulse-labeled for 10 min at 20°C with Trans ³⁵S-label mix and chased for 45 min at 20°C with methionine and cysteine (see Methods, 3.3.6). The cytosolic proteins were precipitated with anti-CPY or anti-Gas1p antibodies (see Figs 4.16 and 4.17). No effect on CPY maturation was observed, but a slight delay of Gas1p maturation was seen with the *ypt1^{Q67L}/Δgyp5* mutant (Fig. 4.17). This is probably due to the growth defect of these cells. In fact, a similar delay of Gas1p secretion was observed also in the cell cycle mutant *cdc28* at non permissive condition (data not shown).

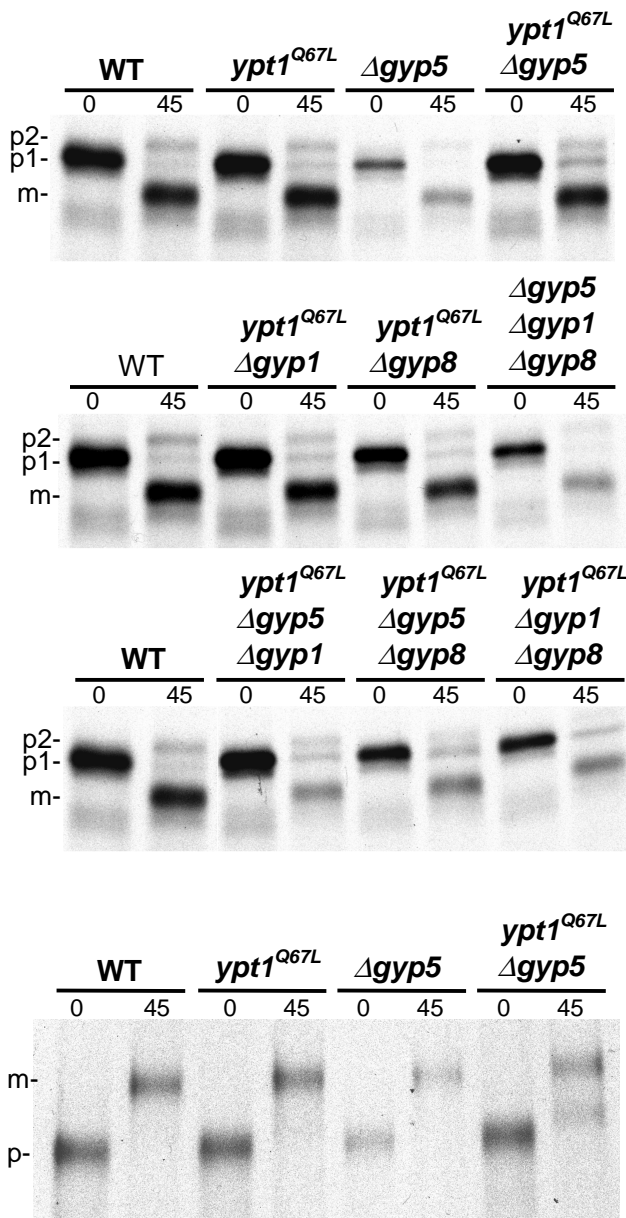


Fig. 4.16 CPY transport in MSUC-3D based strains: *ypt1^{Q67L}* (ADY49), *Δgyp5* (ADY41/K), *ypt1^{Q67L}/Δgyp5* (ADY51/K), *ypt1^{Q67L}/Δgyp1* (ADY50), *ypt1^{Q67L}/Δgyp8* (ADY53), *Δgyp5/Δgyp1/Δgyp8* (ADY47), *ypt1^{Q67L}/Δgyp5/Δgyp1* (ADY54), *ypt1^{Q67L}/Δgyp5/Δgyp8* (ADY55) and *ypt1^{Q67L}/Δgyp1/Δgyp8* (ADY56).

All the strains were grown to an OD₆₀₀ of 0.5, incubated for 1 h at 20°C, pulsed for 10 min and chased for 45 min at 20 °C. p1= ER core-glycosylated CPY, p2= Golgi-modified CPY, m= mature CPY. There is no evident difference in terms of secretion in the mutant strains as compared to the wild type.

Fig. 4.17 Gas1p secretion in MSUC-3D based strains: *ypt1^{Q67L}* (ADY49), *Δgyp5* (ADY41/K), and *ypt1^{Q67L}/Δgyp5* (ADY51/K). All the strains were grown to an OD₆₀₀ of 0.5, incubated for 1 h at 20°C, pulsed for 10 min and chased for 45 min at 20 °C. p= ER proform, m= mature form. There is a slight delay of Gas1p maturation in the double mutant *ypt1^{Q67L}/Δgyp5*.

4.1.10 Gyp5p is primarily a cytosolic protein

Genomic *GYP5* was changed in such a way that Gyp5p became tagged at the C-terminus with 2xMYC, or 3xHA or 3xVSV epitopes by PCR-mediated epitope tagging (see Methods 3.3.3). Yeast strains (ADY14, ADY15, ADY16) expressing tagged Gyp5 proteins were lysed and the lysates fractionated by differential centrifugation (see Methods 3.4.10.a). The different proteins were detected by immunoblotting. As shown in Fig. 4.18, Gyp5p is almost exclusively present in the supernatant (after a 100.000g centrifugation). To be sure that the fractionation was done correctly, soluble and membrane proteins were detected as well. Hxk2p (Hexokinase II), a cytosolic protein, Bos1p, a SNARE protein that fractionates with Golgi and ER membranes and Wbp1p (oligosaccharyltransferase β subunit), an ER integral membrane protein, fractionated as predicted either as soluble proteins (fraction S) or as integral membrane proteins (in the P10-P100 pellets). Bos1p and Wbp1p became soluble only by treatment of cell lysates with detergent.

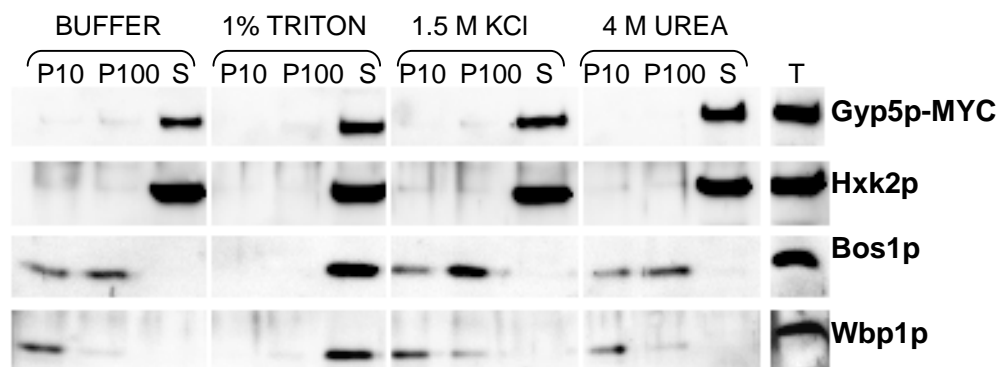


Fig. 4.18 Cell fractionation by differential centrifugation. The different fractions, "P10" (pellet after 10.000g centrifugation), "P100" (pellet after 100.000g centrifugation), "S" (supernatant after 100.000g centrifugation), "T" (total protein extract after 500g centrifugation), were separated by SDS-PAGE (12% polyacrylamide gel). Proteins were detected by immunoblotting using anti-MYC, anti-Hxk2p, anti-Bos1p and anti-Wbp1p antibodies.

4.1.11 Electron microscopic inspection of $\Delta gyp5/ypt1^{Q67L}$ mutant cells

To analyze the morphology of our mutant cells, an electron-microscopic inspection of potassium permanganate-fixed or cryo-fixed/cryo-substituted cells was performed (see Figs. 4.19 and 4.20). Wild type (MSUC-3D), $ypt1^{Q67L}$ (ADY49), $\Delta gyp5$ (ADY41/K⁻) and $ypt1^{Q67L}/\Delta gyp5$ (ADY51/K⁻) strains were grown at 30°C. The liquid cultures were divided into two parts and before fixation one part was incubated at 30°C and the second part at 15°C for 2 h. The $ypt1^{Q67L}$, but much more the $ypt1^{Q67L}/\Delta gyp5$ mutant cells exhibited a surprisingly altered morphology. Cells of these strains exhibited an accumulation of ER membranes and of various membrane-bounded structures already at the permissive temperature. These included vesicles of different sizes, and structures resembling autophagosomes. In addition, the vacuoles were fragmented and often showed large invaginations resembling autophagic tubes (Müller *et al.*, 2000) and engulfed multivesicular bodies. This was most clearly observed in cryo-fixed and cryo-substituted samples (see Figs. 4.20.C and 4.20.D). Incubation at 15°C for 2 h before fixation did not show dramatic differences in comparison with cells incubated at 30°C, probably because two hours are too little to induce visible changes.

4.1.12 Visualization of vacuolar membranes in living cells by FM 4-64 vital staining

The peculiar behavior of vacuolar compartments could also be shown in living cells by using the lipophilic styryl dye FM 4-64 (see Methods 3.6.2). As can be seen in Fig. 4.21, in $\Delta gyp5/ypt1^{Q67L}$ mutants (ADY51/K⁻) the vacuolar membrane forms invaginations and convoluted structures inside the vacuole itself. This phenomenon could be partially observed in $ypt1^{Q67L}$ (ADY49) mutants, too. A similar phenomenon was described by (Müller *et al.*, 2000) studying the formation of autophagic tubes.

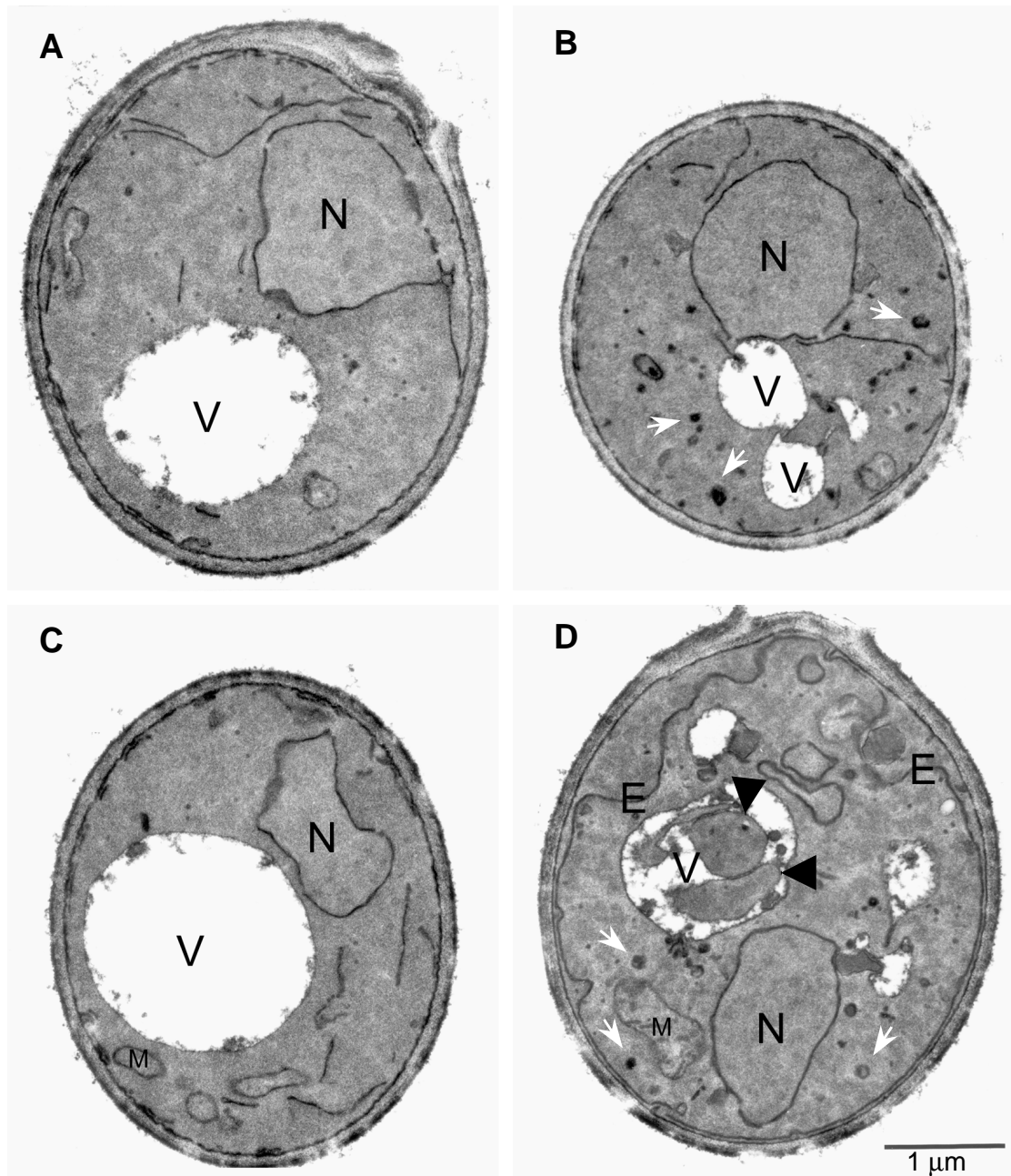


Fig. 4.19 Thin-section electron micrographs of wild type (MSUC-3D; **A**) *ypt1*^{Q67L} (ADY49; **B**), Δ *gyp5* (ADY41/k⁻; **C**) and Δ *gyp5/ypt1*^{Q67L} (ADY51/k⁻; **D**) mutant cells. Cells were grown in YEPG medium at 30 °C and then subjected to potassium permanganate fixation. In *ypt1*^{Q67L}, but more accentuated in the double Δ *gyp5/ypt1*^{Q67L} mutant, the vacuoles are fragmented in addition to ER proliferation and an accumulation of membrane-bounded structures (indicated by white arrows). In the Δ *gyp5/ypt1*^{Q67L} double mutant the vacuoles contain large membrane-bounded structures filled with cytosol which resemble autophagic tubes (indicated by black arrowheads in panel D). This is most clearly observed in Fig. 4.20. N= nucleus, V= vacuole, E= ER, M= mitochondria.

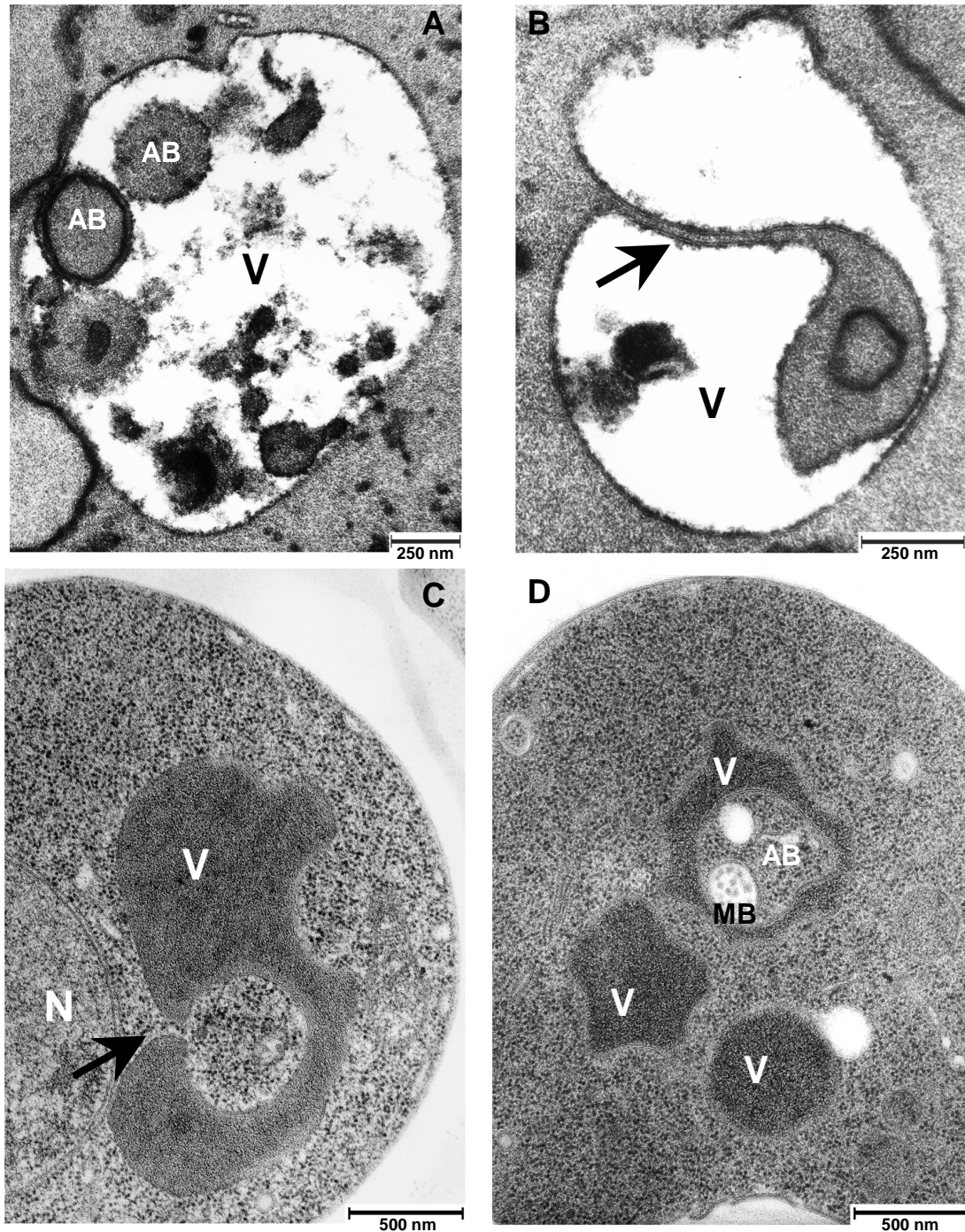


Fig. 4.20 Thin-section electron micrographs of the $\Delta gyp5/ypt1^{Q67L}$ double mutant (ADY51/k) grown at 30°C. (A-B) Potassium permanganate-fixed cells. (C-D) Cryo-fixed and cryo-substituted cells. Large invaginations of the vacuolar membrane can be observed (indicated by arrows). The lumen of the vacuolar invaginations is continuous with the cytosol. These structures resemble the autophagic tubes described by (Müller *et al*, 2000). In the vacuoles putative autophagic bodies are also visible. N= nucleus, V= vacuole, AB= autophagic body, MB= multi-vesicular body.

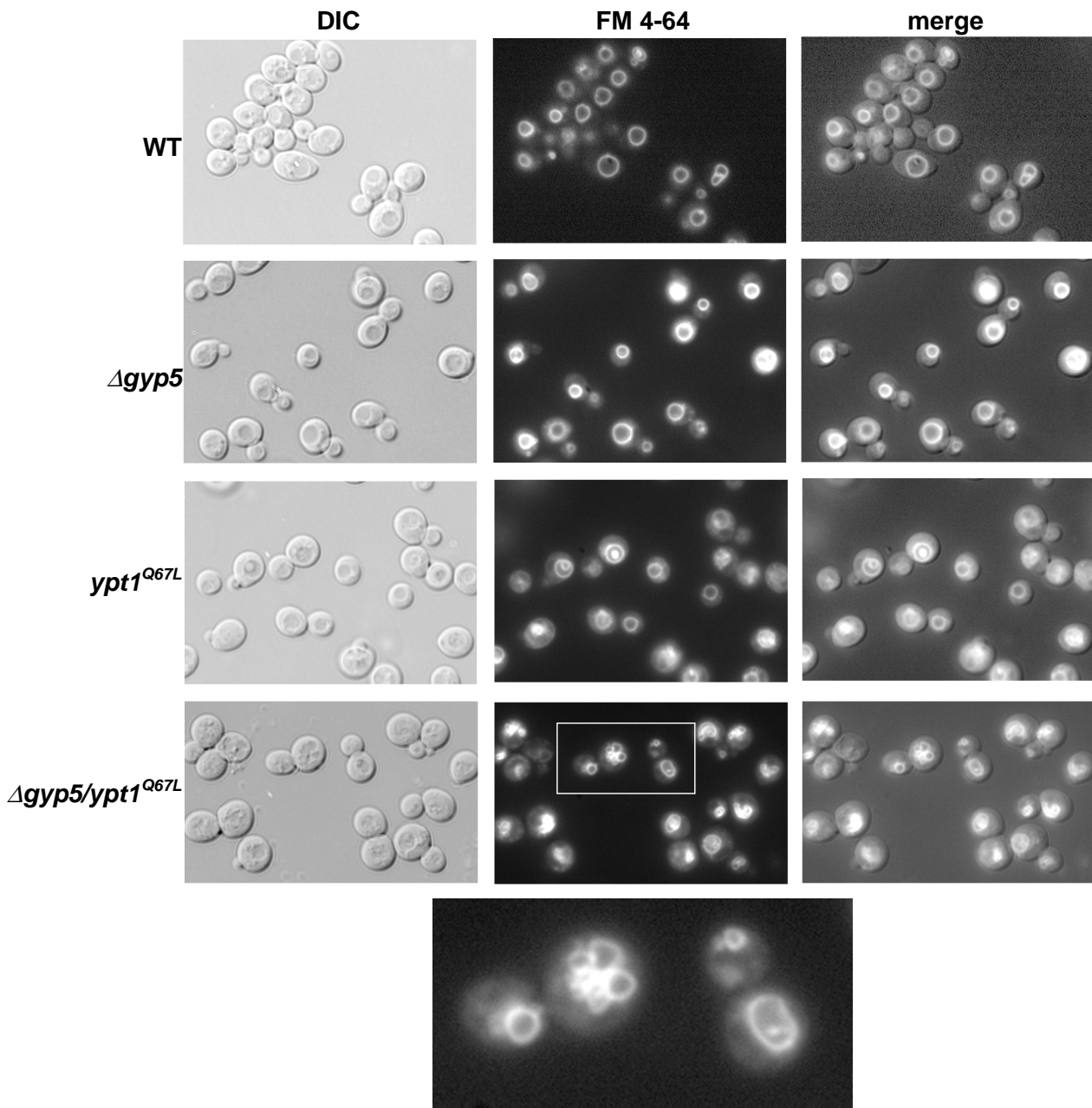


Fig. 4.21 Wild type (MSUC-3D), *ypt1*^{Q67L} (ADY49), Δ *gyp5/ypt1*^{Q67L} (ADY51/k⁻) and Δ *gyp5* (ADY41/k⁻) mutants stained with FM-4-64. Cells were incubated at 30°C for 15 min with 30 μ M FM-4-64 in YEPG medium, then "chased" for 1h at 30°C with fresh YEPG medium. Finally, the cells were resuspended in water and viewed under a fluorescence microscope with a 546 nm filter (for FM 4-64), or by DIC (differential interference contrast).

4.2 SECTION II (Sec24p family)

The Ypt1p-dependent transport vesicle docking/fusion with Golgi organelle(s) is preceded of course by the budding of vesicles from the ER membrane. Sec24p complexed with Sec23p is an essential component of the COPII coat which itself is involved in curving the ER membrane and, most likely, in integral membrane cargo selection (see Introduction 1.3.1). As already mentioned in the Introduction (1.3.2), in *S. cerevisiae* there are two close orthologues to Sec24p, named Sfb2p and Sfb3 (the acronym "Sfb" stands for **S**ed-**f**ive **b**inding). The name "Sfb" was given to them after it was demonstrated that Sec24p is able to bind Sed5p *in vitro* (Peng *et al.*, 1999). Sfb2p/lss1p (product of *YNL049c*; lss1p stands for interacting with sec-sixteen) shares 56% sequence identity with Sec24p, Sfb3p/Lst1p (product of *YHR098c*; Lst1 stands for lethal with sec-thirteen) shares 23% sequence identity with Sec24p. The three proteins contain a putative zinc-binding motif (CysX₂CysX₁₈CysX₂Cys), the four conserved cysteines are highlighted in red in Fig. 4.22.

The present study (in collaboration with Dr. R. Peng; Peng *et al.*, 2000) was undertaken to get further insight into the functional relationship between Sec24p, Sfb2p and Sfb3p. It was possible to demonstrate that Sfb2p and Sfb3p are functional COPII components and that they could have a role in specific cargo selection as it was also demonstrated by other research groups (Higashio *et al.*, 2000; Kurihara *et al.*, 2000; Pagano *et al.*, 1999; Roberg *et al.*, 1999; Shimoni *et al.*, 2000).

While *SEC24* is an essential gene, both *SFB2* and *SFB3* are nonessential genes. This was proven by experimental work performed in our laboratory and also in others (Kurihara *et al.*, 2000; Pagano *et al.*, 1999; Peng *et al.*, 2000; Roberg *et al.*, 1999).

4.2.1 Sec24 family proteins are differently expressed in the cell

To study the behavior of Sec24 family proteins, the three different genes in addition to *SEC23* were elongated so that their protein products were tagged at their C-termini with MYC epitopes by PCR-mediated epitope tagging as described in Methods (Section 3.3.3). Total protein extracts from the strains ADY1, ADY2, ADY3 and ADY4 (see Appendix Table 7.2), expressing respectively Sfb2p-MYC, Sfb3p-MYC, Sec23p-MYC and Sec24p-MYC, were used to determine the relative abundance of these proteins (see Fig 4.23). The protein extracts were obtained by alkaline lysis or by sonication as described in Methods (3.4.7.b).

Sec24p	1	MSHHKRVYPQAOLQYQGNATPLQQAQFMPQDPAAGMSYGQMGMPQGAVPVSMGQQQ
Sfb2p	1	MSHHKRVYPQAQVPY-----I-----ASMPIVAEQ-
Sfb3p	1	MSQQNILAASVSAISLDESTVHTGGASS-KKSRRPHRAYHNFSSGTVPTLGNSEPYTTPQL
Sec24p	61	FLTPAQLFOLHQOIDOATTSMNDMHLHN-VPLVDPNAYMQP-QVPVQMGTPLOQQQQPMAA
Sfb2p	27	-----QSQOQOQIDOTAYAMGNLQLN-----NR---A---NSFTQLAQNQO---F
Sfb3p	60	N---QDGFQCPQAFIPKQFGGFNNGSGSVMSTPVMVSOERFGASEASSPYCQSMLDMTA
Sec24p	119	PAYGQPSAAMGQNRPMNQLYPIDLLTELPPPTITDLTLPPPPLVIPPERRMLVPSSELSNAS
Sfb2p	62	PCSG-----K-VVNQLYVDLFTTELPPPIRDLNLPPLPITITISQDNIVTPSEYSNVP
Sfb3p	117	PQPTS-----HIVPTORFEDQAQYLQORSFETCRDSVPPLPTTQ-----FYCVDQGS
Sec24p	179	PDYIRSTLNAPKNSLLKSKLPFLVIRPYQHLYDDIDPP---PLNEDGLIVRCRRCR
Sfb2p	112	YQVIRSTLKAVPKINSLKKTLPFATVIRPYLHLQSDNQV---PLNTDGVIVRCRRCR
Sfb3p	165	PHLMSLSMYNIPSEHLRAATKLPGLTIQPFSTLTPNDAEVPTIPLPMDGTPLRCRRCR
Sec24p	236	SYMNPVVFVLEQGRWRVCRIRLANDVPMQMDQSD-PNDPKS-RYDRNEIKCAVMEYMAP
Sfb2p	169	SYMNPVVFVINQGRKWCNIRCFKNDVDFGFDQNL-QGAPIN-RYERNEIKNSVVDYLAP
Sfb3p	225	AVANPKFQFTYDS-SVICNIRVCMQVGEHFAPMGPNGQRSDLNEKSELHGHGTVDLVE
Sec24p	294	KEYTLRQPP---PATYCFLLDVSQSSIKSGLLATTINTLLQNLDSIPNHDERTRISILCV
Sfb2p	227	VEYSVREPP---PSVYVFLIDVSONAVKNGLLATSARTILENIEFLPNHDGRTRIAICV
Sfb3p	284	STYNATQEKELPLHYVFLIDVSLLANENGSSLAMVEGVRSCIEYISDFQPNCEVAIIIVY
		Y (sec24-11)
Sec24p	351	DNAHYFKIPLDS-----ENNEES-----ADQINMMDIADLEEFPLPR
Sfb2p	284	DHSLHYFYVPLDDDYEVSEDEDEESDGEEDDEDEEEDVDNSETIQMFDIGDLDEPFLPM
Sfb3p	344	DNKLRFFNLRPDL-----DNAQEVIVSELDVDFIEF
Sec24p	389	P-NSMVVSLKACRONIETLLTKIPQIFQS--NLITNFALGPALKSAY----HLIGGVGGK
Sfb2p	344	PSDELVVPVKYCKNLETLLKKIPEIFQD--THSSKFALGPALKAAS----NLIKSTGGK
Sfb3p	375	YNGLFVVKPGNSMKIINDTLIKISGYISTDKYSHVPQVCYGSALQAAKLALDVTGGQGGK
Sec24p	442	IIVVSGTLPLNLGIGKLQRRNESGVVNTSKETAQLLSCQDSFYKNFTIDCSKVQITVDLFL
Sfb2p	398	VEVIVSSITLPLNTGIGKLKRRSEQGIINTPKESSQLLSCKDSFYKFTTIECNKLQITVDMFL
Sfb3p	435	IICSLNSLPTIGNGNLSLKRDN-----AHIAHVKCDNGFYKKLASDFLKSYSISLDLYV
Sec24p	502	ASEDYMDVASLSNLSRFTAGQTHFYPGFSGKNPNDIVKFSSTEFAKHISMDFCMETVMRAR
Sfb2p	458	ASEDYMDVATLSHLGRFSGGQTHFYPGFNATSLNDVTKFTRELSRHLSDISMEAVMRVR
Sfb3p	488	TNAGFIDMATVGHVEMTSGILKYYPHFQOET--DAFTLVNDMVTNVSNIIVGYQALLKVR
Sec24p	562	GSTGLRMSRFYGHFFNRSSDLCAFSTMPRDQSYLFEVNVDESIMA-DYCYVQVAVLLSLN
Sfb2p	518	CSTGLRATSFYGHFFNRSSDLCAFSTMPRDQSYLFGISIEDSLMA-EYCYLQVSTLLTLN
Sfb3p	546	CSTGLSVEQYCDSSDNIDHDPVIPVLRDITLDVLLKYDSKIKTGTDVHFQTALLYTDI
Sec24p	621	NSQRRIRIITLAMPITESLAEVYASADQLAIASFYNSKAVEKALNSSLDDARVLINKSVQ
Sfb2p	577	TGERRIRVMTLALPTSESAREVFASADQLAITDFMTQNAVTKALNSSMYSARDFITKSLE
Sfb3p	606	DVRKVRISINTSGAVSNNIREIFKFINQNPVMRIMIKDVIKTLGDCDFVKIRRLIDDKMV
Sec24p	681	DILATYKKEIVSNNTAGGAPLRLCANLRMFPLLMHSLTKHMAFRSGIVPS--DHRASALN
Sfb2p	637	DILNAYKKEISMSNINSVITSLNLCANLRMLPLLMNGLSKHIALRPGVVPS--DYRASALN
Sfb3p	666	EILTQYRGLVSS---NSSTQLIILPDSIKTLPAYMLAFEKSELKMPNAQSTRGNERIYDIL
Sec24p	739	NLESPLKYLKNTYDPVYSLHMADEAGLPVQTE---DGEATGTVLVPQPINATSSLFE
Sfb2p	695	RLETEPLHYLIKSIYPTVYSLHMDPDEVGLP-----DFEGKTVLPEPINATISLFE
Sfb3p	723	KYDSLNSAQLCYKLYPQIVPFHVLLEETDITFYDANDKLLQINSSSINNLSVRASHSNFI
Sec24p	796	RYGLYLIDNGNELFLWGGDAVPALVDFVFGTQD---IFDIPIGKQEIIPVVENSEFNQRV
Sfb2p	746	RYGLYLIDNSAELFLWGGDAVPELLIDVFNTDT---ISQIPVGKSELPLINDSPFNERL
Sfb3p	783	NGGCYLIFQGDITYLWFNENTNRMLLQDILLSVDESPLVSQLSLSFSGTLPETGTS-INQKA
Sec24p	853	RNIIN---QLRNHD-----DVITYQSLYIVRGASLSEPVNHASARE--VATLRLWA
Sfb2p	803	RRIIG---RIRENN-----DTITFQSLYIIRGPSINEPANLNSEKD--MASLRLWV
Sfb3p	842	SNVTKNWQVVKSSSLPLVLLRPVNDQYYSNVMSQLLCEDKTVNRIESYDNYLVIMHKKI
Sec24p	899	SSTLVEDKILNNEASYREFLQIMKARTSK
Sfb2p	849	LSTLVEDKVLNCASYREYLOSMTSINR
Sfb3p	902	QEKLQKDDFKVSLAATHENIHQKFVQF

Fig. 4.22 Multiple alignment of Sec24p, Sfb2p and Sfb3p. Identical or similar amino acids in two or all three proteins are shown on black or shaded background, respectively. In red are the cysteine residues of the putative zinc-finger domain. The single amino acid change (D351Y) in the *sec24-11* allele in the temperature-sensitive strain is also indicated.

Equal amount of protein extracts from these strains were separated by SDS-PAGE and subjected to immunoblot analysis with monoclonal anti-MYC and polyclonal anti-Sly1p antibodies, the latter serving as control. The relative abundance of the proteins was calculated by measuring the chemiluminescent intensities of the bands using a Lumi-Imager. The values obtained by Lumi-Imager for the MYC-tagged proteins were normalized on the values obtained for Sly1p. As shown in Fig. 4.23, Sec23p was found to be the most abundant of the four proteins and Sfb2p the least abundant. Note that while the calculated molecular masses are 103.6 kDa for Sec24p, 98.9 kDa for Sfb2p and 103.9 kDa for Sfb3p, on SDS-PAGE the apparent molecular mass of Sfb3p is smaller than the calculated.

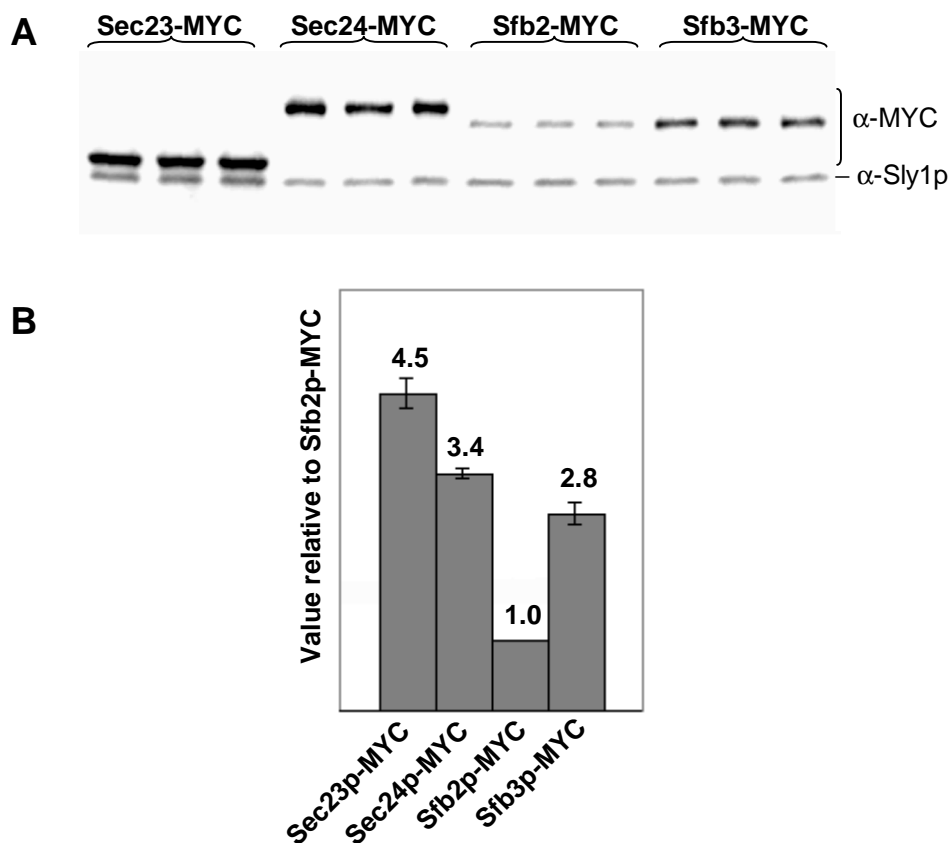


Fig. 4.23 Relative abundance of Sec23p and Sec24p family members. (A) Triplicate samples of total protein after alkaline lysis of MYC-tagged Sec24p-, Sfb2p-, Sfb3p- or Sec23p-producing cells were separated by SDS-PAGE, and subjected to immunoblotting with anti-MYC or anti-Sly1p antibodies. The concentrations were calculated measuring the chemiluminescent intensity of the protein bands with a Lumi-Imager. (B) Histograms representing the relative concentrations of Sec23p, Sec24p and Sfb3p in proportion to Sfb2p as determined by Lumi-Imager analysis. The values were normalized on Sly1p. The data are the average of three measurements derived from two different protein extracts.

4.2.2 Sec24p, Sfb2p and Sfb3p form complexes with Sec23p

It is known that Sec24p forms a stable complex with Sec23p (Hicke *et al.*, 1992). More precisely, it was determined that the binding site for Sec23p lies in between amino acids 56-594 (Peng *et al.*, 1999). To test whether Sfb2p and Sfb3p could also form stable complexes with Sec23p, these proteins were immuno-precipitated and the co-precipitated protein-complexes analyzed. The MYC-tagged proteins were expressed in the previously described ADY1, ADY2, ADY3 and ADY4 strains (see 4.2.1), and were precipitated from 16.000g supernatants (cells lysed in the presence of 1% Triton X-100, see Methods 3.4.13) with polyclonal anti-MYC antibodies. The target and co-precipitated proteins in the "IP" (immunoprecipitation pellet) and the non-precipitated protein in the "supernatant" were separated by SDS-PAGE and probed with polyclonal anti-Sec23p and anti-Sec24p antibodies. As shown in Fig. 4.24, immunoprecipitation of Sfb2p-MYC and Sfb3p-MYC led to co-precipitation of Sec23p but not of Sec24p. Immunoprecipitation of Sec23p-MYC led to the complete co-precipitation of Sec24p. In contrast, complete immunoprecipitation of Sec24p-MYC left some of the Sec23p in the supernatant. This argues for Sec23p being in excess over Sec24p, and the exceeding part should be in complex with Sfb2p or Sfb3p.

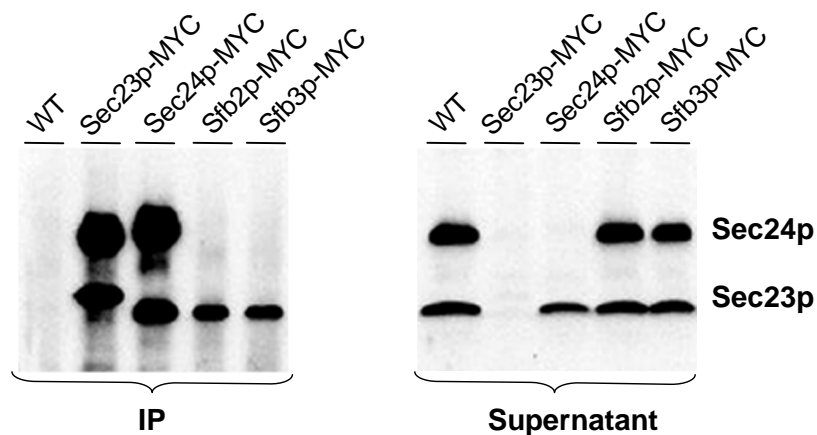


Fig. 4.24 Immunoprecipitation of MYC-tagged proteins with anti-MYC antibodies and analysis of co-precipitated Sec24p and Sec23p. The target and co-precipitated proteins in the "IP" and the non-precipitated protein in the "supernatant" were separated by SDS-PAGE and probed with polyclonal anti-Sec23p and anti-Sec24p antibodies. The amount of supernatant loaded on each lane of the gel corresponds to 1/20 of the total.

The complexes of Sfb2p and Sfb3p with Sec23p were also observed by other researchers (Higashio *et al.*, 2000; Kurihara *et al.*, 2000; Roberg *et al.*, 1999). Similarly, in mammalian cells hSec23Ap could co-immunoprecipitate with hSec24Bp

and hSec24Cp (Pagano *et al.*, 1999). In the same study it was determined, by two-hybrid assay, that the interacting domain of hSec24Cp is located in the region within amino acids 485-807 (corresponding to amino acids 289-611 in Sec24p).

4.2.3 Sfb2p behaves differently from Sec24p and Sfb3p on gel filtration chromatography

For further analysis of Sec23p complexes with either Sec24p or its orthologues, the 100.000g supernatant (obtained in the presence of 0.5% CHAPS) from ADY6 strain (expressing Sfb2p-HA and Sfb3p-MYC proteins, see Table 7.2) was subjected to Sephacryl S-400 gel filtration (see Methods 3.4.11). As can be seen in Fig. 4.25, all the proteins show an overlapping peak at ~ 250-300 kDa. This is a further proof of Sfb2p and Sfb3p forming complexes with Sec23p as was previously shown for Sec24p (Hicke *et al.*, 1992). Interestingly, a significant portion of Sfb2p, in contrast to the other proteins, eluted from the column at a higher molecular mass (~650 kDa). It is therefore possible that part of Sfb2p is in a large complex free of Sec23p.

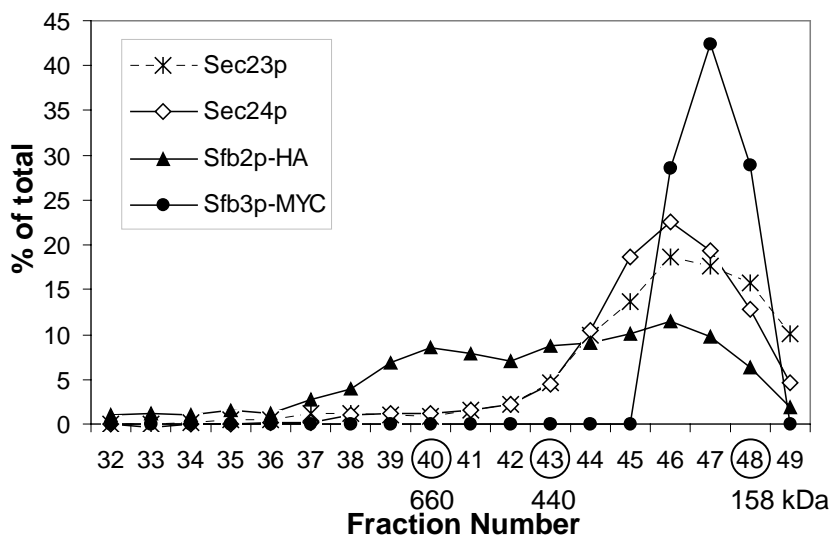


Fig. 4.25 Gel filtration chromatography on S-400 columns (1.6 cm x 65 cm) of 100.000g supernatants obtained in the presence of 0.5% CHAPS. Proteins were separated by SDS-PAGE and subjected to immunoblotting using antibodies specific for the different proteins. The chemiluminescence intensities of the protein bands were evaluated with a Lumi-Imager. The position of molecular size markers used to calibrate the column are indicated.

4.2.4 Intracellular distribution of Sec24p and its orthologues

Previous studies had shown that the Sec23p/Sec24p subcomplex is recruited to the ER membrane in the process of vesicle budding and that it dissociates from vesicles before fusion (Barlowe *et al.*, 1994) (see also Introduction 1.3.1). It is

therefore expected that there is a soluble and a membrane associated pool of the different COPII components.

To see whether Sec23p and Sec24p orthologues form distinguishable complexes and whether the individual proteins might behave differently with respect to membrane association, we examined the distribution of the four COPII components by differential centrifugation of cell lysates (see Methods 3.4.10a and Fig. 4.26), and by sucrose gradients (see Methods 3.4.10b and Fig. 4.26).

By differential centrifugation it is possible to distinguish whether a protein is cytosolic, membrane-associated or part of large protein complexes. As can be seen in Fig. 4.26, all four COPII components were distributed almost evenly between the pellet and supernatant fractions obtained from successive centrifugation at 10.000g and 100.000g. In contrast to Sec24p, a larger fraction of Sfb2p appears to be associated with membranes or in larger pelletable protein complexes. Sfb2p and Sfb3p were more resistant to solubilization with detergent than Sec24p under conditions where the integral membrane protein Bos1p became completely soluble. Treatment of the cell fractions with high salt or urea, conditions expected to dissociate protein complexes, efficiently solubilized all four COPII proteins.

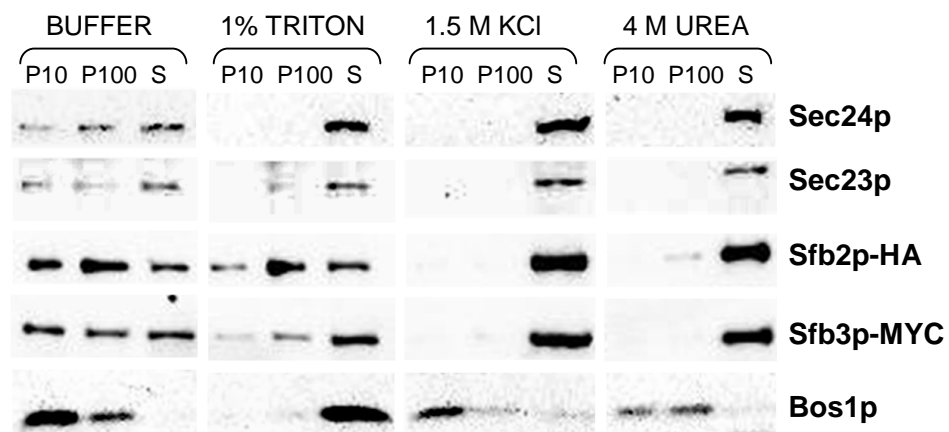


Fig. 4.26 Cell fractionation by differential centrifugation. Cleared cell lysates from the ADY6 strain (expressing Sfb2p-HA and Sfb3-MYC proteins, see Table 7.2) were treated on ice for 15 min with buffer alone, or buffer containing 1% Triton X-100, or 1.5 M KCl, or 4 M urea and then subjected to consecutive centrifugation at 10.000g and 100.000g. The different fractions, "P10" (pellet after 10.000g centrifugation), "P100" (pellet after 100.000g centrifugation), "S" (supernatant after 100.000g centrifugation), were separated by SDS-PAGE (12% polyacrylamide gel). Proteins were detected by immunoblotting using anti-MYC, anti-HA, anti-Sec23p, anti-Sec24p and anti-Bos1p antibodies.

In Fig. 4.27, the distribution of the proteins on a 18%-60% sucrose density gradient is shown. The distribution of the membrane proteins Emp47p, Bos1p and Sec61p were determined as controls. At steady state Emp47p is mostly localized in the Golgi (Schröder *et al.*, 1995), the v-SNARE Bos1p cycles between ER and Golgi (Ossipov *et al.*, 1999) and Sec61p is an ER membrane protein (membrane component of the ER protein translocation apparatus) (Deshaies *et al.*, 1991). Only a minor part of the COPII components tested appeared to be cytosolic (fraction 1-3), the majority fractionated with higher sucrose density of the gradient and partially overlapped with Golgi fractions (fractions 6-10). A very small part of the COPII proteins was found in ER fractions (fractions 11-13). This distribution could be due to either membrane association or to complex formation. There was no significant difference in the distribution of the three different Sec24p family components.

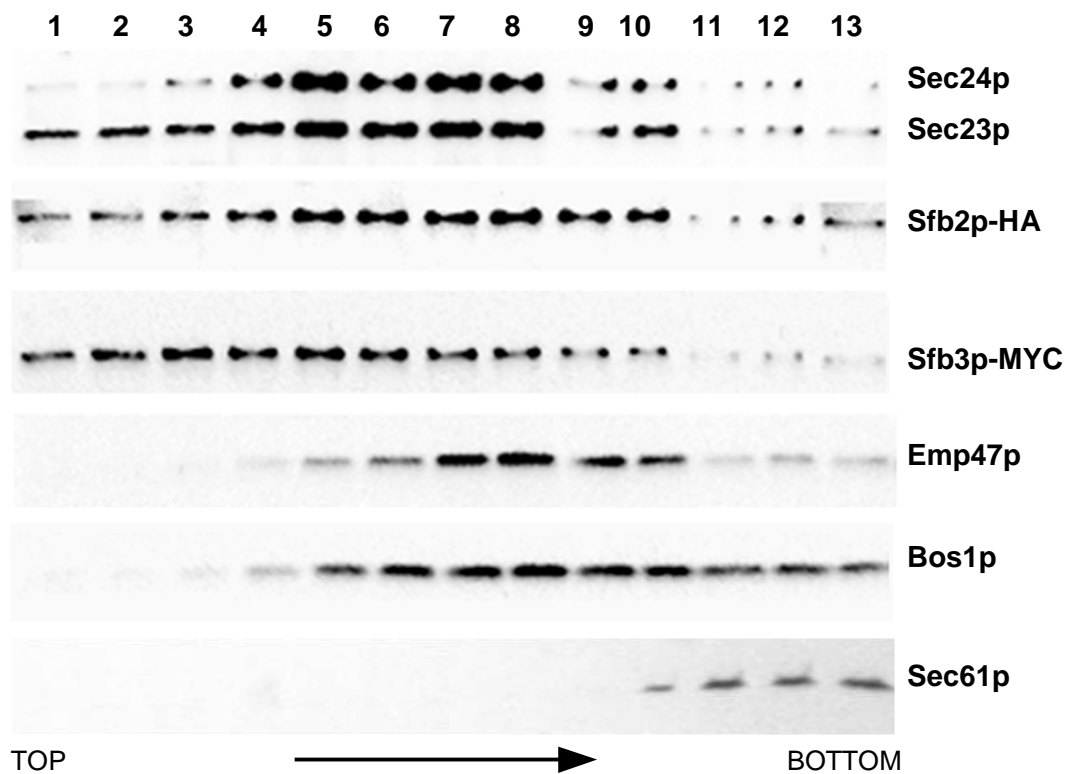


Fig. 4.27 Cell fractionation by velocity sedimentation on 18-60% sucrose gradient of ADY6 cells. Fractions 1 to 13 were collected (top to bottom). Proteins from each fraction were separated by SDS-PAGE (12% polyacrylamide gel) and detected by immunoblotting using anti-MYC, anti-HA, anti-Sec23p, anti-Sec24p, anti-Emp47p anti-Bos1p and anti-Sec61p antibodies.

4.2.5 Sfb2p, like Sec24p, binds Sed5p

Previously it was demonstrated by two-hybrid analysis and affinity chromatography that Sec24p could specifically bind the t-SNARE Sed5p (Peng *et al.*, 1999). It was therefore of interest to investigate whether the two Sec24p orthologues would have the same capability. For that reason an affinity chromatography experiment (see Methods 3.4.12) was performed using the GST fusions of all the known yeast syntaxins (lacking their C-terminal transmembrane domains): the ER localized Ufe1p (Lewis and Pelham, 1996), the *cis*-Golgi Sed5p (Hardwick and Pelham, 1992), the prevacuolar Pep12p (Becherer *et al.*, 1996), the vacuolar Vam3p (Wada *et al.*, 1997), the endosomal and/or late Golgi Tlg1p and Tlg2p (Abeliovich *et al.*, 1998; Holthuis *et al.*, 1998), and the plasma membrane Sso1p and Sso2p (Aalto *et al.*, 1993). The fusion proteins were obtained using the plasmids pTT-VAM3₍₁₋₂₆₁₎, pTT-SSO1₍₂₋₂₆₄₎, pTT-SSO2₍₁₋₂₆₇₎, pTT-TLG1₍₁₋₂₀₄₎, pTT-TLG2₍₁₋₃₁₇₎, pGEX-UFE1ΔC, pGEX-SED5ΔC, pEG-PEP12ΔC (see Tables 7.4, 7.5 and 7.6). Except for GST-Pep12p, which was produced in yeast, all the other proteins were produced in bacteria. 500 μg detergent solubilized proteins from ADY1 and ADY2 strains expressing Sfb2p-MYC and Sfb3p-MYC, respectively, were incubated overnight at 4°C with 1 μg GST or GST fusion SNAREs, previously coupled to glutathione-Sepharose beads, in 200 μl lysis buffer (25 mM HEPES, 1% Triton, 150 mM KOAc, 5 mM MgCl₂, 1 mM DTT, 1 mM EDTA). After extensive washing with lysis buffer proteins were separated by SDS-PAGE and analyzed by immunoblotting using anti-MYC antibodies. As can be seen in Fig. 4.28, Sfb2p bound Sed5p specifically while Sfb3p could not (under these conditions). In a similar experiment, using only cytosolic proteins and slightly different buffer conditions, a weak interaction could also be detected for Sfb3p (Peng *et al.*, 2000).

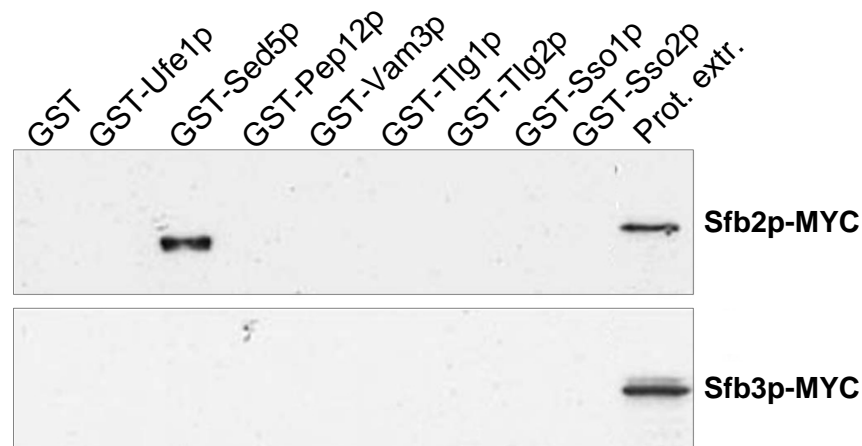


Fig. 4.28 500 μg proteins from detergent-lysed yeast cells were incubated with 1 μg purified GST or GST-fusion t-SNAREs which had previously been immobilized on glutathione-Sepharose beads. After intensive washing, the bound proteins were separated by SDS-PAGE and detected by immunoblotting with polyclonal anti-MYC antibody.

4.2.6 Sfb2p can rescue the growth defect of *sec24-11*

To check whether overexpression of Sfb2p or Sfb3p could compensate the loss of Sec24p function, it was tested if these proteins could rescue the growth defect of the temperature-sensitive *sec24-11* mutant (RPY18). As can be seen in Fig. 4.29, expression of Sfb2p from a high-copy-number vector (2μ) allowed mutant cells to grow whereas high expression of Sfb3p did not. On the contrary, high expression of Sfb3p alone was somehow toxic for the cells (data not shown). Both these data were subsequently confirmed by other researchers (Higashio *et al.*, 2000; Kurihara *et al.*, 2000; Roberg *et al.*, 1999)

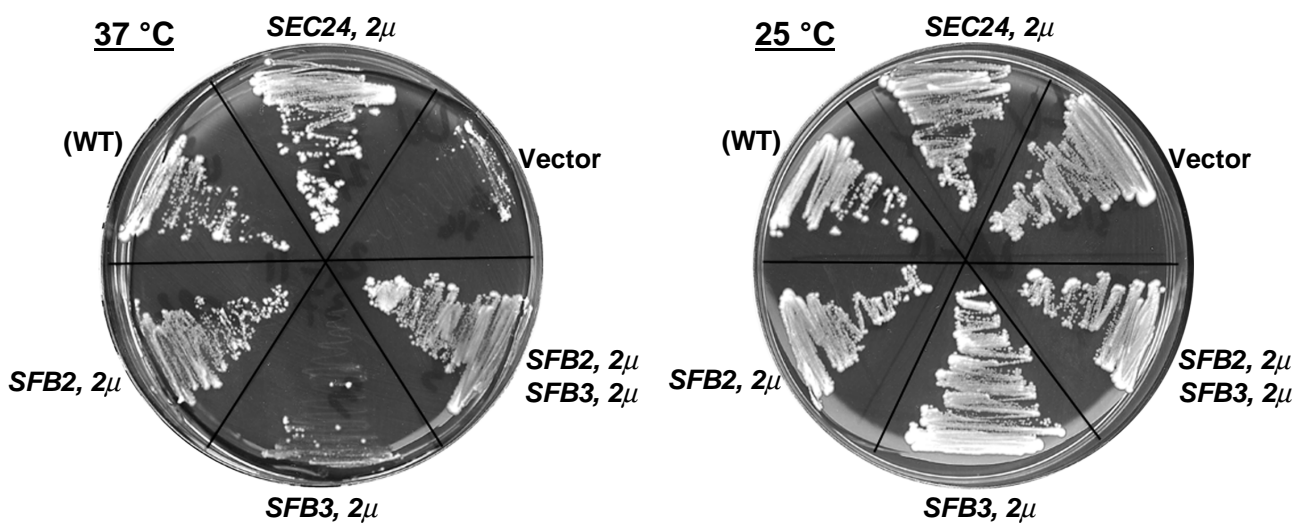


Fig. 4.29 Elevated levels of Sfb2p rescued the growth defect of a *sec24-11* mutant (RPY18) at the non-permissive temperature. *sec24-11* cells were transformed with the 2μ based vectors pRS326-*SFB2*, pRS325-*SFB3* and pRS326-*SEC24* (see Tables 2.5 and 2.6) and grown on selective agar plates for 3 days at 37°C or 25°C. (WT) is MSUC-3D transformed with pRS325 and pRS326.

4.2.7 Effects on protein transport of $\Delta sfb2$ in combination with the *sec24-11* allele

As already mentioned, *SFB2* and *SFB3* are nonessential genes. Cells lacking either *SFB2*, *SFB3* or both genes, grew like wild type cells at temperatures between 15°C and 37°C. Transport of the vacuolar hydrolases carboxypeptidase Y (CPY) and alkaline phosphatase (ALP) and secretion of invertase (see Methods 3.3.5 and 3.3.6) seemed to be unaffected. Invertase was apparently not fully glycosylated in the mutant cells (data not shown).

SEC24 is an essential gene and the *sec24-11* mutant cannot grow at the non-permissive temperature of 37°C (see Fig. 4.29). Surprisingly only a mild effect on transport of CPY, ALP and invertase was observed at 37°C (see Fig. 4.30).

We tried therefore to combine the chromosomally integrated *sec24-11* allele with the deletion of either *SFB2* or *SFB3*. Only the double mutant $\Delta sfb2/sec24-11$ could be obtained, the combination of $\Delta sfb3$ with *sec24-11* led to lethality. In contrast to the single mutants, transport of CPY and ALP was completely blocked in the double mutant $\Delta sfb2/sec24-11$ (see Fig. 4.30.A). In this mutant, accumulation of the ER core-glycosylated form of invertase was also observed, but most of the enzyme appeared to reach the periplasmic space in a somewhat hypoglycosylated form (see Fig 4.30.B).

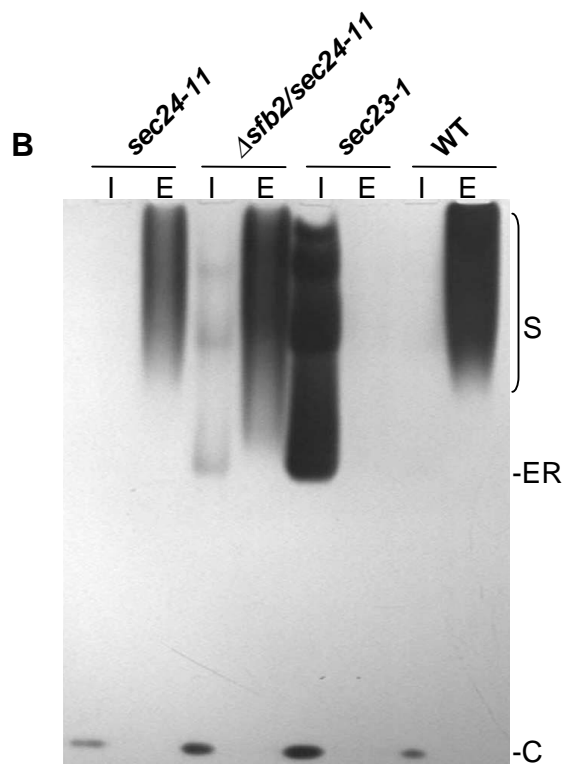
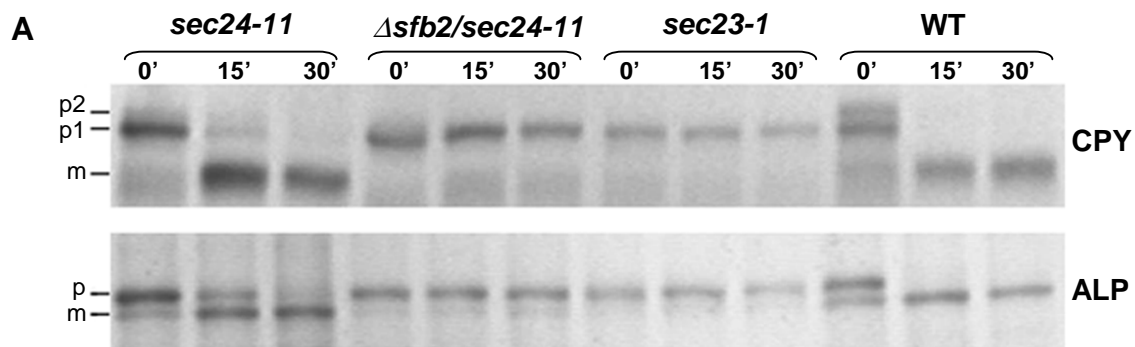


Fig 4.30 (A) Cells from *sec24-11* (RPY18), $\Delta sfb2/sec24-11$ (RPY72), *sec23-1* (RH227-3A) and wild type (MSUC-3D), were grown at 25 °C, transferred to 37 °C for 30 min, pulse-labeled for 10 min and chased for 0, 15 and 30 min at 37 °C. CPY and ALP were immunoprecipitated and separated by SDS-PAGE, followed by autoradiography. "p1"= ER core-glycosylated CPY, "p2"= Golgi-modified CPY, "p"= ER- and Golgi-modified ALP proform and "m"= mature form.

(B) Staining of active invertase in non-denaturing gels. Cells were grown at 25 °C and induced for secreted invertase synthesis at 37°C for 1h. "I"= intracellular fraction, "E"= periplasmic fraction, "S"= secreted form, "ER" = ER form, "C"= cytosolic invertase.

4.2.8 Electron microscopic inspection of the $\Delta sfb2/sec24-11$ mutant

By electron microscopic inspection of potassium permanganate fixed cells we tried to look whether there were morphological differences between wild type (MSUC-3D), $\Delta sfb2$ (RPY61), $sec24-11$ (RPY18) and $\Delta sfb2/sec24-11$ (RPY72) mutants. Cells were grown at 25°C to mid-log phase, then incubated at 37°C for 1h before fixation. Compared to wild type (Fig. 4.31.A), $\Delta sfb2$ (Fig. 4.31.B) and $sec24-11$ (Fig. 4.31.C) mutant cells had an about 2-fold increase in the number of 30-50 nm vesicles (indicated by arrowheads). Interestingly, the $\Delta sfb2/sec24-11$ double mutant (Fig. 4.31.D) exhibited enhanced proliferation of ER membranes, and a further increase (approximately 3-fold compared to wild type) of vesicular structures many of which formed aggregates (Fig. 4.31.E); these aggregates were present in about 20 % of the sections. The aggregated structures were of round and sometimes of short rod-like appearance. In some cases it can be seen that they are surrounded by a membrane.

4.2.9 Immunofluorescence detection of one member of the mammalian Sec24p family in monkey CV1 cells

When this work was started, the mammalian homologues of Sec24p were unknown. By database search, a full-length human cDNA clone named KIAA0079 was found sharing significant homology with Sec24p (GenBank accession number D38555, kindly provided to us by Dr. Nomura from the Kazusa DNA research institute, Japan; (Nomura *et al.*, 1994). The cDNA encodes a 1094 amino acid-long protein with a calculated molecular mass of 118 kDa which is 27.2% identical to Sec24p in 960 overlapping amino acids, 27.8% identical to Sfb2p in 802 overlapping amino acids and 26.4% identical to Sfb3p in 904 overlapping amino acids. The sequence present in the database contains a mistake (an extra base at position 3233 and consequently a frame-shift after amino acid 1040). The sequence shown in Fig. 4.32 is the correct one. This sequence mistake was found after multiple alignment with different ESTs and subsequently confirmed by sequencing.

In order to produce antibodies against this protein, different fragments were cloned and expressed as 6xHis fusion proteins. The two protein fragments, highlighted in Fig. 4.32, corresponding to the sequence regions 365-522 (for simplicity named peptide 2) and 747-992 (peptide 5), respectively, were used as antigens.

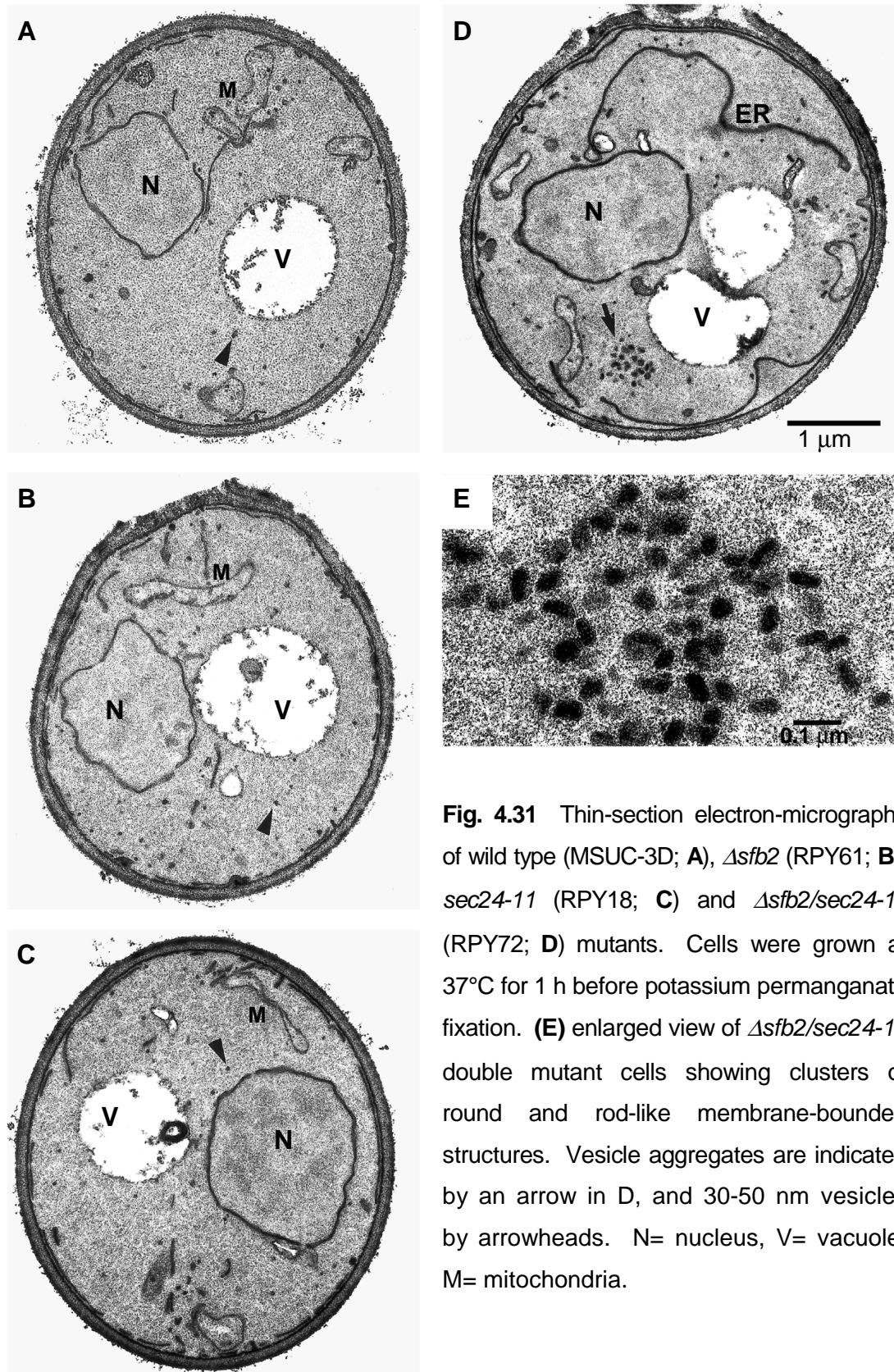


Fig. 4.31 Thin-section electron-micrographs of wild type (MSUC-3D; **A**), $\Delta sfb2$ (RPY61; **B**), *sec24-11* (RPY18; **C**) and $\Delta sfb2/sec24-11$ (RPY72; **D**) mutants. Cells were grown at 37°C for 1 h before potassium permanganate fixation. **(E)** enlarged view of $\Delta sfb2/sec24-11$ double mutant cells showing clusters of round and rod-like membrane-bounded structures. Vesicle aggregates are indicated by an arrow in D, and 30-50 nm vesicles by arrowheads. N= nucleus, V= vacuole, M= mitochondria.

1	MNVNQSVPPV	PPFGQPQPIY	PGYHQSSYGG	QSGSTAPAIP	YGAYNGPVPG
51	YQQTTPQGMS	RAPPSSGAPP	ASTAQAPCGQ	AAYGQFGQGD	VQNGPSSTVQ
101	MQRLPGSQPF	GSPLAPVGNQ	PPVLQPYGPP	PTSAQVATQL	SGMQISGAVA
151	PAPPSSGLGF	GPPTSLASAS	GSFPNSGLYG	SYPQGQAPPL	SQAQGHPIQ
201	TPQRSAPSQA	SSFTPPASGG	PRLPSMTGPL	LPGQSFGGPS	VSQPNHVSSP
251	PQALPPGTQM	TGPLGPLPPM	HSPQQPGYQP	QQNGSFGPAR	GPQSNYGGPY
301	PAAPTFGSQP	GPPQPLPPKR	LDPDAIPSPI	QVIEDDRNNR	GTEPFVTGVR
351	GQVPPLVTTN	FLVKDQGNAS	PRYIRCTSYP	IPCTSDMAKQ	AQVPLAAVIK
401	<u>PLARLPPEEA</u>	<u>SPYVVDHGES</u>	<u>GPLRCNRCKA</u>	<u>YMCPFMQFIE</u>	<u>GGRRFQCCFC</u>
451	SCINDVPPQY	FQHLDHTGKR	VDAYDRPELS	LGSYEFLATV	DYCKNNKFPS
501	PPAFIFMIDV	SYNAIRTGVL	RLLCHEELKSL	LDFLPREGGA	EESAIRVGVF
551	TYNKVLHFYN	VKSSLAQPQM	MVVSVDVDMF	VPLLDGFLVN	VNESRAVITS
601	LLDQIPEMFA	DTRETETVFV	PVIQAGMEAL	KAAECAGKLF	LFHTSLPIAE
651	APGKLNRRDD	RKLINTDKEK	TLFQPQTGAY	QTLAKECVAQ	GCCVDLFLFP
701	NQYVDVATLS	VVPQLTGGSV	YKYASFQVEN	DQERFLSDLR	RDVQKVVGFD
751	AVMRVRTSTG	IRAVDFFGAF	YMSNTTDVEL	AGLDGDKTVT	VEFKHDDRNLN
801	EESGALLQCA	LLYTSCAGQR	RLRIHNLALN	CCTQLADLYR	NCETDTLINY
851	MAKFAYRGVL	NSPVKAVRDT	LITQCAQILA	CYRKNCASPS	SAGQLILPEC
901	MKLLPVYLLNC	VLKSDVLQPG	AEVTTDDRAY	VRQLVTSMDV	TETNVFFYP
951	LLPLTKSPVE	STTEPPAVRA	SEERLSNGDI	YLLEENGLNLF	LWVGASVQQG
1001	VVQSLFSVSS	FSQITSGLSV	LPVLDNPLSK	KVRGLIDSLR	AQRSRYMKL
1051	VVKQEDKMEM	LFKHFLVEDK	SLSGGASYVD	FLCHMHKEIR	QLLS

Fig. 4.32 Protein encoded by the cDNA KIAA0079 (hSec24Cp). The sequences highlighted represent the two fragments (for simplicity named peptides 2 and 5) used to produce anti-KIAA0079-2 and anti-KIAA0079-5 antibodies, respectively. The putative zinc finger domain is underlined.

The two 6xHis-tagged fragments were expressed in bacteria containing the expression plasmids pQE30-KIAA0079₍₃₆₃₋₅₂₂₎, pQE50-KIAA0079₍₃₆₃₋₅₂₂₎ and pQE30-KIAA0079₍₇₄₇₋₉₉₂₎ (see Table 7.6). The methods used to produce and purify these antibodies are described in Section 3.5. In Fig. 4.33 an immunoblot of protein extracts from HeLa and CV1 cells using the antibodies anti-KIAA0079-2 (serum from rabbits 166 and 167) and anti-KIAA0079-5 (serum from rabbits 168 and 169) is shown.

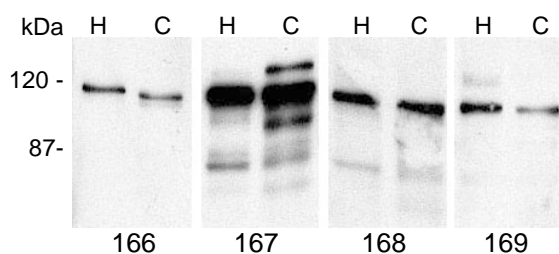


Fig. 4.33 Protein extracts from HeLa (H) and CV1 (C) cells were separated by SDS-PAGE and immunoblotted with serum from two rabbits (166, 167) immunized with "peptide 2" and from two rabbits (168, 169) immunized with "peptide 5". The calculated molecular mass of the KIAA0079-encoded protein is 118 kDa.

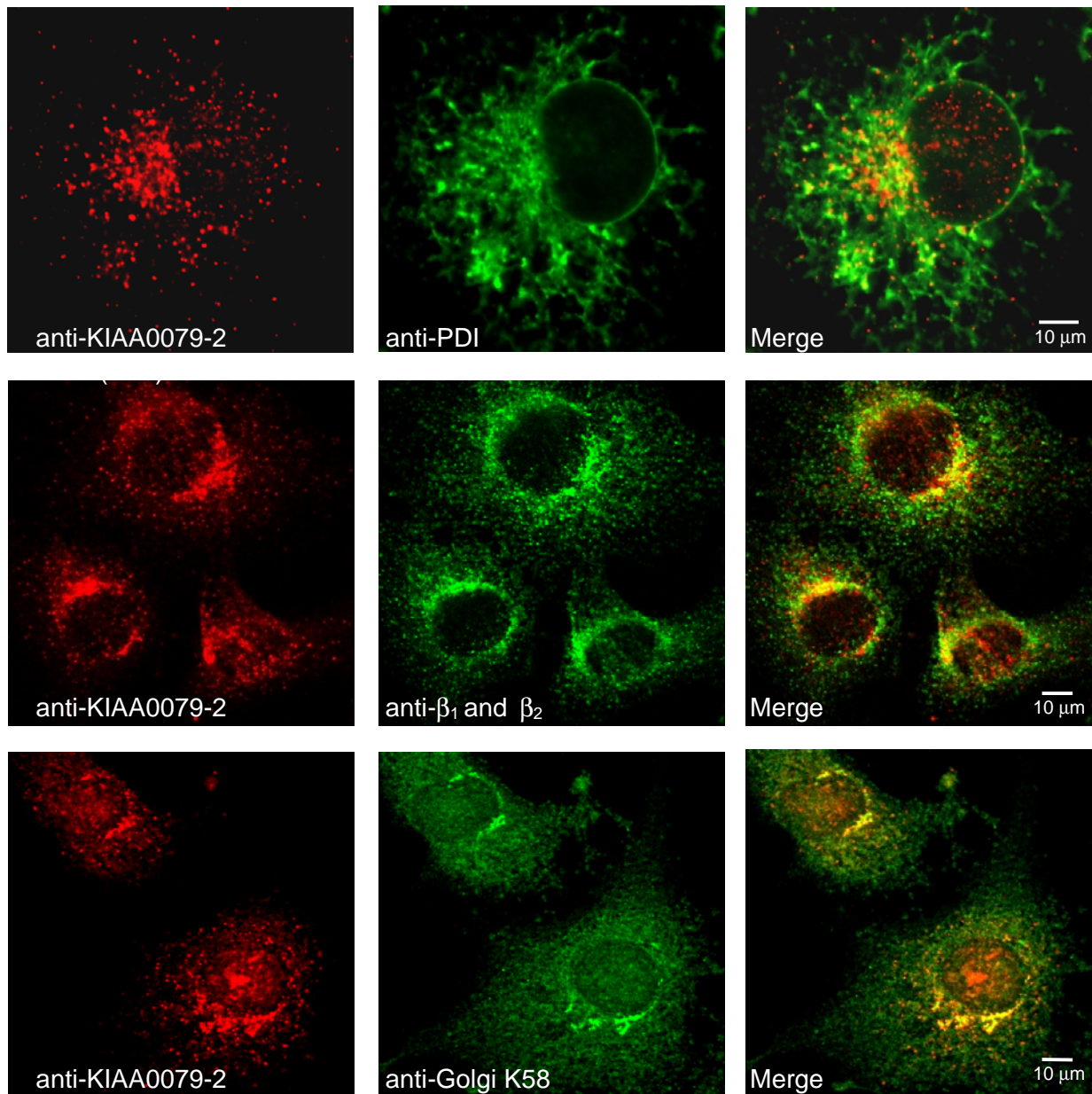


Fig. 4.34 Double immunofluorescence of methanol-acetone fixed CV1 cells using anti-KIAA0079-2 antibody in combination with the antibodies indicated in the panels. The secondary antibodies were rhodamine red-X-conjugated and Oregon-Green-488-conjugated. Confocal images were taken using a Leica TCS NT confocal laser scanning microscope.

By indirect immunofluorescence with anti-KIAA0079 antibodies it was possible to judge the subcellular localization of KIAA0079-encoded protein in methanol-acetone fixed CV1 cells (see Methods 3.6.3). The following proteins were immuno-labeled and used for reference: protein disulfide-isomerase (PDI), β_1 and β_2 adaptins and Golgi 58K. PDI is a soluble ER resident protein containing at its C-terminus the highly conserved KDEL sequence (Kaetzel *et al.*, 1987); β_1 and β_2 adaptins are components of the adaptor complexes AP-1 and AP-2, the antibodies against β_1 and β_2 adaptins

stain clathrin-coated domains at the plasma membrane and at the Golgi region (Ahle *et al.*, 1988); Golgi 58K is a microtubule-binding peripheral Golgi membrane protein (Bloom and Brashear, 1989).

As can be seen in Fig. 4.34, the anti-KIAA0079 antibodies revealed a punctate pattern scattered throughout the cytoplasm along with some concentration at the perinuclear region (overlapping with Golgi markers). Some of the punctate structures were overlapping with ER structures, as can be seen in the double staining with PDI. This distribution pattern is similar to what was previously described for another COPII component, the mammalian Sec13p (Tang *et al.*, 1997). The same was subsequently observed by other research groups (Pagano *et al.*, 1999; Tang *et al.*, 1999; Tani *et al.*, 1999), who described the entire family of mammalian Sec24 proteins: hSec24Ap, hSec24Bp, hSec24Cp, hSec24Dp. The KIAA0079-encoded protein is hSec24C. hSec24Ap and hSec24Bp seem to form one class sharing about 56% identity, while hSec24Cp and hSec24Dp form another class with about 52% identity. There is about 20% identity between the two pairs (Tang *et al.*, 1999), which is almost the same degree of identity observed for Sec24p, Sfb2p (56% identity between them) and Sfb3p (23% identity with Sec24p and 24% with Sfb2p).

4.3 SECTION III (Epitope tagging vectors)

During my Ph.D. work, I created three plasmids containing a multi-purpose cassette for repeated integrative PCR-mediated epitope tagging (see Methods 3.3.3; De Antoni and Gallwitz, 2000). These plasmids were named pU6H2MYC (GenBank accession number AJ132965), pU6H3HA (AJ132966) and pU6H3VSV (AJ132967), because they were created through modification of the plasmid pUG6 (Güldener *et al.*, 1996). A DNA fragment expressing six histidines in combination with either two MYC epitopes (9E10 epitope; Evan *et al.*, 1985), three HA epitopes (12CA5 epitope; Wilson *et al.*, 1984) or three VSV epitopes (P5D4 epitope; Kreis, 1986) was inserted into pUG6. More precisely, three adaptors (see Fig. 4.35) obtained by annealing three pairs of long primers (forward and reverse) were inserted into pUG6 digested with BsiWI and Sall. The resulting plasmids contain the "tag" epitopes fused to the *loxP-kanMX-loxP* cassette (see Fig. 4.36).

6His-2MYC adaptor

BsiWI BamHI

```

GT ACG GGA TCC CAC CAC CAT CAT CAT CAC GGA GAG CAG AAA TTG ATC AGC GAG GAA GAC TTG GGC
c cct agg gtg gtg gta gta gta gtg cct ctc gtc ttt aac tag tcg ctc ctt ctg aac ccg
G S H H H H H H G E Q K L I S E E D I G

GAA CAA AAG CTT ATT TCT GAA GAA GAC TTG TAA TGA G
ctt gtt ttc gaa taa aga ctt ctt ctg aac att act cag ct
E Q K L I S E E D I - - Sall

```

6His-3HA adaptor

BsiWI BamHI

```

GT ACG GGA TCC CAC CAC CAT CAT CAT CAC GGA TAC CCG TAT GAT GTT CCG GAT TAC GCT GGC
c cct agg gtg gtg gta gta gta gtg cct atg ggc ata cta caa ggc cta atg cga ccg
G S H H H H H H G Y P Y D V P D Y A G

TAC CCA TAC GAC GTC CCA GAC TAC GCT GGC TAC CCA TAC GAC GTC CCA GAC TAC GCT TAA TGA G
atg ggt atg ctg cag ggt ctg atg cga ccg atg ggt atg ctg cag ggt ctg atg cga att act cag ct
Y P Y D V P D Y A G Y P Y D V P D Y A - - Sall

```

6His-3VSV adaptor

BsiWI BamHI

```

GT ACG GGA TCC CAC CAC CAT CAT CAT CAC GGA TAC ACC GAT ATC GAG ATG AAC CGT TTG GGT AAG GGC
c cct agg gtg gtg gta gta gta gtg cct atg tgg cta tag ctc tac ttg gca aac cca ttc ccg
G S H H H H H H G Y T D I E M N R L G K G

TAC ACT GAC ATT GAA ATG AAT CGT TTG GGT AAG GGC TAC ACT GAC ATT GAA ATG AAT CGT TTG GGT AAG
atg tga ctg taa ctt tac tta gca aac cca ttc ccg atg tga ctg taa ctt tac tta gca aac cca ttc
Y T D I E M N R L G K G Y T D I E M N R L G K

TAA TGA G
att act cag ct
- - Sall

```

Fig. 4.35 Adaptors used to create pU6H2MYC, pU6H3HA and pU6H3VSV. The adaptors contain the sequences encoding six histidines followed by the sequences encoding either two MYC epitopes, three HA epitopes or three VSV epitopes. The epitope-expressing sequences are followed by two STOP codons. Note that in each adaptor the first epitope (MYC, HA or VSV) is different in nucleotide sequence from the following, so that it is possible to design primers that anneal either in the region of the six histidines or in the region of the first epitope.

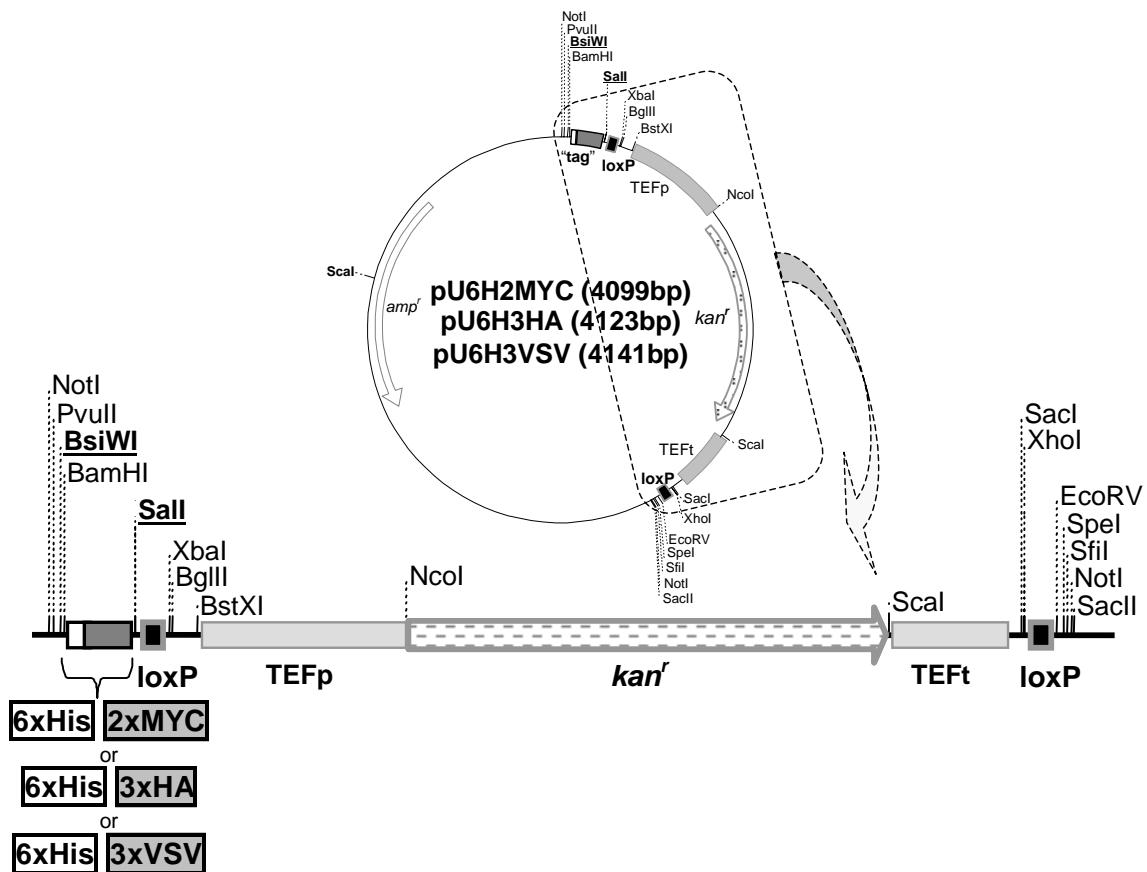


Fig 4.36 Schematic representation of the plasmids pU6H2MYC (4099 bp), pU6H3HA (4123 bp) and pU6H3VSV (4141 bp). The two restriction sites (*BsiWI* and *Sall*) into which the described adaptors were inserted are underlined.

The *kanMX* module (Wach *et al.*, 1994) consists of the kanamycin resistance gene (from the *E. coli* transposon TN903, coding for aminoglycoside phosphotransferase; Oka *et al.*, 1981) fused to the *Ashbya gossypii* TEF (translation elongation factor) promoter and terminator sequences. The aminoglycoside phosphotransferase activity renders *E. coli* kanamycin resistant and *S. cerevisiae* resistant to the aminoglycoside G418. The *loxP* flanking sequences allow for the excision of the marker by induction of the Cre recombinase (Güldener *et al.*, 1996), see also Methods 3.3.2. An example of a strain expressing two tagged proteins is shown in Fig 4.37.

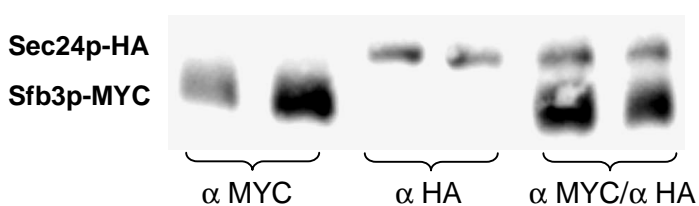


Fig. 4.37 Immunoblot analysis of total cellular proteins from the yeast strain ADY13 expressing simultaneously two tagged proteins, Sec24p-HA and Sfb3p-MYC. The tagged proteins were identified with anti-MYC and anti-HA antibodies. Duplicate samples were analyzed. To separate the proteins, a 7% SDS-polyacrylamide gel was used.

5 DISCUSSION

To maintain their intricate, internal structure of specialized compartments as well as meeting the necessity to react to changes of environmental conditions, eukaryotic cells have evolved an elaborate transport machinery to selectively deliver biochemical components to their various destinations. Vesicular carrier units are used as vehicles of targeted transport by all eukaryotic cell types. Vesicles of various types exist, each serving one or a small number of specialized functions. Every vesicle is generated by a multi-step process known as budding at a donor compartment's membrane. After its formation, including specific cargo-selection, vesicles travel within the cell in a directed manner to finally meet their target membrane and fuse with it. As already mentioned in the Introduction, the formation of transport vesicles, their correct targeting and the specificity of membrane fusion events depend on a considerable array of proteins, lipids and enzyme complexes, some of which function as structural component while others regulate spatial and temporal aspects of these processes.

COPII vesicles are involved in ER-to-Golgi transport. The assembly of the vesicle's protein coat provides the necessary energy to deform the vesicle's membrane into a spherical shell and also serves as an affinity matrix for the selective partitioning of cargo molecules into the vesicle.

Before the fusion process at the vesicle's target membrane a proof-reading process, involving the compartment-specific Ypt/Rab GTPases, plays an essential role in guaranteeing correct delivery of vesicle contents to their respective target location. These GTPases are important regulators during the tethering/docking of vesicles to their target membranes. Ypt1p and Ypt1 GTPase-interacting proteins belong to these regulators in ER-to-Golgi and intra-Golgi transport.

In this thesis, I described the main characteristics of two close orthologues of the COPII component Sec24p. I described how Sec24p orthologues are presumably actively involved in COPII vesicle formation and I showed that they do possess overlapping and distinct functions. In addition to that I reported the characterization of a new member of the Gyp family of GTPase activating proteins (GAPs), named Gyp5p, which shows remarkable specificity for Ypt1p.

5.1 Sec24p family

In addition to the essential Sec24p in *S. cerevisiae*, there are two non-essential but related proteins named Sfb2p/Iss1p (product of the ORF *YNL049c*) and Sfb3p/Lst1p (product of the ORF *YHR098c*), see also Table 1.2. The acronym "SFB" stands for "Sed-five binding". In a previous study, Sec24p was isolated as a protein that interacts with Sed5p (Peng *et al.*, 1999) and therefore the protein was temporally (before being recognized as Sec24p) named Sfb1p. The two homologues were consequently named Sfb2p and Sfb3p. Sfb2p, as does Sec24p, binds Sed5p; Sfb3p instead, binds this protein only weakly. Sfb2p shares 56% sequence identity with Sec24p, while Sfb3p shares only 23% sequence identity with Sec24p. The N-terminal regions of these proteins are the least conserved.

Similarly, in mammalian cells, four proteins were identified as components of a Sec24p family and named hSec24A, hSec24B, hSec24C and hSec24D (Pagano *et al.*, 1999). hSec24Ap shares 56% identity with hSec24Bp, and hSec24Cp shares 52% identity with hSec24Bp and there is about 20% identity between the two pairs.

The four cysteines of the putative Zn²⁺ binding motif are conserved in all the Sec24p homologues from yeast to man (see Fig. 5.1). In a previous study it was demonstrated that a single cysteine change renders the yeast Sec24p nonfunctional, but this does not interfere with Sec23p or Sed5p binding (Peng *et al.*, 1999).

Sec24p	218	D--PPPLNEDGLIVRCRRRCRSYMNPFVTFIEQGRWRRCNFCRLANDVP-MQMDQ
Sfb2p	151	N--QVPLNTDGVIVRCRRRCRSYMNPFVVFINQGRKWQCNICRFKNDVP-FGFDQ
Sfb3p	205	EVPTIPLPMDGTPLRCRRCRAYANPKFQFTYD-SSVICNICRVKMQVPGEHFAP
hSec24Ap	404	---QLPVVTSSTIVRCRSCRTYINPFVVSFLDQ-RRWKCNLCYRVNDVP-EEFLY
hSec24Bp	593	---QLPVITSNTIVRCRSCRTYINPFVVSFIDQ-RRWKCNLCYRVNDVP-EEFMY
hSec24Cp	410	ASPYVDHGESGPIRCNRCKAYMCPFMQFIEGGRRFQCCFCSCINDVPPQYFQH
hSec24Dp	348	SPLYLVNHGESGPVRCNRCKAYMCPFMQFIEGGRRYQCCGFCNCVNDVPPFYFQH

Fig. 5.1 Multiple alignment of the putative Zn²⁺ binding region sequences from human and yeast Sec24p related proteins, highlighted in red are the four cysteine residues of the motif. Identical or similar amino acids in four or more sequences are shown on black or shaded background, respectively.

5.1.1 Sfb2p

Among the three homologues Sfb2p is the least abundant. It was calculated that the intracellular concentrations ratio [Sec24p]:[Sfb2p]:[Sfb3p] is about 3.4:1:2.8.

When overexpressed, Sfb2p can rescue the growth defect of the temperature-sensitive *sec24-11* mutant. Like Sec24p (Hicke *et al.*, 1992), Sfb2p, forms stable complexes with Sec23p *in vivo*, Sec23p but not Sec24p could in fact be immunoprecipitated together with Sfb2p. According to the co-immunoprecipitation analyses, Sec23p is in excess over Sec24p. It is therefore easy to think that the exceeding Sec23p can be in complex with Sfb2p or Sfb3p. By gel filtration chromatography it was found that a portion of Sfb2p was overlapping with the Sec23p peak at about 250-300 kDa, but unlike Sec23p, Sec24p and Sfb3p, a significant portion of Sfb2p eluted from the column with a molecular mass of around 650 kDa. It is therefore possible that Sfb2p might form larger complexes without Sec23p. Cell fractionation experiments also documented that Sfb2p is a membrane-associated protein and a component of complexes. It was found in cellular fractions sedimenting at 10.000g and 100.000g.

Secretion of CPY and ALP was completely blocked in a double Δ *sfb2/sec24-11* mutant at the non permissive temperature, while in the single mutants these proteins were normally processed. Instead, invertase is secreted to a large extent, and only a small portion of invertase is accumulated in its ER core-glycosylated form. This phenomenon is not easily explainable, unless one would hypothesize a more efficient packaging of invertase with Sfb3p being the only functional protein. This could be a clue about a different role in cargo selection of the different Sec24p related proteins.

The electron microscopic inspection of the Δ *sfb2/sec24-11* mutant revealed ER proliferation and the accumulation (about three-fold compared to wild type) of membrane-enclosed vesicular and rod-like structures, sometimes organized in clusters. The accumulated vesicles have an approximate size of 30-50 nm, a size typical for ER-derived transport intermediates that occasionally were also found in clusters in other *sec* mutants with defects in fusion (Kaiser and Schekman, 1990). It is quite difficult to give an explanation for the accumulation of these vesicles in a mutant in which both Sec24p and Sfb2p function is impaired. It might be that Sfb3p is enough to permit vesicle budding, but the vesicles so produced cannot fuse efficiently with their target membrane. This inability to fuse efficiently could be due either to the incorrect packaging into the vesicle of proteins required for docking and fusion or to a direct involvement of Sec24p and Sfb2p in vesicle docking and fusion processes.

Most of the data presented here were confirmed by other researchers (Higashio *et al.*, 2000; Kurihara *et al.*, 2000). In addition they reported that Sfb2p could physically

interact with Sec16p (and for that reason they named this protein *Iss1p* = interacting with *sec-sixteen*), and that there was a synthetic lethal interaction between *ISS1* (*SFB2*) and *SEC22* and *BET1* but not with *SEC12*, *SEC13*, *SEC16*, *SEC23*, *SEC17*, and *SEC18*, as was the case for *SEC24* (Kurihara *et al.*, 2000). They could also demonstrate that purified Sfb2p/Sec23p complexes could drive vesicle formation from the ER *in vitro* and that the vesicles were comparable to those produced with Sec24p/Sec23p complex, but the packaging efficiency was lower in Sfb2p containing vesicles.

5.1.2 Sfb3p

SFB3 encodes a ~100 kDa membrane-associated protein that is expressed at higher levels than Sfb2p but at slightly lower levels than Sec24p. Co-immunoprecipitation and chromatographic experiments revealed that Sfb3p, like Sec24p and Sfb2p, *in vivo* forms complexes with Sec23p that can associate with membranes in cellular fractions sedimenting at 10.000g and 100.000g. Unlike Sfb2p, Sfb3p could not rescue the growth defect of the temperature-sensitive *sec24-11* mutant. On the contrary, its overexpression was toxic for the cells. The deletion of *SFB3* did not induce any visible phenotype but its combination with the *sec24-11* allele resulted in lethality. Since the Δ *sfb2/sec24-11* combination was possible, one could speculate that Sfb3p might have a more critical role in transport than Sfb2p.

Other researchers isolated *SFB3* in a screen for mutants that are lethal in combination with *sec13-1* and named it *LST1* (lethal with *sec-thirteen*) (Roberg *et al.*, 1999). The same investigators found that Δ *lst1* is lethal when combined with mutations in genes required for COPII vesicle budding (*SEC12*, *SEC13*, *SEC16*, *SEC23*, *SEC24*, *SEC31*), but it is not lethal when combined with mutations in genes required for vesicle fusion (*SEC17*, *SEC18*). It was furthermore demonstrated that deletion of *LST1* (*SFB3*) reduces the secretion of a subset of soluble proteins (Pagano *et al.*, 1999) and inhibits the transport of the plasma membrane proton-ATPase (Pma1p) to the cell surface (Roberg *et al.*, 1999). Subsequently it was demonstrated that Sec24p and Lst1p (Sfb3p) are present on the membrane of the same COPII vesicles and cooperate in sorting Pma1p. Vesicles formed with a mixture of Sec23p/Lst1p and Sec23p/Sec24 complexes were morphologically similar and with a similar buoyant density, but ~ 15% larger in diameter than normal COPII vesicles (Shimoni *et al.*, 2000). However, Sec23p/Lst1p (Sfb3p), in contrast to Sec23p/Iss1p (Sfb2p), could not drive vesicle formation efficiently (Shimoni *et al.*, 2000).

5.1.3 Why are there three Sec24 related proteins?

As mentioned above, a family of Sec24p-related proteins exists not only in yeast. As we and other researchers documented, all the members of the family are expressed, even if at different levels, and all can form complexes with Sec23p. This would argue in favor of a direct involvement of all the different Sec24p members in COPII-mediated transport. However, there are differences among the members. In yeast we have seen that only Sec24p is essential for viability, the two others are not. We observed that *SFB3* deletion is lethal when combined with mutation in *SEC24* gene. Instead, in the $\Delta sfb2/sec24-11$ mutant there was a block in transport of the vacuolar enzymes CPY and ALP. Only overexpression of Sfb2p, which is the most similar to Sec24p, and which is the least expressed in the cell, can partially substitute for Sec24p function. Sfb3p on the contrary is somehow toxic when overexpressed, but this effect is overcome when overexpression was performed in combination with Sfb2p or with Sec24p. Previously it was reported that also overproduction of Sec23p impairs cell growth (Kurihara *et al.*, 2000) and that excess of Sec23p inhibits the budding reaction *in vitro* (Yoshihisa *et al.*, 1993). It is therefore probable that an appropriate balance of Sec23p, Sec24p and its related proteins is important for efficient budding. It is also known that during the process of vesicle formation, cargo proteins are specifically packaged, whereas ER resident proteins are excluded (Kuehn *et al.*, 1998; Kuehn and Schekman, 1997; Matsuoka *et al.*, 1998a). A subset of COPII components, Sar1p and Sec23p/Sec24p, is thought to be involved in cargo recognition and recruitment (Aridor *et al.*, 1998; Kuehn *et al.*, 1998; Springer and Schekman, 1998). We also found a direct interaction of Sec24p and Sfb2p with the t-SNARE Sed5p (Peng *et al.*, 2000; Peng *et al.*, 1999). Therefore it is not unreasonable to hypothesize that Sec24p family members are involved in packaging and sorting of the cargo. The two non essential proteins Sfb2p and Sfb3p could be involved in sorting and concentrating of some subtype of cargo into the nascent vesicle. The specificity of Sfb3p for particular proteins was actually demonstrated (Pagano *et al.*, 1999; Roberg *et al.*, 1999; Shimoni *et al.*, 2000).

We also found that Sfb2p could be part of a large (~650 kDa) protein complex. There is therefore the possibility that this COPII component acts in processes other than budding and cargo selection. Finally, the interaction observed for both Sec24p and Sfb2p with Sed5p could also be an indication for the involvement of these

proteins in another step of transport, for example tethering/docking. However, the latter hypotheses are simple speculations and require further investigations.

5.2 Ypt/Rab proteins as regulators of protein transport

Once the cargo-containing vesicles have pinched off from the donor organelle membrane, they must be targeted to and fuse with the correct target membrane. As was shown in the Introduction, many proteins are involved in tethering, docking and fusion events. Ypt/Rab proteins are important regulators of the tethering/docking processes. They might be involved in recruiting tethering and docking factors and/or in the removal of inhibitors of SNARE complex assembly, as could be proteins of the Sec1 family. Ypt/Rab proteins are GTPases that cycle between a GDP-bound (inactive) and a GTP-bound (active) form. This functional cycle is tightly controlled through the interaction with guanine nucleotide exchange factors (GEFs) which stimulate the exchange of GDP for GTP, and GTPase activating proteins (GAPs) which accelerate the slow intrinsic GTPase activity of Ypt/Rab proteins. In yeast these GTPase activating proteins were named Gyp (**G**ap for **Y**pt) (Strom *et al.*, 1993).

The GTPase that regulates the transport between the endoplasmic reticulum and the Golgi apparatus is Ypt1p. Here, I report on a new Gyp protein the preferred substrate of which turned out to be Ypt1p.

5.3 Gyp proteins and the "GYP domain"

Advanced homology search algorithms (Neuwald, 1997) identified sequence motifs (termed motifs A, B, C, D, E, F, see Fig. 4.2) shared among three known Gyp proteins (Gyp1p, Gyp6p, Gyp7p) and many other proteins from different species, among them several yeast proteins with unknown function. The six motifs are localized within the catalytic domain of Gyp proteins (Albert *et al.*, 1999), therefore we referred to this region as the "GYP domain". However, additional sequences C-terminal of the GYP domain are required for GAP activity (see below). The six motifs harbor three highly conserved "fingerprint sequences" (RxxxW, in motif A; lxxDxxR, in motif B; and YxQ, in motif C) and in addition a conserved aspartic acid residue in motif F (see Figs. 4.2 and 5.2).

A detailed mutational analysis of the catalytically active regions of Gyp1p and Gyp7p (Albert *et al.*, 1999) revealed that the arginine residue in motif B (R343 in Gyp1p) is critical for the catalytic activity. This was an indication for a generalized "arginine finger" mechanism of GTPase activation as described for Ras- and Rho-GAP (Scheffzek *et al.*, 1998). After the crystal structure of Gyp1p GAP-domain had been resolved (Rak *et al.*, 2000), it was seen that the critical catalytic arginine is positioned in the presumed GTPase binding cleft of the molecule (see Fig. 1.9) and forms a salt bridge with the conserved aspartic acid in motif B (see Fig. 5.2). The conserved residues are clustered in two different areas of the Ypt1-GAP domain.

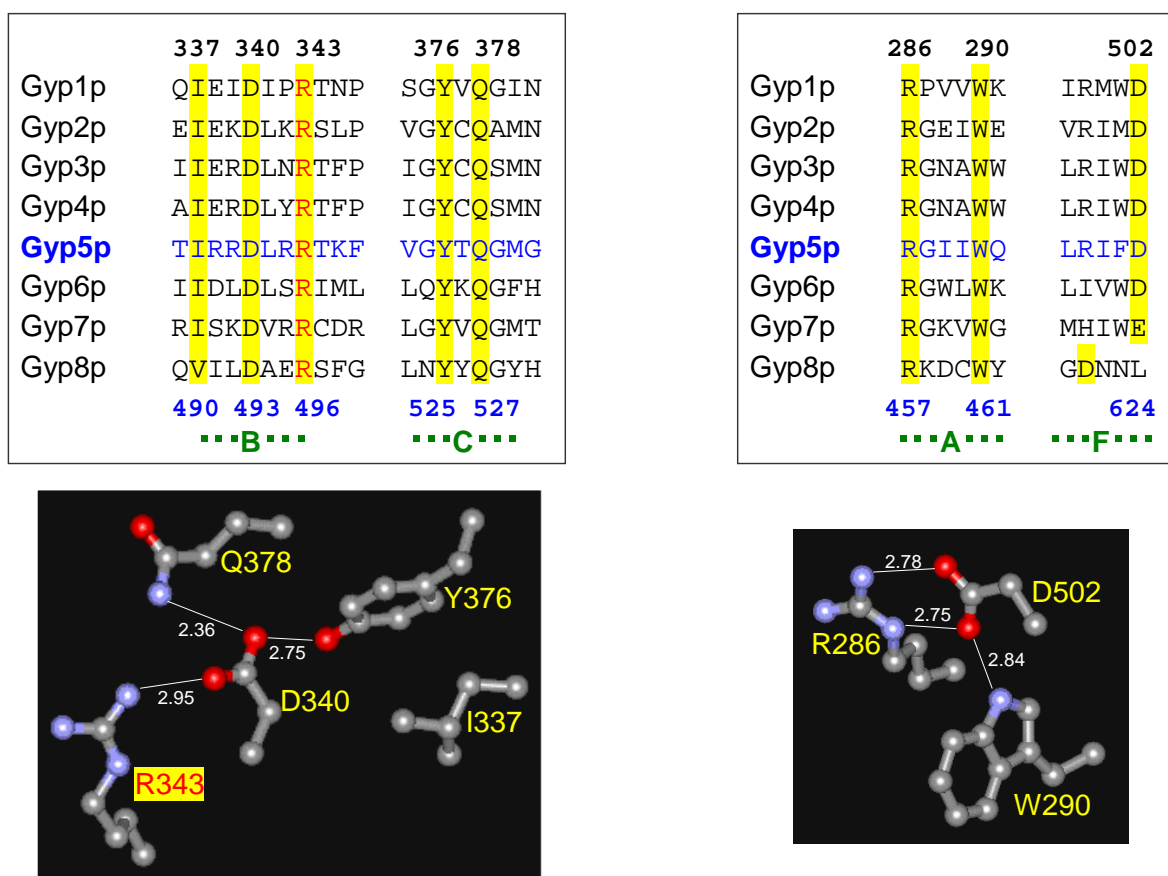


Fig. 5.2 Multiple alignment of the regions containing the "fingerprint sequences" lxxDxxR (in motif B), YxQ (in motif C), RxxxW (in motif A) and the conserved aspartic acid (in motif F). The numbers at the top indicate the residues' positions relative to Gyp1p, the blue numbers at the bottom indicate the residues' positions relative to Gyp5p. Under each alignment group the ball-and-stick representation (visualized with WebLab Viewer) of the conserved residues' side chains in Gyp1p is given. The residues can interact via hydrogen and ionic bonds (H-bond are detected when the distance between donor and acceptor atom is from 2.35 up to 3.2 Angstroms). The oxygen atoms are in red, the nitrogen atoms are in blue. White numbers and sticks indicate the distance between the atoms (in Angstroms).

The residues of the IxxDxxR and YxQ "fingerprint sequences" cluster at the surface of the potential binding cleft of the molecule and can interact via hydrogen and ionic bonds. The conserved aspartic acid in motif F can interact with the conserved residues of the RxxxW "fingerprint sequence". These residues cluster in the central core of the molecule and their interaction seems to be important for the stability of Gyp1p (see Fig. 5.2). To date there are eight yeast proteins proven to be Ypt-GAPs (see Table 1.3) among them Gyp5p.

5.4 Gyp5p

One of the unknown yeast proteins containing the GYP domain was the product of the ORF *YPL249c*, and we named it Gyp5p. Gyp5p is a 101.8 kDa (894 amino acids) cytosolic protein, as could be demonstrated by cell fractionation. The GYP domain is contained between the amino acids 451-624 (see Figs. 4.2 and 4.3), but for catalytic activity additional C-terminal regions are required. Expressing different fragments of Gyp5p as 6xHis fusion proteins it was possible to determine that the catalytic region of the protein was situated in the C-terminal half of the molecule. The N-terminal 430 amino acids were dispensable for GAP activity, whereas the deletion of the C-terminal 261 amino acids rendered this GAP inactive. The minimum active fragment obtained was comprised of amino acids 400-759 (see Fig. 4.3). We do not know the function of the N-terminal half of the protein. It might serve a role in regulating the activity through the interaction with other proteins or it could be necessary for the recruitment of the GAP to a specific cellular location where its activity is required. Computer analysis with the program COILS revealed also a potential coiled-coil region at the C-terminus of Gyp5, between the amino acids 730-870. This part of the molecule (at least after amino acid 759) is dispensable for GAP activity but it could be involved in protein-protein interactions.

5.4.1 Ypt1p is the preferred substrate of Gyp5p

The Gyp5₍₄₀₀₋₈₉₂₎ fragment was tested for its GAP activity on different GTPases in a standard HPLC-based GAP assay (20 μ M GTP-loaded GTPases and 0.1 μ M Gyp5p₍₄₀₀₋₈₉₂₎). Ypt1p turned out to be the best substrate by far. At standard conditions, the intrinsic GTPase activity of Ypt1p was accelerated 150-fold, that of Sec4p 20-fold and those of other GTPases were not accelerated at all.

For further characterization of the Gyp5p₍₄₀₀₋₈₉₂₎/ Ypt1p interaction, the K_m and k_{cat} values were calculated from single time curves using the integrated Michaelis-Menten equation. A K_m of 400 μM and a k_{cat} of 9 s^{-1} were calculated. Given an intrinsic GTP hydrolysis rate of 0.0035 min^{-1} , the GTPase activity of Ypt1p is maximally accelerated 1.6×10^5 -fold by the action of Gyp5p₍₄₀₀₋₈₉₂₎. Therefore, although Gyp5p₍₄₀₀₋₈₉₂₎ has a very low affinity for its preferred substrate, Ypt1p, the activation rate of the GTPase is comparable with the values obtained for other GAPs (see Table 5.1)

Table 5.1 Catalytic properties of different GTPase activating proteins

GAP	GTPase	K_m (μM)	k_{cat} (s^{-1})	Activation (-fold)	References
Gyp5p ₍₄₀₀₋₈₉₂₎	Ypt1p	400	9	1.6×10^5	This work
Gyp1-46p	Ypt51p	143	3.9	4.5×10^4	(Albert <i>et al.</i> , 1999)
Gyp3p/Msb3p	Sec4p	154	13.3	5×10^5	(Albert and Gallwitz, 1999)
GST-Gyp6p	Ypt6p	592	18.8	5.1×10^6	(Will and Gallwitz, 2001)
Gyp7p	Ypt7p	400	7.5	2×10^5	(Albert <i>et al.</i> , 1999)
Gyp7-47p	Ypt7p	42	30	7.8×10^5	(Albert <i>et al.</i> , 1999)
p120-GAP	H-Ras	9.7	19	1.6×10^5	(Gideon <i>et al.</i> , 1992)
GAP-334	H-Ras	19	4.2	3.5×10^4	(Gideon <i>et al.</i> , 1992)
NF1-230	H-Ras	0.65	7.3	6.1×10^4	(Ahmadian <i>et al.</i> , 1996)
P190	RhoA	1.79	1.61	4.4×10^3	(Zhang and Zheng, 1998)
p50RhoGAP	RhoA	2.83	0.99	2.7×10^3	(Zhang and Zheng, 1998)
Ran-GAP	Ran/TC4	0.43	2.1	1.2×10^5	(Klebe <i>et al.</i> , 1995)

5.4.2 Gyp5, like other Gyp proteins, contains a putative catalytic arginine finger

It was previously demonstrated that Gyp1p, Gyp7p (Albert *et al.*, 1999) and Gyp6p (Will and Gallwitz, 2001), contain an arginine residue in motif B (R343 in Gyp1p, R458 in Gyp7p and R155 in Gyp6p) that is absolutely critical for GAP activity. This led to the hypothesis that an arginine finger mechanism similar to that described for Ras- and Rho-GAPs (Scheffzek *et al.*, 1997; Scheffzek *et al.*, 1998; Wittinghofer *et al.*, 1997) could have been adopted by all Gyp proteins. Here, I demonstrate that also Gyp5p contains a critical catalytic arginine (R496) in motif B. Arginine-496 of the active fragment Gyp5p₍₄₀₀₋₈₉₂₎ was mutated to either alanine or lysine (conservative exchange) and the accelerating activity of these mutant proteins on Ypt1p was evaluated. By kinetic analysis under standard conditions (0.2 μM Gyp5p and 20 μM Ypt1p) I observed

that both the R496A and the R496K mutations resulted in an apparently complete inactivation of Gyp5p₍₄₀₀₋₈₉₂₎. Only by strongly increasing the concentration of the R496K mutant (11 μM Gyp5p^{R496K} and 55 μM Ypt1p) a 4-fold acceleration of GTP hydrolysis could be observed. This shows that even mutated Gyp5p^{R496K} is able to interact with its substrate but its activity is severely compromised.

5.4.3 Gyp5p can accelerate the GTPase activity of the Ypt1p^{Q67L} mutant

The Q67L mutation of Ypt1p is analogous to the oncogenic Q61L mutation of p21^{ras}. This Ras mutant has an impaired intrinsic GTPase and is insensitive towards GAP (Bollag and McCormick, 1991; Der *et al.*, 1986). It was proposed that during the GTPase reaction, glutamine-61 would activate a water molecule for a nucleophilic attack of the γ -phosphate (Krengel *et al.*, 1990; Pai *et al.*, 1990; Sprang, 1997). Alternatively, it was proposed that the role of glutamine-61 is involved in the transition-state stabilization of the hydrolysis reaction (Privé *et al.*, 1992).

The Ypt1p^{Q67L} mutant has a strongly decreased intrinsic GTPase activity ($<0.0002 \text{ min}^{-1}$, wt = 0.0035 min^{-1}). Surprisingly, Gyp5p, in contrast to Ras-Gap, can accelerate the GTPase activity of Ypt1p^{Q67L}. The GTPase activity of 20 μM Ypt1p^{Q67L} in the presence of 2 μM Gyp5p₍₄₀₀₋₈₉₂₎ can be accelerated ~400-fold. Therefore, against common belief, a mutant analogous to Q61L Ras was sensitive towards GAP action. We don't know the molecular mechanism that allows the hydrolysis of GTP bound to Ypt1p^{Q67L}. Glutamine-67 of Ypt1p seems to be important for GTP hydrolysis, in fact the intrinsic GTPase activity is drastically reduced. A possible hypothesis is that Gyp5p supplies amino acid residues for the glutamine of the GTPase that can mimic its function in the activation of the water molecule for the nucleophilic attack of the γ -phosphate or in the transition-state stabilization. Gyp proteins could therefore constitute a new class of GAPs able to activate GTPases mutated in the critical conserved glutamine.

5.4.4 Is GTP hydrolysis important *in vivo*?

Deletion of *GYP5* alone or in combination with *GYP1* and *GYP8* (the proteins product of which are known to be GAPs for Ypt1p, too) did not induce any particular mutant phenotype. Therefore, we thought to combine the *GYP* gene deletions with *ypt1*^{Q67L}. Analyzing growth at different temperatures of the different mutant strains it was observed that *ypt1*^{Q67L} became cold-sensitive (at 15°C) when the *GYP* genes

were missing. The strongest growth defect was observed for strains lacking *GYP5*. This was the first indication for an interaction of Gyp5p and Ypt1p *in vivo*, and also an indication that Ypt1p is more conditioned by Gyp5p than by the other two Gyp proteins (that *in vitro* were also active on Ypt1p).

When the *ypt1*^{Q67L} allele replaced the wild type *YPT1* gene in the protease deficient strain cl3-ABYS-86, it was observed that the cells could not grow at 15°C. This growth defect could be partially rescued by overexpression of Gyp5p₍₈₋₈₉₂₎ but not by the catalytically active fragment Gyp5p₍₄₀₀₋₈₉₂₎. Therefore, the N-terminal part of the protein, that is not important *in vitro* for the catalytic activity, became important *in vivo*. This region could be important to target and concentrate the enzyme to a specific cellular location where GAP activity is required.

We tested whether the different *gyp* null mutants in combination with *ypt1*^{Q67L} had secretion defects. Transport of CPY and invertase were not affected at the restrictive temperature. Only a slight retardation in Gas1p maturation was observed, but this was probably due to the growth defects of these cells and not to a transport defect.

Surprisingly, the *ypt1*^{Q67L} mutant, but much more the double mutant $\Delta gyp5/ypt1^{Q67L}$, exhibited an altered morphological phenotype, visible under the electron microscope, and also under the fluorescence microscope by FM 4-64 staining (that visualizes vacuolar membranes). The double mutant cells exhibited, already at the permissive temperature, an accumulation of ER membranes and of various membrane bounded structures. These included vesicles of different size and structures resembling autophagosomes. In addition, vacuoles were fragmented and often showed large invaginations resembling autophagic tubes (Müller *et al.*, 2000) and engulfed multivesicular bodies.

Therefore, despite a lack of transport defects, as expected for mutants of proteins involved in docking/fusion processes, growth defects and morphological changes were observed. We should keep in mind that Ypt1p in the double mutant $\Delta gyp5/ypt1^{Q67L}$ is probably kept in a "permanently" active state. This could make vesicle transport more active, up to the point that too much material is transported and accumulated. The different membraneous structures accumulated in the cytoplasm and inside the vacuoles could be due to an overload of material that cannot be used and needs to be eliminated, probably through autophagocytosis. Autophagocytosis is a major protein degradation process that allows the transfer of cytosolic proteins and organelles into lysosomes (for review see Klionsky and Emr,

2000; Seglen and Bohley, 1992). It operates at the constitutive level, but can be induced under condition of stress such as starvation. In our case, the stress condition could be due to over-active transport with a subsequent overload of materials that have to be eliminated. Autophagocytosis is distinguished into macro- and microautophagocytosis. Macroautophagocytosis occurs through the formation of autophagosomes which are specialized vesicle bounded by double or multiple membranes (Scott and Klionsky, 1998). The origin of these vesicles is unknown, both ER and Golgi have been proposed as precursors. Microautophagocytosis induces direct invagination of lysosomes (vacuoles in yeast), leading to the formation of autophagic tubes and single membrane bounded vesicles in the vacuolar lumen that are rapidly degraded. Microautophagocytosis was proposed to be directly connected to macroautophagocytosis (Müller *et al.*, 2000). In our electron micrographs, membrane-bounded structures, resembling both autophagosomes and autophagic tubes, could be detected.

It is interesting to note that autophagocytosis could be demonstrated in yeast with proteinase-deficient mutants (Takeshige *et al.*, 1992), because cellular components sequestered in the vacuoles could not be degraded and accumulated. We observed that *ypt1*^{Q67L} mutants in the c13-ABYS-86 strain background (a protease deficient strain) showed more severe growth defects than mutants in the MSUC-3D background. In addition, it was impossible to replace the wild type *YPT1* gene with the *ypt1*^{Q67L} allele in $\Delta gyp5/\Delta gyp1$, $\Delta gyp5/\Delta gyp8$ and $\Delta gyp1/\Delta gyp8$ mutants in c13-ABYS-86 strain background. This could be due to the fact that mutant cells, where vesicular transport is "over-active", accumulate material that needs to be eliminated, but in proteinase deficient strains, cellular components sequestered in the vacuoles cannot be degraded, and therefore, proteinase deficient strains suffer more than others from the "permanently" activated state of Ypt1p.

The effects induced by the Q67L mutation in Ypt1p were studied also by other researchers (Richardson *et al.*, 1998). These investigators could not observe any particular altered phenotype in *ypt1*^{Q67L} and concluded that GTP hydrolysis is not important for Ypt1p GTPase function *in vivo*, but only for recycling of Ypt1p between compartments. Their conclusions, however, did not take into proper consideration the action of GAP proteins.

Other investigators analyzed *sec4*^{Q79L}, *rab2*^{Q65L}, *rab5*^{Q79L} and *rab6*^{Q72L}. *sec4*^{Q79L} cells were cold sensitive at 14°C, and the investigators observed that a decrease in GTPase activity led to a loss of Sec4p function (Walworth *et al.*, 1992). *Rab2p*^{Q65L}

was found to be an inhibitor of ER-to-Golgi transport when overexpressed (Tisdale *et al.*, 1992). This was attributed to the fact that this mutant protein could stimulate vesicle formation from pre-Golgi compartments altering the correct distribution of VTCs (vesicular tubular clusters) (Tisdale, 1999). Rab5p^{Q79L} stimulated membrane fusion in endocytosis (Stenmark *et al.*, 1994), and subsequently it was suggested that GTP hydrolysis acts as a timer that determines the frequency of membrane docking/fusion events (Rybin *et al.*, 1996). Rab6p is involved in intra-Golgi transport, and overexpression of Rab6p^{Q72L} induces a brefeldinA-like effect redistributing Golgi resident proteins into the ER (Martinez *et al.*, 1997).

Our data would support a role of the GTPase control as a timer, as it was previously postulated (Rybin *et al.*, 1996), regulating the velocity and efficiency of transport depending on the needs of the cell. When this timer is blocked, as it is the case in our $\Delta gyp5/ypt1^{Q67L}$ mutant, there is accumulation of materials that find a different way to be eliminated, as for example by autophagocytosis .

6 SUMMARY

In this thesis, I described the main characteristics of two close orthologues of the COPII component Sec24p. These proteins were named Sfb2p and Sfb3p. I described how Sec24p orthologues are most likely actively involved in COPII vesicle formation and in cargo selection. It was found that *SFB2* and *SFB3* are dispensable, but combining $\Delta sfb2$ null with the *sec24-11* conditional allele led to serious secretion defects. The combination of $\Delta sfb3$ with the *sec24-11* allele resulted in lethality. Both Sfb2p and Sfb3p form stable complexes with Sec23p. Sfb2p was also found in a large complex without Sec23p. It was also observed that Sfb2p, like Sec24p, interacts with Sed5p, while the interaction of Sfb3p with Sed5p is very weak.

In addition to that, I characterized a new member of the Gyp family of Ypt/Rab-specific GTPase activating proteins (GAPs), named Gyp5p, which shows remarkable specificity for Ypt1p. Furthermore, I investigated the biological function of Ypt1p GTP hydrolysis in the cells. I demonstrated that Gyp5p, like other GAP proteins, contains a critical catalytic arginine and that it is able to accelerate the GTP hydrolysis not only of Ypt1p but also that of the Ypt1p^{Q67L} mutant. The $\Delta gyp5/ypt1^{Q67L}$ mutant is cold-sensitive at 15°C and shows morphological alterations (also at 30°C) that are reminiscent of autophagy.

7 APPENDIX

7.1 Bacterial and yeast strains and mammalian cell lines

7.1.1 Bacterial *E. coli* strains

Table 7.1

Strain	Genotype	Source
DH5 α	F ϕ 80 <i>dlacZ</i> Δ M15 Δ (<i>lacZYA-argF</i>)U169 <i>endA1 recA1 hsdR17</i> (<i>r_k⁻ m_k⁺</i>) <i>deoR thi-1 supE44 λ⁻ gyrA96 relA1</i>	Gibco-BRL (Karlsruhe, Germany)
DH5 α F'IQ	F' <i>pro AB⁺ lacI^q Z</i> Δ M15 <i>zzf::Tn5</i> [Kan ^r]/ ϕ 80 <i>dlacZ</i> Δ M15 Δ (<i>lacZYA-argF</i>)U169 <i>endA1 recA1 hsdR17</i> (<i>r_k⁻ m_k⁺</i>) <i>deoR thi-1 supE44 λ⁻ gyrA96 relA1</i>	Gibco-BRL
XI1Blu	<i>endA1 recA1 gyrA96 thi⁻ hsd R17</i> (<i>r_k⁻ m_k⁺</i>) <i>supE44 relA1 lac⁻ [F ϕtraD36 proAB lacI^q Z</i> Δ M15 <i>Tn10</i> (Tc ^r)	Stratagene (Heidelberg, Germany)
Origami (DE3)	Δ <i>ara-leu7697</i> Δ <i>lacX74</i> Δ <i>phoAPvull phoR araD139 galE galK rspL F [lac⁻(lacI^f)pro] gor522::Tn10</i> (Tc ^r) <i>trxB::kan</i> (DE3)	Novagen (Darmstadt, Germany)
BL21	F <i>ompT hsdS</i> (<i>r_{B-mB-}</i>) <i>gal dcm</i>	Novagen
BL21(DE3)	F <i>ompT hsdS</i> (<i>r_{B-mB-}</i>) <i>gal dcm</i> (DE3)	Novagen
M15[pREP4]	F <i>Nal^S Str^S Rif^S Thi⁻ Lac⁻ Ara⁻ Gal⁻ Mti⁻ recA⁺ Uvr⁺ Lon⁺</i>	QIAGEN (Hilden)

For a description of gene nomenclature see (Bachmann, 1987).

7.1.2 Yeast strains

Table 7.2

Strain	Genotype	Source
cl3-ABYS-86	MAT α <i>ura3-Δ5 leu2-3 112 his3 pra1-1 prb1-1 prc1-1 cps1-3 can^R</i>	D. H. Wolf, Univ. of Stuttgart, Germany
MSUC-3D	MAT α <i>ura3 trp1 leu2 his3 lys2</i>	This Department
MSUC-IA	MAT α <i>ura3 trp1 leu2 his3 ade8</i>	This Department
<i>sec18-1</i>	MAT α <i>leu2</i>	Dr. H. D. Schmitt, this Department
BHY11	MAT α <i>ura3-52 his3Δ200 trp1Δ901 ade2-101 suc2-Δ9 leu2-3 112::pBHY11 (CPY-InvLEU2)</i>	(Horazdovsky <i>et al.</i> , 1994)
RH227-3A	MAT α <i>ura3 leu2 his3 sec23-1</i>	Prof. H. Riezman, Univ. of Basel, Switzerland
RPY18	MAT α <i>ura3 trp1 leu2 his3 ade8 sec24-11</i>	(Peng <i>et al.</i> , 1999)
RPY61	MAT α <i>ura3 trp1 leu2 his3 ade8 sfb2::kanMX4</i>	(Peng <i>et al.</i> , 2000)
RPY63	MAT α <i>ura3 trp1 leu2 his3 lys2 sfb2::kanMX4 sfb2::LEU</i>	(Peng <i>et al.</i> , 2000)
RPY72	MAT α <i>ura3 trp1 leu2 his3 ade8 sec24-11 sfb2::kanMX4</i>	(Peng <i>et al.</i> , 2000)

ADY1	MAT α <i>ura3-Δ5 leu2-3 112 his3 pra1-1 prb1-1 prc1-1 cps1-3 can^R SFB2-6His-2MYC-loxP-KanMX-loxP</i>	(De Antoni and Gallwitz, 2000; Peng <i>et al.</i> , 2000); This work
ADY1/K ⁻	MAT α <i>ura3-Δ5 leu2-3 112 his3 pra1-1 prb1-1 prc1-1 cps1-3 can^R SFB2-6His-2MYC-loxP</i>	This work
ADY2	MAT α <i>ura3-Δ5 leu2-3 112 his3 pra1-1 prb1-1 prc1-1 cps1-3 can^R SFB3-6His-2MYC-loxP-KanMX-loxP</i>	(De Antoni and Gallwitz, 2000; Peng <i>et al.</i> , 2000); This work
ADY2/K ⁻	MAT α <i>ura3-Δ5 leu2-3 112 his3 pra1-1 prb1-1 prc1-1 cps1-3 can^R SFB3-6His-2MYC-loxP</i>	This work
ADY3	MAT α <i>ura3-Δ5 leu2-3 112 his3 pra1-1 prb1-1 prc1-1 cps1-3 can^R SEC23-6His-2MYC-loxP-KanMX-loxP</i>	(De Antoni and Gallwitz, 2000; Peng <i>et al.</i> , 2000); This work
ADY4	MAT α <i>ura3-Δ5 leu2-3 112 his3 pra1-1 prb1-1 prc1-1 cps1-3 can^R SEC24-6His-2MYC-loxP-KanMX-loxP</i>	(De Antoni and Gallwitz, 2000; Peng <i>et al.</i> , 2000); This work
ADY5	MAT α <i>ura3-Δ5 leu2-3 112 his3 pra1-1 prb1-1 prc1-1 cps1-3 can^R SFB2-6His-2MYC-loxP SFB3-6His-3HA-loxP-KanMX-loxP</i>	(Peng <i>et al.</i> , 2000); This work
ADY6	MAT α <i>ura3-Δ5 leu2-3 112 his3 pra1-1 prb1-1 prc1-1 cps1-3 can^R SFB2-6His-3HA-loxP-KanMX-loxP SFB3-6His-2MYC-loxP</i>	(Peng <i>et al.</i> , 2000); This work
ADY7	MAT α <i>ura3-Δ5 leu2-3 112 his3 pra1-1 prb1-1 prc1-1 cps1-3 can^R SEC24-6His-3HA-loxP-KanMX-loxP</i>	(De Antoni and Gallwitz, 2000); This work
ADY8	MAT α <i>ura3-Δ5 leu2-3 112 his3 pra1-1 prb1-1 prc1-1 cps1-3 can^R SFB2-6His-3HA-loxP-KanMX-loxP</i>	(De Antoni and Gallwitz, 2000); This work
ADY9	MAT α <i>ura3-Δ5 leu2-3 112 his3 pra1-1 prb1-1 prc1-1 cps1-3 can^R SFB3-6His-3HA-loxP-KanMX-loxP</i>	(De Antoni and Gallwitz, 2000); This work.
ADY10	MAT α <i>ura3-Δ5 leu2-3 112 his3 pra1-1 prb1-1 prc1-1 cps1-3 can^R SEC24-6His-3VSV-loxP-KanMX-loxP</i>	(De Antoni and Gallwitz, 2000); This work
ADY11	MAT α <i>ura3-Δ5 leu2-3 112 his3 pra1-1 prb1-1 prc1-1 cps1-3 can^R SFB2-6His-3VSV-loxP-KanMX-loxP</i>	(De Antoni and Gallwitz, 2000); This work
ADY12	MAT α <i>ura3-Δ5 leu2-3 112 his3 pra1-1 prb1-1 prc1-1 cps1-3 can^R SFB3-6His-3VSV-loxP-KanMX-loxP</i>	(De Antoni and Gallwitz, 2000); This work
ADY13	MAT α <i>ura3-Δ5 leu2-3 112 his3 pra1-1 prb1-1 prc1-1 cps1-3 can^R SEC24-6His-3HA-loxP-KanMX-loxP SFB3-6His-2MYC-loxP</i>	(De Antoni and Gallwitz, 2000); This work
ADY14	MAT α <i>ura3-Δ5 leu2-3 112 his3 pra1-1 prb1-1 prc1-1 cps1-3 can^R GYP5-6His-2MYC-loxP-KanMX-loxP</i>	This work
ADY15	MAT α <i>ura3-Δ5 leu2-3 112 his3 pra1-1 prb1-1 prc1-1 cps1-3 can^R GYP5-6His-3HA-loxP-KanMX-loxP</i>	This work
ADY16	MAT α <i>ura3-Δ5 leu2-3 112 his3 pra1-1 prb1-1 prc1-1 cps1-3 can^R GYP5-6His-3VSV-loxP-KanMX-loxP</i>	This work.
ADY20	MAT α <i>ura3-Δ5 leu2-3 112 his3 pra1-1 prb1-1 prc1-1 cps1-3 can^R gyp1::loxP-KanMX-loxP</i>	This work
ADY20/K ⁻	MAT α <i>ura3-Δ5 leu2-3 112 his3 pra1-1 prb1-1 prc1-1 cps1-3 can^R gyp1::loxP</i>	This work
ADY21	MAT α <i>ura3-Δ5 leu2-3 112 his3 pra1-1 prb1-1 prc1-1 cps1-3 can^R gyp5::loxP-KanMX-loxP</i>	This work
ADY21/K ⁻	MAT α <i>ura3-Δ5 leu2-3 112 his3 pra1-1 prb1-1 prc1-1 cps1-3 can^R gyp5::loxP</i>	This work
ADY23	MAT α <i>ura3-Δ5 leu2-3 112 his3 pra1-1 prb1-1 prc1-1 cps1-3 can^R gyp8::loxP-KanMX-loxP</i>	This work

ADY24	MAT α <i>ura3-Δ5 leu2-3 112 his3 pra1-1 prb1-1 prc1-1 cps1-3 can^R gyp5::loxP gyp1::loxP-KanMX-loxP</i>	This work
ADY24/K ⁻	MAT α <i>ura3-Δ5 leu2-3 112 his3 pra1-1 prb1-1 prc1-1 cps1-3 can^R gyp5::loxP gyp1::loxP</i>	This work
ADY25	MAT α <i>ura3-Δ5 leu2-3 112 his3 pra1-1 prb1-1 prc1-1 cps1-3 can^R gyp5::loxP gyp8::loxP-KanMX-loxP</i>	This work
ADY25/K ⁻	MAT α <i>ura3-Δ5 leu2-3 112 his3 pra1-1 prb1-1 prc1-1 cps1-3 can^R gyp5::loxP gyp8::loxP</i>	This work
ADY26	MAT α <i>ura3-Δ5 leu2-3 112 his3 pra1-1 prb1-1 prc1-1 cps1-3 can^R gyp1::loxP gyp8::loxP-KanMX-loxP</i>	This work
ADY27	MAT α <i>ura3-Δ5 leu2-3 112 his3 pra1-1 prb1-1 prc1-1 cps1-3 can^R gyp5::loxP gyp1::loxP gyp8::loxP-KanMX-loxP</i>	This work
ADY28	MAT α <i>ura3-Δ5 leu2-3 112 his3 pra1-1 prb1-1 prc1-1 cps1-3 can^R gyp5::loxP gyp8::loxP gyp1::loxP-KanMX-loxP</i>	This work
ADY29	MAT α <i>ura3-Δ5 leu2-3 112 his3 pra1-1 prb1-1 prc1-1 cps1-3 can^R ypt1^{Q67L}-LEU2</i>	This work
ADY30	MAT α <i>ura3-Δ5 leu2-3 112 his3 pra1-1 prb1-1 prc1-1 cps1-3 can^R gyp1::loxP-KanMX-loxP ypt1^{Q67L}-LEU2</i>	This work
ADY31	MAT α <i>ura3-Δ5 leu2-3 112 his3 pra1-1 prb1-1 prc1-1 cps1-3 can^R gyp5::loxP-KanMX-loxP ypt1^{Q67L}-LEU2</i>	This work
ADY32	MAT α <i>ura3-Δ5 leu2-3 112 his3 pra1-1 prb1-1 prc1-1 cps1-3 can^R gyp7::loxP-KanMX-loxP ypt1^{Q67L}-LEU2</i>	This work
ADY33	MAT α <i>ura3-Δ5 leu2-3 112 his3 pra1-1 prb1-1 prc1-1 cps1-3 can^R gyp8::loxP-KanMX-loxP ypt1^{Q67L}-LEU2</i>	This work
ADY40	MAT α <i>ura3 trp1 leu2 his3 lys2 gyp1::loxP-KanMX-loxP</i>	This work
ADY40/K ⁻	MAT α <i>ura3 trp1 leu2 his3 lys2 gyp1::loxP</i>	This work
ADY41	MAT α <i>ura3 trp1 leu2 his3 lys2 gyp5::loxP-KanMX-loxP</i>	This work
ADY41/K ⁻	MAT α <i>ura3 trp1 leu2 his3 lys2 gyp5::loxP</i>	This work
ADY42	MAT α <i>ura3 trp1 leu2 his3 lys2 gyp7::loxP-KanMX-loxP</i>	This work
ADY43	MAT α <i>ura3 trp1 leu2 his3 lys2 gyp8::loxP-KanMX-loxP</i>	This work
ADY43/K ⁻	MAT α <i>ura3 trp1 leu2 his3 lys2 gyp8::loxP</i>	This work
ADY44 ⁻	MAT α <i>ura3 trp1 leu2 his3 lys2 gyp5::loxP gyp1::loxP-KanMX-loxP</i>	This work
ADY44/K	MAT α <i>ura3 trp1 leu2 his3 lys2 gyp5::loxP gyp1::loxP</i>	This work
ADY45	MAT α <i>ura3 trp1 leu2 his3 lys2 gyp5::loxP gyp8::loxP-KanMX-loxP.</i>	This work
ADY45/K	MAT α <i>ura3 trp1 leu2 his3 lys2 gyp5::loxP gyp8::loxP</i>	This work
ADY46	MAT α <i>ura3 trp1 leu2 his3 lys2 gyp1::loxP gyp8::loxP-KanMX-loxP.</i>	This work
ADY47	MAT α <i>ura3 trp1 leu2 his3 lys2 gyp5::loxP gyp1::loxP gyp8::loxP-KanMX-loxP.</i>	This work
ADY48	MAT α <i>ura3 trp1 leu2 his3 lys2 gyp5::loxP gyp8::loxP gyp1::loxP-KanMX-loxP.</i>	This work
ADY49	MAT α <i>ura3 trp1 leu2 his3 lys2 ypt1^{Q67L}-LEU2.</i>	This work
ADY50	MAT α <i>ura3 trp1 leu2 his3 lys2 gyp1::loxP-KanMX-loxP ypt1^{Q67L}-LEU2.</i>	This work
ADY51/K ⁻	MAT α <i>ura3 trp1 leu2 his3 lys2 gyp5::loxP ypt1^{Q67L}-LEU2</i>	This work
ADY52	MAT α <i>ura3 trp1 leu2 his3 lys2 gyp7::loxP-KanMX-loxP ypt1^{Q67L}-LEU2</i>	This work

ADY53	MAT α <i>ura3 trp1 leu2 his3 lys2 gyp8::loxP-KanMX-loxP ypt1^{Q67L}-LEU2</i>	This work
ADY54	MAT α <i>ura3 trp1 leu2 his3 lys2 gyp5::loxP gyp1::loxP-KanMX-loxP ypt1^{Q67L}-LEU2</i>	This work
ADY55	MAT α <i>ura3 trp1 leu2 his3 lys2 gyp5::loxP gyp8::loxP-KanMX-loxP ypt1^{Q67L}-LEU2</i>	This work
ADY56	MAT α <i>ura3 trp1 leu2 his3 lys2 gyp1::loxP gyp8::loxP-KanMX-loxP ypt1^{Q67L}-LEU2</i>	This work

For a description of gene nomenclature see (Rose *et al.*, 1990; Sherman, 1991).

7.1.3 Mammalian tissue culture cell lines

The cell lines, the equipment, and materials for cell culture were gently provided by Prof. Mary Osborn (department of biochemistry and cell biology, MPI for Biophysical Chemistry). Cells were cultivated on Petri dishes in DME 10% FCS medium at 37 °C 95% humidity 7% CO₂ (I was helped for cell culture by Heinz Juergen Dehne and Susanne Brandfass)

Table 7.3

Strain	Origin	Cell type	Source
HeLa	Human cervix adenocarcinoma	epithelioid	ATCC
CV1	African green monkey kidney	fibroblastic	ATCC

7.2 Plasmids

7.2.1 *E. coli* cloning and expression vectors

Table 7.4

Vector	Description	Source
pBluescript SK ⁺	General cloning vector. Ampicillin resistance.	Stratagene (Heidelberg, Germany)
pQE50	Expression vector. T5 promoter, <i>lac</i> operator, ampicillin resistance	QIAGEN (Hilden, Germany)
pQE30	Expression vector for production of N-terminus 6xHis tagged proteins. T5 promoter, <i>lac</i> operator, ampicillin resistance	QIAGEN
pET12c	Expression vector. T7 promoter, ampicillin resistance	Novagen
pET30a	Expression vector for production of N- terminus 6xHis-tag and S-tag proteins or C-terminus 6xHis fusion proteins. T7 promoter, <i>lac</i> operator, <i>lacI</i> repressor, kanamycin resistance	Novagen. (Darmstadt, Germany)
pET32a	Expression vector for production of N- terminus Trx-tag, 6xHis-tag and S-tag proteins or C-terminus 6xHis fusion proteins. T7 promoter, <i>lac</i> operator, <i>lacI</i> repressor, ampicillin resistance	Novagen

pGEX-TT	Expression vector for production of GST fusion proteins. Contains the polylinker from pEG-KT, tac promoter, <i>lacI^f</i> repressor, ampicillin resistance	Dr. S. Albert, this Department
pMAL-c2	Expression vector for production of MBP fusion proteins,. Ptac promoter, <i>lacI^f</i> repressor, ampicillin resistance	New England Biol. (Frankfurt, Germany)
pET12c-YPT1	Plasmid for Ypt1p expression.	S. Albert, this Dep.
KIAA0079	Plasmid containing <i>hSEC24c</i> cDNA (KIAA0079)	(Nomura <i>et al.</i> , 1994)
pGEX-SED5ΔC	for expression of GST-Sed5p (amino acids 1-319)	Dr. R Grabowski, this Department
pGEX-UFE1ΔC	for expression of GST-Ufe1p (amino acids 1-326)	Dr. R. Peng, this Dept.

7.2.2 Yeast vectors

Table 7.5

Vector	Description	Source
pUG6	Plasmid containing the loxP-KanMX-loxP gene disruption cassette.	(Güldener <i>et al.</i> , 1996)
pSH47	Vector containing <i>cre</i> , <i>GAL1</i> promoter, CEN, <i>URA3</i>	(Güldener <i>et al.</i> , 1996)
pU6H2MYC	Plasmid containing the <i>6His-2MYC-loxP-KanMX-loxP</i> cassette for PCR mediated epitope tagging.	(De Antoni and Gallwitz, 2000); this work
pU6H3HA	Plasmid containing the <i>6His-3HA-loxP-KanMX-loxP</i> cassette for PCR mediated epitope tagging	(De Antoni and Gallwitz, 2000); this work
pU6H3VSV	Plasmid containing the <i>6His-3VSV-loxP-KanMX-loxP</i> cassette for PCR mediated epitope tagging	(De Antoni and Gallwitz, 2000); this work
pEG(KT)	2μ vector containing GST, galactose-inducible <i>CYC1</i> promoter, <i>URA3</i>	(Mitchell <i>et al.</i> , 1993)
pRS315	CEN, <i>LEU2</i>	(Sikorski and Hieter, 1989)
pRS316	CEN, <i>URA3</i>	(Sikorski and Hieter, 1989)
pRS325	2μ, <i>LEU2</i>	(Tsukada and Gallwitz, 1996)
pRS326	2μ, <i>URA3</i>	(Vollmer and Gallwitz, 1995)
pYX112	CEN, <i>URA3</i> , <i>TPI</i> -promoter	R&D-Systems (Wiesbaden, Germany)
pYX143	CEN, <i>LEU2</i> , <i>GAL1</i> -promoter	R&D-Systems
pYX212	2μ, <i>URA3</i> , <i>TPI</i> -promoter	R&D-Systems
pYX243	2μ, <i>LEU2</i> , <i>GAL1</i> -promoter	R&D-Systems
pRE-YPT1 ^{Q67L}	Plasmid containing <i>TUB2-YPT1^{Q67L}-LEU2-ACT1</i> , to replace <i>YPT1</i> gene with <i>YPT1^{Q67L}</i> allele	Dr. U. Vespermann, this Dept.; (Schmitt <i>et al.</i> , 1988)
pRS326-SEC24	2μ vector containing <i>SEC24</i> and its promoter	(Peng <i>et al.</i> , 1999)
pEG-SEC24 ₍₅₆₋₅₄₉₎ (pEG-SEC24N)	Galactose inducible GST-Sec24 ₍₅₆₋₅₄₉₎	(Peng <i>et al.</i> , 1999)
pEG-SEC24N ^{C231S}	Galactose inducible GST-Sec24N ^{C231S}	(Peng <i>et al.</i> , 1999)
pEG-SEC24N ^{C231S-C234S}	Galactose inducible GST-Sec24N ^{C231S-C234S}	(Peng <i>et al.</i> , 1999)
pRS326-SFB2	2μ vector containing <i>SFB2</i> and its promoter	(Peng <i>et al.</i> , 2000)
pMG28 (pEG-PEP12ΔC)	galactose inducible GST-Pep12 ₍₁₋₂₂₀₎	Dr. M. Götte this Dept.

7.2.3 Recombinant plasmids created in this work

Table 7.6

GYP5 constructs				
Construct	Insert preparation	Vector preparation	Features	Prot. expression
pET30- <i>GYP5</i> _{(8-448)A} (or pET30-pep0 _A)	PCR fragment from genomic DNA (primers: <i>GYP5_f1/GYP5_r1</i>) NdeI-Sall digested	pET30a NdeI-XhoI digested	C-terminus 6xHis-Tag	Poorly expressed
pET30- <i>GYP5</i> _{(8-448)B} (or pET30-pep0 _B)	PCR fragment from genomic DNA (<i>GYP5_f1/GYP5_r1</i>) NcoI-NotI digested	pET30a NcoI-NotI digested	N-terminus 6xHis-Tag, S-Tag	Poorly expressed
pET32- <i>GYP5</i> ₍₈₋₄₄₈₎ (or pET32-pep0)	PCR fragment from genomic DNA (<i>GYP5_f1/GYP5_r1</i>) NcoI-NotI digested	pET32a NcoI-NotI digested	N-terminus Trx-Tag, 6xHis-Tag, S-Tag	Good
pTT- <i>GYP5</i> ₍₈₋₃₈₈₎	PCR fragment from genomic DNA (<i>GYP5_f1/GYP5_r1</i>) NcoI-HindIII digested	pGEX-TT NcoI-NotI digested	N-terminus GST-Tag	Good
pY212- <i>GYP5</i> -6H ₍₈₋₄₄₈₎ (or pY212-pep0) (<u>yeast shuttle vector</u>)	PCR fragment from genomic DNA (<i>GYP5_f1/GYP5_r1</i> _{6H}) NcoI-XmaI digested	pYX212 NcoI-XmaI digested	C-terminus 6xHis-Tag. 2 μ , URA3, TPI promoter	Good
pET32- <i>GYP5</i> ₍₈₋₈₉₂₎ (or pET32-pep1)	PCR fragment from genomic DNA (<i>GYP5_f1/GYP5_r3</i>) NcoI-NotI digested	pET32a NcoI-NotI digested	N-terminus Trx-Tag, 6xHis-Tag, S-Tag	Poorly expressed
pY212- <i>GYP5</i> -6H ₍₈₋₈₉₂₎ (or pY212-pep1) (<u>yeast shuttle vector</u>)	<i>GYP5</i> containing fragment from pET32-pep1 NcoI-Sall digested	pYX212-6H from pY212-pep0 NcoI-Sall digested	C-terminus 6xHis-Tag. 2 μ , URA3, TPI promoter	Good
pET30- <i>GYP5</i> _{(400-892)A} (or pET30-pep2 _A)	PCR fragment from genomic DNA (<i>GYP5_f2/GYP5_r3</i>) NdeI-Sall digested	pET30a NdeI-XhoI digested	C-terminus 6xHis-Tag	Good
pET30- <i>GYP5</i> _{(400-892)B} (or 30-pep2 _B)	PCR fragment from genomic DNA (<i>GYP5_f2/GYP5_r3</i>) NcoI-NotI digested	pET30a NcoI-NotI digested	N-terminus 6xHis-Tag, S-Tag	Good
pET32- <i>GYP5</i> ₍₄₀₀₋₈₉₂₎ (or pET32-pep2)	<i>GYP5</i> containing fragment from pET30-pep2 _B NcoI-XhoI digested	pET32a NcoI-NotI digested	N-terminus Trx-Tag, 6xHis-Tag, S-Tag	Good
pY212- <i>GYP5</i> -6H ₍₄₀₀₋₈₉₂₎ (or pY212-pep2) (<u>yeast shuttle vector</u>)	<i>GYP5</i> containing fragment from pET32-pep2 NcoI-Sall digested	pYX212-6H from pY212-pep0 NcoI-Sall digested	C-terminus 6xHis-Tag. 2 μ , URA3, TPI promoter	Good
pET30- <i>GYP5</i> _{(429-892)A} (or pET30-pep3 _A)	PCR fragment from genomic DNA (<i>GYP5_f3/GYP5_r3</i>) NdeI-Sall digested	pET30a NdeI-XhoI digested	C-terminus 6His-Tag.	Good

pET30- <i>GYP5</i> _{(429-892)B} (or pET30-pep3 _B)	PCR fragment from genomic DNA (<i>GYP5_f3/GYP5_r3</i>) NcoI-NotI digested	pET30a NcoI-NotI digested	N-terminus 6xHis-Tag, S-Tag	Good
pET32- <i>GYP5</i> ₍₄₂₉₋₈₉₂₎ (or pET32-pep3)	PCR fragment from genomic DNA (<i>GYP5_f3/GYP5_r3</i>) NcoI-NotI digeste	pET32a NcoI-NotI digested	N-terminus Trx-Tag, 6xHis-Tag, S-Tag	Good
pET30- <i>GYP5</i> _{(451-892)A} (or pET30-pep4 _A)	PCR fragment from genomic DNA (<i>GYP5_f4/GYP5_r3</i>) NdeI-SalI digested	pET30a NdeI-XhoI digested	C-terminus 6His-Tag	Good
pET32- <i>GYP5</i> ₍₄₅₁₋₈₉₂₎ (or pET32-pep4)	PCR fragment from genomic DNA (<i>GYP5_f4/GYP5_r3</i>) NcoI-NotI digested	pET32a NcoI-NotI digested	N-terminus Trx-Tag, 6xHis-Tag, S-Tag	Good
pET30- <i>GYP5</i> _{(8-633)A} (or pET30-pep5 _A)	PCR fragment from genomic DNA (<i>GYP5_f1/GYP5_r2</i>) NdeI-SalI digested	pET30a NdeI-XhoI digested	C-terminus 6His-Tag.	Good
pET32- <i>GYP5</i> ₍₈₋₆₃₃₎ (or pET32-pep5)	PCR fragment from genomic DNA (<i>GYP5_f1/GYP5_r2</i>) NcoI-NotI digested	pET32a NcoI-NotI digested	N-terminus Trx-Tag, 6xHis-Tag, S-Tag.	Good
pET30- <i>GYP5</i> _{(400-633)A} (or pET30-pep6 _A)	PCR fragment from genomic DNA (<i>GYP5_f2/GYP5_r2</i>) NdeI-SalI digested	pET30a NdeI-XhoI digested	C-terminus 6His-Tag	Good
pET30- <i>GYP5</i> _{(400-633)B} (or pET30-pep6 _B)	PCR fragment from genomic DNA (<i>GYP5_f2/GYP5_r2</i>) NcoI-NotI digested	pET30a NcoI-NotI digested	N-terminus 6xHis-Tag, S-Tag	Good
pET32- <i>GYP5</i> ₍₄₀₀₋₆₃₃₎ (or pET32-pep6)	PCR fragment from genomic DNA (<i>GYP5_f2/GYP5_r2</i>) NcoI-NotI digested	pET32a NcoI-NotI digested	N-terminus Trx-Tag, 6xHis-Tag, S-Tag	Good
pET30- <i>GYP5</i> _{(429-633)A} (or pET30-pep7 _A)	PCR fragment from genomic DNA (<i>GYP5_f3/GYP5_r2</i>). NdeI-SalI digested.	pET30a NdeI-XhoI digested	C-terminus 6xHis-Tag	Good
pET30- <i>GYP5</i> _{(429-633)B} (or pET30-pep7 _B)	PCR fragment from genomic DNA (<i>GYP5_f3/GYP5_r2</i>) NcoI-NotI digested	pET30a NcoI-NotI digested	N-terminus 6xHis-Tag, S-Tag	Good
pET32- <i>GYP5</i> ₍₄₂₉₋₆₃₃₎ (or pET32-pep7)	PCR fragment from genomic DNA (<i>GYP5_f3/GYP5_r2</i>) NcoI-NotI digested	pET32a NcoI-NotI digested	N-terminus Trx-Tag, 6xHis-Tag, S-Tag	Good
pET30- <i>GYP5</i> _{(451-633)A} (or pET30-pep8 _A)	PCR fragment from genomic DNA (<i>GYP5_f4/GYP5_r2</i>). NdeI-SalI digested	pET30a NdeI-XhoI digested	C-terminus 6xHis-Tag	Good
pET30- <i>GYP5</i> _{(451-633)B} (or pET30-pep8 _B)	PCR fragment from genomic DNA (<i>GYP5_f4/GYP5_r2</i>) NcoI-NotI digested	pET30a NcoI-NotI digested	N-terminus 6xHis-Tag, S-Tag	Good

pET32- <i>GYP5</i> ₍₄₅₁₋₆₃₃₎ (or pET32-pep8)	PCR fragment from genomic DNA (<i>GYP5_f4/GYP5_r2</i>) NcoI-NotI digested	pET32a NcoI-NotI digested	N-terminus Trx-Tag, 6xHis-Tag, S-Tag	Good
pET30- <i>GYP5</i> _{(8-759)_A} (or pET30-pep9 _A)	PCR fragment from genomic DNA (<i>GYP5_f1/GYP5_r4</i>). NdeI-SalI digested.	pET30a NdeI-XhoI digested	C-terminus 6xHis-Tag	Moderately good
pET30- <i>GYP5</i> _{(400-759)_A} (or pET30-pep10 _A)	PCR fragment from genomic DNA (<i>GYP5_f2/GYP5_r4</i>) NdeI-SalI digested	pET30a NdeI-XhoI digested	C-terminus 6xHis-Tag	Good
pET30- <i>GYP5</i> _{(400-786)_A} (or pET30-pep14 _A)	PCR fragment from genomic DNA (<i>GYP5_f2/GYP5_r5</i>) NdeI-SalI digested	pET30a NdeI-XhoI digested	C-terminus 6xHis-Tag	Good
pET32- <i>GYP5</i> ₍₄₀₀₋₇₈₆₎ (or pET32-pep14)	PCR fragment from genomic DNA (<i>GYP5_f2/GYP5_r5</i>). NcoI-NotI digested	pET32a NcoI-NotI digested	N-terminus Trx-Tag, 6xHis-Tag, S-Tag	Good
pET30- <i>GYP5</i> ^{R496K} _{(400-892)_A} (or pET30-pep2 _A ^{R496K})	R496K mutation induced in pET30-pep2 _A using the primers <i>GYP5-R/K_f</i> and <i>GYP5-R/K_r</i>			
pET30- <i>GYP5</i> ^{R496A} _{(400-892)_A} (or pET30-pep2 _A ^{R496A})	R496A mutation induced in pET30-pep2 _A using the primers <i>GYP5-R/A_f</i> and <i>GYP5-R/A_r</i>			
<i>YPT1</i>^{Q67L} construct				
pET12c- <i>YPT1</i> ^{Q67L}	point mutation induced in pET12c- <i>YPT1</i> using the primers <i>YPT1-Q/L_f</i> and <i>YPT1-Q/L_r</i>			
Yeast <i>SEC24</i> family constructs				
Construct	Insert preparation	Vector preparation	Features	Prot. expression
pKT- <i>SEC24</i> (<u>yeast shuttle vector</u>)	PCR fragment from genomic DNA (<i>SEC24_f0/SEC24_r0</i>) XmaI/XbaI digested.	pEG(KT) XmaI/XbaI digested.	N-terminus GST-Tag; 2 μ , <i>URA3</i> , <i>GAL1</i>	Moderately good
pKT- <i>SEC24</i> -6H-2MYC (<u>yeast shuttle vector</u>)	PCR fragment from ADY4 genomic DNA (<i>SEC24_f0/ TAGuniv_r1</i>) XmaI/XbaI digested.	pEG(KT) XmaI/XbaI digested	N-terminus GST-Tag; C-terminus 6xHis-2MYC; 2 μ , <i>URA3</i> , <i>GAL1</i>	Moderately good
pY243- <i>SEC24</i> (<u>yeast shuttle vector</u>)	<i>SEC24</i> containing fragment from pKT- <i>SEC24</i> AvrII/XhoI digested	pYX243 AvrII/XhoI digested	2 μ , <i>LEU2</i> , <i>GAL1</i>	Good
pY243- <i>SEC24</i> -6H-2MYC (<u>yeast shuttle vector</u>)	<i>SEC24</i> containing fragment from pKT- <i>SEC24</i> -6H-2MYC, AvrII/XhoI digested	pYX243 AvrII/XhoI digested	C-terminus 6His-2MYC; 2 μ , <i>LEU2</i> , <i>GAL1</i>	Good
pTT- <i>SEC24</i> ₍₁₇₄₋₃₃₀₎	PCR fragment from genomic DNA (<i>SEC24_f5/SEC24_r6</i>). XmaI/XhoI digested	pGEX-TT XmaI/XhoI digested	N-terminus GST-Tag	Bad
pTT- <i>SEC24</i> ^{C231S} ₍₁₇₄₋₃₃₀₎ (pTT- <i>SEC24</i> ^m)	PCR fragment from pEG- <i>SEC24</i> N ^{C231S} (<i>SEC24_f5/SEC24_r6</i>) XmaI/XhoI digested.	pGEX-TT XmaI/XhoI digested.	N-terminus GST-Tag	Bad

pTT- <i>SEC24N</i> ^{C231S-C234S} (pTT- <i>SEC24</i> ^{m2}) (174-330)	PCR fragment from pEG- <i>SEC24N</i> ^{C231S-C234S} (<i>SEC24_f5/SEC24_r6</i>) XmaI/XhoI digested	pGEX-TT XmaI/XhoI digested.	N-terminus GST-Tag	Bad
pMAL- <i>SEC24</i> ₍₁₇₄₋₃₃₀₎	<i>SEC24</i> containing fragment from pTT- <i>SEC24</i> ₍₁₇₄₋₃₃₀₎ BamHI/HindIII digested	pMAL-c2 BamHI/HindIII digested	N-terminus MBP-Tag	Good
pMAL- <i>SEC24</i> ^{C231S} (174-330)	<i>SEC24</i> containing fragment from pTT- <i>SEC24</i> ^m BamHI/HindIII digested	pMAL-c2 BamHI/HindIII digested.	N-terminus MBP-Tag	Good
pMAL- <i>SEC24N</i> ^{C231S-C234S} (174-330)	<i>SEC24</i> containing fragment from pTT- <i>SEC24</i> ^{m2} BamHI/HindIII digested	pMAL-c2 BamHI/HindIII digested	N-terminus MBP-Tag	Good
pET32- <i>SEC24</i> ₍₁₇₄₋₃₃₀₎	<i>SEC24</i> containing fragment from pTT- <i>SEC24</i> ^m BamHI/HindIII digested	pET32 BamHI/HindIII digested.	N-terminus Trx- Tag, 6xHis-Tag, S-Tag	Good
pET32- <i>SEC24</i> ^{C231S} (174-330)	<i>SEC24</i> containing fragment from pTT- <i>SEC24</i> ^m BamHI/HindIII digested	pET32 BamHI/HindIII digested.	N-terminus Trx-Tag, 6xHis- Tag, S-Tag	Good
pET32- <i>SEC24N</i> ^{C231S-C234S} (174-330)	<i>SEC24</i> containing fragment from pTT- <i>SEC24</i> ^{m2} BamHI/HindIII digested	pET32 BamHI/HindIII digested.	N-terminus Trx-Tag, 6xHis- Tag, S-Tag	Good
pKT- <i>SFB2</i> (<u>yeast shuttle vector</u>)	PCR fragment from genomic DNA (<i>SFB2_f0/SFB2_r0</i>). XmaI/XbaI digested	pEG(KT) XmaI/XbaI digested	N-terminus GST-Tag; 2 μ , <i>URA3</i> , <i>GAL1</i>	Moderately good
pY243- <i>SFB2</i> (<u>yeast shuttle vector</u>)	<i>SFB2</i> containing frag- ment from pKT- <i>SFB2</i> . AvrII/XhoI digested.	pYX243 AvrII/XhoI digested	2 μ , <i>LEU2</i> , <i>GAL1</i>	
pY243- <i>SFB2</i> -6H-2MYC (<u>yeast shuttle vector</u>)	PCR fragment from ADY1 genomic DNA (<i>SFB2_f0/TAGuniv_r1</i>) AvrII/XhoI digested.	pYX243 AvrII/XhoI digested.	C-terminus 6xHis-2MYC; 2 μ , <i>LEU2</i> , <i>GAL1</i>	Good
pRS325- <i>SFB3</i> (<u>yeast shuttle vector</u>)	PCR fragment from genomic DNA (<i>SFB3_f1/SFB3_r4</i>) XhoI-BamHI digested	pRS326 XhoI-BamHI digested.	2 μ , <i>LEU2</i>	
pKT- <i>SFB3</i> -6H-3HA (<u>yeast shuttle vector</u>)	PCR fragment from ADY9 genomic DNA (<i>SFB3_f0/TAGuniv_r1</i>) XmaI/XbaI digested	pEG(KT) XmaI/XbaI digested	N-terminus GST- Tag; C-terminus, 6xHis-3HA; 2 μ , <i>URA3</i> , <i>GAL1</i>	Moderately good
pTT- <i>SFB3</i>	PCR fragment from genomic DNA (<i>SFB3_f0/ SFB3_r0.Xh</i>) XmaI/XhoI digested	pGEX-TT XmaI/XhoI digested.	N-terminus GST-Tag	Bad
pY243- <i>SFB3</i> (<u>yeast shuttle vector</u>)	<i>SFB3</i> containing fragment from pTT- <i>SFB3</i> AvrII/XhoI digested	pYX243 AvrII/XhoI digested	2 μ , <i>LEU2</i> , <i>GAL1</i>	
pY243- <i>SFB3</i> -6H-3HA (<u>yeast shuttle vector</u>)	<i>SFB3</i> containing fragment from pKT- <i>SFB3</i> -6H-3HA AvrII/XhoI digested	pYX243 AvrII/XhoI digested	C-terminus 6xHis-3HA; 2 μ , <i>LEU2</i> , <i>GAL1</i>	Moderately good

Human <i>SEC24C</i> constructs				
Construct	Insert preparation	Vector preparation	Features	Prot. expression
pQE30-KIAA0079 ₍₂₋₁₀₂₎ (fragment-1)	PCR fragment from KIAA0079 (<i>hSEC24_f1/hSEC24_r2</i>) BamHI/HindIII digested	pQE30 BamHI/HindIII digested	N-terminus 6His-Tag	Bad
pQE30-KIAA0079 ₍₃₆₃₋₅₂₂₎ (fragment-2)	PCR fragment from KIAA0079 (<i>hSEC24_f3/hSEC24_r4</i>) BamHI/HindIII digested	pQE30 BamHI/HindIII digested	N-terminus 6His-Tag	Good
pQE50-KIAA0079 ₍₃₆₃₋₅₂₂₎ (fragment-2)	PCR fragment from KIAA0079 (<i>hSEC24_f3/hSEC24_r4_{6H}</i>) BamHI/HindIII digested	pQE50 BamHI/HindIII digested	C-terminus 6His-Tag	Good
pMAL-KIAA0079 ₍₃₆₃₋₅₂₂₎ (fragment-2)	PCR fragment from KIAA0079 (<i>hSEC24_f3/hSEC24_r4</i>) BamHI/HindIII digested	pMAL-c2 BamHI/HindIII digested	N-terminus MBP-Tag	Good
pQE30-KIAA0079 ₍₅₇₀₋₇₁₅₎ (fragment-3)	PCR fragment from KIAA0079 (<i>hSEC24_f5/hSEC24_r6</i>). BamHI/HindIII digested	pQE30 BamHI/HindIII digested	N-terminus 6His-Tag	Bad
pQE30-KIAA0079 ₍₆₃₅₋₈₂₇₎ (fragment-4)	PCR fragment from KIAA0079 (<i>hSEC24_f7/hSEC24_r8</i>). BamHI/HindIII digested	pQE30 BamHI/HindIII digested.	N-terminus 6His-Tag	Bad
pQE30-KIAA0079 ₍₇₄₇₋₉₉₂₎ (fragment-5)	PCR fragment from KIAA0079 (<i>hSEC24_f9/hSEC24_r10</i>) BamHI/HindIII digested	pQE30 BamHI/HindIII digested.	N-terminus 6His-Tag	Good
pMAL-KIAA0079 ₍₇₄₇₋₉₉₂₎ (fragment-5)	PCR fragment from KIAA0079 (<i>hSEC24_f3/hSEC24_r4</i>) BamHI/HindIII digested	pMAL-c2 BamHI/HindIII digested.	N-terminus MBP-Tag	Good
t-SNAREs constructs				
pTT-VAM3 ₍₁₋₂₆₁₎	PCR fragment from genomic DNA (<i>VAM3_f/VAM3_r</i>) NcoI/XhoI digested.	pGEX-TT NcoI/XhoI digested.	N-terminus GST-Tag	Moderately good
pTT-SSO1 ₍₂₋₂₆₄₎	PCR fragment from genomic DNA (<i>SSO1_f/SSO1_r</i>) XbaI/XhoI digested	pGEX-TT XbaI/XhoI digested.	N-terminus GST-Tag	Good
pTT-SSO2 ₍₁₋₂₆₇₎	PCR fragment from genomic DNA (<i>SSO2_f/SSO2_r</i>) NcoI/XhoI digested	pGEX-TT NcoI/XhoI digested.	N-terminus GST-Tag.	Good
pTT-TLG1 ₍₁₋₂₀₄₎	PCR fragment from genomic DNA (<i>TLG1_f/TLG1_r</i>) NcoI/XhoI digested	pGEX-TT NcoI/XhoI digested	N-terminus GST-Tag.	Good
pTT-TLG2 ₍₁₋₃₁₇₎	PCR fragment from genomic DNA (<i>TLG2_f/TLG2_r</i>) NcoI/XhoI digested	pGEX-TT NcoI/XhoI digested	N-terminus GST-Tag	Good

7.3 Oligonucleotides

Oligonucleotides used in this work were custom-synthesized by Eurogentec company (Belgium) or by NAPS company (Göttingen, Germany). Here is a list with

the primer used, note that "f" or "r" indicate whether a primer is in the "forward" or in the "reverse" direction of a sequence.

Table 7.7

Name	Sequence	Peculiarities
GYP5-specific oligonucleotides		
GYP5_f0	5'-ATT ACG AGG GCT TAT TCA GAA G-3'	
GYP5_f1	5'-CG <u>GGA TCC CAT ATG GCC ATG GAG</u> AAA AAT ACA GAT ACG ATC GCC-3'	BamHI, NdeI, NcoI underlined; in bold aa n° 8
GYP5_f2	5'-CG <u>GGA TCC CAT ATG GCC ATG GAG</u> AAC TTG TCC GAG TAT AAC GAA G-3'	BamHI, NdeI, NcoI underlined; in bold aa n° 400
GYP5_f3	5'-CG <u>GGA TCC CAT ATG GCC ATG GTA</u> GTT ATT GAT TAT GCT ACA GTG GC-3'	BamHI, NdeI, NcoI underlined; in bold aa n° 429
GYP5_f4	5'-CG <u>GGA TCC CAT ATG GCC ATG GGG</u> ATA CCA CCA CAA ATT CGA GG-3'	BamHI, NdeI, NcoI underlined; in bold aa n° 451
GYP5_Seq.f0	5'-TTT GGA TCG AAC GTA ATT GA-3'	Sequencing primer
GYP5_Seq.f1	5'-CAA CGC CAT CAG ACC AAT AT-3'	Sequencing primer
GYP5_Seq.f2	5'-GGA TGT GCA AGC CCC AAA-3'	Sequencing primer
GYP5_Seq.f3	5'-CCC AGA AAG GTC GTC AGA A-3'	Sequencing primer
GYP5_Seq.f4	5'-TTC CAC CGC CAC TAG AGG A-3'	Sequencing primer
GYP5_Seq.f5	5'-TTG TCC GAG TAT AAC GAA GTG-3'	Sequencing primer
GYP5_Seq.f6	5'-GCC GAG GAC AAA ATG GAG T-3'	Sequencing primer
GYP5_Seq.f7	5'-TCA CCT TCT TTG TAC AAT CGC T-3'	Sequencing primer
GYP5_Seq.f8	5'-TCT TTT CGT TCA TGA TGC AAT-3'	Sequencing primer
GYP5_Seq.r0	5'-GTG GAT GTA CGG GTG AAA ATA-3'	Sequencing primer
GYP5_Mf	5'-TGG CAG CTG ATG GCG AAT-3'	Sequencing primer
GYP5_Mr	5'-GAA CCC CAT GCC TTG CGT-3'	Sequencing primer
GYP5_r0	5'-GGA AAC AAA AAC CCA ACA CAT-3'	
GYP5_r1	5'-T <u>TTC CCG GGC GGC CGC TTA GTC GAC</u> ATG GGC TTC TAA ATT TTC TGG TTC-3'	XmaI, NotI, Sall underlined; in bold STOP codon and aa n° 448
GYP5_r1 _{6H}	5'-T <u>CCC CCC GGG TTA GTG ATG ATG ATG</u> <u>GTG GTG GTC GAC</u> ATG GGC TTC TAA ATT TTC TGG TTC-3'	XmaI, Sall underlined. 6xHis double underlined; in bold STOP codon and aa n° 448.
GYP5_r2	5'-T <u>TTC CCG GGC GGC CGC TTA GTC GAC</u> TTC AAT ACC CTC TAC GAA TAC AAT ATC-3'	XmaI, NotI, Sall underlined; in bold STOP codon and aa n° 633.
GYP5_r3	5'-T <u>TTC CCG GGC GGC CGC TTA GTC GAC</u> TTT TTT AAA ACC AGT CCA GCC TTT C-3'	XmaI, NotI, Sall underlined. In bold STOP codon and aa n° 892.
GYP5_r4	5'-T <u>TTC CCG GGC GGC CGC TTA GTC GAC</u> <u>TTC</u> TAG CTT CTG CGC CTC TCT TTG-3'	XmaI, NotI, Sall underlined; in bold STOP codon and aa n° 759
GYP5_r5	5'-T <u>TTC CCG GGC GGC CGC TTA GTC GAC</u> <u>CAG</u> CAT CTC CAT ATT CAA TCT GTT CT-3'	XmaI, NotI, Sall underlined; in bold STOP codon and aa n° 786
GYP5-R/K_f	5'-A CGT AGA GAT TTA AGG <u>AAA</u> ACG AAG TTT GTG GCC GAG GAC-3'	R496K mutation bold and underlined
GYP5-R/K_r	5'-GTC CTC GGC CAC AAA CTT CGT <u>TTT</u> CCT TAA ATC TCT ACG T-3'	R496K mutation bold and underlined

<i>GYP5-R/A_f</i>	5'-A CGT AGA GAT TTA AGG <u>GCA</u> ACG AAG TTT GTG GCC GAG GAC-3'	R496A mutation bold and underlined
<i>GYP5-R/A_r</i>	5'-GTC CTC GGC CAC AAA CTT CGT <u>TGC</u> CCT TAA ATC TCT ACG T-3'	R496A mutation bold and underlined
<i>GYP5-SeqM.f</i>	5'-GGC AGC TGA TGG CGA ATT-3'	Sequencing primer
<i>GYP5-SeqM.r</i>	5'-GAA CCC CAT GCC TTG CGT-3'	Sequencing primer
<i>GYP1, GYP7, GYP8</i> oligonucleotides		
<i>GYP1_f0</i>	5'-ACA ACA ACA ACC ACC AAT ACC-3'	
<i>GYP1_r0</i>	5'-CAC GTT CCT CAG GAT TTA TGA-3'	
<i>GYP7_f0</i>	5'-TAT GGG GCA AAG TTC TGC TCT AT-3'	
<i>GYP7_r0</i>	5'-CGG ATG TAT TGA TGA TTA TGT GG-3'	
<i>GYP8_f0</i>	5'-GCA AAT GAC ATA GAA CAA GCC A-3'	
<i>GYP8_r0</i>	5'-GCA GCG AAT TTT AAA GAA GCA-3'	
<i>YPT1</i>-specific oligonucleotides		
<i>YPT1_f0</i>	5'-GCA CCA GTT TTG AGG ATA T-3'	
<i>YPT1_f1</i>	5'-GAT TAC CTG TTC AAA CTG CTG T-3'	
<i>YPT1_f1_b</i>	5'-T TCG GAC GAC ACA TAT ACC AA-3'	
<i>YPT1_f2</i>	5'-GAA CTG GAC GGC AAG ACT G-3'	
<i>YPT1_r0</i>	5'-TAT GTT CTC GCG TGT GTC TTA-3'	
<i>YPT1_r0_b</i>	5'-CGC TTC CCC ACA CAT TTT G-3'	
<i>YPT1_r1</i>	5'-CCA CAT CTT CAC GCC GTT-3'	
<i>YPT1_r1_b</i>	5'-T CTC TTG CAG CCA CAT CTT CA-3'	
<i>YPT1-Q/L_f</i>	5'-CAG ATT TGG GAC ACT GCA GGT <u>CTA</u> GAA CGT TTC CGT ACT ATC ACT-3'	Q67L mutation bold and underlined
<i>YPT1-Q/L_r</i>	5'-AGT GAT AGT ACG GAA ACG TTC <u>TAG</u> ACC TGC AGT GTC CCA AAT CTG-3'	Q67L mutation bold and underlined
Yeast <i>Sec24</i> family oligonucleotides		
<i>SEC24_f0</i>	5'-TG GCC CCG GGA <u>CCT AGG</u> ATG TCT CAT CAC AAG AAA CGT G-3'	XmaI, AvrII underlined; in bold aa n° 1
<i>SEC24_f3</i>	5'-GGG AAG TTG CAA CGC TAA G-3'	
<i>SEC24_f5</i>	5'-TG GCC CCG GGT <u>CCT AGG</u> TTG TCC AAT GCG TCT CCA GAT TAT-3'	XmaI, AvrII underlined; in bold aa n° 174
<i>SEC24_r0</i>	5'-GC <u>TCT AGA</u> TTA TTA TTT GCT AAT TCT GGC TTT CA-3'	XbaI, underlined. In bold STOP codon.
<i>SEC24_r6</i>	5'-CCG <u>CTC GAG</u> TTA TTA CAA AAG GGT GTT GAT GGT AGT GGC-3'	XhoI, underlined; in bold STOP codon and aa n° 330
<i>SFB2-f0</i>	5'-TG GCC CCG GGA <u>CCT AGG</u> ATG TCT CAT CAT AAG AAG AGG GTG-3'	XmaI, AvrII underlined. In bold aa n° 1
<i>SFB2-f3</i>	5'-CGC CAA CCT AAA CTC CGA A-3'	
<i>SFB2_r0</i>	5'-GC <u>TCT AGA</u> TTA TTA TCT GTT GAT ACT AGT CTT CAT ACT-3'	XbaI, underlined; in bold STOP codon
<i>SFB3_f0</i>	5'-TG GCC CCG GGA <u>CCT AGG</u> ATG TCT CAG CAG AAT ATT TTG GC-3'	XmaI, AvrII underlined; in bold aa n° 1
<i>SFB3_f1</i>	5'-CCG <u>CTC GAG</u> CCG ATT TTG TTG GTG TTG TTT ATT-3'	XhoI underlined
<i>SFB3-f3</i>	5'-ACA AGA CCG TCA ACA GAA TCG-3'	
<i>SFB3-f5</i>	5'-G GGT GAA GGT GTC AGG TCA T-3'	
<i>SFB3_r0</i>	5'-GC <u>TCT AGA</u> TTA GGA GGC TCA AAA CTG CAC AAA-3'	XbaI, underlined; in bold STOP codon
<i>SFB3_r0.Xh</i>	5'-CCG <u>CTC GAG</u> TTA GGA GGC TCA AAA CTG CAC AAA-3'	XhoI underlined; in bold STOP codon
<i>SFB3_r2</i>	5'-A GTA GTA CTG TTC CAC AGA TAG CC-3'	

SFB3_r4	5'-CGG <u>GAT CCT</u> GCA AGA TTT ACC AGA AGA CAG TC-3'	BamHI underlined
SFB3_r6	5'-GGT TCC TGT TTT TAT TTT ACT-3'	
SFB3_Seq1f	5'-GAA ATG CGC GTG TCC GTA A-3'	Sequencing primer
SFB3_Seq2f	5'-CA GCG CTC CTT GAT GAA-3'	Sequencing primer
SFB3_Seq3f	5'-AC AAC ATC CCC GAA AGT GAA-3'	Sequencing primer
SFB3_Seq4f	5'-GC AGT AAC TCA TCA ACG CAA-3'	Sequencing primer
SFB3_Seq5f	5'-CCT GAG ACG GGC ACT AGT AT-3'	Sequencing primer
SFB3_Seq6r	5'-CC GCC ACT AAT CAA CTC CT-3'	Sequencing primer
SFB3_Seq7r	5'-G GGG TGT AGT GTA GGG TGA-3'	Sequencing primer
SFB3_Seq8f	5'-G AGT CAA GAG CGA TTC GGT-3'	Sequencing primer
SFB3_Seq9r	5'-CAA AGG CGT ACC ATC CAT T-3'	Sequencing primer
SFB3_Seq10f	5'-A GTC GAT TTC TTG GTG CCA-3'	Sequencing primer
SFB3_Seq11f	5'-CC GGA AAC TCG ATG AAA AT-3'	Sequencing primer
SFB3_Seq12r	5'-GGT ACT TTG AGC GTT TGG C-3'	Sequencing primer
SFB3_Seq13r	5'-CCT CAA CAA GAC TAA CGG CA-3'	Sequencing primer
Human SEC24c-specific oligonucleotides		
hSEC24_f1	5'-CGC <u>GGA TCC AAC</u> GTC AAC CAG TCA GTT CCA CCT-3'	BamHI underlined; in bold aa n° 2
hSEC24_f3	5'-CGC <u>GGA TCC</u> GTG AAA GAC CAA GGG AAT GCA AGT-3'	BamHI underlined; in bold aa n° 363
hSEC24_f5	5'-CGC <u>GGA TCC</u> ATG ATG GTT GTG TCT GAT GTG GCT-3'	BamHI underlined; in bold aa n° 570
hSEC24_f7	5'-CGC <u>GGA TCC</u> TGT GCA GGG AAG CTC TTT CTA TTC-3'	BamHI underlined; in bold aa n° 635
hSEC24_f9	5'-CGC <u>GGA TCC</u> GTT GGC TTT GAT GCT GTG ATG CGG-3'	BamHI underlined; in bold aa n° 747
hSEC24_r2	5'-CCG <u>AAG CTT</u> TTA TTG CAT CTG AAC AGT GGA GCT TGG-3'	HindIII, underlined; in bold STOP codon and aa n° 102
hSEC24_r4	5'-CCC <u>AAG CTT</u> TTA GAG CCT AAC AAG ACC AGT CCT GAT -3'	HindIII, underlined; in bold STOP codon and aa n° 522
hSEC24_r4 _{6H}	5'-CCC <u>AAG CTT</u> TTA <u>GTG ATG GTG ATG GTG</u> ATG GAG CCT AAC AAG ACC AGT CCT GAT-3'	HindIII, underlined; in bold STOP codon and aa n° 522 6-His double underlined.
hSEC24_r6	5'-TTT <u>AAG CTT</u> TTA GAG CTG GGG CAC AAC AGA GAG TGT-3'	HindIII, underlined; in bold STOP codon and aa n° 715
hSEC24_r8	5'-GCG <u>AAG CTT</u> TTA CAG ATT ATG GAT GCG GAG CCG ACG-3'	HindIII, underlined; in bold STOP codon and aa n° 827
hSEC24_r10	5'-GCG <u>AAG CTT</u> TTA CCA GAG GAA GAG GTT GAG CCC ATT-3'	HindIII, underlined; in bold STOP codon and aa n° 992
t-SNAREs oligonucleotides		
VAM3_f	5'-CTT <u>GCC ATG GTT</u> GAG ATT ATG TCC TTT TTC GA-3'	NcoI underlined; in bold aa n° 1
VAM3_r	5'-CGG <u>CTC GAG</u> TTA TTT GTT ACG GTC CCT CTG ATG-3'	XhoI, underlined; in bold STOP codon and aa n° 261
SSO1_f	5'-T <u>GCT CTA GAG</u> AGT TAT AAT AAT CCG TAC CAG-3'	XbaI underlined; in bold aa n° 2
SSO1_r	5'-CCG <u>CTC GAG</u> TTA AAT CTT GTT CTT TCT TGC TTT TC-3'	XhoI, underlined; in bold STOP codon and aa n° 264
SSO2_f	5'-CAA <u>GCC ATG GCA</u> ATG AGC AAC GCT AAT CCT TA-3'	NcoI underlined; in bold amino acid n° 1
SSO2_r	5'-CCG <u>CTC GAG</u> TTA TTT GTT TTT TCT TGC TTT TCT GG-3'	XhoI, underlined; in bold STOP codon and aa n° 267

TLG1_f	5'-CAT <u>GCC ATG GAA</u> ATG AAC AAC AGT GAA GAT CCG-3'	NcoI underlined; in bold amino acid n° 1
TLG1_r	5'-CCG <u>CTC GAG</u> TTA ATC GTC GTA TTT TTC TTT ATT TT-3'	XhoI, underlined; in bold STOP codon and aa n° 204
TLG2_f	5'-CAT <u>GCC ATG GCA</u> AAC ATG TTT AGA GAT AGA ACT A-3'	NcoI underlined; in bold amino acid n° 1
TLG2_r	5'-CCG <u>CTC GAG</u> TTA TTT ACA TTT TTG AGT TCT CTT CTG-3'	XhoI, underlined; in bold STOP codon and aa n° 317
Vectors-specific oligonucleotides		
Tag.univ_r1	5'-C <u>CCC TCG AGG</u> CAA GCT AAA CAG ATC-3'	Anneals inside <i>loxP-kanMX</i> ; XhoI underlined
Tag.univ_r2	5'-G <u>GGG ATC CTA</u> TAG GGA GAC CGG CAG ATC-3'	Anneals after <i>kanMX-loxP</i> ; BamHI underlined
pU-f0	5'-AAC GCG GCT ACA ATT AAT AC-3'	For pU vectors
pU-r0	5'-AT TCT GGG CCT CCA TGT C-3'	Anneals inside <i>loxP-kanMX</i>
pU-r2	5'-GG ATG TAT GGG CTA AAT G-3'	Anneals inside <i>loxP-kanMX</i>
pU-r4	5'-CTA TAG GGA GAC CGG CAG ATC-3'	Anneals after <i>kanMX-loxP</i>
6H-f	5'-CAC CAC CAT CAT CAT CAC G-3'	For pUtag vectors
TL15_f	5'-C CTC GAC ATC ATC TGC CC-3'	Anneals inside <i>kanMX</i>
TL20_r	5'-CCC ATG GTT GTT TAT GTT CG-3'	Anneals inside <i>kanMX</i>
MYC-f	5'-GAA CAA AAG CTT ATT TCT GAA-3'	
HA-f	5'-TAC CCA TAC GAC GTC CCA GAC-3'	
VSV-f	5'-TAC ACT GAC ATT GAA ATG AAT-3'	
TPI-f	5'-AGG GAA TAT AAA GGG CAG CA-3'	For sequencing inserts in pYX112 and pYX212
pYX243_f	5'-CGG TTT GTA TTA CTT CTT ATT C-3'	for sequencing inserts in pYX143 and pYX243
pYX_r	5'-AAA GGG ATG TAT CGG TCA GTC A-3'	For sequencing inserts in pYX vectors
pET30_Seqlf	5'-TGA AAG AAA CCG CTG CTG C-3'	For sequencing inserts in pET30
pET30_f	5'-CCG GCG TAG AGG ATC GAG A -3'	For pET30 and pET32
pET30_r	5'-GAG CCG TTT AGA GGC CCC A-3'	For pET30 and pET32
pET32_Seqlf	5'-GAA AGA AAC CGC TGC TGC T-3'	For sequencing inserts in pET32
GST_f	5'-GCA AGT ATA TAG CAT GGC C-3'	For sequencing inserts in pGEX-TT and pEG(KT)
TT_f1	5'-GAC CAT CCT CCA AAA TCG G-3'	For sequencing inserts in pGEX-TT and pEG(KT)
TT_r2	5'-GAG GCA GAT CGT CAG TCA G-3'	For sequencing inserts in pGEX-TT and pEG(KT)
pMAL_f	5'-GGT CGT CAG ACT GTC GAT GAA GCC-3'	For sequencing inserts in pMAL
pMAL_r	5'-CGC CAG GGT TTT CCC AGT CAC GAC-3'	For sequencing inserts in pMAL
pQE_f	5'-GAA TTC ATT AAA GAG GAG AAA-3'	For sequencing inserts in pQE vectors
pQE_r	5'-CAT TAC TG ATC TAT CAA CAG G-3'	For sequencing inserts in pQE30, pQE50
oligonucleotides for PCR mediated gene deletion		
GYP5DEL_f1	5'-ACA GCT CCT ACC ACC AGT GTA AAG TAG AAC GTT AAT AGA GCA <u>TCC CAC CAC CAT CAT CAT CAC</u> -3'	For GYP5 deletion, it anneals (underlined sequence) with pUtag vectors
GYP5DEL_r = Gyp5-tag_r2	5'-CAA CAA CAT TGT CTA AAC GAG TCG TGA TGC ATT TTT TAA CAC <u>ACT ATA GGG AGA CCG GCA GAT</u> C-3'	For GYP5 deletion, it anneals (underlined sequence) with pUtag vectors

<i>GYP1DEL_f</i>	5'-AAC AAC CAC CAA TAC CGA CCA CTT AAT AAA AGT AAC CAT ATA <u>GCT TAA TGA GTC GAC</u> AAC CCT-3'	For <i>GYP1</i> deletion, it anneals (underlined seq.) with pU6H3HA
<i>GYP1DEL_r</i>	5'-GAG ATT TTT GTT TTA TAT TAT TAC ATA CTA TAC AGT AAG TAA <u>ACT ATA GGG AGA</u> CCG GCA GAT C-3'	For <i>GYP1</i> deletion, it anneals (underlined seq.) with pU6H3HA
<i>GYP8DEL_f</i> = SA170	5'-AAT ACG ATG CCA TTA AGG TCA TTA TTT CAT ACT AAT CAG AGT <u>CAG CTG AAG CTT CGT ACG C-3'</u>	For <i>GYP8</i> deletion, it anneals (underlined seq.) with pUG6
<i>GYP8DEL_r</i>	5'-CTA TCT AGT TGG ATG CCC CAG TTT CAA AAT GTC CCT AAT CGG <u>GCA TAG GCC ACT AGT GGA TCT G-3'</u>	For <i>GYP8</i> deletion, it anneals (underlined seq.) with pUG6
SA88_f	5'-CAT CCC CTG ATG AGT AAG ATA CTA TTC TGC AAA TCT <u>CAG CTG AAG CTT CGT ACG C-3'</u>	For <i>GYP7</i> deletion, it anneals (underlined seq.) with pUG6
SA89_r	5'-CCA CTA TTT AAC GGA ATT TTT GCT CCT TTG CCC TTC <u>GCA TAG GCC ACT AGT GGA TCT -3'</u>	For <i>GYP7</i> deletion, it anneals (underlined seq.) with pUG6
oligonucleotides for PCR mediated epitope tagging		
<i>GYP5-tag_fa</i>	5'-AAA GGG AGG AAA GGC TGG ACT GGT TTT AAA AAA GTT GTT AAA <u>TCC CAC CAC CAT CAT</u> CAT CAC-3'	For <i>GYP5</i> tagging, it anneals (underlined sequence) with pUtag vectors
<i>GYP5-tag_r2</i>	5'-CAA CAA CAT TGT CTA AAC GAG TCG TGA TGC ATT TTT TAA CAC <u>ACT ATA GGG AGA CCG GCA</u> GAT C-3'	For <i>GYP5</i> tagging, it anneals (underlined sequence) with pUtag vectors
<i>SEC23-tag_f1</i>	5'-TTC ATG ACT CAC TTA CAA CAA GTA GCC GTC TCT GGT CAG GCA <u>TCC CAC CAC CAT</u> CAT CAT CAC-3'	For <i>SEC23</i> tagging, it anneals (underlined sequence) with pUtag vectors
<i>SEC23-tag_r4</i>	5'-GGA AAA TTC TTG CAC GCG CAA TGG ACT GAA CAG GCC TTA TAT <u>ACT ATA GGG AGA CCG GCA</u> GAT C-3'	For <i>SEC23</i> tagging, it anneals (underlined sequence) with pUtag vectors
<i>SEC24-tag_f1</i>	5'-TAC AGA GAA TTC TTA CAA ATC ATG AAA GCC AGA ATT AGC AAA <u>TCC CAC CAC CAT CAT</u> CAT CAC-3'	For <i>SEC24</i> tagging, it anneals (underlined sequence) with pUtag vectors
<i>SEC24-tag_r2</i>	5'-AAC TGT TCA ATA TAC ATA ATA TAA TTG GAA AGC AAA AAT GCA <u>ACT ATA GGG AGA</u> CCG GCA GAT C-3'	For <i>SEC24</i> tagging, it anneals (underlined sequence) with pUtag vectors
<i>SFB2-tag_f1</i>	5'-TAT AGA GAA TAC TTA CAG AGT ATG AAG ACT AGT ATC AAC AGA <u>TCC CAC CAC CAT</u> CAT CAT CAC-3'	For <i>SFB2</i> tagging, It anneals (underlined sequence) with pUtag vectors
<i>SFB2-tag_r6</i>	5'-CGA TTT ACT TTT ATT TCT ATC TGT ATT GTA TAT CAA AAT CTA <u>ACT ATA GGG AGA CCG GCA</u> GAT C-3'	For <i>SFB2</i> tagging, It anneals (underlined sequence) with pUtag vectors
<i>SFB3-tag_f1</i>	5'-GCC GCA ACT CAC GAA AAT ATC CAT CAA AAA TTT GTG CAG TTT <u>TCC CAC CAC CAT CAT</u> CAT CAC-3'	For <i>SFB3</i> tagging, It anneals (underlined sequence) with pUtag vectors
<i>SFB3-tag_r4</i>	5'-TCC TAT GTA GAA TTT CAC CCT TTC TCT GCC AGC GTT TCA CAT <u>ACT ATA GGG AGA CCG GCA</u> GAT C-3'	For <i>SFB3</i> tagging, It anneals (underlined sequence) with pUtag vectors

7.4 Antibodies

Antibodies against different proteins or epitopes were produced according to standard procedures in rabbits.

7.4.1 Primary antibodies

Table 7.8

Antibody	source
Rabbit anti-KIAA0079-2 (anti-hSec24c-2), polyclonal Antigen: 6xHis recombinant hSec24cp(363-522)	This work
Rabbit anti-KIAA0079-5 (anti-hSec24c-5), polyclonal Antigen: 6xHis recombinant hSec24cp(570-992)	This work.
Rabbit anti-Sec24p, polyclonal	(Peng <i>et al.</i> , 1999)
Rabbit anti-Sec23p, polyclonal	Dr. R. Peng, this Department
Rabbit anti-Sly1p, polyclonal	This department
Rabbit anti-Emp47, polyclonal	Dr. S. Schröder, this Department
Rabbit anti-Kar2p, polyclonal	(Benli <i>et al.</i> , 1996)
Rabbit anti-Bos1p, polyclonal	This department
Rabbit anti-Sed5p, polyclonal	Dr. R. Grabowski this Department
Rabbit anti-Gyp1, polyclonal	Dr. S. Albert, this Department
Rabbit anti-Ypt1p, polyclonal	Dr. X. Yang, this Department
Rabbit anti-Sec61p, polyclonal	
Rabbit anti-Hxk2p, polyclonal	Prof. H. Riezman, Univ. of Basel
Rabbit anti-Gas1p, polyclonal	Prof. H. Riezman, Univ. of Basel
Rabbit anti-CPY, polyclonal	This Department, (Benli <i>et al.</i> , 1996)
Rabbit anti-ALP, polyclonal	This Department, (Benli <i>et al.</i> , 1996)
Rabbit anti-GST, polyclonal	Pharmacia (Freiburg, Germany)
Mouse anti-6xhis, monoclonal	Gibco (Karlsruhe, Germany)
Mouse anti-HA (12CA5), monoclonal	Roche (Mannheim, Germany)
Mouse anti-VSV-G (P5D4), monoclonal	Roche (Mannheim, Germany)
Mouse anti-c-myc (9E10), monoclonal	Santa Cruz Biotech. (USA)
Rabbit anti-c-myc, polyclonal	Santa Cruz Biotech. (USA)
Mouse anti-calnexin (AF18), monoclonal	DIANOVA, Hamburg, Germany
Mouse anti-PDI (RL77), monoclonal	DIANOVA, Hamburg, Germany
Mouse anti- β_1 and β_1 -adaptins (100/1), monoclonal	Sigma, Deisenhofen, Germany
Mouse anti-Golgi 58K (58K-9), monoclonal	Sigma, Deisenhofen, Germany

7.4.2 Secondary antibodies

Table 7.9

Antibody	source
Sheep anti-mouse-IgG, HRP conjugated.	Amersham-Buchler (Braunschweig, Germany)
Donkey anti-rabbit-IgG, HRP conjugated	Amersham-Buchler
Anti-mouse-IgG, Cy3 conjugated	Dianova (Hamburg, Germany)
Anti-rabbit-IgG, Cy3 conjugated	Dianova
Anti-mouse-IgG, Rhodamine Red-X conjugated	Dianova
Anti-mouse-IgG, Rhodamine Red-X conjugated	Dianova
goat anti-rabbit IgG, Oregon Green 488 conjugated	Molecular Probe Inc. (Leiden, The Netherlands)
goat anti-rabbit IgG, Oregon Green 488 conjugated	Molecular Probe Inc.

8 ABBREVIATION

aa	amino acid	GDI	GDP dissociation inhibitor
ALP	alkaline phosphatase	GDP	guanosine diphosphate
APS	ammoniumpersulfate	GEF	guanine nucleotide exchange factor
ARF	ADP-ribosylation factor	GMP	guanosine monophosphate
ARS	autonomous replication sequences	GMP-PNP	5'-guanylyl imidodiphosphate
3-AT	3 amino 1,2,4 triazol	GPI	glycosyl phosphatidyl inositol
ATCC	American Type Culture Collection	GST	glutathione S-transferase
BSA	bovine serum albumin	GTP	guanosine triphosphate
<i>CEN</i>	centromere elements	h	hour(s)
COPI/II	coatamer protein complex I/II	HA	influenza virus hemagglutinin epitope
CPY	carboxypeptidase Y	HEPES	N-(2-Hydroxyethyl)piperazine-N'-(2-ethanesulfonic acid)
Cy3	indigocarbocyanine	HP	high performance
Dept.	Department	HPLC	high performance liquid chromatography
dH ₂ O	deionized H ₂ O	HR	high resolution
DIC	differential interference contrast	HRP	horseradish peroxidase
dsDNA	double strand DNA	Ig	immunoglobulin
DTT	dithiothreitol	IPTG	isopropylthio-β-D-galactoside
ECL	enhanced chemiluminescence	Iss1	interacting with sec-sixteen
EDTA	ethylenediaminetetraacetic acid	k_{cat}	catalytic rate constant
EEA1	early endosome associated protein	kDa	kilo Dalton
ER	endoplasmic reticulum	k_m	Michaelis constant
ERGIC	ER Golgi intermediate compartment	KOAc	potassium acetate
FCS	foetal calf serum	l	litre
FM 4-64	N-(3-triethylammmoniumpropyl)-4-(p-diethylaminophenylhexatrienyl) pyridinium dibromide	LiOAc	lithium acetate
5-FOA	5-fluoroorotic acid	Lma1	low molecular weight activity
FPLC	fast protein liquid chromatography	Lst1	lethal with sec-thirteen
g	gram	m	meter
<i>g</i>	gravity	M	molar (mol x l ⁻¹)
GAP	GTPase activating protein	mA	milli Amper
Gap1	general amino acid permease	MBP	maltose binding protein
Gas1p	glycophospholipid-anchored surface protein	2-ME	β-mercaptoethanol

mg	milligram (10^{-3} g)	ssDNA	single strand DNA
µg	microgram (10^{-6} g)	tab.	tablet
MgOAc	magnesium acetate	TBS	tris buffered saline
min	minute(s)	TCA	trichloroacetic acid
ml	millilitre (10^{-3} l)	TEF	translation elongation factor
µl	microlitre (10^{-6} l)	TEMED	1,2-bis-(dimethylamino)-ethane
µm	micrometer (10^{-6} m)	tER	transitional ER
mM	millimolar (10^{-3} M)	TGN	<i>trans</i> -Golgi network
µM	micromolar (10^{-6} M)	<i>TPI</i>	tris phosphate isomerase
MPI	Max Planck Insitute	TRAPP	transport protein particle
MYC	c-myc epitope	Tris	tris(hydroxymethyl)aminomethane
NaOAc	sodium acetate	Trx	thioredoxin
Ni-NTA	nickel-nitrilotriacetic acid	YEPEG	yeast extract, peptone, glucose
nm	nanometer (10^{-9} m)	VAMP	vesicle associated membrane protein
NSF	N-ethylmaleimide sensitive fusion	VSV	vesicular stomatitis virus glycoprotein epitope
OD	optical density	VTCS	vesicular tubular clusters
ON	overnight	v/v	volume/volume
ORF	open reading frame	w/o	without
ori	origin of replication	wt	wild type
PAGE	polyacrylamide gel electrophoresis	w/v	weight/volume
PBS	phosphate buffered saline	∅	diameter
PCR	polymerase chain reaction		
PES	polyethylene sodium sulfonate		
pI	isoelectric point		
Pma1	plasma membrane ATPase		
PMSF	phenyl methyl sulfonyl fluoride		
Rab	rat brain		
Ras	rat sarcoma		
Rnase	ribonuclease		
Rpm	rotation per minute		
RT	room temperature		
SD	synthetic dextrose		
SDS	sodium dodecyl sulfate		
Sfb	Sed-five bynding		
SMM	semi-minimal medium		
SNAP	soluble NSF attachment protein		
SNARE	SNAP receptor		

Amino acids abbreviations:

Alanine	Ala	A
Arginine	Arg	R
Asparagine	Asn	N
Aspartic acid	Asp	D
Cysteine	Cys	C
Glutamic acid	Glu	E
Glutamine	Gln	Q
Glycine	Gly	G
Histidine	His	H
Isoleucine	Ile	I
Leucine	Leu	L
Lysine	Lys	K
Methionine	Met	M
Phenylalanine	Phe	F
Proline	Pro	P
Serine	Ser	S
Threonine	Thr	T
Tryptophan	Trp	W
Tyrosine	Tyr	Y
Valine	Val	V

Species abbreviations:

<i>A. gossypii</i>	<i>Ashbya gossypii</i>
<i>A. thaliana</i>	<i>Arabidopsis thaliana</i>
<i>C. elegans</i>	<i>Caenorhabditis elegans</i>
<i>D. melanogaster</i>	<i>Drosophila melanogaster</i>
<i>E. coli</i>	<i>Escherichia coli</i>
<i>H. sapiens</i>	<i>Homo sapiens</i>
<i>S. cerevisiae</i>	<i>Saccharomyces cerevisiae</i>
<i>S. pombe</i>	<i>Schizosaccharomyces pombe</i>
<i>X. laevis</i>	<i>Xenopus laevis</i>

9 REFERENCES

- Aalto, M.K., Ronne, H. and Keranen, S.** (1993). Yeast syntaxins Sso1p and Sso2p belong to a family of related membrane proteins that function in vesicular transport. *Embo J.* 12: 4095-4104.
- Abeliovich, H., Grote, E., Novick, P. and Ferro-Novick, S.** (1998). Tlg2p, a yeast syntaxin homolog that resides on the Golgi and endocytic structures. *J. Biol. Chem.* 273: 11719-11727.
- Ahle, S., Mann, A., Eichelsbacher, U. and Ungewickell, E.** (1988). Structural relationships between clathrin assembly proteins from the Golgi and the plasma membrane. *Embo J.* 7: 919-929.
- Ahmadian, M.R., Stege, P., Scheffzek, K. and Wittinghofer, A.** (1997). Confirmation of the arginine-finger hypothesis for the GAP-stimulated GTP-hydrolysis reaction of Ras. *Nat. Struct. Biol.* 4: 686-689.
- Ahmadian, M.R., Wiesmuller, L., Lautwein, A., Bischoff, F.R. and Wittinghofer, A.** (1996). Structural differences in the minimal catalytic domains of the GTPase-activating proteins p120GAP and neurofibromin. *J. Biol. Chem.* 271: 16409-16415.
- Albert, S. and Gallwitz, D.** (1999). Two new members of a family of Ypt/Rab GTPase activating proteins. Promiscuity of substrate recognition. *J. Biol. Chem.* 274: 33186-33189.
- Albert, S. and Gallwitz, D.** (2000). Msb4p, a protein involved in Cdc42p-dependent organization of the actin cytoskeleton, is a Ypt/Rab-specific GAP. *Biol. Chem.* 381: 453-456.
- Albert, S., Will, E. and Gallwitz, D.** (1999). Identification of the catalytic domains and their functionally critical arginine residues of two yeast GTPase-activating proteins specific for Ypt/Rab transport GTPases. *Embo J.* 18: 5216-5225.
- Allan, B.B., Moyer, B.D. and Balch, W.E.** (2000). Rab1 recruitment of p115 into a cis-SNARE complex: programming budding COPII vesicles for fusion. *Science* 289: 444-448.
- Appenzeller, C., Andersson, H., Kappeler, F. and Hauri, H.P.** (1999). The lectin ERGIC-53 is a cargo transport receptor for glycoproteins. *Nat. Cell. Biol.* 1: 330-334.
- Aridor, M. and Balch, W.E.** (1996). Principle of selective transport: coat complexes hold the key. *Trends. Cell Biol.* 6: 315-320.
- Aridor, M. and Balch, W.E.** (2000). Kinase signaling initiates COPII recruitment and export from the mammalian endoplasmic reticulum. *J. Biol. Chem.* 275: 35673-35676.
- Aridor, M., Fish, K.N., Bannykh, S., Weissman, J., Roberts, T.H., Lippincott-Schwartz, J. and Balch, W.E.** (2001). The Sar1 GTPase Coordinates Biosynthetic Cargo Selection with Endoplasmic Reticulum Export Site Assembly. *J. Cell Biol.* 152: 213-230.
- Aridor, M., Weissman, J., Bannykh, S., Nuoffer, C. and Balch, W.E.** (1998). Cargo selection by the COPII budding machinery during export from the ER. *J. Cell Biol.* 141: 61-70.

- Ausubel, F.M., Brent, R., Kingston, R.E., Moore, D., Seidman, J.G., Smith, J.A. and Struhl, K.** (1997). "Current protocols in molecular biology", John Wiley & Sons Inc., New York. Vol. 1-3.
- Bachmann, B.J.** (1987). Linkage map of *Escherichia coli* K12. In "Escherichia coli and Salmonella typhimurium - cellular and molecular biology", American Society for Microbiology, Washington D. C., USA. : pp. 807-876.
- Baker, D., Hicke, L., Rexach, M., Schleyer, M. and Schekman, R.** (1988). Reconstitution of SEC gene product-dependent intercompartmental protein transport. *Cell* 54: 335-344.
- Balch, W.E., McCaffery, J.M., Plutner, H. and Farquhar, M.G.** (1994). Vesicular stomatitis virus glycoprotein is sorted and concentrated during export from the endoplasmic reticulum. *Cell* 76: 841-852.
- Bannykh, S.I. and Balch, W.E.** (1997). Membrane dynamics at the endoplasmic reticulum-Golgi interface. *J. Cell Biol.* 138: 1-4.
- Bannykh, S.I., Rowe, T. and Balch, W.E.** (1996). The organization of endoplasmic reticulum export complexes. *J. Cell. Biol.* 135: 19-35.
- Barlowe, C.** (1997). Coupled ER to Golgi transport reconstituted with purified cytosolic proteins. *J. Cell. Biol.* 139: 1097-1108.
- Barlowe, C., d'Enfert, C. and Schekman, R.** (1993). Purification and characterization of SAR1p, a small GTP-binding protein required for transport vesicle formation from the endoplasmic reticulum. *J. Biol. Chem.* 268: 873-879.
- Barlowe, C., Orci, L., Yeung, T., Hosobuchi, M., Hamamoto, S., Salama, N., Rexach, M.F., Ravazzola, M., Amherdt, M. and Schekman, R.** (1994). COPII: a membrane coat formed by Sec proteins that drive vesicle budding from the endoplasmic reticulum. *Cell* 77: 895-907.
- Barlowe, C. and Schekman, R.** (1993). SEC12 encodes a guanine-nucleotide-exchange factor essential for transport vesicle budding from the ER. *Nature* 365: 347-349.
- Barrett, T., Xiao, B., Dodson, E.J., Dodson, G., Ludbrook, S.B., Nurmahomed, K., Gamblin, S.J., Musacchio, A., Smerdon, S.J. and Eccleston, J.F.** (1997). The structure of the GTPase-activating domain from p50rhoGAP. *Nature* 385: 458-461.
- Barrowman, J., Sacher, M. and Ferro-Novick, S.** (2000). TRAPP stably associates with the Golgi and is required for vesicle docking. *Embo J.* 19: 862-869.
- Baumert, M., Maycox, P.R., Navone, F., De Camilli, P. and Jahn, R.** (1989). Synaptobrevin: an integral membrane protein of 18,000 daltons present in small synaptic vesicles of rat brain. *Embo J.* 8: 379-384.
- Becherer, K.A., Rieder, S.E., Emr, S.D. and Jones, E.W.** (1996). Novel syntaxin homologue, Pep12p, required for the sorting of luminal hydrolases to the lysosome-like vacuole in yeast. *Mol. Biol. Cell* 7: 579-594.
- Becker, J., Tan, T.J., Trepte, H.H. and Gallwitz, D.** (1991). Mutational analysis of the putative effector domain of the GTP-binding Ypt1 protein in yeast suggests specific regulation by a novel GAP activity. *Embo J.* 10: 785-792.
- Beckers, C.J., Block, M.R., Glick, B.S., Rothman, J.E. and Balch, W.E.** (1989). Vesicular transport between the endoplasmic reticulum and the Golgi stack requires the NEM-sensitive fusion protein. *Nature* 339: 397-398.

- Bednarek, S.Y., Orci, L. and Schekman, R.** (1996). Traffic COPs and the formation of vesicle coats. *Trends. Cell Biol.* 6: 468-473.
- Benli, M., Doring, F., Robinson, D.G., Yang, X. and Gallwitz, D.** (1996). Two GTPase isoforms, Ypt31p and Ypt32p, are essential for Golgi function in yeast. *Embo J.* 15: 6460-6475.
- Bennett, M.K., Calakos, N. and Scheller, R.H.** (1992). Syntaxin: a synaptic protein implicated in docking of synaptic vesicles at presynaptic active zones. *Science* 257: 255-259.
- Bennett, M.K. and Scheller, R.H.** (1993). The molecular machinery for secretion is conserved from yeast to neurons. *Proc. Natl. Acad. Sci. USA* 90: 2559-2563.
- Block, M.R., Glick, B.S., Wilcox, C.A., Wieland, F.T. and Rothman, J.E.** (1988). Purification of an N-ethylmaleimide-sensitive protein catalyzing vesicular transport. *Proc. Natl. Acad. Sci. USA* 85: 7852-7856.
- Bloom, G.S. and Brashear, T.A.** (1989). A novel 58-kDa protein associates with the Golgi apparatus and microtubules. *J Biol Chem* 264: 16083-92.
- Bollag, G. and McCormick, F.** (1991). Differential regulation of rasGAP and neurofibromatosis gene product activities. *Nature* 351: 576-579.
- Bonifacino, J.S., Dasso, M., Harford, J.B., Linpincott-Swhartz, J. and Yamada, K.M.** (1999). "Current protocols in cell biology", John Wiley & Sons Inc., New York, USA.
- Bourne, H.R., Sanders, D.A. and McCormick, F.** (1990). The GTPase superfamily: a conserved switch for diverse cell functions. *Nature* 348: 125-132.
- Bourne, H.R., Sanders, D.A. and McCormick, F.** (1991). The GTPase superfamily: conserved structure and molecular mechanism. *Nature* 349: 117-127.
- Bradford, M.M.** (1976). A rapid and sensitive method for the quantitation of microgram quantities of protein utilizing the principle of protein-dye binding. *Anal. Biochem.* 72: 248-254.
- Brennwald, P. and Novick, P.** (1993). Interactions of three domains distinguishing the Ras-related GTP-binding proteins Ypt1 and Sec4. *Nature* 362: 560-563.
- Brondyk, W.H., McKiernan, C.J., Burstein, E.S. and Macara, I.G.** (1993). Mutants of Rab3A analogous to oncogenic Ras mutants. Sensitivity to Rab3A-GTPase activating protein and Rab3A-guanine nucleotide releasing factor. *J. Biol. Chem.* 268: 9410-9415.
- Brondyk, W.H., McKiernan, C.J., Fortner, K.A., Stabila, P., Holz, R.W. and Macara, I.G.** (1995). Interaction cloning of Rabin3, a novel protein that associates with the Ras-like GTPase Rab3A. *Mol. Cell Biol.* 15: 1137-1143.
- Burnette, W.N.** (1981). "Western blotting": electrophoretic transfer of proteins from sodium dodecyl sulfate--polyacrylamide gels to unmodified nitrocellulose and radiographic detection with antibody and radioiodinated protein A. *Analytical Biochemmistry* 112: 195-203.
- Burstein, E.S. and Macara, I.G.** (1992). Characterization of a guanine nucleotide-releasing factor and a GTPase-activating protein that are specific for the ras-related protein p25rab3A. *Proc. Natl. Acad. Sci. USA* 89: 1154-1158.
- Campbell, J.L. and Schekman, R.** (1997). Selective packaging of cargo molecules into endoplasmic reticulum-derived COPII vesicles. *Proc. Natl. Acad. Sci. USA* 94: 837-842.

- Cao, X., Ballew, N. and Barlowe, C.** (1998). Initial docking of ER-derived vesicles requires Uso1p and Ypt1p but is independent of SNARE proteins. *Embo J.* 17: 2156-2165.
- Cao, X. and Barlowe, C.** (2000). Asymmetric requirements for a Rab GTPase and SNARE proteins in fusion of COPII vesicles with acceptor membranes. *J. Cell. Biol.* 149: 55-66.
- Carr, C.M., Grote, E., Munson, M., Hughson, F.M. and Novick, P.J.** (1999). Sec1p binds to SNARE complexes and concentrates at sites of secretion. *J. Cell Biol.* 146: 333-344.
- Chavrier, P., Gorvel, J.P., Stelzer, E., Simons, K., Gruenberg, J. and Zerial, M.** (1991). Hypervariable C-terminal domain of rab proteins acts as a targeting signal. *Nature* 353: 769-772.
- Chen, M. and Christen, P.** (1997). Removal of chromosomal DNA by Mg²⁺ in the lysis buffer: an improved lysis protocol for preparing Escherichia coli whole-cell lysates for sodium dodecyl sulfate-polyacrylamide gel electrophoresis. *Anal. Biochem.* 246: 263-264.
- Chen, Y. and Scheller, R.** (2001). Snare-mediated membrane fusion. *Nature Rev. Mol. Cell Biol.* 2: 98-106.
- Cherfils, J. and Chardin, P.** (1999). GEFs: structural basis for their activation of small GTP-binding proteins. *Trends Biochem. Sci.* 24: 306-311.
- Clabecq, A., Henry, J.P. and Darchen, F.** (2000). Biochemical characterization of Rab3-GTPase-activating protein reveals a mechanism similar to that of ras-GAP. *J. Biol. Chem.* 275: 31786-31791.
- Clary, D.O., Griff, I.C. and Rothman, J.E.** (1990). SNAPs, a family of NSF attachment proteins involved in intracellular membrane fusion in animals and yeast. *Cell* 61: 709-721.
- Coligan, J.E., Dunn, B.N., Ploegh, H.L., Speicher, D.W. and Wingfield, P.T.** (1997). "Current protocols in protein science", John Wiley & Sons Inc., New York. Vol. 1-2.
- Cosson, P. and Letourneur, F.** (1997). Coatamer (COPI)-coated vesicles: role in intracellular transport and protein sorting. *Curr. Opin. Cell Biol.* 9: 484-487.
- Cox, A.D. and Der, C.J.** (1992). Protein prenylation: more than just glue? *Curr. Opin. Cell Biol.* 4: 1008-1016.
- Cuif, M.H., Possmayer, F., Zander, H., Bordes, N., Jollivet, F., Couedel-Courteille, A., Janoueix-Lerosey, I., Langsley, G., Bornens, M. and Goud, B.** (1999). Characterization of GAPCenA, a GTPase activating protein for Rab6, part of which associates with the centrosome. *Embo J.* 18: 1772-1782.
- Dascher, C., Ossig, R., Gallwitz, D. and Schmitt, H.D.** (1991). Identification and structure of four yeast genes (SLY) that are able to suppress the functional loss of YPT1, a member of the RAS superfamily. *Mol. Cell Biol.* 11: 872-885.
- Day, G.J., Mosteller, R.D. and Broek, D.** (1998). Distinct subclasses of small GTPases interact with guanine nucleotide exchange factors in a similar manner. *Mol Cell Biol* 18: 7444-7454.
- De Antoni, A. and Gallwitz, D.** (2000). A novel multi-purpose cassette for repeated integrative epitope tagging of genes in *Saccharomyces cerevisiae*. *Gene* 246: 179-185.
- De Camilli, P., Emr, S.D., McPherson, P.S. and Novick, P.** (1996). Phosphoinositides as regulators in membrane traffic. *Science* 271: 1533-1539.

- de Duve, C.** (1975). Exploring cells with a centrifuge. *Science* 189: 186-194.
- Der, C.J., Finkel, T. and Cooper, G.M.** (1986). Biological and biochemical properties of human rasH genes mutated at codon 61. *Cell* 44: 167-176.
- Deshaies, R.J., Sanders, S.L., Feldheim, D.A. and Schekman, R.** (1991). Assembly of yeast Sec proteins involved in translocation into the endoplasmic reticulum into a membrane-bound multisubunit complex. *Nature* 349: 806-808.
- Diaz, E., Schimmoller, F. and Pfeffer, S.R.** (1997). A novel Rab9 effector required for endosome-to-TGN transport. *J Cell Biol* 138: 283-90.
- Dirac-Svejstrup, A.B., Sumizawa, T. and Pfeffer, S.R.** (1997). Identification of a GDI displacement factor that releases endosomal Rab GTPases from Rab-GDI. *Embo J.* 16: 465-472.
- Dominguez, M., Dejgaard, K., Fullekrug, J., Dahan, S., Fazel, A., Paccaud, J.P., Thomas, D.Y., Bergeron, J.J. and Nilsson, T.** (1998). gp25L/emp24/p24 protein family members of the cis-Golgi network bind both COP I and II coatomer. *J. Cell Biol.* 140: 751-765.
- Du, L.L., Collins, R.N. and Novick, P.J.** (1998). Identification of a Sec4p GTPase-activating protein (GAP) as a novel member of a Rab GAP family. *J. Biol. Chem.* 273: 3253-3256.
- Duggleby, R.G. and Clarke, R.B.** (1991). Experimental designs for estimating the parameters of the Michaelis-Menten equation from progress curves of enzyme-catalyzed reactions. *Biochim. Biophys. Acta* 1080: 231-236.
- Echard, A., Jollivet, F., Martinez, O., Lacapere, J.J., Rousselet, A., Janoueix-Lerosey, I. and Goud, B.** (1998). Interaction of a Golgi-associated kinesin-like protein with Rab6. *Science* 279: 580-585.
- Esmon, B., Novick, P. and Schekman, R.** (1981). Compartmentalized assembly of oligosaccharides on exported glycoproteins in yeast. *Cell* 25: 451-460.
- Espenshade, P., Gimeno, R.E., Holzmacher, E., Teung, P. and Kaiser, C.A.** (1995). Yeast SEC16 gene encodes a multidomain vesicle coat protein that interacts with Sec23p. *J. Cell. Biol.* 131: 311-324.
- Evan, G.I., Lewis, G.K., Ramsay, G. and Bishop, J.M.** (1985). Isolation of monoclonal antibodies specific for human c-myc proto-oncogene product. *Mol. Cell Biol.* 5: 3610-3616.
- Fasshauer, D., Antonin, W., Margittai, M., Pabst, S. and Jahn, R.** (1999). Mixed and non-cognate SNARE complexes. Characterization of assembly and biophysical properties. *J Biol Chem* 274: 15440-6.
- Fasshauer, D., Sutton, R.B., Brunger, A.T. and Jahn, R.** (1998). Conserved structural features of the synaptic fusion complex: SNARE proteins reclassified as Q- and R-SNAREs. *Proc. Natl. Acad. Sci. USA* 95: 15781-15786.
- Ferro-Novick, S. and Jahn, R.** (1994). Vesicle fusion from yeast to man. *Nature* 370: 191-193.
- Fiedler, K., Veit, M., Stamnes, M.A. and Rothman, J.E.** (1996). Bimodal interaction of coatomer with the p24 family of putative cargo receptors. *Science* 273: 1396-1399.
- Frech, M., Darden, T.A., Pedersen, L.G., Foley, C.K., Charifson, P.S., Anderson, M.W. and Wittinghofer, A.** (1994). Role of glutamine-61 in the hydrolysis of GTP by p21H-ras: an experimental and theoretical study. *Biochemistry* 33: 3237-3244.

- Fukui, K., Sasaki, T., Imazumi, K., Matsuura, Y., Nakanishi, H. and Takai, Y.** (1997). Isolation and characterization of a GTPase activating protein specific for the Rab3 subfamily of small G proteins. *J. Biol. Chem.* 272: 4655-4658.
- Gallwitz, D., Donath, C. and Sander, C.** (1983). A yeast gene encoding a protein homologous to the human c-ha/bas proto-oncogene product. *Nature* 306: 704-707.
- Gamblin, S.J. and Smerdon, S.J.** (1998). GTPase-activating proteins and their complexes. *Curr. Opin. Struct. Biol.* 8: 195-201.
- Garcia-Ranea, J.A. and Valencia, A.** (1998). Distribution and functional diversification of the ras superfamily in *Saccharomyces cerevisiae*. *FEBS Lett.* 434: 219-225.
- Garrett, M.D., Zahner, J.E., Cheney, C.M. and Novick, P.J.** (1994). GDI1 encodes a GDP dissociation inhibitor that plays an essential role in the yeast secretory pathway. *Embo J.* 13: 1718-1728.
- Gerst, J.E.** (1999). SNAREs and SNARE regulators in membrane fusion and exocytosis. *Cell Mol. Life. Sci.* 55: 707-734.
- Gideon, P., John, J., Frech, M., Lautwein, A., Clark, R., Scheffler, J.E. and Wittinghofer, A.** (1992). Mutational and kinetic analyses of the GTPase-activating protein (GAP)-p21 interaction: the C-terminal domain of GAP is not sufficient for full activity. *Mol. Cell Biol.* 12: 2050-2056.
- Gimeno, R.E., Espenshade, P. and Kaiser, C.A.** (1996). COPII coat subunit interactions: Sec24p and Sec23p bind to adjacent regions of Sec16p. *Mol. Biol. Cell.* 7: 1815-18123.
- Götte, M., Lazar, T., Yoo, J.S., Scheglmann, D. and Gallwitz, D.** (2000). The full complement of yeast Ypt/Rab-GTPases and their involvement in exo- and endocytic trafficking. In "Subcell. Biochem.", Plenum Press, New York, USA. Vol. 34: pp. 133-173.
- Gournier, H., Stenmark, H., Rybin, V., Lippe, R. and Zerial, M.** (1998). Two distinct effectors of the small GTPase Rab5 cooperate in endocytic membrane fusion. *Embo J.* 17: 1930-1940.
- Grabowski, R. and Gallwitz, D.** (1997). High-affinity binding of the yeast cis-Golgi t-SNARE, Sed5p, to wild-type and mutant Sly1p, a modulator of transport vesicle docking. *FEBS Lett.* 411: 169-172.
- Grossmann, M.K. and Zimmermann, F.K.** (1979). The structural genes of internal invertases in *Saccharomyces cerevisiae*. *Mol. Gen. Genet.* 175: 223-229.
- Grote, E. and Novick, P.J.** (1999). Promiscuity in Rab-SNARE interactions. *Mol. Biol. Cell* 10: 4149-4161.
- Güldener, U., Heck, S., Fiedler, T., Beinhauer, J. and Hegemann, J.H.** (1996). A new efficient gene disruption cassette for repeated use in budding yeast. *Nucleic Acids Res.* 24: 2519-2524.
- Guo, W., Sacher, M., Barrowman, J., Ferro-Novick, S. and Novick, P.** (2000). Protein complexes in transport vesicle targeting. *Trends. Cell Biol.* 10: 251-255.
- Halachmi, N. and Lev, Z.** (1996). The Sec1 family: a novel family of proteins involved in synaptic transmission and general secretion. *J Neurochem.* 66: 889-897.
- Hama, H., Tall, G.G. and Horazdovsky, B.F.** (1999). Vps9p is a guanine nucleotide exchange factor involved in vesicle-mediated vacuolar protein transport. *J. Biol. Chem.* 274: 15284-15291.

- Hanahan, D., Jessee, J. and Bloom, F.R.** (1991). Plasmid transformation of *Escherichia coli* and other bacteria. In *"Methods in Enzymology"*, Academic Press, Inc., San Diego, USA. Vol. 204: pp. 63-113.
- Hardwick, K.G. and Pelham, H.R.** (1992). SED5 encodes a 39-kD integral membrane protein required for vesicular transport between the ER and the Golgi complex. *J. Cell Biol.* 119: 513-521.
- Harlow, E. and Lane, D.** (1999). *"Using Antibodies. A laboratory manual"*, Cold Spring Harbor Press, Cold Spring Harbor, New York, USA.
- Haubruck, H., Disela, C., Wagner, P. and Gallwitz, D.** (1987). The ras-related ypt protein is an ubiquitous eukaryotic protein: isolation and sequence analysis of mouse cDNA clones highly homologous to the yeast YPT1 gene. *Embo J.* 6: 4049-4053.
- Haucke, V. and Gottfried, S.** (1997). Import of proteins into mitochondria and chloroplasts. *Trends. Cell Biol.* 7: 103-106.
- Hauri, H.P., Kappeler, F., Andersson, H. and Appenzeller, C.** (2000). ERGIC-53 and traffic in the secretory pathway. *J. Cell. Sci.* 113: 587-596.
- Herrmann, J.M., Malkus, P. and Schekman, R.** (1999). Out of the ER--outfitters, escorts and guides. *Trends Cell Biol.* 9: 5-7.
- Hettema, E.H., Distel, B. and Tabak, H.F.** (1999). Import of proteins into peroxisomes. *Biochim. Biophys. Acta.* 1451: 17-34.
- Hicke, L. and Schekman, R.** (1989). Yeast Sec23p acts in the cytoplasm to promote protein transport from the endoplasmic reticulum to the Golgi complex in vivo and in vitro. *Embo J.* 8: 1677-1684.
- Hicke, L., Yoshihisa, T. and Schekman, R.** (1992). Sec23p and a novel 105-kDa protein function as a multimeric complex to promote vesicle budding and protein transport from the endoplasmic reticulum. *Mol. Biol. Cell.* 3: 667-676.
- Higashio, H., Kimata, Y., Kiriya, T., Hirata, A. and Kohno, K.** (2000). Sfb2p, a yeast protein related to Sec24p, can function as a constituent of COPII coats required for vesicle budding from the endoplasmic reticulum. *J. Biol. Chem.* 275: 17900-17908.
- Holthuis, J.C., Nichols, B.J., Dhruvakumar, S. and Pelham, H.R.** (1998). Two syntaxin homologues in the TGN/endosomal system of yeast. *Embo J.* 17: 113-126.
- Horazdovsky, B.F., Busch, G.R. and Emr, S.D.** (1994). VPS21 encodes a rab5-like GTP binding protein that is required for the sorting of yeast vacuolar proteins. *Embo J.* 13: 1297-1309.
- Horiuchi, H., Lippe, R., McBride, H.M., Rubino, M., Woodman, P., Stenmark, H., Rybin, V., Wilm, M., Ashman, K., Mann, M. and Zerial, M.** (1997). A novel Rab5 GDP/GTP exchange factor complexed to Rabaptin-5 links nucleotide exchange to effector recruitment and function. *Cell* 90: 114911-59.
- Jahn, R. and Südhof, T.C.** (1999). Membrane fusion and exocytosis. *Annu. Rev. Biochem.* 68: 863-911.
- Janknecht, R., de Martynoff, G., Lou, J., Hipskind, R.A., Nordheim, A. and Stunnenberg, H.G.** (1991). Rapid and efficient purification of native histidine-tagged protein expressed by recombinant vaccinia virus. *Proc. Natl. Acad. Sci. USA.* 88: 8972-8976.

- Janson, J.C. and Ryden, L.** (1989). "*Protein purification*", VCH, New York, USA.
- Jedd, G., Richardson, C., Litt, R. and Segev, N.** (1995). The Ypt1 GTPase is essential for the first two steps of the yeast secretory pathway. *J. Cell Biol.* 131: 583-590.
- Jones, S., Newman, C., Liu, F. and Segev, N.** (2000). The TRAPP complex is a nucleotide exchanger for ypt1 and Ypt31/32. *Mol. Biol. Cell* 11: 4403-4411.
- Kaetzel, C.S., Rao, C.K. and Lamm, M.E.** (1987). Protein disulphide-isomerase from human placenta and rat liver. Purification and immunological characterization with monoclonal antibodies. *Biochem J.* 241: 39-47.
- Kahn, R.A., Der, C.J. and Bokoch, G.M.** (1992). The ras superfamily of GTP-binding proteins: guidelines on nomenclature [news]. *Faseb J.* 6: 2512-2513.
- Kaiser, C.A. and Schekman, R.** (1990). Distinct sets of SEC genes govern transport vesicle formation and fusion early in the secretory pathway. *Cell* 61: 723-733.
- Kamal, A. and Goldstein, L.S.** (2000). Connecting vesicle transport to the cytoskeleton. *Curr. Opin. Cell Biol.* 12: 503-508.
- Kappeler, F., Klopfenstein, D.R., Foguet, M., Paccaud, J.P. and Hauri, H.P.** (1997). The recycling of ERGIC-53 in the early secretory pathway. ERGIC-53 carries a cytosolic endoplasmic reticulum-exit determinant interacting with COPII. *J. Biol. Chem.* 272: 31801-31808.
- Katz, L. and Brennwald, P.** (2000). Testing the 3Q:1R "Rule": mutational analysis of the ionic "Zero" layer in the yeast exocytic SNARE complex reveals No requirement for arginine. *Mol. Biol. Cell* 11: 3849-3858.
- Kirchhausen, T.** (1999). Adaptors for clathrin-mediated traffic. *Annu. Rev. Cell Dev. Biol.* 15: 705-732.
- Kirchhausen, T.** (2001). Three ways to make a vesicle. *Nature Rev. Mol. Cell Biol.* 1: 187-198.
- Kjeldgaard, M., Nyborg, J. and Clark, B.F.** (1996). The GTP binding motif: variations on a theme. *Faseb J.* 10: 1347-1368.
- Klebe, C., Bischoff, F.R., Ponstingl, H. and Wittinghofer, A.** (1995). Interaction of the nuclear GTP-binding protein Ran with its regulatory proteins RCC1 and RanGAP1. *Biochemistry* 34: 639-647.
- Klionsky, D.J. and Emr, S.D.** (2000). Autophagy as a regulated pathway of cellular degradation. *Science* 290: 1717-1721.
- Kreis, T.E.** (1986). Microinjected antibodies against the cytoplasmic domain of vesicular stomatitis virus glycoprotein block its transport to the cell surface. *Embo J.* 5: 931-941.
- Krengel, U., Schlichting, L., Scherer, A., Schumann, R., Frech, M., John, J., Kabsch, W., Pai, E.F. and Wittinghofer, A.** (1990). Three-dimensional structures of H-ras p21 mutants: molecular basis for their inability to function as signal switch molecules. *Cell* 62: 539-548.
- Kuehn, M.J., Herrmann, J.M. and Schekman, R.** (1998). COPII-cargo interactions direct protein sorting into ER-derived transport vesicles. *Nature* 391: 187-190.
- Kuehn, M.J. and Schekman, R.** (1997). COPII and secretory cargo capture into transport vesicles. *Curr. Opin. Cell Biol.* 9: 477-483.

- Kuge, O., Dascher, C., Orci, L., Rowe, T., Amherdt, M., Plutner, H., Ravazzola, M., Tanigawa, G., Rothman, J.E. and Balch, W.E.** (1994). Sar1 promotes vesicle budding from the endoplasmic reticulum but not Golgi compartments. *J. Cell Biol.* 125: 51-65.
- Kurihara, T., Hamamoto, S., Gimeno, R.E., Kaiser, C.A., Schekman, R. and Yoshihisa, T.** (2000). Sec24p and Iss1p function interchangeably in transport vesicle formation from the endoplasmic reticulum in *Saccharomyces cerevisiae*. *Mol. Biol. Cell.* 11: 983-998.
- Laemmli, U.K.** (1970). Cleavage of structural proteins during the assembly of the head of bacteriophage T4. *Nature* 227: 680-685.
- Lazar, T., Götte, M. and Gallwitz, D.** (1997). Vesicular transport: how many Ypt/Rab-GTPases make a eukaryotic cell? *Trends Biochem. Sci.* 22: 468-472.
- Lewis, M.J. and Pelham, H.R.** (1996). SNARE-mediated retrograde traffic from the Golgi complex to the endoplasmic reticulum. *Cell* 85: 205-215.
- Lian, J.P., Stone, S., Jiang, Y., Lyons, P. and Ferro-Novick, S.** (1994). Ypt1p implicated in v-SNARE activation. *Nature* 372: 698-701.
- Lin, R.C. and Scheller, R.H.** (1997). Structural organization of the synaptic exocytosis core complex. *Neuron* 19: 1087-1094.
- Lupas, A., Van Dyke, M. and Stock, J.** (1991). Predicting coiled coils from protein sequences. *Science* 252: 1162-1164.
- Lupashin, V.V. and Waters, M.G.** (1997). t-SNARE activation through transient interaction with a rab-like guanosine triphosphatase. *Science* 276: 1255-1258.
- Mackay, J.P. and Crossley, M.** (1998). Zinc fingers are sticking together. *Trends Biochem. Sci.* 23: 1-4.
- Malhotra, V., Orci, L., Glick, B.S., Block, M.R. and Rothman, J.E.** (1988). Role of an N-ethylmaleimide-sensitive transport component in promoting fusion of transport vesicles with cisternae of the Golgi stack. *Cell* 54: 221-227.
- Manivasakam, P., Weber, S.C., McElver, J. and Schiestl, R.H.** (1995). Micro-homology mediated PCR targeting in *Saccharomyces cerevisiae*. *Nucleic Acids Res.* 23: 2799-2800.
- Martinez, O., Antony, C., Pehau-Arnaudet, G., Berger, E.G., Salamero, J. and Goud, B.** (1997). GTP-bound forms of rab6 induce the redistribution of Golgi proteins into the endoplasmic reticulum. *Proc. Natl. Acad. Sci. USA* 94: 1828-1833.
- Martinez, O. and Goud, B.** (1998). Rab proteins. *Biochim. Biophys. Acta* 1404: 101-112.
- Matern, H., Yang, X., Andrusis, E., Sternglanz, R., Trepte, H.H. and Gallwitz, D.** (2000). A novel golgi membrane protein is part of a GTPase-binding protein complex involved in vesicle targeting. *Embo J.* 19: 4485-4492.
- Matozaki, T., Nakanishi, H. and Takai, Y.** (2000). Small G-protein networks: Their crosstalk and signal cascades. *Cell. Signal.* 12: 515-524.
- Matsuoka, K., Morimitsu, Y., Uchida, K. and Schekman, R.** (1998a). Coat assembly directs v-SNARE concentration into synthetic COPII vesicles. *Mol. Cell.* 2: 703-708.

- Matsuoka, K., Orci, L., Amherdt, M., Bednarek, S.Y., Hamamoto, S., Schekman, R. and Yeung, T.** (1998b). COPII-coated vesicle formation reconstituted with purified coat proteins and chemically defined liposomes. *Cell* 93: 263-275.
- McMahon, H.T. and Sudhof, T.C.** (1995). Synaptic core complex of synaptobrevin, syntaxin, and SNAP25 forms high affinity alpha-SNAP binding site. *J. Biol. Chem.* 270: 2213-2217.
- McNew, J.A., Parlati, F., Fukuda, R., Johnston, R.J., Paz, K., Paumet, F., Sollner, T.H. and Rothman, J.E.** (2000). Compartmental specificity of cellular membrane fusion encoded in SNARE proteins. *Nature* 407: 153-159.
- Mellman, I. and Warren, G.** (2000). The road taken: past and future foundations of membrane traffic. *Cell* 100: 99-112.
- Milburn, M.V., Tong, L., deVos, A.M., Brunger, A., Yamaizumi, Z., Nishimura, S. and Kim, S.H.** (1990). Molecular switch for signal transduction: structural differences between active and inactive forms of protooncogenic ras proteins. *Science* 247: 939-945.
- Mitchell, D.A., Marshall, T.K. and Deschenes, R.J.** (1993). Vectors for the inducible overexpression of glutathione S-transferase fusion proteins in yeast. *Yeast* 9: 715-722.
- Müller, O., Sattler, T., Flotenmeyer, M., Schwarz, H., Plattner, H. and Mayer, A.** (2000). Autophagic tubes: vacuolar invaginations involved in lateral membrane sorting and inverse vesicle budding. *J. Cell Biol.* 151: 519-528.
- Muniz, M., Nuoffer, C., Hauri, H.P. and Riezman, H.** (2000). The Emp24 complex recruits a specific cargo molecule into endoplasmic reticulum-derived vesicles. *J. Cell Biol.* 148: 925-930.
- Nakano, A. and Muramatsu, M.** (1989). A novel GTP-binding protein, Sar1p, is involved in transport from the endoplasmic reticulum to the Golgi apparatus. *J. Cell Biol.* 109: 2677-2691.
- Nelson, D.S., Alvarez, C., Gao, Y.S., Garcia-Mata, R., Fialkowski, E. and Sztul, E.** (1998). The membrane transport factor TAP/p115 cycles between the Golgi and earlier secretory compartments and contains distinct domains required for its localization and function. *J. Cell. Biol.* 143: 319-331.
- Neuwald, A.F.** (1997). A shared domain between a spindle assembly checkpoint protein and Ypt/Rab-specific GTPase-activators. *Trends Biochem. Sci.* 22: 243-244.
- Neuwald, A.F., Liu, J.S., Lipman, D.J. and Lawrence, C.E.** (1997). Extracting protein alignment models from the sequence database. *Nucleic Acids Res.* 25: 1665-1677.
- Nichols, B.J., Holthuis, J.C. and Pelham, H.R.** (1998). The Sec1p homologue Vps45p binds to the syntaxin Tlg2p. *Eur. J. Cell Biol.* 77: 263-268.
- Nickel, W., Brugger, B. and Wieland, F.T.** (1998). Protein and lipid sorting between the endoplasmic reticulum and the Golgi complex. *Semin. Cell Dev. Biol.* 9: 493-501.
- Nielsen, E., Severin, F., Backer, J.M., Hyman, A.A. and Zerial, M.** (1999). Rab5 regulates motility of early endosomes on microtubules. *Nat. Cell Biol.* 1: 376-382.
- Nishimura, N. and Balch, W.E.** (1997). A di-acidic signal required for selective export from the endoplasmic reticulum. *Science* 277: 556-8.

- Nishimura, N., Bannykh, S., Slabough, S., Matteson, J., Altschuler, Y., Hahn, K. and Balch, W.E.** (1999). A di-acidic (DXE) code directs concentration of cargo during export from the endoplasmic reticulum. *J. Biol. Chem.* 274: 15937-15946.
- Nomura, N., Nagase, T., Miyajima, N., Sazuka, T., Tanaka, A., Sato, S., Seki, N., Kawarabayasi, Y., Ishikawa, K. and Tabata, S.** (1994). Prediction of the coding sequences of unidentified human genes. II. The coding sequences of 40 new genes (KIAA0041-KIAA0080) deduced by analysis of cDNA clones from human cell line KG-1 (supplement). *DNA Res.* 1: 251-262.
- Novick, P. and Zerial, M.** (1997). The diversity of Rab proteins in vesicle transport. *Curr. Opin. Cell Biol.* 9: 496-504.
- Odorizzi, G., Babst, M. and Emr, S.D.** (2000). Phosphoinositide signaling and the regulation of membrane trafficking in yeast. *Trends Biochem. Sci.* 25: 229-235.
- Ogden, R.C. and Adams, D.A.** (1987). Electrophoresis in agarose and acrylamide gels. In "Methods in Enzymology", Academic Press, Inc., San Diego, USA. Vol. 152: pp. 61-87.
- Oka, A., Sugisaki, H. and Takanami, M.** (1981). Nucleotide sequence of the kanamycin resistance transposon Tn903. *J. Mol. Biol.* 147: 217-226.
- Oka, T., Nishikawa, S. and Nakano, A.** (1991). Reconstitution of GTP-binding Sar1 protein function in ER to Golgi transport. *J. Cell Biol.* 114: 671-679.
- Orci, L., Ravazzola, M., Meda, P., Holcomb, C., Moore, H.P., Hicke, L. and Schekman, R.** (1991). Mammalian Sec23p homologue is restricted to the endoplasmic reticulum transitional cytoplasm. *Proc. Natl. Acad. Sci. USA* 88: 8611-8615.
- Ossig, R., Dascher, C., Trepte, H.H., Schmitt, H.D. and Gallwitz, D.** (1991). The yeast SLY gene products, suppressors of defects in the essential GTP-binding Ypt1 protein, may act in endoplasmic reticulum-to-Golgi transport. *Mol. Cell Biol.* 11: 2980-2993.
- Ossig, R., Schmitt, H.D., de Groot, B., Riedel, D., Keranen, S., Ronne, H., Grubmuller, H. and Jahn, R.** (2000). Exocytosis requires asymmetry in the central layer of the SNARE complex. *EMBO J.* 19: 6000-6010.
- Ossipov, D., Schröder-Kohne, S. and Schmitt, H.D.** (1999). Yeast ER-Golgi v-SNAREs Bos1p and Bet1p differ in steady-state localization and targeting. *J. Cell Sci.* 112: 4135-4142.
- Otto, H., Hanson, P.I. and Jahn, R.** (1997). Assembly and disassembly of a ternary complex of synaptobrevin, syntaxin, and SNAP-25 in the membrane of synaptic vesicles. *Proc. Natl. Acad. Sci. USA* 94: 6197-201.
- Paccaud, J.P., Reith, W., Carpentier, J.L., Ravazzola, M., Amherdt, M., Schekman, R. and Orci, L.** (1996). Cloning and functional characterization of mammalian homologues of the COPII component Sec23. *Mol. Biol. Cell* 7: 1535-1546.
- Pagano, A., Letourneur, F., Garcia-Estefania, D., Carpentier, J.L., Orci, L. and Paccaud, J.P.** (1999). Sec24 proteins and sorting at the endoplasmic reticulum. *J. Biol. Chem.* 274: 7833-7840.
- Pai, E.F., Kregel, U., Petsko, G.A., Goody, R.S., Kabsch, W. and Wittinghofer, A.** (1990). Refined crystal structure of the triphosphate conformation of H-ras p21 at 1.35 Å resolution: implications for the mechanism of GTP hydrolysis. *Embo J.* 9: 2351-2359.

- Palade, G.** (1975). Intracellular aspects of the process of protein synthesis. *Science* 189: 347-358.
- Parlati, F., McNew, J.A., Fukuda, R., Miller, R., Sollner, T.H. and Rothman, J.E.** (2000). Topological restriction of SNARE-dependent membrane fusion. *Nature* 407: 194-198.
- Pelham, H.R.** (1999). SNAREs and the secretory pathway-lessons from yeast. *Exp. Cell Res.* 247: 1-8.
- Pelham, H.R. and Rothman, J.E.** (2000). The debate about transport in the Golgi--two sides of the same coin? *Cell* 102: 713-719.
- Peng, R., De Antoni, A. and Gallwitz, D.** (2000). Evidence for overlapping and distinct functions in protein transport of coat protein Sec24p family members. *J. Biol. Chem.* 275: 11521-11528.
- Peng, R., Grabowski, R., De Antoni, A. and Gallwitz, D.** (1999). Specific interaction of the yeast cis-Golgi syntaxin Sed5p and the coat protein complex II component Sec24p of endoplasmic reticulum-derived transport vesicles. *Proc. Natl. Acad. Sci. U S A* 96: 3751-6
- Peranen, J., Auvinen, P., Virta, H., Wepf, R. and Simons, K.** (1996). Rab8 promotes polarized membrane transport through reorganization of actin and microtubules in fibroblasts. *J. Cell Biol.* 135: 153-167.
- Peter, M., Chavrier, P., Nigg, E.A. and Zerial, M.** (1992). Isoprenylation of rab proteins on structurally distinct cysteine motifs. *J. Cell Sci.* 102: 857-865.
- Peters, C., Andrews, P.D., Stark, M.J., Cesaro-Tadic, S., Glatz, A., Podtelejnikov, A., Mann, M. and Mayer, A.** (1999). Control of the terminal step of intracellular membrane fusion by protein phosphatase 1. *Science* 285: 1084-1087.
- Peters, C. and Mayer, A.** (1998). Ca²⁺/calmodulin signals the completion of docking and triggers a late step of vacuole fusion [see comments]. *Nature* 396: 575-580.
- Pfeffer, S.R.** (1999). Transport-vesicle targeting: tethers before SNAREs. *Nat. Cell Biol.* 1: E17-22.
- Pfeffer, S.R., Dirac-Svejstrup, A.B. and Soldati, T.** (1995). Rab GDP dissociation inhibitor: putting rab GTPases in the right place. *J. Biol. Chem.* 270: 17057-17059.
- Poirier, M.A., Xiao, W., Macosko, J.C., Chan, C., Shin, Y.K. and Bennett, M.K.** (1998). The synaptic SNARE complex is a parallel four-stranded helical bundle. *Nat. Struct. Biol.* 5: 765-769.
- Pringle, J.R., Adams, A.E., Drubin, D.G. and Haarer, B.K.** (1991). Immunofluorescence methods for yeast. In *"Methods in Enzymology"*, Academic Press, Inc., San Diego, USA. Vol. 194: pp. 565-602.
- Privé, G.G., Milburn, M.V., Tong, L., de Vos, A.M., Yamaizumi, Z., Nishimura, S. and Kim, S.H.** (1992). X-ray crystal structures of transforming p21 ras mutants suggest a transition-state stabilization mechanism for GTP hydrolysis. *Proc. Natl. Acad. Sci. USA* 89: 3649-3653.
- Pruyne, D.W., Schott, D.H. and Bretscher, A.** (1998). Tropomyosin-containing actin cables direct the Myo2p-dependent polarized delivery of secretory vesicles in budding yeast. *J Cell Biol* 143: 1931-1945.
- Pryer, N.K., Salama, N.R., Schekman, R. and Kaiser, C.A.** (1993). Cytosolic Sec13p complex is required for vesicle formation from the endoplasmic reticulum in vitro. *J. Cell. Biol.* 120: 865-875.

- Rak, A., Fedorov, R., Alexandrov, K., Albert, S., Goody, R.S., Gallwitz, D. and Scheidig, A.J.** (2000). Crystal structure of the GAP domain of Gyp1p: first insights into interaction with Ypt/Rab proteins. *Embo J.* 19: 5105-5113.
- Ren, M., Zeng, J., De Lemos-Chiarandini, C., Rosenfeld, M., Adesnik, M. and Sabatini, D.D.** (1996). In its active form, the GTP-binding protein rab8 interacts with a stress-activated protein kinase. *Proc. Natl. Acad. Sci. USA* 93: 5151-5.
- Rexach, M.F. and Schekman, R.W.** (1991). Distinct biochemical requirements for the budding, targeting, and fusion of ER-derived transport vesicles. *J. Cell Biol.* 114: 219-229.
- Richardson, C.J., Jones, S., Litt, R.J. and Segev, N.** (1998). GTP hydrolysis is not important for Ypt1 GTPase function in vesicular transport. *Mol. Cell Biol.* 18: 827-838.
- Rittinger, K., Walker, P.A., Eccleston, J.F., Nurmahomed, K., Owen, D., Laue, E., Gamblin, S.J. and Smerdon, S.J.** (1997a). Crystal structure of a small G protein in complex with the GTPase-activating protein rhoGAP. *Nature* 388: 693-697.
- Rittinger, K., Walker, P.A., Eccleston, J.F., Smerdon, S.J. and Gamblin, S.J.** (1997b). Structure at 1.65 Å of RhoA and its GTPase-activating protein in complex with a transition-state analogue. *Nature* 389: 758-762.
- Roberg, K.J., Crotwell, M., Espenshade, P., Gimeno, R. and Kaiser, C.A.** (1999). LST1 is a SEC24 homologue used for selective export of the plasma membrane ATPase from the endoplasmic reticulum. *J. Cell Biol.* 145: 659-672.
- Rose, M.D., Winston, F. and Hieter, P.** (1990). "*Methods in yeast genetics a laboratory course manual*", Cold Spring Harbor Laboratory Press, Cold Spring Harbor, New York, USA.
- Rothman, J.E.** (1994). Mechanisms of intracellular protein transport. *Nature* 372: 55-63.
- Rothman, J.E. and Warren, G.** (1994). Implications of the SNARE hypothesis for intracellular membrane topology and dynamics. *Curr. Biol.* 4: 220-233.
- Rybin, V., Ullrich, O., Rubino, M., Alexandrov, K., Simon, I., Seabra, M.C., Goody, R. and Zerial, M.** (1996). GTPase activity of Rab5 acts as a timer for endocytic membrane fusion. *Nature* 383: 266-269.
- Sacher, M., Barrowman, J., Schieltz, D., Yates, J.R., 3rd and Ferro-Novick, S.** (2000). Identification and characterization of five new subunits of TRAPP. *Eur. J. Cell Biol.* 79: 71-80.
- Sacher, M., Jiang, Y., Barrowman, J., Scarpa, A., Burston, J., Zhang, L., Schieltz, D., Yates, J.R., 3rd, Abeliovich, H. and Ferro-Novick, S.** (1998). TRAPP, a highly conserved novel complex on the cis-Golgi that mediates vesicle docking and fusion. *Embo J.* 17: 2494-2503.
- Saiki, R.K., Gelfand, D.H., Stoffel, S., Scharf, S.J., Higuchi, R., Horn, G.T., Mullis, K.B. and Erlich, H.A.** (1988). Primer-directed enzymatic amplification of DNA with a thermostable DNA polymerase. *Science* 239: 487-491.
- Salama, N.R., Chuang, J.S. and Schekman, R.W.** (1997). Sec31 encodes an essential component of the COPII coat required for transport vesicle budding from the endoplasmic reticulum. *Mol. Biol. Cell.* 8: 205-217.
- Salama, N.R., Yeung, T. and Schekman, R.W.** (1993). The Sec13p complex and reconstitution of vesicle budding from the ER with purified cytosolic proteins. *Embo J.* 12: 4073-4082.

- Salminen, A. and Novick, P.J.** (1987). A ras-like protein is required for a post-Golgi event in yeast secretion. *Cell* 49: 527-538.
- Sambrook, J., Fritsh, E.F. and Maniatis, T.** (1989). "*Molecular cloning. A laboratory manual*", second edition, Cold Spring Harbor Press, Cold Spring Harbor, New York, USA. Vol. 1-3.
- Sapperstein, S.K., Lupashin, V.V., Schmitt, H.D. and Waters, M.G.** (1996). Assembly of the ER to Golgi SNARE complex requires Uso1p. *J. Cell Biol.* 132: 755-767.
- Sapperstein, S.K., Walter, D.M., Grosvenor, A.R., Heuser, J.E. and Waters, M.G.** (1995). p115 is a general vesicular transport factor related to the yeast endoplasmic reticulum to Golgi transport factor Uso1p. *Proc. Natl. Acad. Sci. USA* 92: 522-526.
- Saraste, J., Lahtinen, U. and Goud, B.** (1995). Localization of the small GTP-binding protein rab1p to early compartments of the secretory pathway. *J. Cell Sci.* 108: 1541-1552.
- Sato, T.K., Rehling, P., Peterson, M.R. and Emr, S.D.** (2000). Class C Vps protein complex regulates vacuolar SNARE pairing and is required for vesicle docking/fusion. *Mol. Cell* 6: 661-671.
- Sauer, B.** (1987). Functional expression of the cre-lox site-specific recombination system in the yeast *Saccharomyces cerevisiae*. *Mol. Cell Biol.* 7: 2087-2096.
- Saxena, K., Gaitatzes, C., Walsh, M.T., Eck, M., Neer, E.J. and Smith, T.F.** (1996). Analysis of the physical properties and molecular modeling of Sec13: A WD repeat protein involved in vesicular traffic. *Biochemistry* 35: 15215-15221.
- Scales, S.J., Bock, J.B. and Scheller, R.H.** (2000a). The specifics of membrane fusion. *Nature* 407: 144-146.
- Scales, S.J., Gomez, M. and Kreis, T.E.** (2000b). Coat proteins regulating membrane traffic. *Int. Rev. Cytol.* 195: 67-144.
- Schatz, G.** (1996). The protein import system of mitochondria. *J. Biol. Chem.* 271: 31763-6.
- Schauer, I., Emr, S., Gross, C. and Schekman, R.** (1985). Invertase signal and mature sequence substitutions that delay intercompartmental transport of active enzyme. *J. Cell Biol.* 100: 1664-1675.
- Scheffzek, K., Ahmadian, M.R., Kabsch, W., Wiesmuller, L., Lautwein, A., Schmitz, F. and Wittinghofer, A.** (1997). The Ras-RasGAP complex: structural basis for GTPase activation and its loss in oncogenic Ras mutants. *Science* 277: 333-8.
- Scheffzek, K., Ahmadian, M.R. and Wittinghofer, A.** (1998). GTPase-activating proteins: helping hands to complement an active site. *Trends Biochem. Sci.* 23: 257-262.
- Scheffzek, K., Lautwein, A., Kabsch, W., Ahmadian, M.R. and Wittinghofer, A.** (1996). Crystal structure of the GTPase-activating domain of human p120GAP and implications for the interaction with Ras. *Nature* 384: 591-596.
- Schekman, R. and Orci, L.** (1996). Coat proteins and vesicle budding. *Science* 271: 1526-1533.
- Schiestl, R.H. and Gietz, R.D.** (1989). High efficiency transformation of intact yeast cells using single stranded nucleic acids as a carrier. *Curr. Genet.* 16: 339-346.

- Schimmoller, F., Simon, I. and Pfeffer, S.R.** (1998). Rab GTPases, directors of vesicle docking. *J. Biol. Chem.* 273: 22161-22164.
- Schimmoller, F., Singer-Kruger, B., Schröder, S., Kruger, U., Barlowe, C. and Riezman, H.** (1995). The absence of Emp24p, a component of ER-derived COPII-coated vesicles, causes a defect in transport of selected proteins to the Golgi. *Embo J.* 14: 1329-1339.
- Schleiff, E. and Soll, J.** (2000). Travelling of proteins through membranes: translocation into chloroplasts. *Planta* 211: 449-456.
- Schlichting, I., Almo, S.C., Rapp, G., Wilson, K., Petratos, K., Lentfer, A., Wittinghofer, A., Kabsch, W., Pai, E.F., Petsko, G.A. and et al.** (1990). Time-resolved X-ray crystallographic study of the conformational change in Ha-Ras p21 protein on GTP hydrolysis. *Nature* 345: 309-315.
- Schmitt, H.D., Puzicha, M. and Gallwitz, D.** (1988). Study of a temperature-sensitive mutant of the ras-related YPT1 gene product in yeast suggests a role in the regulation of intracellular calcium. *Cell* 53: 635-647.
- Schmitt, H.D., Wagner, P., Pfaff, E. and Gallwitz, D.** (1986). The ras-related YPT1 gene product in yeast: a GTP-binding protein that might be involved in microtubule organization. *Cell* 47: 401-412.
- Schott, D., Ho, J., Pruyn, D. and Bretscher, A.** (1999). The COOH-terminal domain of Myo2p, a yeast myosin V, has a direct role in secretory vesicle targeting. *J. Cell Biol.* 147: 791-808.
- Schröder, S., Schimmoller, F., Singer-Kruger, B. and Riezman, H.** (1995). The Golgi-localization of yeast Emp47p depends on its di-lysine motif but is not affected by the ret1-1 mutation in alpha-COP. *J. Cell Biol.* 131: 895-912.
- Schweins, T., Geyer, M., Kalbitzer, H.R., Wittinghofer, A. and Warshel, A.** (1996). Linear free energy relationships in the intrinsic and GTPase activating protein-stimulated guanosine 5'-triphosphate hydrolysis of p21ras. *Biochemistry* 35: 14225-14231.
- Scott, S.V. and Klionsky, D.J.** (1998). Delivery of proteins and organelles to the vacuole from the cytoplasm. *Curr. Opin. Cell Biol.* 10: 523-529.
- Seals, D.F., Eitzen, G., Margolis, N., Wickner, W.T. and Price, A.** (2000). A Ypt/Rab effector complex containing the Sec1 homolog Vps33p is required for homotypic vacuole fusion. *Proc. Natl. Acad. Sci. USA* 97: 9402-9407.
- Segev, N.** (1991). Mediation of the attachment or fusion step in vesicular transport by the GTP-binding Ypt1 protein. *Science* 252: 1553-1556.
- Segev, N., Mulholland, J. and Botstein, D.** (1988). The yeast GTP-binding YPT1 protein and a mammalian counterpart are associated with the secretion machinery. *Cell* 52: 915-924.
- Seglen, P.O. and Bohley, P.** (1992). Autophagy and other vacuolar protein degradation mechanisms. *Experientia* 48: 158-172.
- Shaywitz, D.A., Espenshade, P.J., Gimeno, R.E. and Kaiser, C.A.** (1997). COPII subunit interactions in the assembly of the vesicle coat. *J. Biol. Chem.* 272: 25413-25416.
- Shen, K.A., Hammond, C.M. and Moore, H.P.** (1993). Molecular analysis of SAR1-related cDNAs from a mouse pituitary cell line. *FEBS Lett.* 335: 380-385.

- Sherman, F.** (1991). Getting started with yeast. In *"Methods in Enzymology"*, Academic Press, Inc., San Diego, USA. Vol. 194: pp. 3-21.
- Shimoni, Y., Kurihara, T., Ravazzola, M., Amherdt, M., Orci, L. and Schekman, R.** (2000). Lst1p and Sec24p Cooperate in Sorting of the Plasma Membrane ATPase into COPII Vesicles in *Saccharomyces cerevisiae*. *J. Cell Biol.* 151: 973-984.
- Shirataki, H., Kaibuchi, K., Sakoda, T., Kishida, S., Yamaguchi, T., Wada, K., Miyazaki, M. and Takai, Y.** (1993). Rabphilin-3A, a putative target protein for smg p25A/rab3A p25 small GTP-binding protein related to synaptotagmin. *Mol. Cell Biol.* 13: 2061-2068.
- Sigal, I.S., Gibbs, J.B., D'Alonzo, J.S. and Scolnick, E.M.** (1986). Identification of effector residues and a neutralizing epitope of Ha-ras-encoded p21. *Proc. Natl. Acad. Sci. USA* 83: 4725-4729.
- Sikorski, R.S. and Hieter, P.** (1989). A system of shuttle vectors and yeast host strains designed for efficient manipulation of DNA in *Saccharomyces cerevisiae*. *Genetics* 122: 19-27.
- Simonsen, A., Lippe, R., Christoforidis, S., Gaullier, J.M., Brech, A., Callaghan, J., Toh, B.H., Murphy, C., Zerial, M. and Stenmark, H.** (1998). EEA1 links PI(3)K function to Rab5 regulation of endosome fusion. *Nature* 394: 494-498.
- Singer-Kruger, B., Stenmark, H. and Zerial, M.** (1995). Yeast Ypt51p and mammalian Rab5: counterparts with similar function in the early endocytic pathway. *J. Cell Sci.* 108: 3509-3521.
- Siniosoglou, S., Peak-Chew, S.Y. and Pelham, H.R.** (2000). Ric1p and rgp1p form a complex that catalyses nucleotide exchange on ypt6p. *Embo J.* 19: 4885-4894.
- Siniosoglou, S., Wimmer, C., Rieger, M., Doye, V., Tekotte, H., Weise, C., Emig, S., Segref, A. and Hurt, E.C.** (1996). A novel complex of nucleoporins, which includes Sec13p and a Sec13p homolog, is essential for normal nuclear pores. *Cell* 84: 265-275.
- Smith, D.B. and Johnson, K.S.** (1988). Single-step purification of polypeptides expressed in *Escherichia coli* as fusions with glutathione S-transferase. *Gene* 67: 31-40.
- Sogaard, M., Tani, K., Ye, R.R., Geromanos, S., Tempst, P., Kirchhausen, T., Rothman, J.E. and Sollner, T.** (1994). A rab protein is required for the assembly of SNARE complexes in the docking of transport vesicles. *Cell* 78: 937-948.
- Soldati, T., Rancano, C., Geissler, H. and Pfeffer, S.R.** (1995). Rab7 and Rab9 are recruited onto late endosomes by biochemically distinguishable processes. *J. Biol. Chem.* 270: 25541-25548.
- Soldati, T., Shapiro, A.D., Svejstrup, A.B. and Pfeffer, S.R.** (1994). Membrane targeting of the small GTPase Rab9 is accompanied by nucleotide exchange. *Nature* 369: 76-78.
- Söllner, T., Bennett, M.K., Whiteheart, S.W., Scheller, R.H. and Rothman, J.E.** (1993a). A protein assembly-disassembly pathway in vitro that may correspond to sequential steps of synaptic vesicle docking, activation, and fusion. *Cell* 75: 409-418.
- Söllner, T., Whiteheart, S.W., Brunner, M., Erdjument-Bromage, H., Geromanos, S., Tempst, P. and Rothman, J.E.** (1993b). SNAP receptors implicated in vesicle targeting and fusion. *Nature* 362: 318-324.
- Southern, E.M.** (1975). Detection of specific sequences among DNA fragments separated by gel electrophoresis. *J. Mol. Biol.* 98: 503-517.

- Sprang, S.R.** (1997). G protein mechanisms: insights from structural analysis. *Annu. Rev. Biochem.* 66: 639-678.
- Sprang, S.R. and Coleman, D.E.** (1998). Invasion of the nucleotide snatchers: structural insights into the mechanism of G protein GEFs. *Cell* 95: 155-158.
- Springer, S., Chen, E., Duden, R., Marzioch, M., Rowley, A., Hamamoto, S., Merchant, S. and Schekman, R.** (2000). The p24 proteins are not essential for vesicular transport in *Saccharomyces cerevisiae*. *Proc. Natl. Acad. Sci. USA* 97: 4034-4039.
- Springer, S. and Schekman, R.** (1998). Nucleation of COPII vesicular coat complex by endoplasmic reticulum to Golgi vesicle SNAREs. *Science* 281: 698-700.
- Springer, S., Spang, A. and Schekman, R.** (1999). A primer on vesicle budding. *Cell* 97: 145-148.
- Stamnes, M.A., Craighead, M.W., Hoe, M.H., Lampen, N., Geromanos, S., Tempst, P. and Rothman, J.E.** (1995). An integral membrane component of coatamer-coated transport vesicles defines a family of proteins involved in budding [published erratum appears in PNAS 1995 Nov 7;92(23):10816]. *Proc. Natl. Acad. Sci USA* 92: 8011-8015.
- Stenmark, H., Parton, R.G., Steele-Mortimer, O., Lutcke, A., Gruenberg, J. and Zerial, M.** (1994). Inhibition of rab5 GTPase activity stimulates membrane fusion in endocytosis. *Embo J.* 13: 1287-1296.
- Stenmark, H., Vitale, G., Ullrich, O. and Zerial, M.** (1995). Rabaptin-5 is a direct effector of the small GTPase Rab5 in endocytic membrane fusion. *Cell* 83: 423-432.
- Stone, S., Sacher, M., Mao, Y., Carr, C., Lyons, P., Quinn, A.M. and Ferro-Novick, S.** (1997). Bet1p activates the v-SNARE Bos1p. *Mol. Biol. Cell* 8: 1175-1181.
- Strom, M., Vollmer, P., Tan, T.J. and Gallwitz, D.** (1993). A yeast GTPase-activating protein that interacts specifically with a member of the Ypt/Rab family. *Nature* 361: 736-739.
- Sutton, R.B., Fasshauer, D., Jahn, R. and Brunger, A.T.** (1998). Crystal structure of a SNARE complex involved in synaptic exocytosis at 2.4 Å resolution. *Nature* 395: 347-353.
- Swaroop, A., Yang-Feng, T.L., Liu, W., Gieser, L., Barrow, L.L., Chen, K.C., Agarwal, N., Meisler, M.H. and Smith, D.I.** (1994). Molecular characterization of a novel human gene, SEC13R, related to the yeast secretory pathway gene SEC13, and mapping to a conserved linkage group on human chromosome 3p24-p25 and mouse chromosome 6. *Hum. Mol. Genet.* 3: 1281-1286.
- Takehige, K., Baba, M., Tsuboi, S., Noda, T. and Ohsumi, Y.** (1992). Autophagy in yeast demonstrated with proteinase-deficient mutants and conditions for its induction. *J. Cell Biol.* 119: 301-311.
- Tang, B.L., Kausalya, J., Low, D.Y., Lock, M.L. and Hong, W.** (1999). A family of mammalian proteins homologous to yeast Sec24p. *Biochem. Biophys. Res. Commun.* 258: 679-684.
- Tang, B.L., Peter, F., Krijnse-Locker, J., Low, S.H., Griffiths, G. and Hong, W.** (1997). The mammalian homolog of yeast Sec13p is enriched in the intermediate compartment and is essential for protein transport from the endoplasmic reticulum to the Golgi apparatus. *Mol. Cell Biol.* 17: 256-266.

- Tang, B.L., Zhang, T., Low, D.Y., Wong, E.T., Horstmann, H. and Hong, W.** (2000). Mammalian homologues of yeast sec31p. An ubiquitously expressed form is localized to endoplasmic reticulum (ER) exit sites and is essential for ER-Golgi transport. *J. Biol. Chem.* 275: 13597-13604.
- Tani, K., Oyama, Y., Hatsuzawa, K. and Tagaya, M.** (1999). Hypothetical protein KIAA0079 is a mammalian homologue of yeast Sec24p. *FEBS Lett.* 447: 247-250.
- Tisdale, E.J.** (1999). A Rab2 mutant with impaired GTPase activity stimulates vesicle formation from pre-Golgi intermediates. *Mol. Biol. Cell* 10: 1837-1849.
- Tisdale, E.J., Bourne, J.R., Khosravi-Far, R., Der, C.J. and Balch, W.E.** (1992). GTP-binding mutants of rab1 and rab2 are potent inhibitors of vesicular transport from the endoplasmic reticulum to the Golgi complex. *J. Cell. Biol.* 119: 749-761.
- Touchot, N., Chardin, P. and Tavitian, A.** (1987). Four additional members of the ras gene superfamily isolated by an oligonucleotide strategy: molecular cloning of YPT-related cDNAs from a rat brain library. *Proc. Natl. Acad. Sci. USA* 84: 8210-8214.
- Trainor, C.D., Evans, T., Felsenfeld, G. and Boguski, M.S.** (1990). Structure and evolution of a human erythroid transcription factor. *Nature* 343: 92-96.
- Trimble, W.S., Cowan, D.M. and Scheller, R.H.** (1988). VAMP-1: a synaptic vesicle-associated integral membrane protein. *Proc. Natl. Acad. Sci. USA* 85: 4538-4542.
- Tsukada, M. and Gallwitz, D.** (1996). Isolation and characterization of SYS genes from yeast, multicopy suppressors of the functional loss of the transport GTPase Ypt6p. *J. Cell Sci.* 109: 2471-2481.
- Tucker, J., Sczakiel, G., Feuerstein, J., John, J., Goody, R.S. and Wittinghofer, A.** (1986). Expression of p21 proteins in *Escherichia coli* and stereochemistry of the nucleotide-binding site. *Embo J.* 5: 1351-1358.
- Ullrich, O., Horiuchi, H., Bucci, C. and Zerial, M.** (1994). Membrane association of Rab5 mediated by GDP-dissociation inhibitor and accompanied by GDP/GTP exchange. *Nature* 368: 157-160.
- Ullrich, O., Stenmark, H., Alexandrov, K., Huber, L.A., Kaibuchi, K., Sasaki, T., Takai, Y. and Zerial, M.** (1993). Rab GDP dissociation inhibitor as a general regulator for the membrane association of rab proteins. *J. Biol. Chem.* 268: 18143-18150.
- Ungermann, C., Nichols, B.J., Pelham, H.R. and Wickner, W.** (1998). A vacuolar v-t-SNARE complex, the predominant form in vivo and on isolated vacuoles, is disassembled and activated for docking and fusion. *J. Cell Biol.* 140: 61-69.
- Valencia, A., Chardin, P., Wittinghofer, A. and Sander, C.** (1991). The ras protein family: evolutionary tree and role of conserved amino acids. *Biochemistry* 30: 4637-4648.
- VanRheenen, S.M., Cao, X., Lupashin, V.V., Barlowe, C. and Waters, M.G.** (1998). Sec35p, a novel peripheral membrane protein, is required for ER to Golgi vesicle docking. *J. Cell Biol.* 141: 1107-1119.
- VanRheenen, S.M., Cao, X., Sapperstein, S.K., Chiang, E.C., Lupashin, V.V., Barlowe, C. and Waters, M.G.** (1999). Sec34p, a protein required for vesicle tethering to the yeast Golgi apparatus, is in a complex with Sec35p. *J. Cell Biol.* 147: 729-742.

- Vida, T.A. and Emr, S.D.** (1995). A new vital stain for visualizing vacuolar membrane dynamics and endocytosis in yeast. *J. Cell Biol.* 128: 779-792.
- Vogel, U.S., Dixon, R.A., Schaber, M.D., Diehl, R.E., Marshall, M.S., Scolnick, E.M., Sigal, I.S. and Gibbs, J.B.** (1988). Cloning of bovine GAP and its interaction with oncogenic ras p21. *Nature* 335: 90-93.
- Vollmer, P. and Gallwitz, D.** (1995). High expression cloning, purification, and assay of Ypt-GTPase-activating proteins. In *"Methods in Enzymology"*, Academic Press, Inc., San Diego, USA. Vol. 257: pp. 118-128.
- Vollmer, P., Will, E., Scheglmann, D., Strom, M. and Gallwitz, D.** (1999). Primary structure and biochemical characterization of yeast GTPase-activating proteins with substrate preference for the transport GTPase Ypt7p. *Eur. J. Biochem.* 260: 284-290.
- Wach, A., Brachat, A., Pohlmann, R. and Philippsen, P.** (1994). New Heterologous Modules for Classical or PCR-based Gene Disruptions in *Saccharomyces Cerevisiae*. *Yeast* 10: 1793-1808.
- Wada, Y., Nakamura, N., Ohsumi, Y. and Hirata, A.** (1997). Vam3p, a new member of syntaxin related protein, is required for vacuolar assembly in the yeast *Saccharomyces cerevisiae*. *J. Cell Sci.* 110: 1299-1306.
- Wagner, P., Hengst, L. and Gallwitz, D.** (1992). Ypt proteins in yeast. In *"Methods in Enzymology"*, Academic Press, Inc., San Diego, USA. Vol. 219: pp. 369-387.
- Walch-Solimena, C., Collins, R.N. and Novick, P.J.** (1997). Sec2p mediates nucleotide exchange on Sec4p and is involved in polarized delivery of post-Golgi vesicles. *J. Cell Biol.* 137: 1495-509.
- Walworth, N.C., Brennwald, P., Kabcenell, A.K., Garrett, M. and Novick, P.** (1992). Hydrolysis of GTP by Sec4 protein plays an important role in vesicular transport and is stimulated by a GTPase-activating protein in *Saccharomyces cerevisiae*. *Mol Cell Biol* 12: 2017-28.
- Wang, L., Ungermann, C. and Wickner, W.** (2000a). The docking of primed vacuoles can be reversibly arrested by excess Sec17p (alpha-SNAP). *J. Biol. Chem.* 275: 22862-22867.
- Wang, W., Sacher, M. and Ferro-Novick, S.** (2000b). TRAPP Stimulates Guanine Nucleotide Exchange on Ypt1p. *J. Cell Biol.* 151: 289-296.
- Wang, Y., Okamoto, M., Schmitz, F., Hofmann, K. and Sudhof, T.C.** (1997). Rim is a putative Rab3 effector in regulating synaptic-vesicle fusion. *Nature* 388: 593-598.
- Waters, M.G., Clary, D.O. and Rothman, J.E.** (1992). A novel 115-kD peripheral membrane protein is required for intercisternal transport in the Golgi stack. *J. Cell Biol.* 118: 1015-1026.
- Waters, M.G. and Pfeffer, S.R.** (1999). Membrane tethering in intracellular transport. *Curr.Opin. Cell. Biol.* 11: 453-459.
- Weber, T., Parlati, F., McNew, J.A., Johnston, R.J., Westermann, B., Sollner, T.H. and Rothman, J.E.** (2000). SNAREpins are functionally resistant to disruption by NSF and alphaSNAP. *J. Cell Biol.* 149: 1063-1072.

- Weber, T., Zemelman, B.V., McNew, J.A., Westermann, B., Gmachl, M., Parlati, F., Söllner, T.H. and Rothman, J.E.** (1998). SNAREpins: minimal machinery for membrane fusion. *Cell* 92: 759-772.
- Wickner, W. and Haas, A.** (2000). Yeast homotypic vacuole fusion: a window on organelle trafficking mechanisms. *Annu. Rev. Biochem.* 69: 247-275.
- Will, E., Albert, S. and Gallwitz, D.** (2001). Expression, purification and biochemical properties of Ypt/Rab GAPs of the GYP family. In "*Methods in Enzymology*", Academic Press, Inc., San Diego, USA. Vol. 329: pp. 50-58.
- Will, E. and Gallwitz, D.** (2001). Biochemical characterization of Gyp6p, a Ypt/Rab-specific GTPase-activating protein from yeast. *J. Biol. Chem.* (in process citation)
- Wilson, I.A., Niman, H.L., Houghten, R.A., Cherenon, A.R., Connolly, M.L. and Lerner, R.A.** (1984). The structure of an antigenic determinant in a protein. *Cell* 37: 767-778.
- Wittinghofer, A. and Pai, E.F.** (1991). The structure of Ras protein: a model for a universal molecular switch. *Trends Biochem. Sci.* 16: 382-387.
- Wittinghofer, A., Scheffzek, K. and Ahmadian, M.R.** (1997). The interaction of Ras with GTPase-activating proteins. *FEBS Lett.* 410: 63-7.
- Wooding, S. and Pelham, H.R.** (1998). The dynamics of golgi protein traffic visualized in living yeast cells. *Mol. Biol. Cell* 9: 2667-2680.
- Wurmser, A.E., Sato, T.K. and Emr, S.D.** (2000). New component of the vacuolar class C-Vps complex couples nucleotide exchange on the Ypt7 GTPase to SNARE-dependent docking and fusion. *J Cell Biol* 151: 551-62.
- Xu, Z., Mayer, A., Muller, E. and Wickner, W.** (1997). A heterodimer of thioredoxin and I(B)2 cooperates with Sec18p (NSF) to promote yeast vacuole inheritance. *J. Cell Biol.* 136: 299-306.
- Xu, Z., Sato, K. and Wickner, W.** (1998). LMA1 binds to vacuoles at Sec18p (NSF), transfers upon ATP hydrolysis to a t-SNARE (Vam3p) complex, and is released during fusion. *Cell* 93: 1125-1134.
- Yang, B., Steegmaier, M., Gonzalez, L.C., Jr. and Scheller, R.H.** (2000). nSec1 binds a closed conformation of syntaxin1A. *J. Cell Biol.* 148: 247-252.
- Yang, X., Matern, H.T. and Gallwitz, D.** (1998). Specific binding to a novel and essential Golgi membrane protein (Yip1p) functionally links the transport GTPases Ypt1p and Ypt31p. *Embo J.* 17: 4954-4963.
- Yeung, T., Barlowe, C. and Schekman, R.** (1995a). Uncoupled packaging of targeting and cargo molecules during transport vesicle budding from the endoplasmic reticulum. *J. Biol. Chem.* 270: 30567-30570.
- Yeung, T., Yoshihisa, T. and Schekman, R.** (1995b). Purification of Sec23p-Sec24p complex. In "*Methods in Enzymology*", Academic Press, Inc., San Diego, USA. Vol. 257: pp. 145-151.
- Yoshihisa, T., Barlowe, C. and Schekman, R.** (1993). Requirement for a GTPase-activating protein in vesicle budding from the endoplasmic reticulum. *Science* 259: 1466-1468.

- Zeng, J., Ren, M., Gravotta, D., De Lemos-Chiarandini, C., Lui, M., Erdjument-Bromage, H., Tempst, P., Xu, G., Shen, T.H., Morimoto, T., Adesnik, M. and Sabatini, D.D.** (1999). Identification of a putative effector protein for rab11 that participates in transferrin recycling. *Proc. Natl. Acad. Sci. USA* 96: 2840-5.
- Zerial, M. and Huber, L.** (1995). "*Guidebook to Small GTPases*", Oxford University Press.
- Zerial, M. and McBride, H.** (2001). Rab proteins as membrane organizers. *Nature Rev. Mol. Cell Biol.* 2: 107-117.
- Zhang, B. and Zheng, Y.** (1998). Regulation of RhoA GTP hydrolysis by the GTPase-activating proteins p190, p50RhoGAP, Bcr, and 3BP-1. *Biochemistry* 37: 5249-5257.

Publications

- ❖ **De Antoni, A.** and Gallwitz, D. (2000). A novel multi-purpose cassette for repeated integrative epitope tagging of genes in *Saccharomyces cerevisiae*. *Gene* 246 (1-2): 179–185.
- ❖ Peng, R.[#], **De Antoni, A.[#]** and Gallwitz, D. (2000). Evidence for overlapping and distinct functions in protein transport of coat protein Sec24p family members. *J. Biol. Chem.* 275 (15): 11521-11528. ([#] the two authors contributed equally to this work)
- ❖ Peng, R., Grabowski, R., **De Antoni, A.** and Gallwitz, D. (1999). Specific interaction of the yeast cis-Golgi syntaxin Sed5p and the coat protein complex II component Sec24p of endoplasmic reticulum-derived transport vesicles. *Proc. Natl. Acad. Sci. USA* 96 (7): 3751-3756.
- Philippsen, P., Kleine, K., Pohlmann, R., Dusterhoft, A., Hamberg, K., Hegemann, J.H., Obermaier, B., Urrestarazu, L.A., Aert, R., Albermann, K., Altmann, R., Andre, B., Baladron, V., Ballesta, J.P., Becam, A.M., Beinhauer, J., Boskovic, J., Buitrago, M.J., Bussereau, F., Coster, F., Crouzet, M., D'Angelo, M., Dal Pero, F., **De Antoni, A.**, Hani, J. *et al.* (1997). The nucleotide sequence of *Saccharomyces cerevisiae* chromosome XIV and its evolutionary implications. *Nature* 387 (supp.): 93-98.
- **De Antoni, A.**, Foli, A., Lisziewicz, J., and Lori, F. (1997). Mutations in the pol gene of HIV-1 infected patients receiving didanosine and hydroxyurea combination therapy *J. Infect. Dis* 176 (4): 899-903
- Lori, F., Malykh, A.G., Foli, A., Maserati, R., **De Antoni, A.**, Minoli, L., Padriani, D., Degli Antoni, A., Barchi, E., Jessen, H., Wainberg, M.A., Gallo, R.C. and Lisziewicz, J. (1997). Combination of a drug targeting the cell with a drug targeting the virus controls human immunodeficiency virus type 1 resistance. *AIDS Res. Hum. Retroviruses* 13 (16): 1403-1409.
- Valle, G., Faulkner, G., **De Antoni, A.**, Pacchioni, B., Pallavicini, A., Pandolfo, D., Tiso, N., Toppo, S., Trevisan, S. and Lanfranchi, G. (1997). Telethonin, a novel sarcomeric protein of heart and skeletal muscle. *FEBS Lett* 415 (2): 163-168.
- **De Antoni, A.**, D'Angelo, M., Dal Pero, F., Sartorello, F., Pandolfo, D., Pallavicini, A., Lanfranchi, G. and Valle, G. (1997a). The DNA sequence of cosmid 14-13b from chromosome XIV of *Saccharomyces cerevisiae* reveals an unusually high number of overlapping open reading frames. *Yeast* 13 (3): 261-266.
- Pandolfo, D., **De Antoni, A.**, Lanfranchi, G. and Valle, G. (1996). The DNA sequence of cosmid 14-5 from chromosome XIV reveals 21 open reading frames including a novel gene encoding a globin-like domain. *Yeast* 12 (10B): 1071-1076.

(❖ indicates the publications related to this work)

Curriculum Vitae

Name: Anna De Antoni
Date of Birth: February 1st, 1968
Place of Birth: Vicenza , Italy
Citizenship: Italian
Parents: Angelo De Antoni
Gianfranca De Antoni, born Santamaria

Education:

1974 - 1979 Primary school, Scuola elementare P. Lioy, Vicenza, Italy.
1979 - 1982 Secondary school, Scuola media Monte Berico, Vicenza, Italy.
1982 - 1987 High school, Liceo Scientifico P. Lioy, Vicenza, Italy

Studies:

1987 - 1994 Biological Sciences faculty, University of Padua, Italy .

1992 - 1994 Department of Biology, University of Padua, Italy. "Internato di laurea" (research activity for "laurea" degree) under the leadership of Dr. G. Valle. Final Thesis titled: "Caratterizzazione del recettore KDEL ed osservazioni sulla regolazione di proteine del reticolo endoplasmatico in *Xenopus laevis*" (Characterization of the KDEL receptor and observations on the regulation of endoplasmic reticulum proteins in *Xenopus laevis*)

March 14th, 1994 "Laurea" degree in Biological Sciences, University of Padua, Italy.

Nov. 1997 - Apr. 2001 Molecular Genetics department, Max Planck Institute for Biophysical Chemistry, Göttingen, Germany. Ph.D. studies under the leadership of Prof. Dr. D. Gallwitz

Other research activities:

Jun. - Oct., 1991 Department of Genetics, University of Groningen, Holland:
Molecular studies on *Lactococcus lactis*.
Scholarship granted by the Erasmus Program .
Research Director Dr. A. Haandrkman and Dr. J. Kok.

- 1994 - 1995 Department of Biology, University of Padua, Italy:
Sequencing of a 38Kb fragment of the chromosome XIV of *S. cerevisiae*. Gene Bank accession number: z69382.
Part of the EU project BIOTECH I for the complete sequencing of the genome of *Saccharomyces cerevisiae*.
Research Director: Dr. G. Valle.
- 1995 - 1996 Department of Biology, University of Padua, Italy:
Project aimed at obtaining the full length sequences of some unknown genes of human skeletal muscle tissue.
Part of the Telethon Program.
Scholarship granted by the Telethon Program.
Research Directors: Dr. G. Valle and Dr. G. Lanfranchi.
- 1996 - 1997 Research Institute for Genetic and Human Therapy (R.I.G.H.T.),
Gaithersburg, Maryland, USA: Molecular studies on the human immunodeficiency virus (HIV). Identification of mutations in the *pol* gene of HIV-1 in infected patients receiving didanosine and hydroxyurea combination therapy.
Scholarship granted by R.I.G.H.T..
Research Directors: Dr. F. Lori and Dr. J. Lisziewicz.